

University of Nebraska - Lincoln

DigitalCommons@University of Nebraska - Lincoln

Student Research Projects, Dissertations, and
Theses - Chemistry Department

Chemistry, Department of

5-2015

Analysis of Free Solute Fractions and Solute-Protein Interactions Using Ultrafast Affinity Extraction and Affinity Microcolumns

Xiwei Zheng

University of Nebraska-Lincoln, xiwei@huskers.unl.edu

Follow this and additional works at: <http://digitalcommons.unl.edu/chemistrydiss>



Part of the [Analytical Chemistry Commons](#)

Zheng, Xiwei, "Analysis of Free Solute Fractions and Solute-Protein Interactions Using Ultrafast Affinity Extraction and Affinity Microcolumns" (2015). *Student Research Projects, Dissertations, and Theses - Chemistry Department*. 52.

<http://digitalcommons.unl.edu/chemistrydiss/52>

This Article is brought to you for free and open access by the Chemistry, Department of at DigitalCommons@University of Nebraska - Lincoln. It has been accepted for inclusion in Student Research Projects, Dissertations, and Theses - Chemistry Department by an authorized administrator of DigitalCommons@University of Nebraska - Lincoln.

ANALYSIS OF FREE SOLUTE FRACTIONS AND SOLUTE-PROTEIN
INTERACTIONS USING ULTRAFAST AFFINITY EXTRACTION AND AFFINITY
MICROCOLUMNS

by

Xiwei Zheng

A DISSERTATION

Presented to the Faculty of
The Graduate College at the University of Nebraska

In Partial Fulfillment of Requirements

For the Degree of Doctor of Philosophy

Major: Chemistry

Under the Supervision of Professor David S. Hage

Lincoln, Nebraska

May, 2015

ANALYSIS OF FREE SOLUTE FRACTIONS AND SOLUTE-PROTEIN
INTERACTIONS USING ULTRAFAST AFFINITY EXTRACTION AND AFFINITY
MICROCOLUMNS

Xiwei Zheng, Ph.D.

University of Nebraska, 2015

Advisor: David S. Hage

This dissertation describes the use of a high-performance affinity chromatography method based on ultrafast affinity extraction and microcolumns to study biological interactions.

In the first project, a new method was created and based on ultrafast affinity extraction to determine both the dissociation rate constants (k_d) and association equilibrium constants (K_a) for drug-protein interactions in solution. Various conditions to optimize the use of ultrafast affinity extraction for equilibrium and kinetic studies were considered.

The objective of the next portion of this dissertation was to develop a chromatographic approach to measure free drug fractions in more complex samples. This was accomplished by combining ultrafast affinity extraction with a multi-dimensional HPAC system. In the first project in this section, the target of interest was *R*- and *S*-warfarin, which have slightly different binding strengths for the serum transport protein human serum albumin (HSA). A multi-dimensional HPAC system was developed to study the binding of each enantiomer with HSA. This system was used to simultaneously

measure the free fraction of each enantiomer and its K_a value with HSA. The second project used ultrafast affinity extraction and a multi-dimensional affinity system to measure the free fractions and global affinity constants of several sulfonylurea drugs in the presence of normal HSA or glycated HSA. A third project used a similar approach to measure the free fractions and K_a value of various drugs in serum

The next project used ultrafast affinity extraction to study the interactions of a steroid hormone (i.e., testosterone) with its serum transport proteins, HSA and sex hormone binding globulin (SHBG). Both the k_d and K_a values for these systems were determined. The free fractions of testosterone in samples containing HSA or SHBG at physiological concentration were also estimated.

The last project sought to develop a method to increase the binding capacity and activity of proteins in small affinity columns. This was accomplished by combining a traditional covalent immobilization method with protein cross-linking/modification. It was found that up to a 75-113% increase in total protein content could be obtained by this method when compared with more traditionally prepared supports.

ACKNOWLEDGEMENTS

I would like to thank many people who have provided me with great help throughout my graduate studies. First of all, I would like to express my most gratitude to Dr. David S. Hage for his mentorship and support in my research over the past five years. Your generous guidance and brilliant advice throughout my graduate studies exposed me to fantastic academic areas and helped me to become a good researcher. I appreciate all of your help in my paper writing and editing. I also want to specially thank you for your understanding and offering me time to return to China to reunite with my family. I would also like to thank my committee members, Dr. Lai, Dr. Dussault, Dr. Guo and Dr. Subramanian. I really appreciate all the valuable suggestions and guidance you gave me during my Ph.D. studies. Many thanks also go to Dr. Lai for providing me with the opportunity to start my journey at UNL.

I also would like to thank the members of the Hage lab in the past and at present. Ryan Matsuda, Penny and Zhao, I am very grateful and fortunate to have met all of you. You gave me countless help, support and happiness over the past years. Thank you for accompanying with me all the time. I know my graduate life would have been very helpless, lonely and pale without any of you. I also would like to say many thanks to Maria for your great assistance in my research and paper writing. It was so amazing to work with you during the past three years. I also would like to thank my friends outside of the Hage group whom I met before or after I came to Lincoln. Thank you, Weiwei, Yunyun, Xi, Tong, and Haotong for bringing me many wonderful moments and happy memories. Every Chinese New Year Festival we celebrated together made me feel like I

was back at our home country. I also would like to thank Yunan and Jiahan for always being there for me in every possible way. Your support and trust made me believe that I can be strong and brave enough to overcome all the challenges in my life and studies.

Most of all, I owe my deepest gratitude to my family. Baba and Mama, thanks for your understanding and allowing me to leave home for five years to some place that is super far away from you. I am so sorry that, as your only kid, I missed five years in your life and could not accompany with and take care of both of you. Instead, I made you two worry and miss me all the time. You are the most awesome parents I could ever have. Your wisdom and sincerity lead me to know how to be a good person. Your love has always overcome the time difference and geographical distance between us and gave me the encouragement and support to cross any difficulties I encountered. At last, many thanks to my fiancé, Lei, for everything! You are the biggest treasure I have here. I cannot describe to you how you have brightened my life and how happy you make me. You make me believe that everything is possible and we can make it through no matter how hard it is. Thank you for being with me.

TABLE OF CONTENTS

CHAPTER 1

General Introduction

Basic Principles of Affinity Chromatography and HPAC	1
Types of Affinity Microcolumns	3
Zonal Elution and Affinity Microcolumns	10
<i>Principles of zonal elution</i>	10
<i>Estimating binding strength and retention using affinity microcolumns</i>	14
<i>Competition and displacement studies using affinity microcolumns</i>	17
<i>Ultrafast affinity extraction method</i>	25
<i>Other applications of zonal elution with affinity microcolumns</i>	29
Frontal Analysis and Affinity Microcolumns	34
<i>Principles of frontal analysis</i>	34
<i>Estimating binding strength and number of sites using affinity microcolumns</i>	37
<i>Competition and displacement studies using affinity microcolumns</i>	39
<i>Other applications of frontal analysis with affinity microcolumns</i>	43
Overall Goal and Summary of Work	45
References	48

CHAPTER 2

Analytical Methods for Kinetic Studies of Biological Interactions

Introduction	61
Stopped-Flow Analysis	62
<i>General principles</i>	62
<i>Applications involving single-molecule reactions</i>	66
<i>Applications involving bimolecular reactions</i>	70
<i>Applications involving competition studies</i>	74
<i>Applications involving multistep reactions</i>	77
<i>Advantages and potential limitations</i>	80
Surface Plasmon Resonance	81
<i>General principles</i>	81
<i>Data analysis methods</i>	84
<i>Applications in kinetic studies</i>	86
<i>Advantages and potential limitations</i>	90
Affinity Chromatography	92
<i>General principles</i>	92
<i>Band broadening methods</i>	95

<i>Peak fitting methods</i>	100
<i>Split-peak method</i>	103
<i>Peak decay method</i>	105
<i>Advantages and potential limitations</i>	109
Capillary Electrophoresis	111
<i>General principles</i>	111
<i>Analysis of slow biological reactions</i>	111
<i>Kinetic capillary electrophoresis</i>	115
<i>Advantages and potential limitations</i>	122
Conclusions	123
References	125

CHAPTER 3

Improvement of Ultrafast Affinity Extraction for Determination of both the Kinetics and Thermodynamics of Drug-Protein Interactions

Introduction	140
Experimental	144
<i>Materials and reagents</i>	144
<i>Apparatus</i>	145

<i>Column preparation</i>	145
<i>Chromatographic studies</i>	146
Results and Discussion	147
<i>Optimization of free drug fraction measurements</i>	147
<i>Determination of dissociation rate constants</i>	153
<i>Measurement of association equilibrium constants</i>	158
<i>Estimation of association rate constants</i>	162
Conclusions	163
References	165

CHAPTER 4

Combination of Ultrafast Affinity Extraction and Multi-Dimensional HPAC for the Analysis of Free Fractions for Chiral Drugs

Introduction	169
Experimental	171
<i>Materials and reagents</i>	171
<i>Apparatus</i>	171
<i>Column preparation</i>	172
<i>Chromatographic studies</i>	172

<i>Ultrafiltration studies</i>	178
Results and Discussion	179
<i>Optimization of conditions for multi-dimensional affinity system</i>	179
<i>Measurement of free drug fractions for warfarin enantiomers</i>	185
<i>Simultaneous estimation of association equilibrium constants for R- and S-warfarin with soluble HSA</i>	188
Conclusions	191
References	193

CHAPTER 5

The Use of Ultrafast Affinity Extraction and Multi-Dimensional HPAC to Study the Interactions of Sulfonylurea Drugs with Normal or Glycated Human Serum Albumin

Introduction	195
Experimental	200
<i>Materials and reagents</i>	200
<i>Apparatus</i>	200
<i>Column preparation and protein glycation</i>	201
<i>Chromatographic studies</i>	202
Results and Discussion	206

<i>Optimization of conditions for ultrafast affinity extraction</i>	206
<i>Optimization of conditions for multi-dimensional affinity system</i>	211
<i>Measurement of free fractions for sulfonylurea drugs</i>	217
<i>Estimation of affinity for sulfonylurea drugs with normal HSA or glycated HSA</i> ..	220
Conclusions	223
References	225

CHAPTER 6

The Use of Ultrafast Affinity Extraction for Free Fraction Measurements of Various Drugs in Clinical Samples

Introduction	229
Experimental	231
<i>Materials and reagents</i>	231
<i>Apparatus</i>	232
<i>Column preparation</i>	233
<i>Chromatographic studies</i>	234
<i>Ultrafiltration studies</i>	238
Results and Discussion	239
<i>Optimization of conditions for ultrafast affinity extraction</i>	239

<i>Optimization of conditions for multi-dimensional affinity system</i>	244
<i>Measurement of free fractions and binding of drugs to HSA in serum</i>	251
Conclusions	254
References	257

CHAPTER 7

The Use of Ultrafast Affinity Extraction to Study the Interactions of Steroid Hormone with Human Serum Albumin and Sex Hormone Binding Globulin

Introduction	260
Experimental	263
<i>Materials and reagents</i>	263
<i>Apparatus</i>	263
<i>Column preparation</i>	264
<i>Preparation of Testosterone Solutions</i>	265
<i>Chromatographic studies</i>	266
Results and Discussion	271
<i>Optimization of ultrafast affinity extraction for testosterone-protein binding studies</i>	271
<i>Determination of binding strength for testosterone with HSA</i>	280
<i>Determination of rate constants for interactions of testosterone with HSA</i>	283

<i>Determination of the binding strength for testosterone with SHBG</i>	284
<i>Determination of rate constants for the interactions of testosterone with SHBG ...</i>	287
Conclusions.....	290
References	292

CHAPTER 8

Development of High Capacity Affinity Microcolumns Based on Hybrid Cross- Linking and Protein Immobilization Methods

Introduction.....	295
Experimental	299
<i>Materials and reagents</i>	299
<i>Apparatus.....</i>	300
<i>Preparation of affinity supports</i>	301
<i>Chromatographic studies</i>	302
Results and Discussion.....	305
<i>Optimization of HSA modification.....</i>	305
<i>Effects of protein modification on retention</i>	307
<i>Use of BMH-treated HSA microcolumns with a sulfhydryl-reactive drug</i>	313
<i>Use of BMH-treated HSA microcolumns in ultrafast affinity extraction</i>	317

Conclusions.....	323
References	325

CHAPTER 9

Summary and Future Work

Summary of Work.....	328
Future Work	332

CHAPTER 1

General Introduction

Portion of this chapter have previously appeared in X. Zheng, Z. Li, S. Beeram, M. Podariu, R. Matsuda, E.L. Pfaunmiller, C.J. White II, N. Carter, D.S. Hage "Analysis of Biomolecular Interactions Using Affinity Microcolumn: A Review" Journal of Chromatography B 2014, 968, 49-63.

Basic Principles of Affinity Chromatography and HPAC

Affinity chromatography is a liquid chromatographic technique that uses a biologically-related binding agent, or "affinity ligand", as the stationary phase to separate or analyze sample components.¹⁻⁸ This stationary phase can be created by covalently attaching, entrapping, absorbing or in some other way immobilizing the affinity ligand to a chromatographic support.³⁻⁵ This solid support and the stationary phase are placed within a column or capillary that can then be used for the purification, separation or analysis of targets capable of binding to the affinity ligand.⁵⁻¹⁴ The retention and separation of a target from other sample components is based on the specific and reversible interactions that characterize many biological interactions, such as the binding of an antibody with an antigen or a hormone with a receptor.^{1-3,5-8} If the interaction is strong (i.e., with an association equilibrium constant greater than 10^5 - 10^6 M⁻¹), an elution buffer and a change in the pH, temperature, or mobile phase composition may be required to remove the target from the column.¹⁵⁻¹⁷ If weaker binding is present (i.e., an association equilibrium constant of 10^5 - 10^6 M⁻¹ or less), it may be possible to elute the target under isocratic conditions. This latter method is sometimes referred to as weak

affinity chromatography (WAC).¹⁸⁻¹⁹ The variety of elution formats, immobilized ligands, and columns that can be used in affinity chromatography has made this method a valuable tool for the study of biomolecular interactions,^{1-3,20-29} as will be discussed in this chapter.

In any type of affinity chromatography, the support that is used for the immobilized affinity ligand should have low non-specific binding to sample components and yet be easy to modify for ligand attachment.^{4-8,30-33} Traditional affinity chromatography typically employs relatively inexpensive supports and non-rigid materials with low-to-moderate efficiencies, such as agarose gels or other carbohydrate-based materials.^{3,6,7,30} In the method of HPAC, which is the type of affinity chromatography utilized with most affinity microcolumns, the support is a material that has sufficient mechanical stability and efficiency for use in HPLC.^{3,5,8,30-31} This type of support, in turn, tends to provide HPAC with better speed and precision than traditional affinity chromatography, along with greater ease of automation through the use of HPLC systems.^{1,5,30,33} Possible supports for HPAC include particulate materials based on modified silica or glass, azalactone beads, and hydroxylated polystyrene media.^{1,3,5,30,31} Various types of monolithic supports have also been considered for use in HPAC and affinity chromatography, such as those based on organic polymers, silica monoliths, cryogels and modified forms of agarose.^{30,75-39} The recent interest in monoliths for these affinity-based separations is due to several useful features of these supports, including their rapid mass transfer properties, low back pressures, and ability to be made in a variety of shapes and sizes.^{30,32,33,36,39}

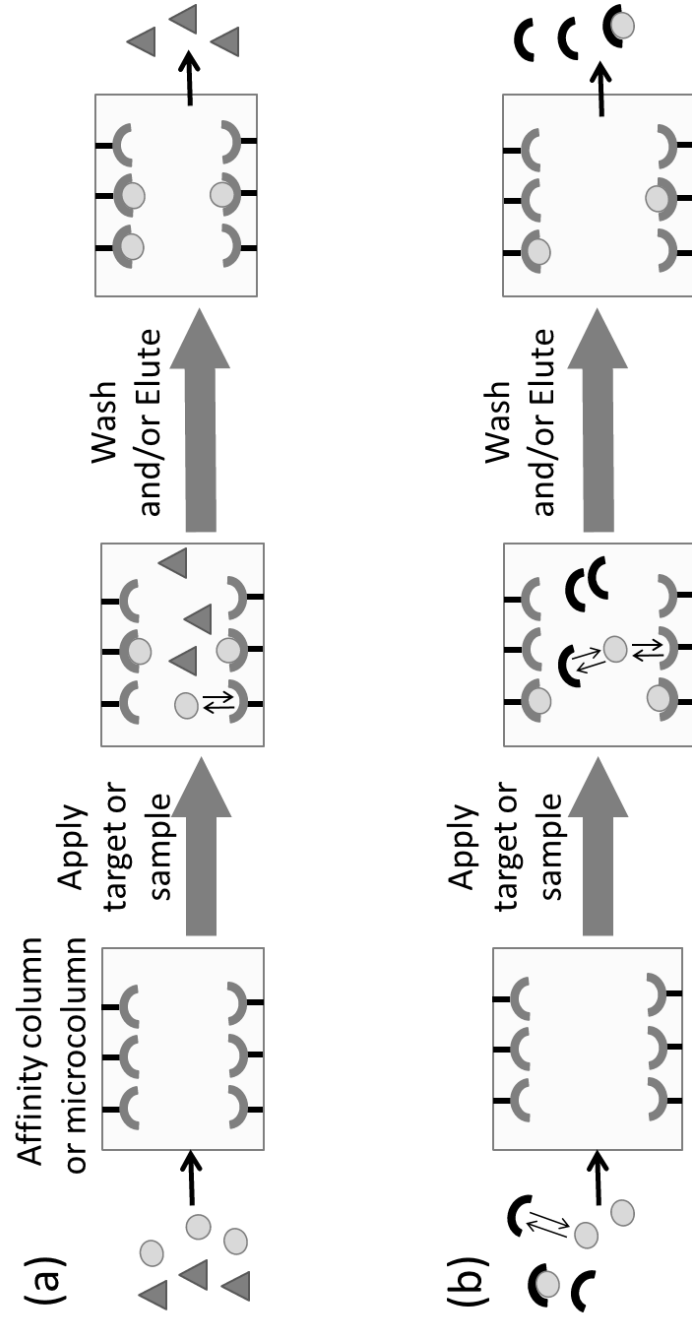
The use of affinity chromatography and HPAC for the study of biomolecular

interactions is sometimes referred to as analytical affinity chromatography, quantitative affinity chromatography, or biointeraction chromatography.^{2,3,20-29,40-41} This type of approach either examines the interaction of an applied target with the immobilized affinity ligand or uses the affinity ligand to examine interactions of the target with another binding agent in the mobile phase (see Figure 1.1).^{2,5,20} A great deal of information can be obtained through such experiments, including data on the number of interaction sites for the target with a binding agent, the equilibrium constants for this process, and the rate of the interaction.^{2,5,20,21,25,27,40-42} Data can also be obtained on the types of competition the target may have with other compounds for interactions with the binding agent, and the structure and location of the sites that are involved in these interactions.^{20,27,42}

Types of Affinity Microcolumns

A reduction in column size has been of interest in the fields of HPLC and chromatographic separations for many years. This interest initially appeared due to some common limitations with traditional 10-25 cm \times 4.6 mm i.d. HPLC columns, such as issues related to high backpressure, solvent consumption, and difficulties in working with small sample volumes.⁴³ To overcome these limitations, work began in the 1970s to reduce the size of columns in chromatographic systems and to produce various types of small-volume columns.⁴⁴⁻⁴⁶ Examples of approaches that have been used specifically in HPAC and affinity chromatography to produce affinity microcolumns are shown in Figure 1.2.^{15,47-51}

Figure 1.1 Two general schemes for the use of HPAC and affinity chromatography to study biomolecular interactions based on (a) the binding of an applied target with the immobilized affinity ligand or (b) use of the affinity ligand to examine interactions of the target with another binding agent in solution. Reproduced with permission from X. Zheng, Z. Li, S. Beeram, M. Podariu, R. Matsuda, E.L. Pfaunmiller, C.J. White II, N. Carter, D.S. Hage, *J. Chromatogr. B* 968 (2014) 49-63.



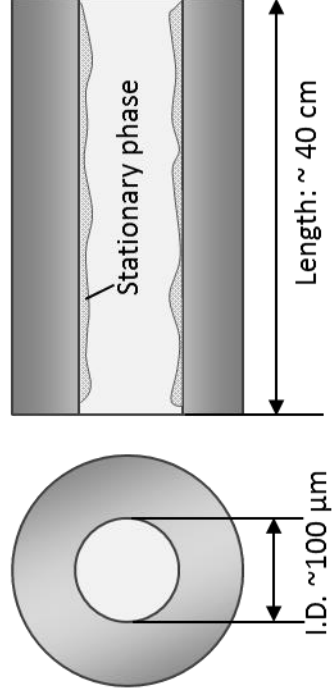
The first approach for reducing the size of a chromatographic column is to decrease the column's inner diameter, as is illustrated in Figure 1.2(a). This change is usually accompanied by an increase in column length to maintain or provide high efficiency for the system while still giving an overall decrease in volume versus traditional columns. This approach may involve the use of either open-tubular capillary columns or packed capillary columns.⁴³ Open-tubular capillaries that have been used with affinity ligands for binding studies have generally had an inner diameter of 100 μm and lengths of 30-40 cm, giving total volumes of approximately 2-4 μL .⁴⁷⁻⁴⁹ Packed capillaries that have been used with affinity ligands and binding studies have had an inner diameter of up to 0.5 mm and a length that ranges from 5-15 cm (volumes, 10-30 μL).⁴⁷⁻⁶⁰

There are several advantages to using the open-tubular or packed capillary columns in affinity-based binding studies. For instance, the flow rates applied to such columns are usually quite low (i.e., in the nL/min to $\mu\text{L}/\text{min}$ range) and the efficiencies can be high, resulting in a significant reduction in mobile phase consumption and sample size requirements.^{43,61} One potential disadvantage is that these capillary columns often require specialized equipment designed for work at low flow rates and high efficiencies (e.g., microbore or nano-HPLC systems).^{43,52,61} However, these columns are attractive for use with on-line detection by mass spectrometry, which can provide high sensitivity in detecting small amounts of targets and can be used to confirm the identity of a target in a mixture of applied compounds.⁶²⁻⁶⁴

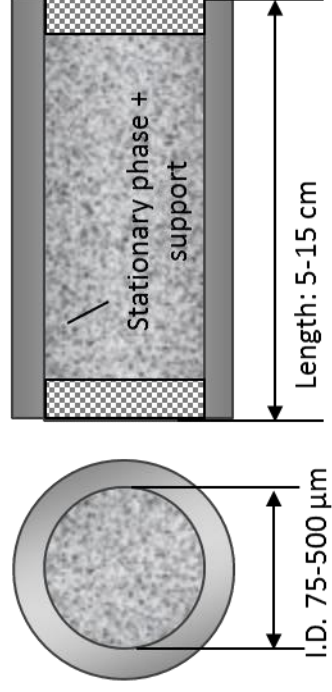
Another approach to decreasing the column size is to reduce the length of the column, as shown in Figure 1.2(b). This type of design can be employed in separations that do not require high efficiencies, such as those based on simple adsorption/desorption

Figure 1.2 Examples of affinity microcolumns that have been used for studying biomolecular interactions including designs based on (a) open-tubular or packed capillaries and (b) short microcolumns or sandwich microcolumns. Reproduced with permission from X. Zheng, Z. Li, S. Beeram, M. Podariu, R. Matsuda, E.L. Pfaunmiller, C.J. White II, N. Carter, D.S. Hage, J. Chromatogr. B 968 (2014) 49-63.

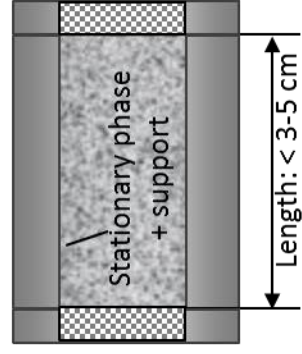
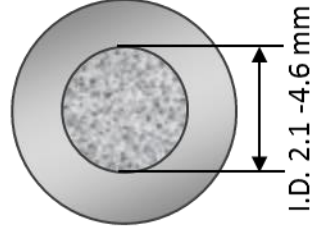
(a) Open-tubular capillary



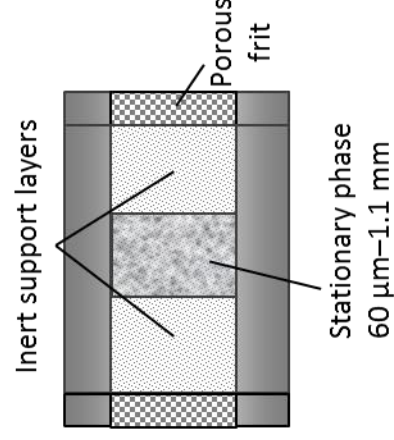
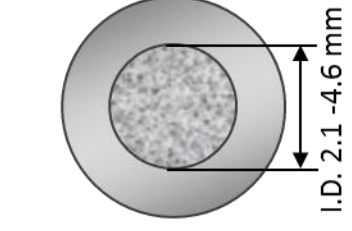
Packed capillary



(b) Short microcolumn



Sandwich microcolumn



mechanisms and selective binding for affinity separations involving moderate-to-high strength interactions.^{3-5,28,65} Various types of short microcolumns based on particulate supports or monolithic materials have been developed for affinity separations and binding studies. These columns often have an inner diameter of 2.1 mm or smaller and lengths of 1-5 cm (i.e., volumes less than 35-175 μL). Other possible formats include affinity disks, with an inner diameter of 4.6 mm and lengths of 1-2 mm,^{37,66-68} or sandwich affinity microcolumns, with effective lengths as small as 60-250 μm and volumes of only 0.2-0.9 μL .⁶⁹ A few advantages of using these columns in binding studies is that they are easy to employ with traditional HPLC systems, and they require only a small amount of support and binding agent. This type of column is often capable of withstanding high flow rates, because of its low backpressure, and can provide sample residence times in the second to millisecond range.^{50,70,71}

One advantage to utilizing either type of affinity microcolumn is that they are compatible with a variety of detection approaches. These detection forms include absorbance, fluorescence and near-infrared fluorescence, chemiluminescence, matrix-assisted laser desorption/ionization mass spectrometry, and electrospray ionization mass spectrometry.^{47-58,70,71} The small volumes of affinity microcolumns^{53,72} also leads to a significant decrease in the amount of support and affinity ligand that are needed for binding studies when compared to more traditional affinity columns.^{37,65,69-73} In many cases it is possible to reuse the same binding agent for many experiments, which further helps to improve the precision and to decrease the cost of this method.⁷⁴⁻⁷⁶

Zonal Elution and Affinity Microcolumns

Principles of zonal elution

Zonal elution is one of the most common formats applied in HPAC and affinity chromatography for studying biomolecular interactions. This method was first used with affinity columns in 1974 and is based on the measurement of peak retention times, retention factors or peak profiles.⁷⁷ This approach can be used to provide information on the strength of binding by a target with an affinity ligand and on the competition of the target with other compounds for the binding agent.^{1-3,20, 27,78,79} In this type of experiment, a narrow plug of the target is injected onto the affinity column under isocratic conditions as a detector is used to monitor the elution time or profile for the injected analyte. If relatively fast association and dissociation kinetics are present on the time scale of the experiment, the retention time of the target should be directly related to the target's strength of binding to the immobilized agent and the amount of active binding agent that is present in the column.^{2,40,79} Factors that can be altered during zonal elution experiments include the mobile phase pH, ionic strength and polarity, as well as the temperature, type of target, type of affinity ligand in the column, and the presence of competing or displacing agents in the mobile phase. By monitoring the changes in the retention for the target as these conditions are varied, detailed data can be obtained on the nature of the interactions between the target and the immobilized binding agent.^{2,10,14,19,40, 79-81}

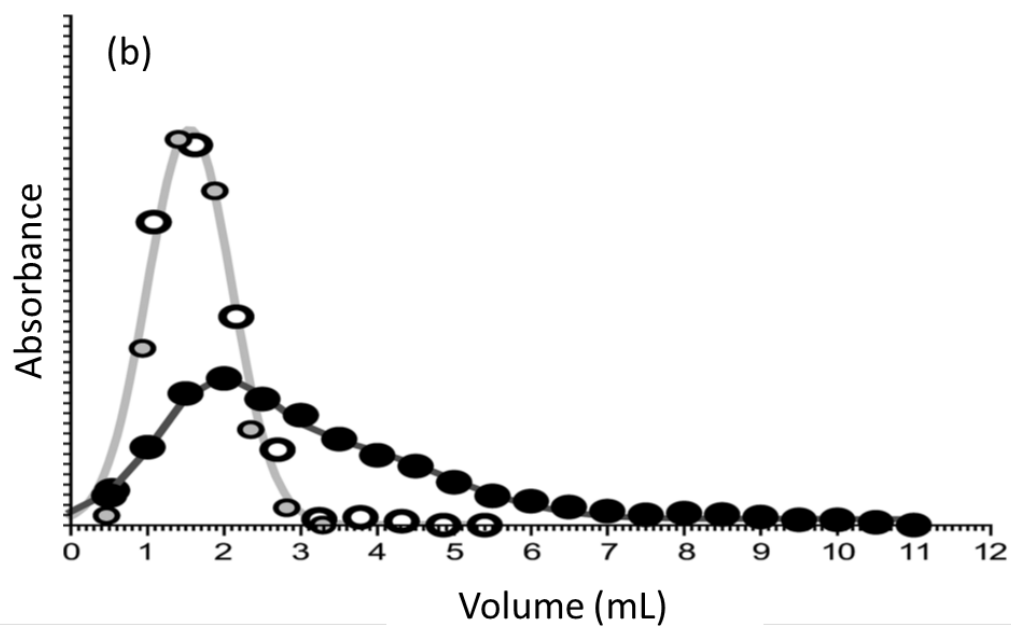
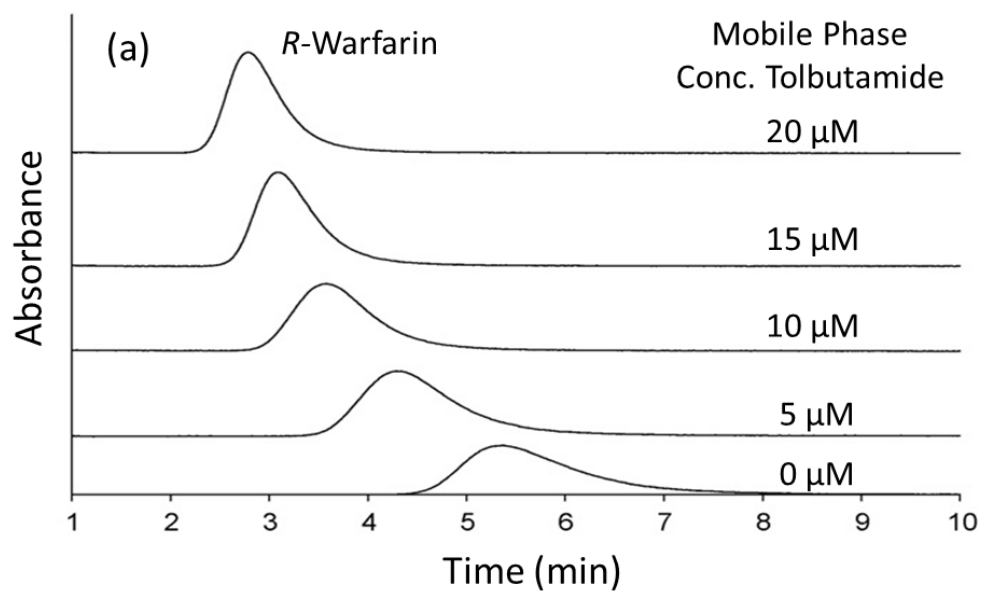
The Figure 1.3(a) shows a typical zonal elution experiment in which competition by a mobile phase additive causes a shift in the retention of an injected target as these two compounds compete for binding sites on an immobilized affinity ligand.⁸⁰ This example

shows the chromatograms generated during injections of the site-selective probe *R*-warfarin onto a 2 cm × 2.1 mm i.d. column (volume, 69 μL) that contained the immobilized protein human serum albumin (HSA), with the drug tolbutamide being placed into the mobile phase as a competing agent. In this specific experiment, a decrease was observed in the retention of *R*-warfarin as the concentration of tolbutamide was increased, indicating that either direct competition or a negative allosteric effect was occurring between these two compounds on HSA.⁸⁰

Another format in which zonal elution has been employed with microcolumns is shown in Figure 1.3(b). In this case, the immobilized binding agent is utilized to examine the binding of a retained target with a second binding agent that is applied in the mobile phase.⁸² The column in this particular example was 275 μL in volume and contained an immobilized form of cellular retinoic acid binding protein (CRABP) that was initially loaded with the target retinoic acid. A sample of a second possible binding agent for retinoic acid (i.e., retinoic acid receptor isoform γ, or RARγ) was then applied to the column and examined for its elution profile. The presence of a shift in the elution profile for this applied binding agent versus a control was used to detect an interaction between RARγ and CRABP during the transfer of retinoic acid between these binding agents.⁸²

One advantage of zonal elution is it requires only a small amount of target for injection. This method can also examine more than one compound in a sample provided there is adequate resolution between the peaks for these compounds or a detection format is employed that can distinguish between these eluting solutes.²⁷ As is illustrated in Figure 1.3(a-b), it is also possible with zonal elution to obtain information on site-specific interactions, on the competition of two targets for the same binding agent^{79,83,84} or on the

Figure 1.3 Examples of the use of zonal elution with affinity microcolumns in examining biomolecular interactions. In (a) competition studies based on zonal elution were carried out using the injection of *R*-warfarin as a site-specific probe onto a microcolumn containing immobilized human serum albumin (HSA) in the presence of various concentrations of tolbutamide in the mobile phase. The results in (b) show the elution profiles for retinoic acid receptor γ (RAR γ) that was applied to columns containing apo-cellular retinoic acid binding protein II (CRABP II) (open circles) or holo-CRABP II (black circles) and in the presence of retinoic acid; the gray-shaded circles represent an elution profile of carbonic anhydrase II (CA II) applied to an apo-CRABP II column. Adapted with permission from Refs.80,82.



competition of two binding agents to the same target.⁸⁵ As will be described in the next few sections, this format can also provide information on the strength of binding and the effects that changes in the structure of a target or binding agent may have on an interaction.

Estimating binding strength and retention using affinity microcolumns

Zonal elution can be used in a variety of ways to obtain information on biomolecular interactions. An important parameter to measure when describing these interactions is the degree or strength of binding that occurs in the system.^{27,40,86-96} This information can be obtained from the retention time or retention factor (k) for a target that is injected onto an affinity column. This retention factor can be calculated from the observed elution times through the following relationship,

$$k = \frac{t_R - t_M}{t_M} \quad (1.1)$$

where t_R is the observed retention time for the injected target, and t_M is the column void time.

If relatively fast association/dissociation kinetics and linear elution conditions are present during the measurement of the retention factor (i.e., the apparent value of k is not affected by the amount of injected sample or the flow rate), Equation 1.2 can be used to relate this retention factor to the number of binding sites for the target in the affinity column and to the association equilibrium constants for the target at these sites.^{81,101}

$$k = \frac{(K_{a1}n_1 + K_{a2}n_2 \dots + K_{an}n_n)m_L}{V_M} \quad (1.2)$$

In this equation, the terms K_{a1} through K_{an} represent the association equilibrium constants for the target at each of its binding sites in the column, n_1 through n_n are the fractions for each type of site in the column, m_L is the total moles of all binding sites in the column, and V_M is the void volume of the column.

The global association equilibrium constant (nK_a') for the interaction of a target with the immobilized binding agent can be obtained from the numerator of Equation 1.2, where nK_a' is the summation of the terms $K_{a1}n_1$ through $K_{an}n_n$. This term is directly proportional to k if all of the binding sites have independent interactions with the target. If the target binds to only one type of site on the affinity ligand and in the column, the multisite equation in Equation 1. 2 can be rearranged to the simpler form that is provided in Equation 1.3,

$$k = \frac{K_a m_L}{V_M} \quad (1.3)$$

where K_a is the association equilibrium constant for the interaction, m_L/V_M represents the molar concentration of the binding sites for this interaction, and other terms are as defined previously.^{81,101}

A few recent studies have examined the ability of short affinity microcolumns to be used with zonal elution for estimates of retention factors and binding strength. One set of experiments were carried out at various flow rates for the drugs carbamazepine and warfarin when applied to HSA affinity microcolumns.⁸⁶ These columns contained 4.6 mm i.d. silica monoliths with lengths of 1-5 mm or 4.6 mm i.d. columns that were 3 mm in

length and that contained HSA immobilized to silica particles. It was found that similar retention factors were obtained for warfarin on 3 to 5 mm long microcolumns, and for carbamazepine when the column length ranged from 1 to 5 mm. These results indicated microcolumns as short as 1-3 mm could be used to provide reproducible retention factors for drug-protein binding studies that involve systems with binding constants in the range of 10^3 to 10^6 M⁻¹.⁸⁶ Additional work was carried out with racemic warfarin and L-tryptophan on 2.1 mm i.d. HSA microcolumns that contained silica particles and that ranged in length from 1 mm to 2 cm. This report also indicated that columns as small as only a few millimeters in length could be used for zonal elution studies of drug-protein binding for systems with affinities of 10^4 to 10^6 M⁻¹.⁷² Some loss of precision in retention measurements did occur with the use of these small columns and there was a greater chance of column overloading.^{72, 86} However, it was noted that the latter effect could be dealt with by decreasing the sample load or by using reference compounds and retention ratios to adjust for shifts in the retention factors.⁷²

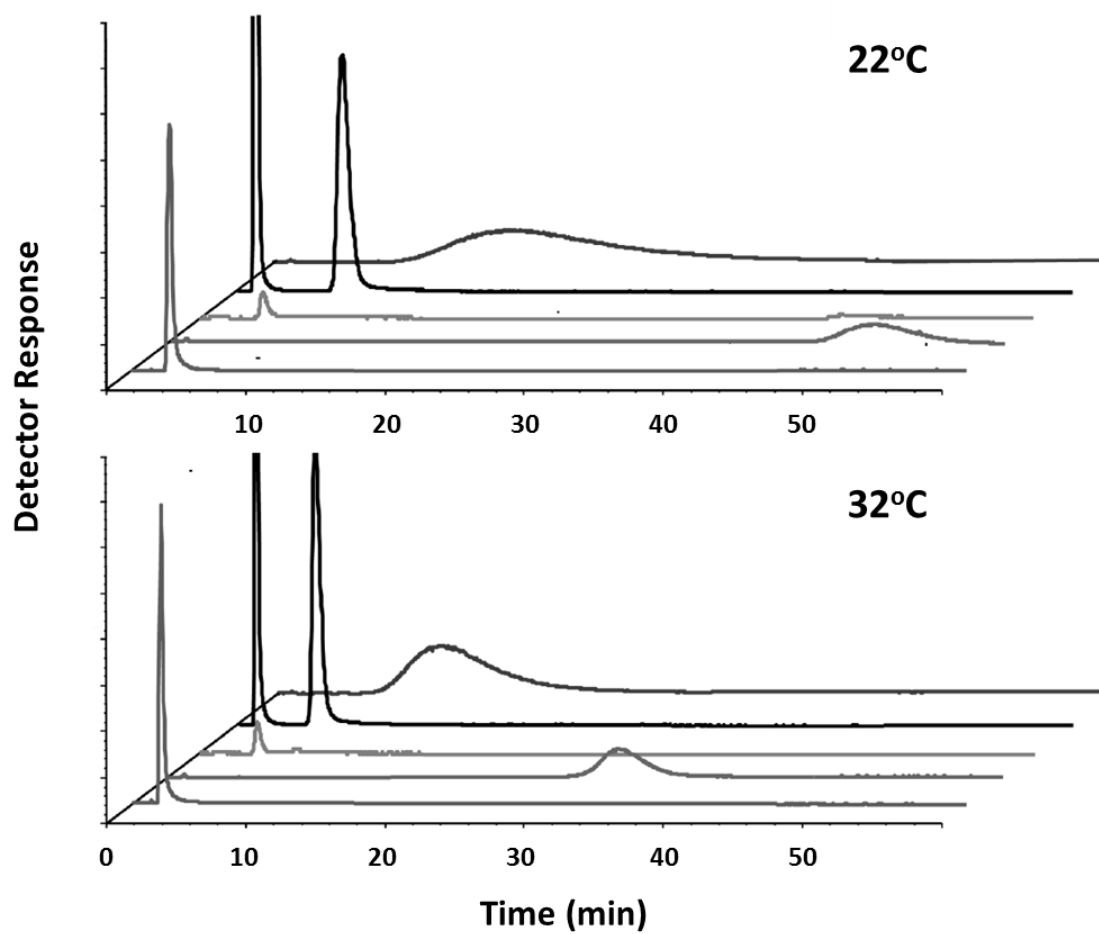
The fact that the retention factor is related both to the association equilibrium constants and number of binding sites for an interaction can be used in a variety of ways. For instance, retention factor measurements of *R*- and *S*-propranolol, as model drugs, have been used in examining the long-term stability of affinity microcolumns that contained high-density lipoprotein (HDL) and low-density lipoprotein (LDL).⁸⁷⁻⁸⁹ If an independent estimate is available for the binding capacity (m_L), it is possible to use this information with measured retention factors and Equations 1.2 or 1.3 to estimate the value of nK_a for a multi-site system, or K_a for a single-site interaction. This method has been used to screen and compare the binding of several site-selective probes and

sulfonylurea drugs on microcolumns containing entrapped samples of HSA or glycated HSA.⁹⁰ Zonal elution data with detection based on mass spectrometry has been combined with binding capacities obtained by frontal analysis on a packed capillary containing cyclin G-associated kinase for drug discovery; the results were then used to estimate and rank the affinity of the kinase for a series of drug fragments.⁹³ A similar method was used to rank the binding constants for various drug fragments with the chaperone protein HSP90 (see Figure 1.4)⁷⁴ and for various carbohydrates in their binding to hen egg-white lysozyme.²⁴ It is also possible to use the ratio of the retention factor to the known amount of binding agent to provide an index that is related to nK_a' or K_a .⁹⁶ This technique has been used to compare the activities and properties for proteins attached within organic-based monoliths that were prepared under various polymerization conditions.⁶⁸

Competition and displacement studies using affinity microcolumns

Zonal elution and traditional HPAC or affinity columns have often been employed in studying the competition and displacement between drugs and other solutes during solute-protein interactions.^{20,27,40,42,105} In this type of experiment, a competing agent is placed at a fixed concentration in the mobile phase. A small pulse of a target or site-selective probe is then injected onto the column and allowed to interact with the immobilized binding agent, as illustrated earlier in Figure 1.3(a). As the target passes through the column, the competing agent may influence binding by the target to the affinity ligand through direct competition or allosteric effects. When these data are fit to the response that is predicted by various models, the types of interactions that are occurring between the target, competing agent and immobilized binding agent can be

Figure 1.4 Use of zonal elution and mass spectrometry with a 0.5 mm i.d. \times 10 cm packed capillary containing the *N*-terminal domain of the protein HSP90 to compare the relative retention of four drug fragments (four upper plots), using adenosine (bottom plot) as a reference. Adapted with permission from Ref. 74.



determined. This, in turn, can provide information on the number of interaction sites, the location of these sites (i.e., through the use of site-selective probes), and the binding strength at particular sites.^{20,97,103}

To illustrate this process, Equation 1.4 shows the response that would be expected between the retention factor for an injected solute and the concentration of a competing agent in the mobile phase if these two solutes have direct competition at a single type of site on an affinity column.^{20,27,40}

$$\frac{1}{k} = \frac{K_{a,IL}V_M[I]}{K_{a,AL}m_L} + \frac{V_M}{K_{a,AL}m_L} \quad (1.4)$$

In this equation, $K_{a,AL}$ and $K_{a,IL}$ are the association equilibrium constants for the interactions of the immobilized binding agent (or affinity ligand, L) with the target/analyte (A) and the competing agent (I) at their site of competition. This relationship predicts that a linear response with a positive slope should be obtained for a plot of $1/k$ versus $[I]$ if A and I have a single site of competition. This relationship, in turn, can be used to provide the value of $K_{a,IL}$ for I at its site of competition with A. If no competition is present between A and I, this type of plot will show only random variations in $1/k$ as $[I]$ is increased. If negative allosteric effects or multisite interactions are present, deviations from a linear response at low concentrations of I should be obtained. If positive allosteric effects are present, the value of $1/k$ should decrease as the concentration of I is increased.^{20,27}

Plots made according to Equation 1.4 have been used in many recent studies involving affinity microcolumns. An example of a plot from a study that used a

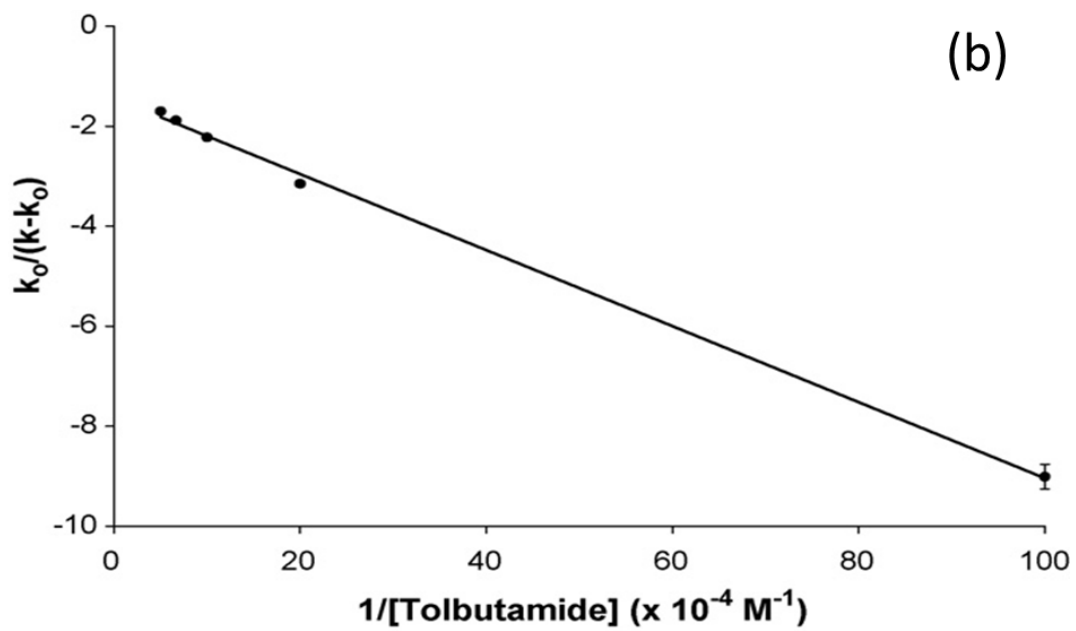
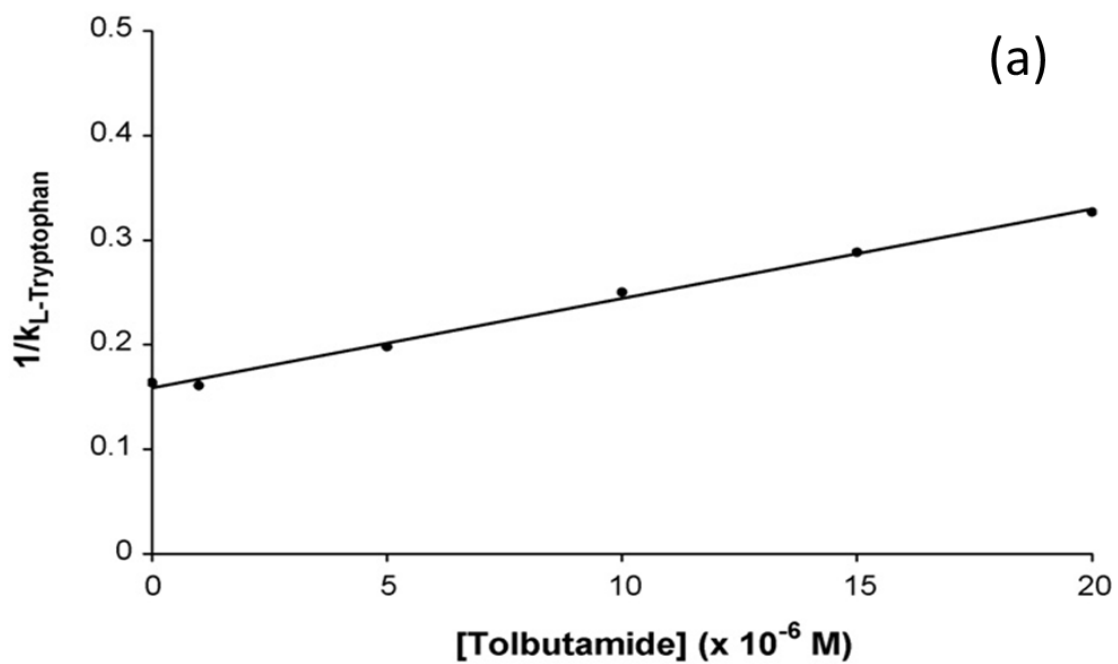
microcolumn containing HSA is shown in Figure 1.5(a).⁸⁰ In this case, a linear response was obtained in a plot of $1/k$ for L-tryptophan as the concentration of tolbutamide was varied in the mobile phase. This result indicated that tolbutamide had direct competition with L-tryptophan at Sudlow site II, the known binding site for the latter compound with HSA. The same approach has been employed with affinity microcolumns to investigate the competition of various probes with a number of other drugs during their interactions with the proteins HSA, glycated HSA, and α_1 -acid glycoprotein (AGP).^{79,80,83,100-105} Alternative forms of Equations 1.3-1.4 have been used with other systems.^{21,23,42,106} One example was the use of competitive zonal elution studies to examine the binding of L-fucose, as a mobile phase additive, to immobilized *Aleuria aurantia* lectin as injections of the oligosaccharide LNF III were made as a probe.²¹

Another type of graph that can be used to analyze both direct competition and allosteric effect using zonal elution data is given in Figure 1.5(b). In this case, a plot of $k_0/(k - k_0)$ versus $1/[I]$ is made according to Equation 1.5, where k_0 and k are the retention factors for injected target A in the absence and presence of the competing agent, respectively.¹⁰⁷

$$\frac{k_0}{k - k_0} = \frac{1}{\beta_{I \rightarrow A} - 1} \cdot \left(\frac{1}{K_{a,IL}[I]} + 1 \right) \quad (1.5)$$

This equation is based on a model where A and I may have direct competition at a single site or allosteric interactions through two different sites. If an allosteric effect is present, the ability of A to bind to L is influenced by the binding of I on L, which causes the association equilibrium constant for A to change from $K_{a,AL}$ to $K'_{a,AL}$. This change can also be described by the coupling constant $\beta_{I \rightarrow A}$, which is equal to the ratio $K'_{a,AL}/K_{a,AL}$.

Figure 1.5 Results of zonal elution competition studies on HSA microcolumns examining the change in retention of (a) L-tryptophan as a probe for Sudlow site II and (b) *R*-warfarin as a probe for Sudlow site I in the presence of tolbutamide as a competing agent. The solid lines show the best-fit responses that were obtained when fitting (a) Equation 1.4 or (b) Equation 1.5 to the data. These results were obtained under similar or identical conditions to those used in Figure 1.3(a). Reproduced with permission from Ref. 80.



A linear relationship obtained from this plot can be used to determine the association equilibrium constant for I with L ($K_{a,IL}$) and the coupling constant, $\beta_{I \rightarrow A}$. A value of $\beta_{I \rightarrow A}$ between 0 and 1 indicates that a negative allosteric effect is present between A and I, while a positive allosteric effect is indicated if $\beta_{I \rightarrow A}$ is larger than 1. A unique advantage of this method is that it can be used to look independently at both directions of an allosteric effect by changing which compound is used as A or I in the experiment.¹⁰⁷⁻¹⁰⁹

Plots made according to Equation 1.5 have been used in various studies of biomolecular interactions based on affinity microcolumns. Figure 1.5(b) is one example, which was used to determine how binding by *R*-warfarin to HSA was affected by tolbutamide as a competing agent. This plot was used to help differentiate between allosteric effects and multi-site binding during the interaction of these two solutes on an HSA microcolumn.⁸⁰ Equation 1.5 and similar plots have been utilized with microcolumns to study the interactions between various fatty acids and sulfonylureas with HSA or glycated HSA¹¹⁰ and allosteric effects that may occur on AGP as it binds to *S*-propranolol and warfarin.⁸³

Experiments based on competition studies and zonal elution can further be used to determine the location and structure of binding regions on proteins or other biomolecules. This is done by using an injected probe compound that is known to bind to a specific site on the protein or affinity ligand, with the competing agent in the mobile phase being the compound for which possible interactions at this site are being examined.²⁰ Such an experiment is illustrated by the examples provided in Figure 1.5. With this technique it is possible to develop a model of both the number of binding regions a solute may have with a protein, or other type of affinity ligand, and the

association equilibrium constants for the solute at each of these sites. This technique has been used with microcolumns containing HSA or modified forms of this protein to study the interactions of drugs such as acetohexamide, tolbutamide, gliclazide, glibenclamide and imipramine at Sudlow sites I and II or the digitoxin site of this protein.^{80,100,103,104,105,111} The same method has been employed to look for common binding regions of drugs and drug enantiomers on microcolumns that contained AGP.⁸³

Ultrafast affinity extraction method

Ultrafast affinity extraction is one of the methods developed based on zonal elution and used for examining biomolecular interactions.^{37,69,71,73,50,51} This approach examines the interaction of a target and a binding agent that is in solution but uses an affinity microcolumn to probe the non-bound, or free, fraction of the target that remains. In this technique, the target is injected in the presence or absence of the soluble binding agent onto a microcolumn that contains an affinity ligand that can selectively retain the target in its free form. This affinity ligand may be a specific agent, such as an antibody for a given target.^{37,69} Alternatively, the affinity ligand may be a more general binding agent, such as a serum transport protein like HSA for the retention of various drugs.^{50,51,71,73} If the flow rate and column conditions are selected correctly, the residence time for the sample in the column can be made small enough that no significant dissociation will occur of the target from the soluble binding agent as the sample passes through the column. For instance, affinity microcolumns have been used to produce sample residence times down to the low-to-mid millisecond range for this method.^{50,70,73}

This type of study is carried out by using the general scheme shown in Figure 1.6, in which an affinity microcolumn containing HSA is used to separate the free and protein-bound fractions of drug or small target in a sample.⁵⁰ In this example, the protein-bound fraction of the target and the protein in the sample will elute first in the non-retained fraction. This is followed later by elution of the retained free fraction of the target, which can then be determined by comparing the measuring retained peaks for the target in the presence or absence of the soluble binding agent. This information, in turn, can be used to determine the association equilibrium constant for the interaction of the target with the binding agent in the sample if the binding agent's total concentration is also known. For instance, Equations 1.6-1.7 describe the relationship between the observed free fraction (f) and the association equilibrium constant (K_a) for a target (A) and soluble binding agent (P) that have a single-site interaction.

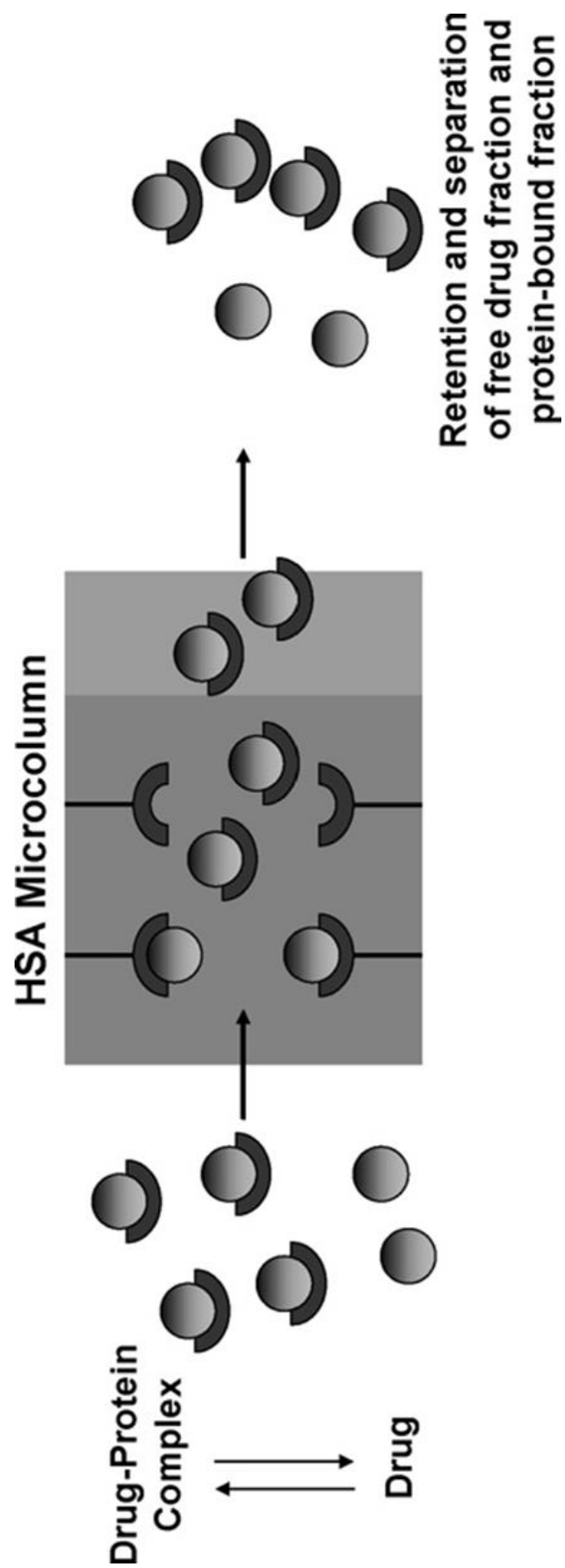
$$f = \frac{C_A - [A-P]}{C_A} \quad (1.6)$$

$$K_a = \frac{[A-P]}{(C_A - [A-P])(C_P - [A-P])} \quad (1.7)$$

In these equations, C_A is the total concentration of the target in the original sample, C_P is the total concentration of soluble binding agent, and $[A-P]$ is the concentration of the target-binding agent complex in the original sample.^{50,70}

One advantage of free fraction analysis is its ability for rapid analysis. This is partly due to the fact that sample residence times in the range of only a few hundred milliseconds or less are used to minimize the possibility that the target may dissociate from soluble binding agent during the analysis.^{50,70,73} It has been shown that the results

Figure 1.6 General scheme for the use of ultrafast affinity extraction with an HSA microcolumn to separate the free and bound fractions of a drug or solute in an injected sample. Reproduced with permission from Ref. 50.



obtained by this technique are comparable to those found with the reference methods such as ultrafiltration and equilibrium dialysis, among others.^{27,50,70} Furthermore, because this method directly examines the interactions between a target and a soluble binding agent, it is not subject to the immobilization effects that can occur with other affinity methods if improper conditions are used to couple the binding agent to the support.^{37,50,51, 69,71,73}

Several recent studies have used ultrafast affinity extraction to examine biomolecular interactions. For instance, this method has been used with immobilized antibodies and fluorescence detection to measure the free drug fraction in mixtures of warfarin and HSA.⁷³ This technique has also been combined with a displacement immunoassay to measure the free fraction of thyroxine and phenytoin in clinical samples by using chemiluminescence or near-infrared fluorescence detection.^{51,71} Use of this scheme to estimate association equilibrium constants has been shown with HSA and drugs such as *R*- or *S*-warfarin, *S*-ibuprofen and imipramine to give good agreement with the values obtained by other methods.⁵⁰

Other applications of zonal elution with affinity microcolumns

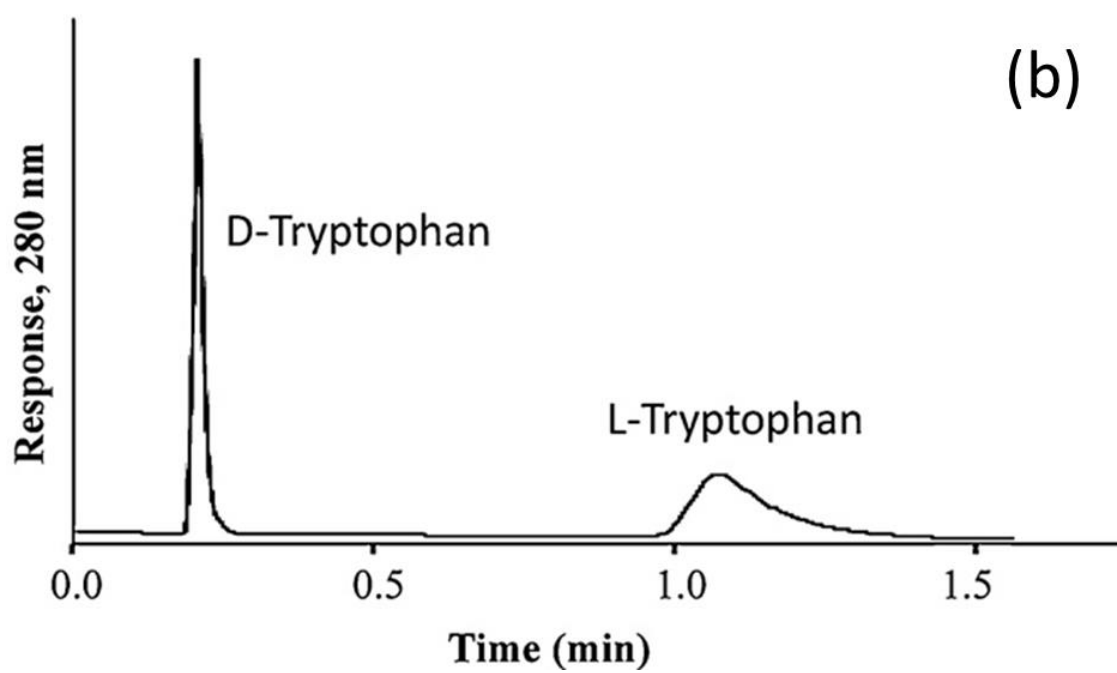
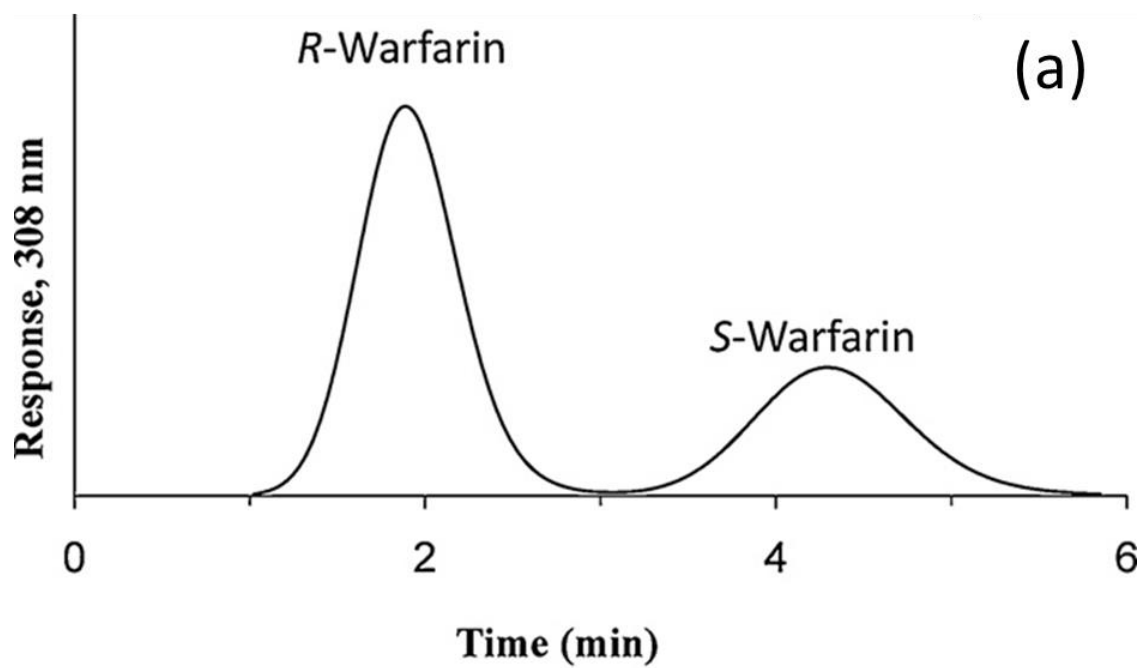
Another application of zonal elution is its use in examining the effects of various conditions on binding of the target with the affinity ligand. Conditions that can be altered during such studies include the temperature, pH, ionic strength and content of the mobile phase.^{10,14,20,81,113,115} For instance, varying the polarity of the mobile phase can be used to alter non-polar interactions between a target and a protein, and/or change the

conformation of the protein or the target. This is a common tactic used with chiral stationary phases based on proteins to alter their retention and stereoselectivity.^{70, 113, 114,116} Some examples are provided in Figure 1.7, in which an organic modifier was used to increase the speed of chiral separations for *R/S*-warfarin and *D/L*-tryptophan on a 4.6 mm i.d. \times 10 mm microcolumn that contained HSA immobilized to an organic monolith.⁶⁸

It is also possible to use zonal elution to examine the effects of changes in the structure of a target on its interactions with a given binding agent. This general approach can involve creating a quantitative structure-retention relationship (QSRR), in which the retention factors for a set of structurally-related molecules are measured on an affinity column under otherwise similar temperature and mobile phase conditions. These data are then compared to various factors that describe the structural components of the applied targets to see which of these factors most affected the retention.^{47,117-120} This technique has been used with traditional HPAC columns to investigate a number of questions: the skin permeation of several organic molecules through the use of a column containing immobilized keratin;¹¹⁷ the binding of HSA to benzodiazepine;¹¹⁸⁻¹²⁰ and the interactions of AGP with antihistamines, beta-adrenolytic drugs, and other agents.¹²¹⁻¹²⁷ In work with affinity microcolumns, the same general method has been used to compare the binding of various sulfonylurea drugs at both Sudlow sites I and II of HSA.¹²⁸

A related approach is to use affinity microcolumns to see how biomolecular interactions change as variations are made in the structure of the immobilized binding agent.¹²⁹⁻¹³¹ This tactic has been used to see how the non-enzymatic glycation of HSA, as occurs during diabetes,^{99,132} may alter the binding of this protein to various drugs and

Figure 1.7 Chiral separations for (a) *R*- and *S*-warfarin and (b) D- and L-tryptophan on a 4.6 mm i.d. \times 10 mm microcolumn containing HSA immobilized to a monolith based on a co-polymer of glycidyl methacrylate and ethylene glycol dimethacrylate. The mobile phase was pH 7.4, 0.067 M phosphate buffer that contained 0.5% 1-propanol and the flow rate was (a) 2.0 mL/min or (b) 3.0 mL/min. Reproduced with permission from Ref. 68.



solutes. These studies have used *R*-warfarin, L-tryptophan and digitoxin as probes (i.e., for Sudlow sites I and II and the digitoxin site of HSA, respectively), along with samples of glycated HSA that had various known levels of modification. The results for *in vitro* glycated samples indicated that changes in the affinities for sulfonylurea drugs and L-tryptophan did occur as the level of glycation for HSA was increased and that these changes differed between solutes and the binding site that was examined.^{105,80,100,103} Similar effects were seen in affinity microcolumns that contained *in vivo* glycated HSA that was obtained from several patients with diabetes.¹⁰⁴

Affinity microcolumns and zonal elution have also been used in the high-throughput screening of compound fragment mixtures based on WAC and mass spectrometry (WAC-MS). This method has been utilized to screen the binding of drugs to albumin¹³³ and binding of compound fragments to protease^{22,134} or kinase targets.⁹³ As an example, one recent study showed that 111 fragments could be screened on capillary column containing the protein HSP90, as illustrated earlier in Figure 1.4. The results of WAC were found to show good agreement with data obtained by NMR, SPR, and isothermal titration calorimetry, as well as crystallographic data.⁷⁴

Zonal elution has also been applied for the study of biomolecular interactions and the kinetic process involved in these interactions. These techniques include peak decay analysis, split-peak analysis, band-broadening measurements and peak fitting methods. The principles behind each of these methods will be described in Chapter 2. The advantages and possible limitations of these methods will be discussed in that chapter, and various examples will be provided to illustrate the use of these techniques with affinity chromatography.

Frontal Analysis and Affinity Microcolumns

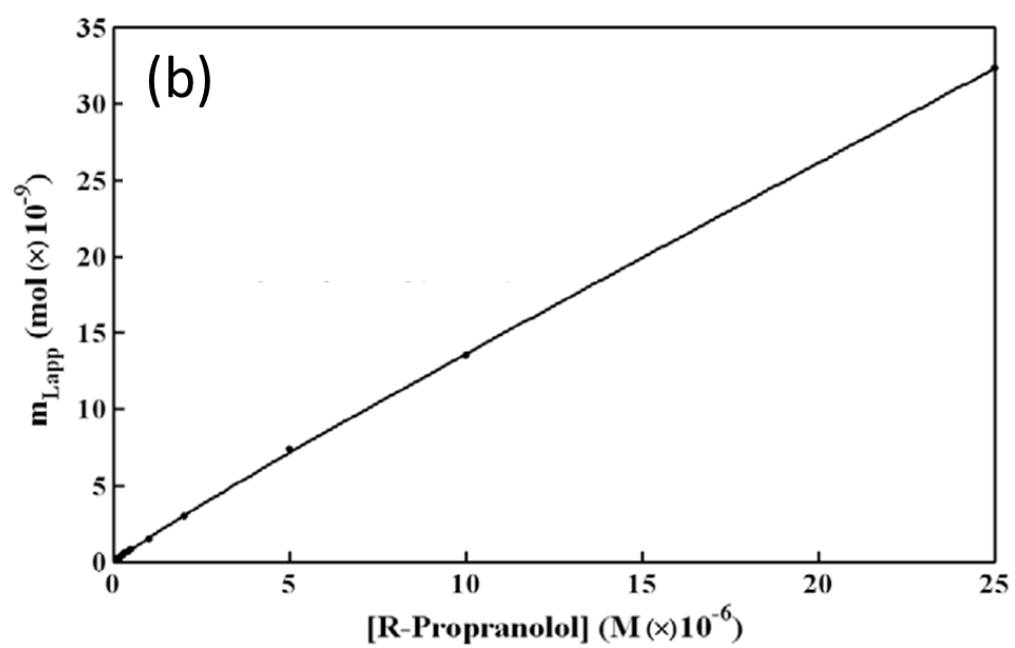
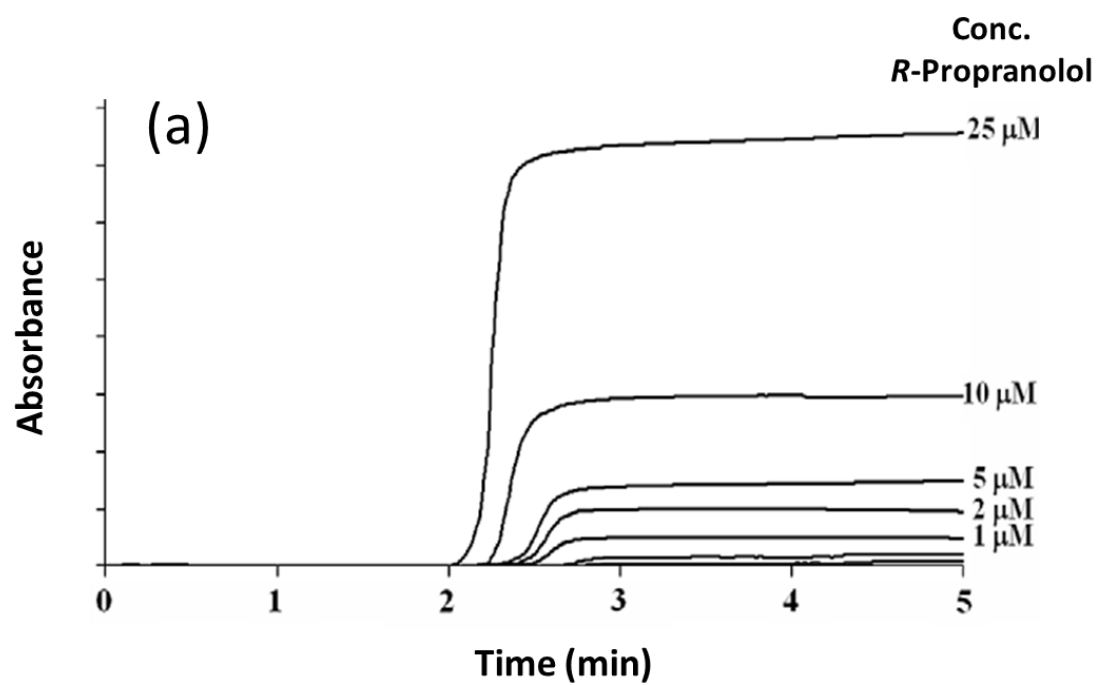
Principles of frontal analysis

Frontal analysis, or frontal affinity chromatography (FAC), is another common technique that is used in HPAC and affinity chromatography to study biomolecular interactions. In this method, a target solution is continuously applied to a column while the amount of target that elutes from the end of the column is monitored.^{27,79,135} As the target binds to the immobilized affinity ligand, the column begins to become saturated and the amount of the target that elutes from the column increases with time or with the volume of applied target.²⁰ The result is the formation of a breakthrough curve, as is illustrated in Figure 1.8(a) for *R*-propranolol that was applied to an affinity microcolumn containing HDL as the binding agent.⁸⁷

Frontal analysis was first used with traditional affinity columns in the mid-to-late 1970s.¹³⁶⁻¹³⁸ In the early 1990s this technique was used with HPAC to study drug-protein binding.¹³⁹ Over the last 10-15 years, this method has been utilized with various types of affinity microcolumns and capillary columns for binding studies; this includes the combination of this method with mass spectrometry, giving a method known as frontal affinity chromatography-mass spectrometry (or FAC-MS).^{54,58,60,87,140}

There are several advantages, and potential disadvantages, to using frontal analysis versus zonal elution to examine a biomolecular interaction. For instance, frontal analysis is easier to use in providing independent information on both the overall number of binding sites for an interaction and the equilibrium constants for these interactions.^{40,20}

Figure 1.8 (a) Typical chromatograms (i.e., breakthrough curves) obtained for a frontal analysis experiment, as obtained here for the application of various solutions R-propranolol to a 5 cm \times 2.1 mm i.d. column containing immobilized high-density lipoprotein (HDL). (b) Analysis of frontal analysis data obtained for R-propranolol on the HDL column by fitting to the results to a model based on a combination of a saturable binding site and a non-saturable interaction. Reproduced with permission from Ref. 87.



On the other hand, zonal elution competition experiments, as discussed in the previous section, are more convenient for identifying interaction sites and measuring binding constants specifically at these sites. Frontal analysis tends to require more solute than zonal elution, but column overloading effects are not a problem in frontal analysis because column saturation is actually a desirable feature for at least part of such an experiment.²⁰ In addition, the higher amounts of a target that are typically used in frontal analysis can make it easier to detect an interaction with this method than when using zonal elution.^{20, 54,58}

Estimating binding strength and number of sites using affinity microcolumns

An important application of frontal analysis is obtaining information on both the overall number of interaction sites an applied target has with an immobilized affinity ligand and the equilibrium constants for these interactions. Data can be obtained for this purpose by applying to the affinity column a wide range of target concentrations, as demonstrated earlier in Figure 1.8(a). The mean position of the breakthrough curve is then measured at each applied concentration of the target, and the resulting data are fit to various binding models, as illustrated in Figure 1.8(b).⁸⁷ For instance, either Equation 1.8 or 1.9 can be used to describe a system in which a single-site interaction is occurring between the target and the immobilized binding agent.²⁰

$$m_{L,app} = \frac{m_L K_a [A]}{1 + K_a [A]} \quad (1.8)$$

$$\frac{1}{m_{L,app}} = \frac{1}{K_a m_L [A]} + \frac{1}{m_L} \quad (1.9)$$

In these equations, $m_{L,app}$ is the apparent moles of target that is required to reach the mean position of the breakthrough curve at a given concentration of the applied target or analyte ($[A]$). The term K_a is the association equilibrium constant for this process, and m_L is the total moles of active binding sites that are involved in this interaction. By using a non-linear fit of $m_{L,app}$ versus $[A]$ to Equation 1.8, or a linear fit of $1/m_{L,app}$ versus $1/[A]$ to Equation 1.9, the values of both K_a and m_L can be obtained for this system. If multiple types of binding sites or interactions are present, alternative binding models and equations can also be fit to the data.^{20,141,142}

An example of this type of analysis when using an affinity microcolumn is provided in Figure 1.8(b). This example shows the use of a model based on both a saturable binding site and a non-saturable interaction to describe the interactions of *R*-propranolol with HDL.⁸⁷ This approach has been employed with small columns in HPAC and with other drugs and serum agents, such as the binding of *S*-propranolol and verapamil with HDL,⁸⁷ the interactions of *R*- and *S*-propranolol with LDL,⁸⁸ the binding of drugs with AGP,^{83,143-147} and the interactions of various drugs and solutes with HSA or modified HSA.^{104,105,78,80,100,103,111} Frontal analysis was used to determine the binding capacity of adenosine on a packed capillary containing cyclin G-associated kinase⁹³ and FAC-MS has been used with open-tubular capillaries containing peroxisome proliferator-activated receptors to compare and rank the binding of the agents to various ureidofibrate-like dual agonists.⁴⁸ Capillary monolith columns containing lectins or enzymes have been employed with FAC-MS to examine the equilibrium constants of applied targets with these affinity ligands.^{52,54, 56} FAC-MS has also been coupled with capillary columns for the high throughput screening of enzyme inhibitors,

oligosaccharides, and other targets for immobilized binding agents.¹⁴⁰

The effect of column size on the results of frontal analysis experiments has been recently examined for systems with low-to-moderate affinity interactions.⁷² This work used HSA as the immobilized binding agent and warfarin as a model target (i.e., a drug with single-site binding to HSA and a well-characterized affinity for this site). Table 1.1 shows the results obtained for 2.1 mm i.d. microcolumns with lengths ranging from 2 cm down to only 1 mm and packed with silica particles. Each of these columns gave a good fit for their frontal analysis data to a single-site model, and the measured binding capacity decreased in proportion to the total column volume. It was also found that all of these columns gave association equilibrium values that were in good agreement with literature values; however, the results obtained for the short columns did have less precision than those obtained for the longer columns. The main benefit of using the shorter columns was the much smaller amount of immobilized binding agent that they required and their shorter residence times. These features made these affinity microcolumns appealing for future use in the high-throughput screening of drug candidates and in rapid studies of drug-protein binding.⁷²

Competition and displacement studies using affinity microcolumns

Frontal analysis, and especially FAC-MS, has also been used to examine the competition between potential targets and immobilized binding agents on affinity microcolumns.^{48,49,27} In this type of study, a competing agent is added with the target in the mobile phase. The resulting chromatograms are then analyzed by measuring the

change in breakthrough time or volume of the target as a function of the competing agent's concentration (see Figure 1.9).⁴⁹ Direct competition or negative allosteric effects between the target and competing agent can be detected when the breakthrough time decreases with an increase in the competing agent's concentration. Alternatively, positive allosteric effects can lead to a larger breakthrough time for the target as the concentration of the competing agent is increased.²⁷

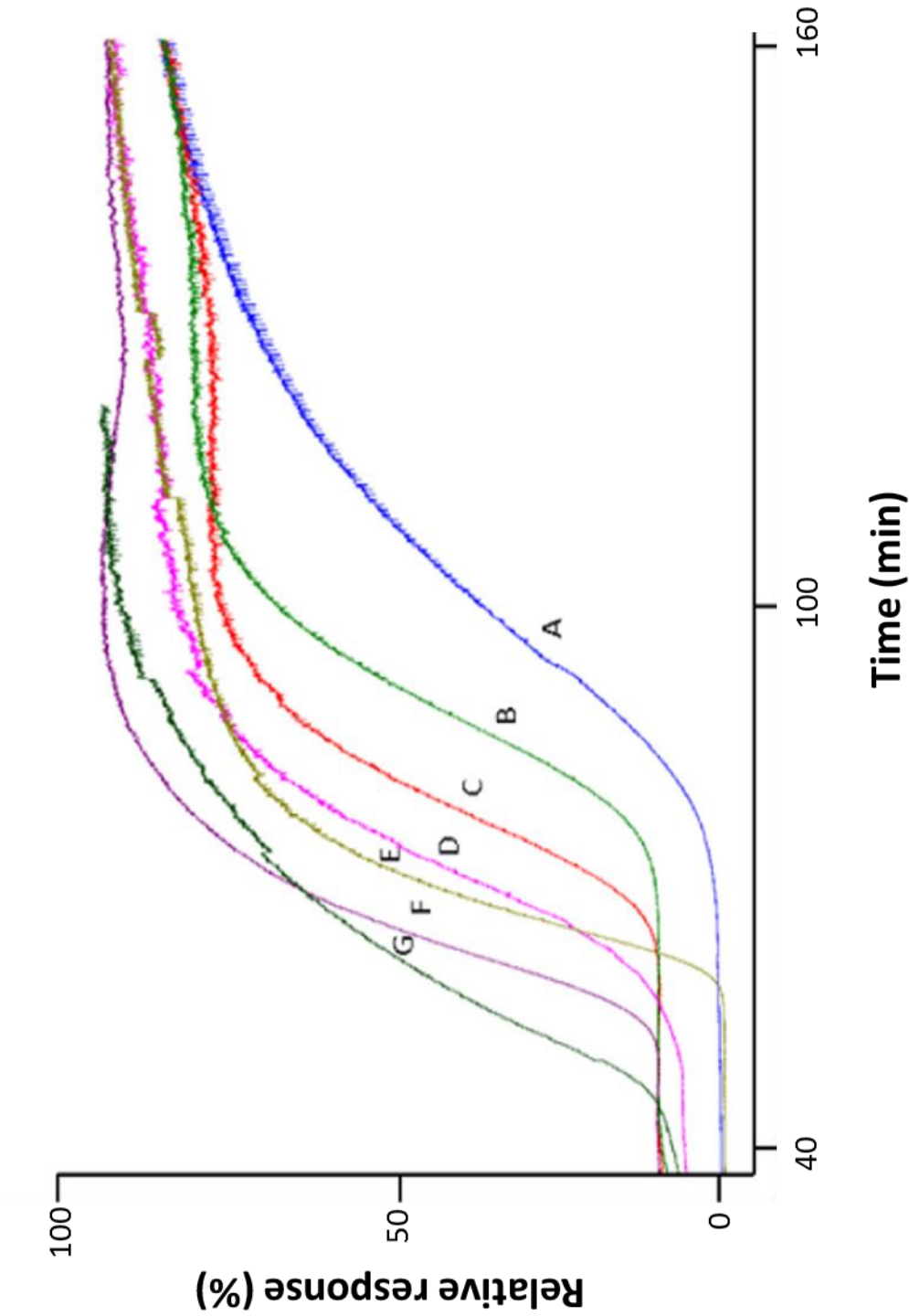
It is possible to obtain a qualitative ranking of the strength of displacing agents based on chromatograms like those in Figure 1.9, but a quantitative analysis of such data is possible as well. For instance, Equation 1.10 has been used to describe the interactions between a competing agent (I) and the target during such an experiment.^{48,49,148-150}

$$V_R - V_{\min} = P/(K_{d,IL} + [I]) \quad (1.10)$$

In this expression, $K_{d,IL}$ is the dissociation equilibrium constant of the competing agent with the immobilized affinity ligand, $[I]$ is the concentration of the competing agent, V_R is the breakthrough volume of the target, and V_{\min} is the breakthrough volume of the target when the interaction being examined is completely suppressed (i.e., as can be determined by running the target with a high concentration of the competing agent). The term P is the product of the number of active binding sites and the term $K_{d,IL}/K_{d,AL}$, where $K_{d,AL}$ is the dissociation equilibrium constant for the target (or analyte) with the immobilized ligand.

Several reports have used Equation 1.10 or equivalent relationships in displacement studies based on FAC-MS and affinity microcolumns.^{48,49} The example in Figure 1.9 utilized an open-tubular capillary that contained the histone deacetylase

Figure 1.9 Example of a displacement experiment using frontal analysis and with detection based on mass spectrometry. These chromatograms show the effects of adding (B) vitexin, (C) naringenin, (D) apigenin, (E) quercetin, (F) kaempferol, or (G) luteolin to a solution containing (A) quercetin as the target and applied to a 30 cm × 100 μm i.d. open-tubular capillary column containing an immobilized form of the histone decarboxylase SIRT6. Adapted with permission from Ref. 49.



SIRT6. This column was used with FAC-MS to estimate the dissociation equilibrium constants for several structurally-related flavonoids based on their ability to displace quercetin, a known inhibitor for SIRT6.⁴⁹ Open-tubular capillaries containing the ligand binding domains of peroxisome proliferator-activated receptors were employed in a similar manner to examine the interactions and rank the affinities of ureidofibrate-like dual agonists with these columns.⁴⁸

Other applications of frontal analysis with affinity microcolumns

As mentioned earlier, changes in factors such as the temperature or mobile phase can alter a biomolecular interaction. Like zonal elution, frontal analysis can be employed to see how such changes may alter an interaction. One advantage of using frontal analysis for this purpose is it can be used to independently examine how both affinity and moles of binding sites are affected by a change in the temperature or reaction conditions.^{20,116} As an example, the effect of temperature on the binding for *R*- and *S*-propranolol with HDL and LDL has been studied using affinity microcolumns.⁸⁷⁻⁸⁹ The results showed that a change in temperature had little effect on either the association equilibrium constants or the binding capacities between these drugs and binding agents.
87-89

Frontal analysis has also been used to examine the binding of solutes to modified proteins. This technique has been utilized to compare the binding of several solutes to HSA that has been modified to various extents by glycation.^{104,105,100,103} Both the affinities and binding capacities for targets such as warfarin, L-tryptophan and

sulfonylurea drugs were investigated in going from normal HSA to *in vitro* or *in vivo* samples of glycated HSA.^{100,103,104, 105} Warfarin and L-tryptophan were found to bind to both sets of proteins through a single-site interaction,^{92,101} but the sulfonylurea drugs interacted through a two-site model that involved a set of high and low affinity sites.¹⁰⁰ The results indicated that the glycation of HSA could affect the affinity of this protein for L-tryptophan and some of the sulfonylurea drugs, but no appreciable change was noted for warfarin under modification conditions similar to those seen in diabetes.^{101,104} Affinity microcolumns and frontal analysis have been used in a growing number of reports for the high-throughput screening of compound mixtures with regards to their binding to biological ligands. This research has used FAC-MS to rank and measure the binding of several applied compounds in a single experiment, as demonstrated with columns that have contained enzymes, antibodies, lectins or human estrogen receptor β .¹⁴⁰ FAC-MS and such columns have been employed to screen the binding of enzyme inhibitors, oligosaccharides and peptide libraries.^{57,140,149,150} For instance, an open-tubular capillary containing an immobilized nuclear receptor was used in FAC-MS to determine the relative affinities for a series of chiral fibrates with this receptor.⁴⁷

Another application of frontal analysis is its use in kinetic studies of biomolecular interactions. This can be performed with frontal analysis by using peak fitting methods. As was mentioned earlier for zonal elution, more details about the principle of this set of kinetic methods will be given in Chapter 2. The advantages and possible limitations of these methods will be considered. Applications of these methods will also be discussed in that chapter.

Overall Goal and Summary of Work

The overall objective of this work is to develop new HPAC methods and affinity microcolumns that could be used to examine the biological interactions and providing information on thermodynamic and kinetic of these binding systems. Chapter 2 will review the analytical methods that have been used for kinetic studies of biological interactions. Chapter 3 will develop a method based on ultrafast affinity extraction and HPAC method to examine both the dissociation rate constants and equilibrium constants for drug-protein interactions in solution in a single experiment. The results will be used to demonstrate that ultrafast affinity extraction can be used as a rapid approach to provide information on both the kinetics and thermodynamics of a drug-protein interaction in solution.

Chapter 4 will develop a multi-dimensional system based on ultrafast affinity extraction and chiral separations to measure the free fractions of drug enantiomers in samples that also contained a binding protein or serum. The binding of each enantiomer with serum transport proteins will also be studied by this method. *R/S*-Warfarin and the HSA will be used as drug and protein models to test this approach. The association equilibrium constants and free fractions of drug enantiomers that are determined by this method will be compared with the results estimated by reference methods (i.e. ultrafiltration) or with the literature values. The work will describe the possibility to automate and complete both the ultrafast extraction and the chiral separation through using a single system.

Chapter 5 will show the use of ultrafast affinity extraction and a multi-

dimensional affinity system to examine the effect of protein modification on drug binding in the sample prepared at therapeutic levels. The model analytes in this chapter will be sulfonylurea drugs, normal HSA or HSA glycosylated at various levels, as are produced during diabetes. The results will indicate how HSA glycation can alter the global affinity constants and free fractions of sulfonylurea drugs at typical therapeutic levels and how the size of this change varies with the level of HSA glycation.

In Chapter 6, a similar system will be used to measure the free fraction of drugs in human serum and to examine the interactions of these drugs with HSA. These studies will be conducted at typical therapeutic drug concentrations that will be prepared in control human serum. Various drugs will be examined in this work including quinidine, diazepam, glimepiride, tolbutamide and acetohexamide. The dissociation rate constant and association equilibrium constants for each drug with HSA in human serum will be determined as well. The results obtained in Chapter 6 should provide important information on the use of ultrafast affinity extraction for examining free drug fractions and drug-protein interaction directly in biological samples.

In Chapter 7, ultrafast affinity extraction method will be used to study the interaction between hormone and protein. The binding of testosterone with human serum albumin and sex hormone binding globulin (SHBG) will be used as models. Both the association equilibrium constants and dissociation rate constants for these interactions will be determined. The free fraction of testosterone in the sample containing HSA or SHBG at clinically-relevant concentrations will also be studied by using a multi-dimensional affinity system. The results of this study should provide a better understanding about the interactions of testosterone with proteins such as HSA and

SHBG, and important information that can be used to extend this approach to alternative hormone-protein systems or other solutes and binding agents.

Chapter 8 will develop and examine a hybrid immobilization method for increasing the binding capacity and activity of protein-based affinity columns. This will be accomplished by combining protein cross-linking/modification and the covalent immobilization. HSA will be used as the model protein for this study. A homobifunctional maleimide, bismaleimido-hexane (BMH), will be used to modify and/or cross-link HSA through the single free sulfhydryl group that is present on this protein. Various studies will be performed to examine the protein content and relative activity of HSA in this affinity column, and the use of this column in drug-protein binding studies and free drug fraction measurement. This method could be extended to other proteins or alternative applications that may require protein-based affinity columns with enhanced binding capacities and activities.

References

1. J.E. Schiel, R. Mallik, S. Soman, K.S. Joseph, D.S. Hage, J. Sep. Sci. 29 (2006) 719-737.
2. I.M. Chaiken, Analytical Affinity Chromatography, CRC Press, Boca Raton, 1987.
3. D.S. Hage, in: D. Corradini, E. Katz, R. Eksteen, P. Shoenmakers, N. Miller (Eds.), Handbook of HPLC, Marcel Dekker, New York, 1998, pp. 483-498.
4. D.S. Hage, P.F. Ruhn, in: D.S. Hage (Ed.), Handbook of Affinity Chromatography, CRC Press, Boca Raton, FL, 2006, pp. 3-13.
5. R.R. Walters, Anal. Chem. 57 (1985) 1099A-1114A.
6. P. Cuatrecasas, M. Wilchek, C.B. Anfinsen, Proc. Natl. Acad. Sci. U.S.A. 61 (1968) 636-643.
7. J. Turkova, Affinity Chromatography, Elsevier, Amsterdam, 1978.
8. D.S. Hage (Ed.), Handbook of Affinity Chromatography, 2nd ed., CRC Press, Boca Raton, FL, 2006.
9. L. Leickt, M. Bergström, D. Zopf, S. Ohlson, Anal. Biochem. 253 (1997) 135-136.
10. S. Ohlson, M. Bergström, P. Pålsson, A. Lundblad, J. Chromatogr. A 758 (1997) 199-208.

11. M. Bergström, A. Lundblad, P. Pålsson, S. Ohlson, *J. Mol. Recognit.* 11 (1998) 110-113.
12. J. Dakour, A. Lundblad, D. Zopf, *Anal. Biochem.* 161 (1987) 140-143.
13. O. Hofstetter, H. Lindstrom, H. Hofstetter, *Anal. Chem.* 74 (2002) 2119-2125.
14. E.J. Franco, H. Hofstetter, O. Hofstetter, *J. Pharm. Biomed. Anal.* 46 (2008) 907-913.
15. J.E. Schiel, D.S. Hage, *J. Sep. Sci.* 32 (2009) 1507–1522.
16. D.S. Hage, T.M. Phillips, in: D.S. Hage (Ed.), *Handbook of Affinity Chromatography*, 2nd ed., CRC Press, Boca Raton, FL, 2006, pp. 127-172.
17. A.C. Moser, D.S. Hage, *Bioanalysis* 2 (2010) 769-790.
18. S. Ohlson, A. Lundblad, D. Zopf, *Anal. Biochem.* 169 (1988) 204-208.
19. D. Zopf, S. Ohlson, *Nature* 346 (1990) 87-88.
20. D.S. Hage, J. Chen, in: D.S. Hage (Ed.), *Handbook of Affinity Chromatography*, CRC Press, Boca Raton, FL, 2006, pp. 595-628.
21. M. Bergström, E. Åström, P. Pålsson, S. Ohlson, *J. Chromatogr. B* 885-886 (2012) 66-72.
22. M.D. Duong-Thi, E. Meiby, M. Bergström, T. Fex, R. Isaksson, S. Ohlson, *Anal. Biochem.* 414 (2011) 138-146.

23. H.A. Engström, R. Johansson, P. Koch-Schmidt, K. Gregorius, S. Ohlson, M. Bergström, *Biomed. Chromatogr.* 22 (2008) 272-277.
24. J. Landström, M. Bergström, C. Hamark, S. Ohlson, G. Widmalm, *Org. Biomol. Chem.* 10 (2012) 3019-3032.
25. A.J. Muller, P.W. Carr, *J. Chromatogr.* 294 (1984) 235-246.
26. S. Patel, I.W. Wainer, W.J. Lough, in: D.S. Hage (Ed.), *Handbook of Affinity Chromatography*, CRC Press, Boca Raton, FL, pp. 663-683.
27. D.S. Hage, *J. Chromatogr. B* 768 (2002) 3-30.
28. D.S. Hage, J.A. Anguizola, A.J. Jackson, R.M. Matsuda, E. Papastavros, E. Pfaunmiller, Z. Tong, M.J. Yoo, X. Zheng, *Anal. Methods* 3 (2011) 1449–1460.
29. D.S. Hage, J.A. Anguizola, C. Bi, R. Li, R. Matsuda, E. Papastavros, E. Pfaunmiller, J. Vargas, X. Zheng, *J. Pharm. Biomed. Anal.* 69 (2012) 93-105.
30. P.E. Gustavsson, P.O. Larsson, in: D.S. Hage (Ed.), *Handbook of Affinity Chromatography*, 2nd ed., CRC Press, Boca Raton, FL, 2006, pp. 15-33.
31. P.O. Larsson, *Methods Enzymol.* 104 (1987) 212-223.
32. M.J. Yoo, D.S. Hage, in: P. Wang (Ed.), *Monolithic Chromatography and its Modern Applications*, ILM Publications, UK, 2010, pp. 3-25.
33. E.L. Pfaunmiller, M.L. Paulemond, C.M. Dupper, D.S. Hage, *Anal. Bioanal. Chem.* 405 (2013) 2133-2145.

34. R. Mallik, T. Jiang, D.S. Hage, *Anal. Chem.* 76 (2004) 7013-7022.
35. M. Schuster, E. Wasserbauer, A. Neubauer, A. Jungbauer, *Bioseparation* 9 (2000) 259-268.
36. E.C. Peters, F. Svec, J.M.J. Frechet, *Adv. Materials* 11 (1999) 1169-1181.
37. T. Jiang, R. Mallik, D.S. Hage, *Anal. Chem.* 77 (2005) 2362-2372.
38. A. Jungbauer, R. Hahn, *J. Sep. Sci.* 27 (2004) 767-778.
39. D. Josic, A. Buchacher, A. Jungbauer, *J. Chromatogr. B* 752 (2001) 191-205.
40. D.S. Hage, S.A. Tweed, *J. Chromatogr. B* 699 (1997) 499-525.
41. D.J. Winzor, in: D.S. Hage (Ed.), *Handbook of Affinity Chromatography*, CRC Press, Boca Raton, FL, 2006, pp. 629-662.
42. D.J. Winzor, *J. Chromatogr. A* 1037 (2004) 351-367.
43. M.V. Novotny, D. Ishii, *Microcolumn Separations*, Elsevier, New York, NY, 1985.
44. R.P.W. Scott, P. Kucera, *J. Chromatogr.* 125 (1976) 251-263.
45. D. Ishii, K. Asai, K. Hibi, T. Jonokuchi, M. Nagaya, *J. Chromatogr.* 144 (1977) 157-168.
46. T. Tsuda, M. Novotny, *Anal. Chem.* 50 (1978) 271-275.
47. E. Calleri, G. Fracchiolla, R. Montanari, G. Pochetti, A. Lavecchia, F. Loiodice, A. Laghezza, L. Piemontese, G. Massolini, C. Temporini, *J. Chromatogr. A* 1232

(2012) 84-92.

48. C. Temporini, G. Pochetti, G. Fracchiolla, L. Piemontese, R. Montanari, R. Moaddel, A. Laghezza, F. Altieri, L. Cervoni, D. Ubiali, E. Prada, F. Loiodice, G. Massolini, E. Calleri, *J. Chromatogr. A* 1284 (2013) 36-43.
49. N. Singh, S. Ravichandran, D.D. Norton, S.D. Fugmann, R. Moaddel, *Anal. Biochem.* 436 (2013) 78-83.
50. R. Mallik, M.J. Yoo, C.J. Briscoe, D.S. Hage, *J. Chromatogr. A* 1217 (2010) 2796-2803.
51. C.M. Ohnmacht, J.E. Schiel, D.S. Hage, *Anal. Chem.* 78 (2006) 7547-7556.
52. K.K.R. Tetala, B. Chen, G.M. Visser, T.A. van Beek, *J. Sep. Sci.* 30 (2007) 2828-2835.
53. M.M. Palcic, B. Zhang, X. Qian, B. Rempel, O. Hindsgaul, *Methods Enzymol.* 362 (2003) 369-372.
54. P. Kovarik, R.J. Hodgson, T. Covey, M.A. Brook, J.D. Brennan, *Anal. Chem.* 77 (2005) 3340-3350.
55. E.S. Ng, F. Yang, A. Kameyama, M.M. Palcic, O. Hindsgaul, D.C. Schriemer, *Anal. Chem.* 77 (2005) 6125-6133.
56. R.J. Hodgson, Y. Chen, Z. Zhang, D. Tleugabulova, H. Long, X. Zhao, M. Organ, M.A. Brook, J.D. Brennan, *Anal. Chem.* 76 (2004) 2780-2790.

57. B. Zhang, M.M. Palcic, D.S. Schriemer, G. Alarez-Manilla, M. Pierce, O. Hindsgaul, *Anal. Biochem.* 299 (2001) 173-182.
58. E.S. Ng, N.W. Chan, D.F. Lewis, O. Hindsgaul, D.S. Schriemer, *Nature Protocols* 2 (2007) 1907-1917.
59. A. Hendrickx, D. Mangelings, Y.V. Heyden, *J. AOAC Int.* 94 (2011) 667-702.
60. D.C. Schriemer, *Anal. Chem.* 76 (2005) 440A-448A.
61. D. Ishii, M. Goto, T. Takeuchi, *J. Pharm. Biomed. Anal.* 2 (1984) 223-231.
62. M.V. Novotny, *Methods Enzymol.* 270 (1996) 101-133.
63. M.V. Novotny, *J. Chromatogr. B* 689 (1997) 55-70.
64. E. Calleri, C. Temporini, G. Caccialanza, G. Massolini, *Chem. Med. Chem.* 4 (2009) 905-916.
65. D.S. Hage, R. R. Walters, H.W. Hethcote, *Anal. Chem.* 58 (1986) 274-279.
66. X. Mao, Y. Luo, Z. Dai, K. Wang, Y. Du, B. Lin, *Anal. Chem.* 76 (2004) 6941-6947.
67. J. Krenkova, F. Foret, *Electrophoresis* 25 (2004) 3550-3563.
68. E.L. Pfaunmiller, M. Hartmann, C.M. Dupper, S. Soman, D.S. Hage, *J. Chromatogr. A* 1269 (2012) 198-207.
69. W. Clarke, D.S. Hage, *Anal. Chem.* 73 (2001) 1366-1373.

70. X. Zheng, M.J. Yoo, D.S. Hage, *Analyst* 138 (2013) 6262-6265.
71. W. Clarke, J.E. Schiel, A. Moser, D.S. Hage, *Anal. Chem.* 77 (2005) 1859-1866.
72. M.J. Yoo, J.E. Schiel, D.S. Hage, *J. Chromatogr. B*, 878 (2010) 1707-1713.
73. W. Clarke, A.R. Chowdhuri, D.S. Hage, *Anal. Chem.* 73 (2001) 2157-2164.
74. E. Meiby, H. Simmonite, L. le Strat, B. Davis, N. Matassova, J.D. Moore, M. Mrosek, J. Murray, R.E. Hubbard, S. Ohlson, *Anal. Chem.* 85 (2013) 6756-6766.
75. B. Loun, D.S. Hage, *J. Chromatogr. B* 665 (1995) 303-314.
76. J. Yang, D.S. Hage, *J. Chromatogr. B* 766 (1997) 15-25.
77. B.M. Dunn, I.M. Chaiken, *Proc. Natl. Acad. Sci. USA* 71 (1974) 2382-2385.
78. H.S. Kim, I.W. Wainer, *J. Chromatogr. B* 870 (2008) 22-26.
79. D.S. Hage, J. Anguizola, O. Barnaby, A. Jackson, M.J. Yoo, E. Papastavros, E. Pfaunmiller, M. Sobansky, Z. Tong, *Curr. Drug Metab.* 12 (2011) 313-328.
80. K.S. Joseph, D.S. Hage, *J. Chromatogr. B* 878 (2010) 1590–1598.
81. D. Zopf, S. Ohlson, J. Dakour, W. Wang, A. Lundblad, *Methods Enzymol.* 179 (1989) 55-64.
82. V. Sjoulund, I. A. Kaltashov, *Anal. Chem.* 84 (2012) 4608–4612.
83. J.A. Anguizola, Ph.D. Dissertation, University of Nebraska, Lincoln, Nebraska, 2013.

84. J.E. Schiel, K.S. Joseph, D.S. Hage, in: N. Grinsberg, E. Grushka (Eds.), *Advances in Chromatography*, Taylor & Francis, New York, 2009, pp. 145-193.
85. N. Jonker, J. Kool, H. Irth, W.M.A. Niessen, *Anal. Bioanal. Chem.* 399 (2011) 2669-2681.
86. M.J. Yoo, D.S. Hage, *J. Sep. Sci.* 32 (2009) 2776-2785.
87. S. Chen, M.R. Sobansky, D.S. Hage, *Anal. Biochem.* 397 (2010) 107-114.
88. M.R. Sobansky, D.S. Hage, *Anal. Bioanal. Chem.* 403 (2012) 563-571.
89. M.R. Sobansky, D.S. Hage, in: L.V. Berhardt (Ed.), *Advances in Medicine and Biology*, Vol. 53, Nova Science Publishers, 2012, Chapter 9.
90. A.J. Jackson, J. Anguizola, E.L. Pfaunmiller, D.S. Hage, *Anal. Bioanal. Chem.*, 405 (2013) 5833-5841.
91. B. Loun, D.S. Hage, *Anal. Chem.* 68 (1996) 1218-1225.
92. K.S. Joseph, A.C. Moser, S. Basiaga, J.E. Schiel, D.S. Hage, *J. Chromatogr. A* 1216 (2009) 3492-3500.
93. E. Meiby, S. Knapp, J. M. Elkins, S. Ohlson, *Anal. Bioanal. Chem.* 404 (2012) 2417-2425.
94. T.A.G. Noctor, M.J. Diaz-Perez, I.W. Wainer, *J. Pharm. Sci.* 82 (1993) 675-676
95. F. Beaudry, M. Coutu, N.K. Brown, *Biomed. Chromatogr.* 13 (1999) 401-406.

96. H.S. Kim, Y.S. Kye, D.S. Hage, *J. Chromatogr. A* 1049 (2004) 51-61.
97. A. Sengupta, D.S. Hage, *Anal. Chem.* 71 (1999) 3821-3827.
98. Z. Zhivkova, V. Russeva, *J. Chromatogr. B* 707 (1998) 143-149.
99. L.C. Maillard, *C.R. Acad. Sci.* 154 (1912) 66-68.
100. K.S. Joseph, J. Anguizola, D.S. Hage, *J. Pharm. Biomed. Anal.* 54 (2011) 426–432.
101. K.S. Joseph, D.S. Hage, *J. Pharm. Biomed. Anal.* 53 (2010) 811-818.
102. R. Matsuda, J. Anguizola, K.S. Joseph, D.S. Hage, *Anal. Bioanal. Chem.* 401 (2011) 2811-2819.
103. K.S. Joseph, J. Anguizola, A.J. Jackson, D.S. Hage, *J. Chromatogr. B* 878 (2010) 2775-2781.
104. J. Anguizola, K.S. Joseph, O.S. Barnaby, R. Matsuda, G. Alvarado, W. Clarke, R.L. Cerny, D.S. Hage, *Anal. Chem.* 85 (2013) 4453-4460.
105. R. Matsuda, J. Anguizola, K.S. Joseph, D.S. Hage, *J. Chromatogr. A* 1265 (2012) 114-122.
106. H. Kakita, K. Nakamura, Y. Kato, *J. Chromatogr.* 543 (1991) 315-326.
107. J. Chen J, D.S. Hage, *Nature Biotechnol.* 22 (2004) 1445–1448.
108. J. Chen, D.S. Hage, *Anal. Chem.* 78 (2006) 2672–2683.

109. R. Mallik, M.J. Yoo, S. Chen, D.S. Hage, J. Chromatogr. B 876 (2008) 69 – 75.
110. S.B.G. Basiaga, Master's Thesis, University of Nebraska, Lincoln, Nebraska, 2009.
111. M.J. Yoo, Q.R. Smith, D.S. Hage, J. Chromatogr. B 877 (2009) 1149-1154.
112. J.E. Schiel, Z. Tong, C. Sakulthaew, D.S. Hage, Anal. Chem. 83 (2011) 9384-9390.
113. S. Allenmark, Chromatographic Enantioseparation: Methods and Applications, 2nd ed., Ellis Horwood, New York, 1991.
114. D.S. Hage, J. Chromatogr. A 906 (2001) 459-481.
115. H.S. Kim, D.S. Hage, J. Chromatogr. B 816 (2005) 57-66.
116. B. Loun, D.S. Hage, Anal. Chem. 66 (1994) 3814-3822.
117. M. Turowski, R. Kaliszan, J. Pharm. Biomed. Anal. 15 (1997) 1325-1333.
118. R. Kaliszan, A. Kaliszan, T.A.G. Noctor, W.P. Purcell, I.W. Wainer, J. Chromatogr. 609 (1992) 69-81.
119. R. Kaliszan, T.A.G. Noctor, I.W. Wainer, Mol. Pharmacol. 42 (1992) 512-517.
120. R. Kaliszan, T.A.G. Noctor, I.W. Wainer, Chromatographia 33 (1992) 546-550.
121. R. Kaliszan, Chemometr. Intell. Lab. Systems 24 (1994) 89-97.
122. A. Nasal, A. Radwanska, K. Osmialowsk, A. Bucinski, R. Kaliszan, G.E. Barker,

- P. Sun, R.A. Hartwick, *Biomed. Chromatogr.* 8 (1994) 125-129.
123. R. Kaliszan, A. Nasal, M. Turowski, *J. Chromatogr. A* 722 (1996) 25-32.
124. A. Karlsson, A. Aspegren, *J. Chromatogr. A* 866 (2000) 15-23.
125. R. Kaliszan, A. Nasal, M. Turowski, *Biomed. Chromatogr.* 707 (1995) 211-215.
126. I. Fitos, J. Visy, M. Simonyi, J. Hermansson, *J. Chromatogr. A* 609 (1992) 163-171.
127. K. Gyimesi-Forras, G. Szasz, A. Gergely, M. Szabo, J. Kokosi, *J. Chromatogr. Sci.* 38 (2000) 430-434.
128. J. Anguizola, R. Matsuda, O.S. Barnaby, K.S. Hoy, C. Wa, E. Debolt, M. Koke, D.S. Hage, *Clin. Chim. Acta* 425 (2013) 64-76.
129. T.A.G. Noctor, I.W. Wainer, *Pharmaceut. Res.* 9 (1992) 480-484.
130. A. Chattopadhyay, T. Tian, L. Kortum, D.S. Hage, *J. Chromatogr. B* 715 (1998) 183-190.
131. C. Bertucci, B. Nanni, A. Raffaelli, P. Salvadori, *J. Pharm. Biomed. Anal.* 18 (1998) 127-136.
132. H. Nursten, *The Maillard Reaction*, Royal Society of Chemistry, Cambridge, UK, 2005.
133. S. Ohlson, S. Shoravi, T. Fex, R. Isaksson, *Anal. Biochem.* 359 (2006) 120-123.

134. M.D. Duong-Thi, M. Bergström, T. Fex, R. Isaksson, S. Ohlson, J. Biomol. Screening 18 (2013) 160–171.
135. D.S. Hage, A. Jackson, M.R. Sobansky, J.E. Schiel, M.J. Yoo, K.S. Joseph, J. Sep. Sci. 32 (2009) 835-853.
136. K.I. Kasai, S.I. Ishii, J. Biochem. 78 (1975) 653-662.
137. N.I. Nakano, T. Oshio, Y. Fujimoto, T. Amiya, J. Pharm. Sci. 67 (1978) 1005-1008.
138. C. Lagercrantz, T. Larsson, H. Karlsson, Anal. Biochem. 99 (1979) 352-364.
139. B. Loun, D.S. Hage, J. Chromatogr. 579 (1992) 225-235.
140. J.J. Slon-Usakiewicz, W. Ng, J-R. Dai, A. Pasternak, P.R. Redden, Drug Discov. Today 10 (2005) 409-416.
141. S.A. Tweed, B. Loun, D.S. Hage, Anal. Chem. 69 (1997) 4790-4798.
142. Z. Tong, D.S. Hage, J. Chromatogr. A 1218 (2011) 8915-8924.
143. H. Xuan, D. S Hage, Anal. Biochem. 346 (2005) 300-310.
144. R. Mallik, H. Xuan, G. Guiochon, D.S. Hage, Anal. Biochem. 376 (2008) 154-156.
145. H. Xuan, K. S. Joseph, C. Wa, D.S. Hage, J. Sep. Sci. 33 (2010) 2294-2301.
146. A.J. Jackson, Ph.D. Dissertation, University of Nebraska, Lincoln, Nebraska,

2011.

- 147. M.J. Yoo, D.S. Hage, J.Chromatogr. A 1218 (2011) 2072-2078.
- 148. R. Moaddel, I. W. Wainer, Nature Protocols, 4 (2009) 197-205.
- 149. D.C. Schriemer, D. R. Bundle, L.Li, O. Hindsgaul, Angew. Chem. Int. Ed. 37 (1998) 3383-3397.
- 150. B. Zhang, M.M. Palcic, H. Mo, I.J. Goldstein, O. Hindsgaul, Glycobiology 11 (2001) 141-147.

CHAPTER 2

Analytical Methods for Kinetic Studies of Biological Interactions

Portion of this chapter have previously appeared in X. Zheng, C. Bi, Z. Li, M. Podariu, D.S. Hage, "Analytical Methods for Kinetic Studies of Biological Interactions: A Review" Journal of Pharmaceutical and Biomedical 2015, in press.

Introduction

Biological interactions are important in determining many of the processes that occur in living systems. For example, enzymes catalyze reactions by binding and modifying their substrates, transport proteins bind to and carry lipids, hormones or nutrients within the circulatory system, and antibodies are utilized by the immune system to bind and remove foreign substances from the body. Many of these events make use of non-covalent binding and may involve proteins, peptides, lipids, nucleic acids, lipids, metal ions, hormones or drugs.¹⁻⁸ Because of the widespread occurrence and importance of these interactions, various techniques have been developed to investigate and characterize such reactions.⁴⁻¹⁹ The overall strength, or thermodynamics, of these processes is one item of interest in these studies; however, the rate of these interactions, or their kinetics, is also important to consider.¹⁻⁸ Obtaining such information can provide a better understanding of the function of individual interactions in a biological system, the mechanisms through which these interactions occur, and the effects that a change in conditions may have on these processes.¹⁻⁸

This chapter examines several analytical techniques that have been used in kinetic studies of biological interactions. The methods that will be discussed include common or traditional techniques such as stopped-flow analysis and surface plasmon resonance (SPR) spectroscopy, as well as separation-based approaches that make use of affinity chromatography or capillary electrophoresis (CE).^{1,3,7,20} The general principles and theory behind each of these techniques will be described, with particular attention being given to the use of each method for investigating the rates of biological interactions. An overview of the conditions and models that are used in each technique for kinetic studies will be provided, and examples of applications will be given to illustrate each approach. Finally, the advantages and possible limitations of each method will be discussed with regards to use of the technique in studying the rate of a biological interaction.

Stopped-Flow Analysis

General principles

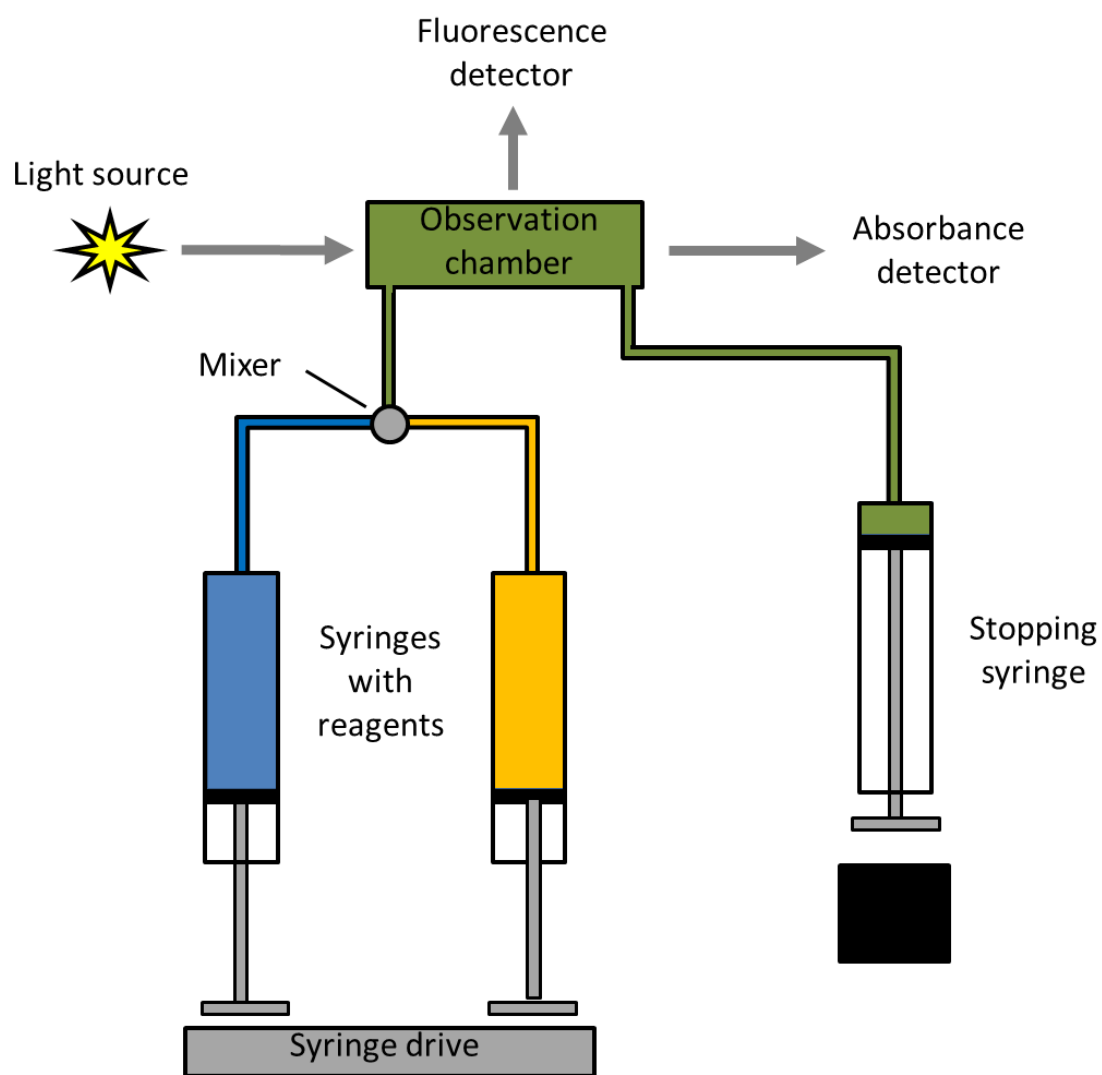
Many methods for kinetic studies are based on the measurement of a change in the concentration of a reagent or product as a function of time after the reagents have been mixed.²¹⁻²⁷ This approach requires that the process of interest be slow enough to give a reaction time that is longer than the time needed for reagent mixing and instrument activation. However, many biological interactions can occur within seconds (s) or milliseconds (ms), a fact which has limited the application of many traditional kinetic methods to such systems.²¹

Stopped-flow analysis is one technique that can be employed to study the kinetics of biological interactions. The mixing time for samples and reagents in stopped-flow analysis can be as short as 1-2 ms, making this approach useful for examining interactions that occur even on the millisecond-to-second timescale. Examples of biological interactions that have been investigated with this method in kinetic studies are protein folding²⁸⁻³⁰, enzyme inhibition.^{31,32}, and the binding of proteins or DNA to hormones, drugs, or small molecules.³³⁻⁴⁰ The reactants that can be used in stopped-flow analysis include proteins, DNA, drugs, hormones, and metal ions, among others.²⁸⁻⁸⁰

In this technique, a small volume of each desired reagent is rapidly applied by a device such as a syringe and passed through a mixer to initiate the reaction (see Figure 2.1). This mixture is then moved into an observation chamber, and the flow is stopped. Data acquisition of a signal that is produced by one of the components in the observation chamber is begun at this time. The time interval between the mixing of the reagents and the beginning of signal observation is usually only 1-2 ms and is referred to as the “dead time”.^{21,24}

Detection in stopped-flow analysis can be accomplished by using various methods that are able to selectively monitor a reagent or product in the reaction. Absorbance and fluorescence are two common detection methods that are employed for this type of experiment.^{21,25,28} For instance, reactants or products with a specific chromophore or fluorophore (e.g., NADH, pyridoxal phosphate, or tryptophan residues on a protein) can be used to follow the rate of a biological reaction.²¹ Alternatively, a tag such as fluorescein can be added to one of the reagents to monitor the progress of the reaction.²¹ Circular dichroism has also been used in stopped-flow analysis for studies involving

Figure 2.1 General design of an instrument for carrying out stopped-flow analysis, as illustrated here for a device that can be used with either fluorescence or absorbance detection. This figure is based on information that was obtained from Refs. 22-24. Reproduced with permission from X. Zheng, C. Bi, Z. Li, M. Podariu, D.S. Hage, J. Pharm. Biomed. Anal. (2015) in press.



protein folding and unfolding.²⁸⁻³⁰ In addition, fluorescence lifetime measurements,^{47,48} nuclear magnetic resonance spectroscopy,^{41,42,49,50} and small-angle X-ray scattering⁵¹ have been coupled with stopped-flow analysis to study the kinetics of protein folding or drug metabolite degradation.

Once the response has been obtained, the data from a stopped-flow experiment are fit to one or more reaction models to obtain rate constants for the desired interaction. These models can range from reactions that involve the conversion of a single type of molecule from one form to another, to a bimolecular interaction or a multistep reaction.²¹ Each of these models and applications will be discussed in more detail in the following sections.

Applications involving single-molecule reactions

The simplest type of reversible reaction that can be examined by stopped-flow analysis is the change of a single molecule from one form or conformation into another. This type of unimolecular reaction is represented by the model in Equation 2.1. In this model, the reversible conversion of molecule P (e.g., a protein) into form P^* is described by the first-order forward and reverse rate constants k_1 and k_{-1} . The ratio of these rate constants also provides the equilibrium constant for this process (K_1), where $K_1 = k_1/k_{-1}$.²¹



An appropriate detector is used during this experiment to monitor the concentration of the probed molecule in either its initial or final form (i.e., P or P^*). The observed signal (S) as a function of the reaction time (t) is then obtained and can be fit to the following equation.^{21,24}

$$S(t) = S_{\text{eq}} - (S_{\text{eq}} - S_0)e^{-k_{\text{obs}}t} \quad (2.2)$$

In Equation 2.2, $S(t)$ is the signal measured at time t , S_0 is the signal observed at the beginning of the experiment ($t = 0$), S_{eq} is the signal obtained at a sufficiently long time that equilibrium has been reached, and $(S_{\text{eq}} - S_0)$ is the total change in signal during the reaction. The term k_{obs} is the observed rate constant for the reaction. This latter parameter is related inversely to τ , the “relaxation time” for the system, where $k_{\text{obs}} = 1/\tau$.

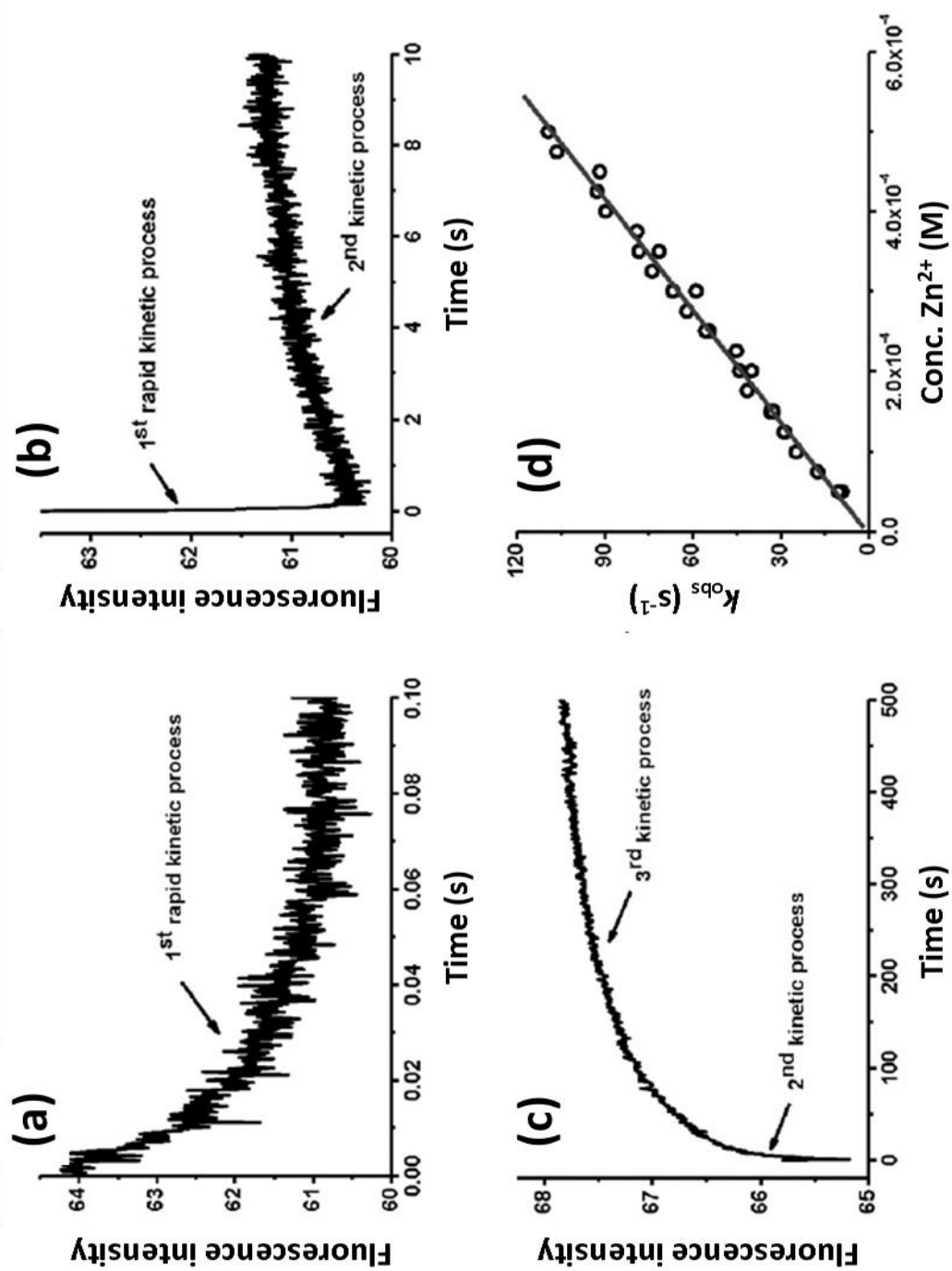
In a unimolecular reaction, the value of k_{obs} in Equation 2.2 will be equal to the sum of k_{-1} and k_1 , regardless of the concentrations of P and P^* .²¹ The values of k_{-1} and k_1 can be obtained from k_{obs} if the value of K_1 is also known, as can be accomplished by using the expressions in Equations 2.3 and 2.4.²¹

$$k_1 = \frac{K_1 k_{\text{obs}}}{1 + K_1} \quad (2.3)$$

$$k_{-1} = \frac{k_{\text{obs}}}{1 + K_1} \quad (2.4)$$

A unimolecular model has been found to describe some conformational changes in proteins. For example, this model has been used to study the conformational changes that occur in apotransferrin following the binding of this protein with Fe^{2+} or Zn^{2+} , as illustrated in Figure 2.2.⁵²

Figure 2.2 Fluorescence intensity measured over time for apotransferrin after mixing a solution of this protein with an excess of Zn^{2+} . The observed processes include (a) a rapid interaction between apotransferrin and Zn^{2+} (i.e., the “1st rapid kinetic process”), as described by Equation 2.5; and (b-c) changes in the conformation of apotransferrin (i.e., the “2nd” and “3rd” kinetic processes), as described by Equation 2.1. The graph in (d) shows a plot of k_{obs} (or τ^{-1}) vs. the concentration of Zn^{2+} during studies of the first kinetic process, which follows the linear relationship that is predicted by Equation 2.6. Adapted with permission from Ref. 52.



Applications involving bimolecular reactions

Another type of reaction that can be examined by stopped-flow analysis is the reversible interaction between two molecules to form a new species. For instance, Equation 2.5 describes a bimolecular reaction between a molecule or protein (P) and a second molecule or ligand (L) that forms the reversible complex or product PL .



The terms k_1 and k_{-1} in this reaction are the second-order association rate constant and first-order dissociation rate constant for the interaction of P with L , respectively. The ratio of these rate constants gives the association equilibrium constant for this reaction (K_1 , where $K_1 = k_1/k_{-1}$).²¹

A bimolecular reaction is often examined in stopped-flow analysis by using conditions that convert this process into a pseudo first-order reaction. This can be achieved by using at least a ten-fold higher concentration of one reagent (X) versus the other reagent. Under these conditions, the concentration of the excess reagent, $[X_{\text{tot}}]$, changes negligibly during the reaction and is approximately constant. The result is that the product of this concentration and the second-order rate constant k_1 can now be used to describe a pseudo first-order rate constant that is equal to $k_1 [X_{\text{tot}}]$. The observed rate constant, k_{obs} , that is measured for this reaction by stopped-flow analysis is described by Equation 2.6.^{21,53}

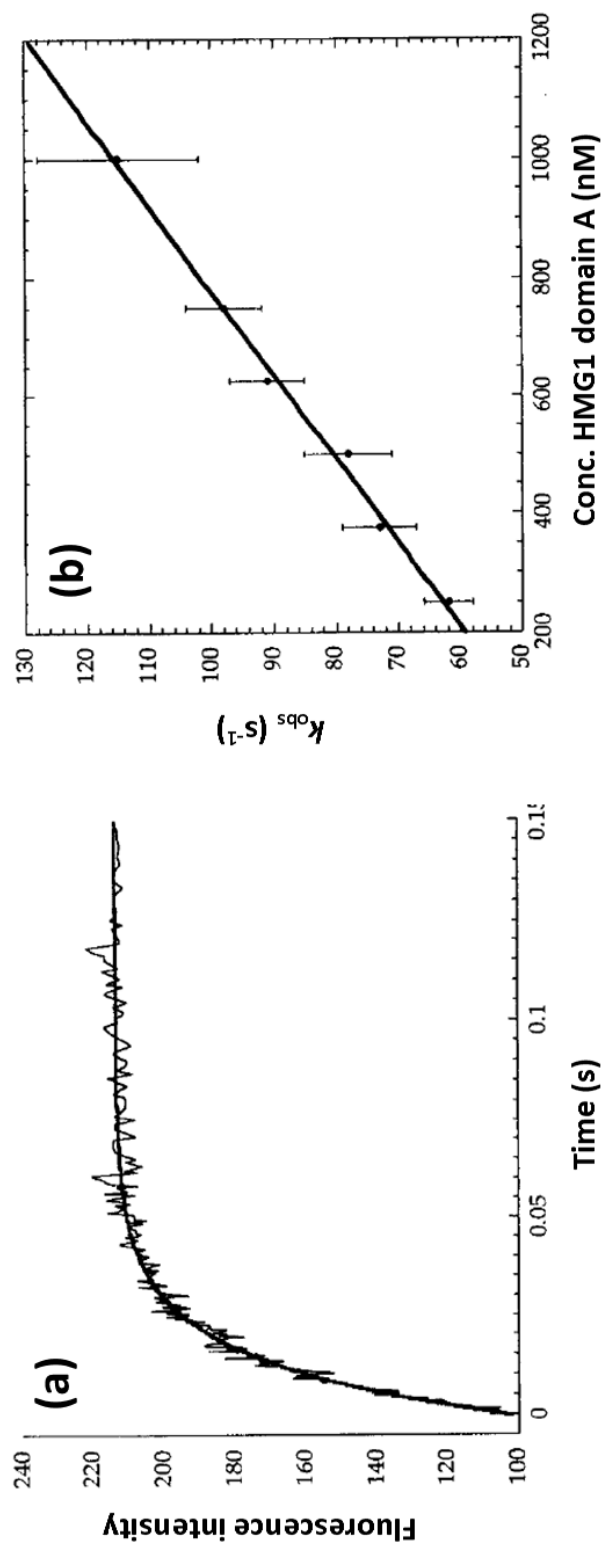
$$k_{\text{obs}} = k_1 [X_{\text{tot}}] + k_{-1} \quad (2.6)$$

The value of the observed rate constant, k_{obs} , is obtained by fitting the stopped-flow analysis data to the expression that was given earlier in Equation 2.2. However, experiments are now usually carried out at various concentrations of X , which is still in excess of the other reagent, and a plot is made of k_{obs} versus $[X_{\text{tot}}]$. If the reaction between P and L is described by Equations 2.5-2.6, a linear relationship should be obtained for this plot, with a slope that is equal to k_1 and a y-intercept that is equal to k_{-1} .^{21,53}

Figure 2.3 shows an example of this approach, in which stopped-flow analysis and fluorescence detection were used to investigate the kinetics of a DNA-protein interaction. This particular application examined the binding of high-mobility group (HMG) domain proteins with cisplatin-modified DNA.⁵⁴ A platinum-containing, fluorescent DNA probe was mixed with an excess of HMG1 or a domain from this protein, which were prepared at various concentrations. The data gave a good fit to Equation 2.2 and the resulting values of k_{obs} were plotted against the total concentrations of HMG1 or its domains in various mixtures. This latter plot provided the association and dissociation rate constants for the DNA-protein interaction.

This type of method has also been used in drug-protein binding studies. Interactions of the drug warfarin with the protein human serum albumin (HSA) have been investigated by using stopped-flow analysis under pseudo first-order conditions (i.e., by mixing HSA with solutions containing a known excess of warfarin).⁵³ The enhancement in the fluorescence of warfarin when binding to HSA was used to examine the kinetics of this interaction. Kinetic data for the interactions between isonicotinic hydrazide and its analogues with *Mycobacterium tuberculosis* catalase-peroxidase (KatG) have also been obtained and analyzed according to this technique, by detecting the change in the

Figure 2.3 Stopped-flow kinetic studies of the reaction between high-mobility group (HMG) 1 domain A and platinated 16-mer DNA probes containing a fluorescein-dU label. The plot in (a) shows the change in fluorescence over time after the mixing of HMG1 domain A with the DNA probes. The plot in (b) shows the relationship that was seen between the observed rate constant (k_{obs}) and the concentration of HMG1 domain A. Equation 2.6 was used with this second plot to determine association and dissociation rate constants for this protein-DNA reaction. Adapted with permission from Ref. 54.

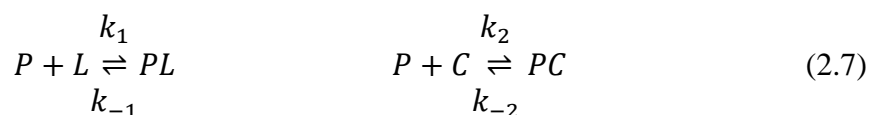


absorbance of KatG as it binds to hydrazide.⁵⁵ In addition, a bimolecular reaction model has been used to investigate enzyme interactions with peptides or coenzymes, protein-protein interactions, the binding of ATP with proteins, and lipid-protein interactions.⁵⁶⁻⁶¹

Even though, in theory, both the association and dissociation rate constants for a bimolecular reaction can be estimated by using Equation 2.6, this equation does have some limitations when it is used to study reactions with relatively high equilibrium constants. For instance, the small dissociation rate constants that can be present for this type of reaction may make it difficult or impractical to determine k_{-1} from the intercept of Equation 2.6. This problem has been noted in the use of stopped-flow analysis to examine the interactions of some drugs or metal ions with proteins and in some enzyme-peptide or protein-protein interactions.^{52,53,56,59}

Applications involving competition studies

Competition experiments can also be utilized in stopped-flow analysis to examine the rates of biological interactions. For instance, this might involve a bimolecular reaction like the one between P and L in Equation 2.5, along with the use of a competing agent (C) that is known to bind to the same site on P as L . In this situation, the addition of C to a pre-incubated mixture of P and L will cause C to displace some of L from its complex with P . The reactions that take place in this system are shown in Equation 2.7.



In these reactions, k_1 and k_{-1} are again the second-order association and first-order dissociation rate constants for the reversible interaction of P with L , while k_2 and k_{-2} are the corresponding association and dissociation rate constants for the reversible interaction of P with C at the same binding region that can be occupied by L .²¹

To study the dissociation rate of L from P in this type of system, the concentration of L in the premixed solution of P and L is chosen to ensure that there is a reasonable, initial saturation of P . However, the concentration of C that is added needs to be present in a large excess compared to the concentrations of both P and L , thus avoiding re-association of L after it has been dissociated from its complex with P . A signal is then measured that reflects a change in one of the products or reactants, and this signal is analyzed according to an expression like Equation 2.2. Ideally, experimental conditions should be selected so that if C and L do compete for sites on P and the concentration of C is sufficiently large, the observed rate constant k_{obs} will be equal to k_{-1} and independent of the concentration of C .^{21,53}

Stopped-flow analysis and the model in Equation 2.7 can be further used to determine the dissociation rate constant for the interaction of C with P . This can be achieved by using a large excess of L to displace C from P in a solution that initially contains a pre-incubated mixture of P and C . Another binding agent, P' , which is able to bind to C , can also be used to displace C from its complex with P by forming the alternative complex, $P'C$.²¹

Competition experiments in stopped-flow analysis have been used to examine the rates of interactions such as drug-protein, DNA-protein, protein-protein, and enzyme-

peptide binding.^{53,54,56,59,62-65} For instance, phenylbutazone has been utilized as a competing agent in kinetic studies of warfarin's interactions with HSA. The observed rate constant was then used to estimate the dissociation rate constant for warfarin from HSA.⁵³ This general approach was also used to measure the dissociation rate constant for DNA from HMG1 domain A, in which a DNA sequence without a fluorescent tag was used as the competing agent.⁵⁴ A similar technique was employed to follow the dissociation of pyrene-labelled actin and ADP from their complexes with myosin by using unlabeled actin or ATP as a competing agent.⁶²⁻⁶⁵

Competition experiments can be modified to measure the association rate constants for the interactions of L and C with P . This can be carried out by premixing solutions of C and L , followed by the addition of P . If the dissociation rate constants for this system (k_{-1} and k_{-2}) are small compared to the pseudo first-order association rate constants, the observed rate constant will now be described by Equation 2.8.

$$k_{\text{obs}} = k_2[C_{\text{tot}}] + k_1[L_{\text{tot}}] \quad (2.8)$$

In this type of experiment, the concentration of C ($[C_{\text{tot}}]$) is varied and mixed with L that has been prepared at a fixed concentration, $[L_{\text{tot}}]$. Both the concentrations of C and L are selected so that they are much higher than the concentration of P that will be present. After P has been added to the premixed solution of C and L , the change in signal for the system is measured as a series of k_{obs} values are obtained for various mixtures of C and L . A plot of k_{obs} versus $[C_{\text{tot}}]$ is then prepared according to Equation 2.8, resulting in a linear relationship with a slope that provides k_2 and a y-intercept that is equal to $k_1 [L_{\text{tot}}]$.

Another use for Equation 2.8 has been in examining the type of competition that solutes may have at their binding sites on a protein. In one report, podophyllotoxin (POD) was used as a competing agent to study binding by tubulin to two analogs of colchicine (2,3,4-trimethoxy-4'-carbomethoxy-1,1'-biphenyl, or TCB, and 2,3,4-trimethoxy-4'-acetyl-1,1'-biphenyl, or TKB); this reaction was followed through stopped-flow analysis by monitoring the increase in fluorescence that occurred upon binding.⁶⁶ A plot of k_{obs} versus the concentration of POD was then made according to Equation 2.8. The linear relationships in this plot indicated that POD was competing with both TCB and TKB for their binding sites on tubulin and provided the association rate constant for POD with this protein. If this system had instead given a non-linear relationship, this would have indicated that a different binding site was involved in the interactions of C and L with P or that a process other than simple direct competition was present in the system.^{66,67}

Applications involving multistep reactions

Even though a reversible bimolecular interaction like the one in Equation 2.5 can be utilized to describe many types of biological interactions, there are situations in which additional steps are needed to provide a suitable description of the system. For instance, the fast binding of P with L to form PL may be followed by a slower conformational change to create an alternative form of this product, PL^* , as is shown in Equation 2.9.



The first step of this process is described by the second-order association and first-order dissociation rate constants k_1 and k_{-1} . The second step, involving a unimolecular change, is described by the first-order forward and reverse rate constants k_2 and k_{-2} , respectively.²¹

The experimental conditions that can be used in stopped-flow analysis to examine this type of system are similar to those described for a simple bimolecular reaction in Section of *Applications involving bimolecular reactions*. One of the reagents (e.g., L) is prepared at a series of concentrations that are much higher than the concentration of the other reagent (e.g., P). To detect a two-step reaction like the one in Equation 2.9, a comparison can be made when the data are fit to both the single-exponential expression in Equation 2.2 and the double-exponential expression given in Equation 2.10, where these two expressions represent one- or two-phase association models.⁶⁶⁻⁷²

$$S(t) = S_0 + F_f(S_{eq} - S_0)e^{-k_{obs1}t} + F_s(S_{eq} - S_0)e^{-k_{obs2}t} \quad (2.10)$$

In Equation 2.10, the terms F_f and F_s are the fractions of the change in response due to the fast and slow reaction steps, where the sum of these fractions is equal to one. In this type of multistep system, the observed rate constant for the fast bimolecular reaction, k_{obs1} , should increase in a linear manner with the value of $[L_{ot}]$ when PL is forming, as is described by Equation 2.6. The term k_{obs2} , which is the observed rate constant for the slower unimolecular reaction, should have a non-linear relationship with $[L_{ot}]$, as indicated by Equation 2.11 for a case in which the concentration of L is much larger than that of P .^{21,68-70,73-75}

$$k_{obs2} = \frac{k_2[L_{tot}]}{K_{-1} + [L_{tot}]} + k_{-2} \quad (2.11)$$

The term K_{-1} in Equation 2.11 is the dissociation equilibrium constant for the fast bimolecular reaction, where $K_{-1} = k_{-1}/k_1$.

This method has been used to examine the interactions of genome-linked protein with wheat germ translation initiation factors.⁶⁸ It was further employed in a study examining the reactions between J-binding protein 1 and its J-DNA-binding domain with DNA oligomers that contained base J or glucosylated 5-hydroxymethylcytosine.⁶⁹ The rate constants for the binding of phosphatidylserine-containing vesicles to lactadherin have also been determined by using Equations 2.10-2.11.⁷⁰ In addition, other biological interactions (e.g., enzyme catalysis) have been investigated by using stopped-flow analysis and a multistep model.⁷³⁻⁷⁵

If the dissociation equilibrium constant K_{-1} is small compared to $[L_{\text{tot}}]$, the value of $k_{\text{obs}2}$ in Equation 2.11 will become independent of $[L_{\text{tot}}]$ and approximately equal to the sum of k_2 and k_{-2} . The kinetic parameters for each step in the reaction can then be determined by employing Equation 2.6 or Equations 2.3-2.4 to analyze data acquired over appropriate time periods during the experiment. This type of analysis has been used in kinetic studies of the binding of Fe^{2+} and Zn^{2+} to human serum transferrin, as illustrated earlier in Figure 2.2.⁵² This model has also been used to investigate the binding and subsequent change in conformation that occurs for the complex between melittin and Ca^{2+} -saturated calmodulin, as well as the interaction of a transcriptional activator-DNA complex with a coactivator, and the interaction of *N*-phenyl-1-naphthylamine with pheromone-binding proteins.⁷⁶⁻⁷⁸

If the value of k_{-2} is small, Equation 2.11 can be simplified to one of the forms shown in Equations 2.12-2.13. For instance, Equation 2.13 indicates that such a system will provide a linear relationship between $1/k_{\text{obs}2}$ and $1/[L_{\text{tot}}]$, which can be used to find the values of k_2 and K_{-1} .

$$k_{\text{obs}2} = \frac{k_2[L_{\text{tot}}]}{K_{-1} + [L_{\text{tot}}]} \quad (2.12)$$

$$\frac{1}{k_{\text{obs}2}} = \frac{K_{-1}}{k_2[L_{\text{tot}}]} + \frac{1}{k_2} \quad (2.13)$$

This type of analysis has been utilized to study the interaction kinetics when an excess of rifampicin is combined with RNA polymerase.⁷² These equations have also been used to study protein-protein interactions.⁷⁹

Advantages and potential limitations

As has been shown in this section, stopped-flow analysis can be applied in studying the kinetics of various biological interactions, including both simple and relatively complex systems. In addition, this technique can be used to examine either slow or relatively fast events. Rate constants that have been determined by stopped-flow analysis have ranged from 10^{-6} to 10^6 s^{-1} for first-order reactions and from 1 to $10^9 \text{ M}^{-1}\text{s}^{-1}$ for second-order reactions.^{40,62,71,76} It is necessary, however, for the observed reaction to have a half-life that is longer than the mixing time and dead time of the stopped-flow instrument, which limits the use of this method in the study of some very fast reactions.⁸⁰

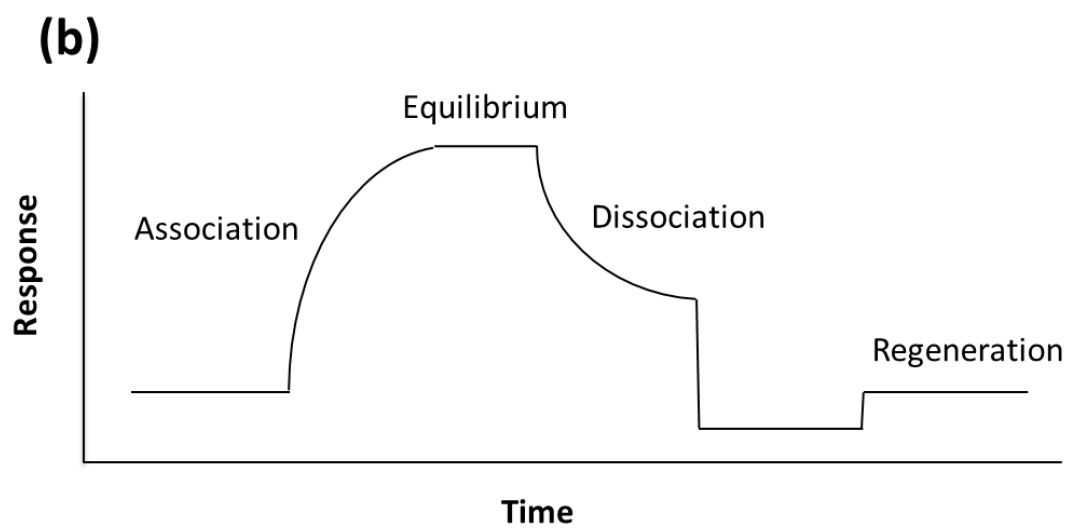
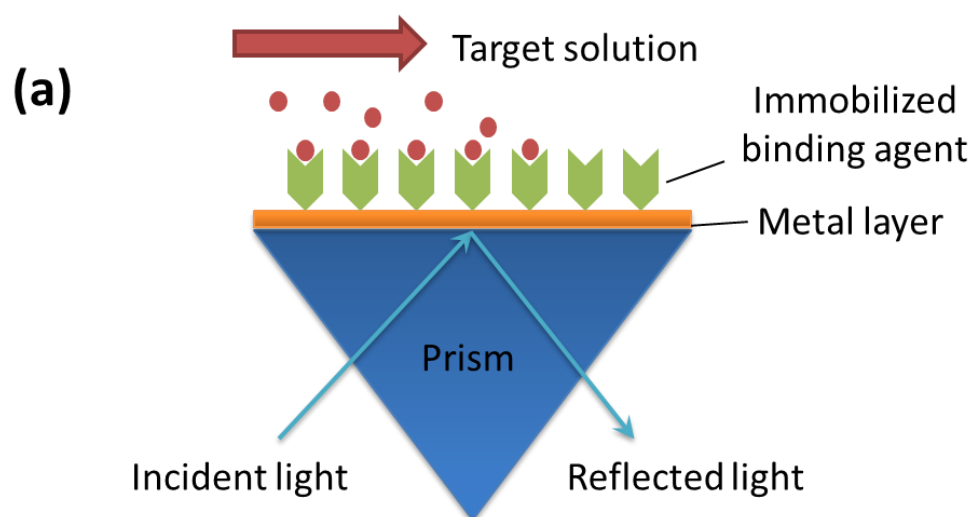
An important advantage of stopped-flow analysis is it can be used directly with solution-phase reactions, provided some means is available to selectively monitor a change in the concentration of a reactant or product in this reaction (e.g., through fluorescence or absorbance detection). It is also necessary to have sufficient volumes of the reagents for use in the solution delivery component of the stopped-flow instrument. A sufficient concentration of the reagents and/or products is also needed for a change in these components to be measured over time. This latter requirement, and the detectable range of the reagent or product, will depend on the detection method that is employed. However, a relatively low detection limit (e.g., low nM levels) can be obtained when a method such as fluorescence is used in stopped-flow analysis.^{21,24,59,69}

Surface Plasmon Resonance

General principles

Surface plasmon resonance (SPR) spectroscopy is another method that has been widely used for the analysis of biological interactions.⁸¹ This method has been utilized to study systems such as protein-ligand, protein-protein, and protein-DNA interactions.^{3-5,82,83} Figure 2.4(a) shows a typical SPR instrument that is used for biological interaction studies. This particular device makes use of prism coupling, but other possible configurations include those based on optical waveguide coupling and grating coupling.^{82,83}

Figure 2.4 (a) Typical design for a surface plasmon resonance (SPR) biosensor based on a prism configuration. The plot in (b) shows a typical experimental cycle and general response (or sensorgram) that can be obtained with this type of instrument in a kinetic analysis for an applied target that is interacting with an immobilized binding agent to form a reversible complex. This figure is based on information that was obtained from Ref. 4. Reproduced with permission from X. Zheng, C. Bi, Z. Li, M. Podariu, D.S. Hage, J. Pharm. Biomed. Anal. (2015) in press.



In an SPR system, a binding agent such as a protein is immobilized onto the sensor surface, which typically consists of a thin film of a metal (e.g., gold or silver) that is placed onto a glass surface.^{82,83} This sensor surface is then placed within a flow cell. A target, or ligand, that is to be tested for its binding to the immobilized agent is then applied to the flow cell and in the presence of an appropriate buffer. Surface plasmons are generated when an incident beam of light is directed towards the metal surface at a critical angle. This critical angle depends on the refractive index of the medium near the surface and changes when targets bind to the immobilized binding agents at this surface.⁸⁴ The change in the refractive index at the surface, as a result of the interaction between the applied target and immobilized agent, is then measured and provides an index of the extent of binding that has occurred.⁸¹⁻⁸⁵

Figure 2.4(b) shows a general plot (or sensorgram) that is obtained with this type of instrument. In this plot, an increase in response is generated as the applied target binds to the immobilized agent in the flow cell. A plateau in this response is obtained as equilibrium is reached between the applied target and the immobilized binding agent. Dissociation of the target from the immobilized binding agent can also be monitored as the bound target is later washed away from the surface. After the bound target has been removed, the surface and binding agent can often be regenerated and are placed back in contact with the initial buffer prior to the application of more target.^{4,83,85}

Data analysis methods

For a bimolecular reaction between P and L , as described earlier in Equation 2.5, the change in the concentration of product PL with time can be described by using Equation 2.14.^{83,86-87}

$$\frac{d[PL]}{dt} = k_1[P][L] - k_{-1}[PL] \quad (2.14)$$

In this equation, k_1 is the second-order association rate constant for the interaction of P with L , and k_{-1} is the first-order dissociation rate constant for this interaction, as defined earlier in Section of *Applications involving single-molecule reactions*. This binding event, and the concentration of PL , is monitored by using the change in the refractive index at the surface of the sensor.

By varying $[L]$, the SPR response for the system in Equation 2.14 can be fit to the following integrated rate expression.^{83,86-87}

$$R_t = \frac{R_{\max}k_1[L]}{k_1[L] + k_{-1}}(1 - e^{-(k_1[L] + k_{-1})t}) \quad (2.15)$$

In Equation 2.15, R_t is the response measured at time t , and R_{\max} is the maximum response that is obtained upon the saturation of P with L . If the value of $[L]$ is varied, a fit of Equation 2.15 to these curves will provide a series of observed rate constants (k_{obs}), in which k_{obs} is equal to the following set of terms.^{83,86-87}

$$k_{\text{obs}} = k_1[L] + k_{-1} \quad (2.16)$$

A plot of k_{obs} versus $[L]$ can then be made according to Equation 2.16, and the values of k_1 and k_{-1} can be determined from the slope and the y-intercept of the best-fit line.

To accurately determine k_{-1} and k_1 by this method, an appropriate range for the concentrations of L should be used. One study examined how k_{obs} varied with the concentration of L during the binding of a 50 kDa target ligand to immobilized chymotrypsin.⁸⁶ Ligand depletion occurred at low ligand concentrations and resulted in curvature in the kinetic plots. This deviation became more pronounced at a higher value for R_{max} and lead to an underestimation of k_1 and an overestimation of k_{-1} . It was determined that these errors could be minimized by using ligand concentrations that were 1-100 times that of the dissociation equilibrium constant for the system (K_{-1} , where $K_{-1} = k_{-1}/k_1$).⁸⁶

Data generated during the dissociation step in SPR can be used to provide additional kinetic information. This can be accomplished by using a first-order expression to describe the release of L from P , as shown in Equation 2.17.^{86,87}

$$R_t = R_0(e^{-k_{-1}t}) \quad (2.17)$$

Most of the terms in this relationship are the same as in Equation 2.15, with the additional term R_0 representing the response at the beginning of the dissociation step. Equation 2.17 is applicable only in the case of the simple, monophasic dissociation of PL , and where the re-association of L to the immobilized binding agent P is negligible after L has dissociated from the surface of the SPR sensor.⁸⁷

Applications in kinetic studies

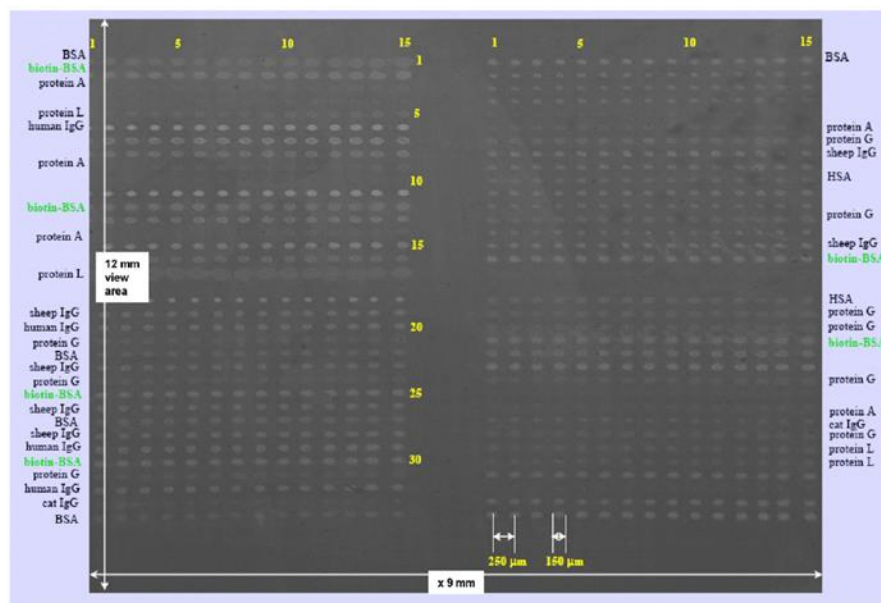
SPR has been widely utilized in dissociation and association rate measurements for various biological systems.^{3-5,88} One recent report examined the choice of suitable conditions for the kinetic analysis of G-protein signaling, based on the use of immobilized native rhodopsin (Rho, a G-protein coupled receptor) and transducin.⁸⁹ A number of antibody-antigen interactions have been examined by using SPR,⁹⁰⁻⁹² and this technique has been applied in studying the DNA-protein interactions.^{93,94} For instance, SPR has been used to measure the interaction rates of DNA-based aptamers with human immunoglobulin E.⁹³

SPR has been further employed in investigating the interaction kinetics between biomacromolecules and small targets.^{3,85,88,95,96} For instance, SPR has been used to examine the interactions of human carbonic anhydrase I with various sulfonamide inhibitors.⁹³ One report used SPR to study the kinetics of small target interactions with modified binding sites on an inverse agonist stabilized receptor of the adenosine A_{2A} receptor.⁹⁶ In another paper, a group of investigators used a commercial SPR instrument to separately characterize the rate constants and binding constants for 10 sulfonamide inhibitors with the enzyme carbonic anhydrase II.⁹⁷

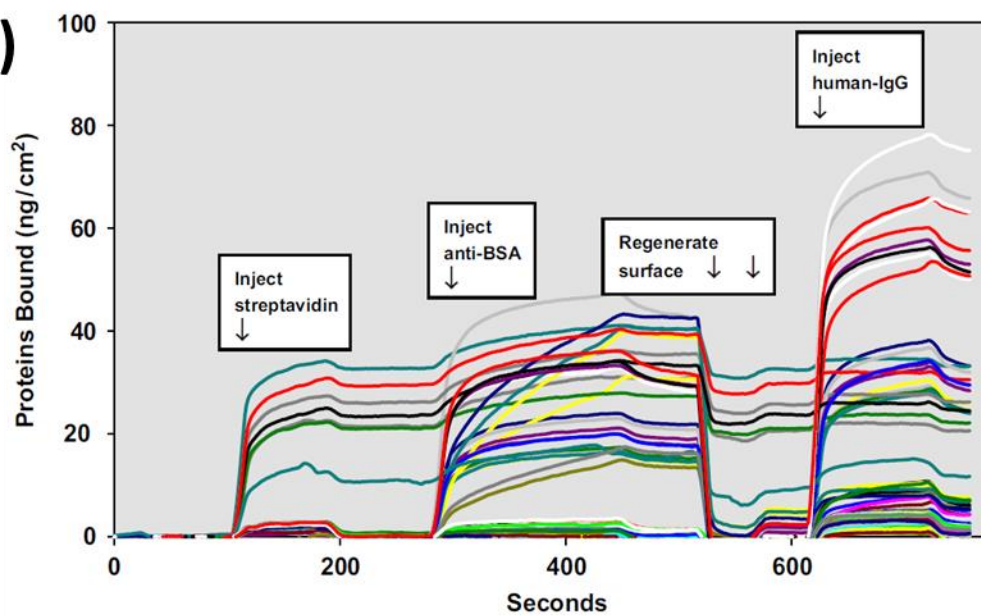
SPR has been used in some situations with a small immobilized binding agent. This format was employed to measure rate constants for the interactions between small targets and FK506 binding protein 12. The results suggested that the use of immobilized targets for the SPR experiments eliminated subtle constraints to the protein's rotational and diffusional freedom that would have been present if the protein were instead immobilized.⁹⁸ Another report that used small immobilized targets involved kinetic

Figure 2.5 (a) A 1020-spot protein microarray as imaged by SPR microscopy, and (b) sensorgrams that were obtained at some of the spots in this protein microarray following the application of streptavidin, anti-bovine serum albumin (BSA) antibodies or human immunoglobulin G (IgG). Adapted with permission from Ref. 88.

(a)



(b)



studies on the binding of streptavidin to mixed biotin-containing alkylthiolate monolayers.⁹⁹

Several variations of SPR systems have been reported. A method for SPR imaging (or SPR microscopy) has been developed for simultaneously monitoring thousands of biomolecular interactions.^{88,104} Figure 2.5 shows an example of an image that was generated for a 1020-spot protein microarray. In this case, twenty different proteins were spotted across the surface of the array and utilized to generate a series of kinetic curves. The results suggested that SPR imaging could be used to carry out kinetic measurements on more than 1000 spots with a one second time resolution, making this approach of interest in applications such as proteomic analysis and drug discovery.^{88,99,101} SPR has also been combined with mass spectrometry, which has been used to provide structural information on interacting proteins.^{81,101-103}

Advantages and potential limitations

There are several advantages in the use of SPR for kinetic studies. One advantage is that this method can be carried out using commercial systems that provide flexible platforms for examining both the equilibrium constants and rate constants for biological interactions.¹⁰⁴ These systems require only a small amount of the binding agent and applied target. The fact that the binding agent is immobilized can also help minimize batch-to-batch variations when the same sensor is used for multiple studies.

The use of SPR as a detection mode is appealing in that it provides a “label free” means for following the course of a biological interaction.^{4,5,85} However, this does require a specific type of surface for the analysis (i.e., one containing a thin metal film such as gold), and it is necessary to immobilize one of the agents that is taking part in the interaction. There are several immobilization methods available for this purpose.^{3,104} Common methods for protein immobilization include the coupling of groups such as amines or thiols on a protein to a coating of dextran on the sensor.⁸¹ It is also possible to capture a biotinylated agent on a surface that contains immobilized streptavidin, or to capture a histidine-labeled agent on a surface that contains immobilized nitrilotriacetic acid and its complex with nickel ions.^{3,81,103} For small molecules, the number and types of functional groups that are present may limit the options for immobilization. Improper coupling conditions, whether it is applied to a large or small molecule, can lead to some changes in the binding properties of the immobilized agent.^{3,5,89} Validation of SPR with reference methods is ideally required when this system is used to study what is normally a solution-phase interaction. However, if the immobilization method and conditions are properly selected, the results obtained by SPR can give good agreement with those seen in solution and by other techniques.^{89,97}

SPR has been used to investigate biological interactions with a wide range of rate constants. This has included second-order association rate constants ranging from 10^2 to $10^8 \text{ M}^{-1} \text{ s}^{-1}$ and first-order dissociation rate constants that have spanned from 10^{-6} to 1 s^{-1}).^{4,81} The level of accuracy and precision of SPR does depend on the rates and affinity of the system being examined, since this will determine the time period over which useful data can be acquired. Systems that have moderate-to-weak interactions (i.e., K_1 values of

10^4 to 10^5 M^{-1} or less) and fast association or dissociation rates are the most difficult to measure by this approach.^{97,106} In addition, mass transfer effects that occur during the transport of the target in solution should be considered when examining the kinetics of biological interactions by SPR.^{81,97,104,106}

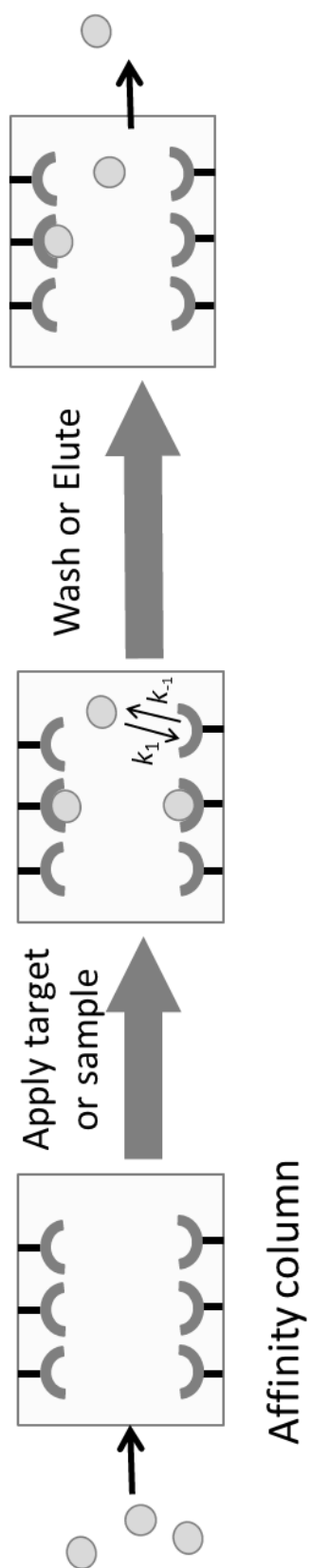
Affinity Chromatography

General principles

Affinity chromatography is a liquid chromatographic technique in which a biologically-related agent known as the “affinity ligand” is used as the stationary phase.¹⁰⁷⁻¹¹¹ The retention and separation of a target analyte from other sample components by this method is based on the specific and reversible interactions that occur in many biological interactions.^{6,8,9,107-111} High-performance affinity chromatography (HPAC) is a type of affinity chromatography that uses the supports and instrumentation of high-performance liquid chromatography to provide both rapid and efficient separations based on biological interactions and affinity ligands.¹¹² The development of HPAC has also lead to the creation of various new or improved techniques that can use affinity chromatography to study the kinetics and thermodynamics of biological interactions.^{6,112,113}

Figure 2.6 shows the general way in which affinity chromatography can be employed for studying biological interactions. Affinity chromatography and HPAC are most often used to examine the binding and/or dissociation of an applied target with an

Figure 2.6 General models for the use of affinity chromatography for kinetic analysis of interactions between an applied target and an immobilized binding agent. The terms k_1 and k_{-1} represent the association rate constant and dissociation rate constant, respectively, for the target with the given binding agent. Reproduced with permission from X. Zheng, C. Bi, Z. Li, M. Podariu, D.S. Hage, J. Pharm. Biomed. Anal. (2015) in press.



immobilized binding agent. These chromatographic-based experiments are similar to SPR in that they can provide information on both binding affinities and association or dissociation rates under typical sample application conditions. It is further possible to use affinity chromatography to examine the binding strength and association/dissociation kinetics under other conditions, such as those that might be used for target elution or for the release of this target from the immobilized binding agent.^{7,106}

Band broadening methods

The use of band broadening measurements was the first method developed in affinity chromatography for kinetic studies of biological interactions.^{7,106} Two variations on this approach are the plate height method and peak profiling.¹⁰⁶ In the plate height method, the total plate height for a small amount of an applied target is measured at several flow rates on both a column that contains an immobilized binding agent and on a control column that contains no binding agent. The resulting plate height and flow rate data are then used to determine the contribution of plate height due stationary phase mass transfer (H_s).

This latter process is of interest because it is directly related to the kinetics for the binding of the applied target with the immobilized binding agent. This process is described by the reaction given earlier in Equation 2.5 and the plate height equation that is shown in Equation 2.18.^{7,106}

$$H_s = \frac{2 u k}{k_{-1} (1 + k)^2} \quad (2.18)$$

In Equation 2.18, u is the linear velocity of the mobile phase in the column, k is the retention factor of the injected target, and k_{-1} is the dissociation rate constant for the target from the immobilized binding agent. When a plot of H_s versus $(u k)/(1 + k)^2$ is prepared, the result is a linear relationship that can provide the value of k_{-1} from the slope.

The plate height method has been used in HPAC to examine the interaction kinetics for drugs and solutes such as *R/S*-warfarin and D/L-tryptophan with HSA.^{114,115} Similar experiments were performed to look at the effects of temperature on the rates of these processes,^{114,115} as well as the effects of pH, ionic strength and solvent polarity on the interaction rates of D/L-tryptophan with HSA.¹¹⁵ This method has also been employed in evaluating the use of small affinity columns and monoliths for screening the interactions of HSA with drugs or solutes such as carbamazepine, L-tryptophan and *R*-warfarin.^{116,117}

The plate height method has generally been used to study systems that have relatively fast interaction rates compared to the time of the chromatographic analysis. For instance, the dissociation rate constants that have been determined by this method have ranged from roughly 10^{-2} to 10^1 s^{-1} .^{6,114,117} This method also has been successfully used with systems that have weak-to-moderate binding (i.e., K_1 values of 10^5 M^{-1} or less).^{6,7,106,114-117} The injection of only a small amount of the target is needed and desirable in this method to ensure that linear elution conditions are present. Also, columns and support materials should be selected for this technique that will minimize or provide reproducible values for other plate height contributions, such as those due to mobile phase mass transfer, eddy diffusion, longitudinal diffusion, and stagnant mobile phase mass transfer.^{6,7,106}

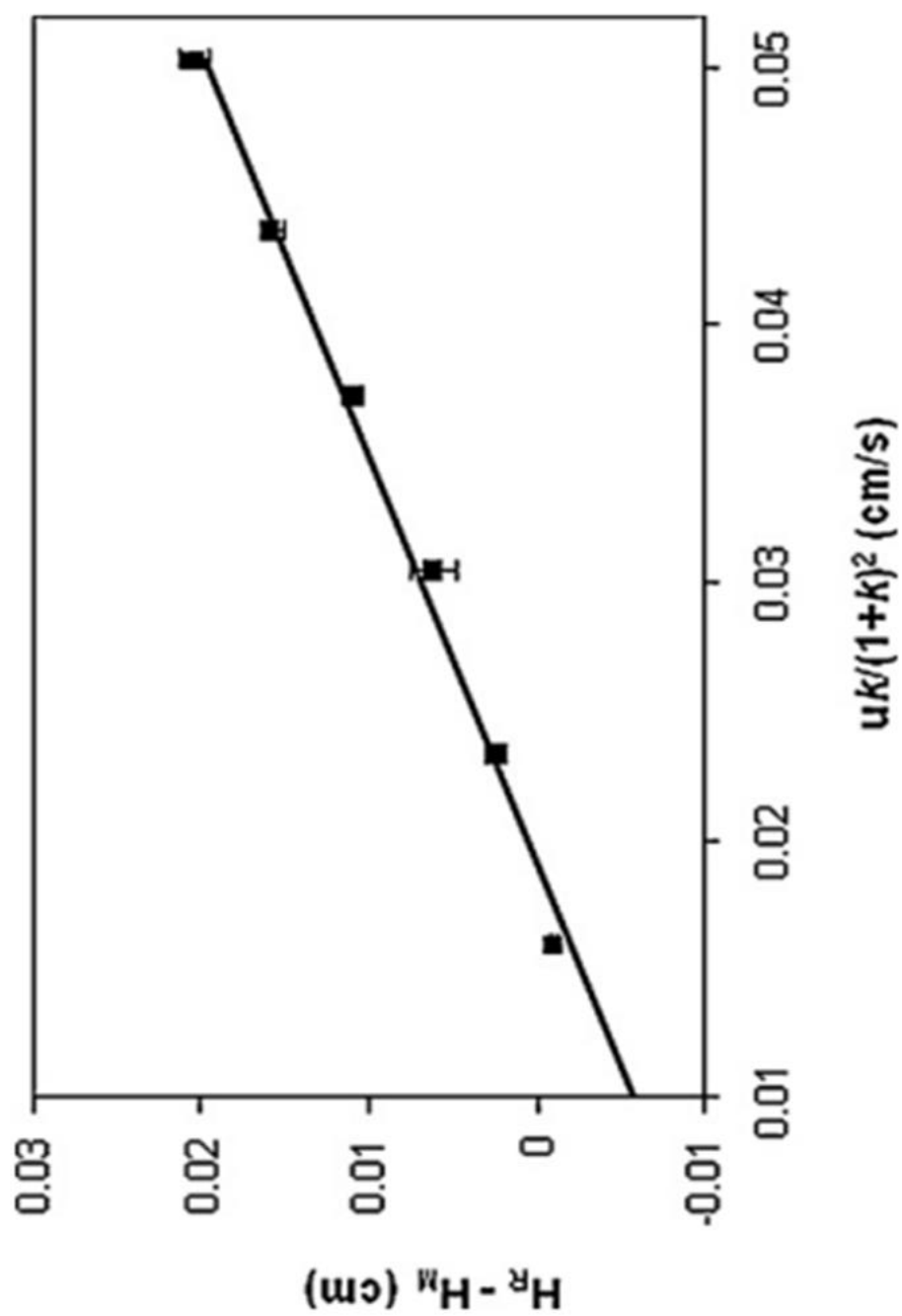
Peak profiling is a related method that examines the band broadening of a target and a non-retained solute on an affinity column (and possibly on a control column) under linear elution conditions.^{106,112} Equation 2.19 is often used in peak profiling studies to provide information on the dissociation rate constant k_{-1} from band broadening data.^{112,118-120}

$$H_R - H_M = \frac{2 u k}{k_{-1} (1+k)^2} = H_s \quad (2.19)$$

In this equation, H_R and H_M refer to the plate heights for the retained target and a non-retained solute on the affinity column, respectively, although the plate height for the target on a control column is also sometimes used for H_M . Equation 2.19 can be used with data obtained at a single flow rate to calculate the value of k_{-1} , or data acquired at several flow rates can be used to construct a plot of $(H_R - H_M)$ versus $(u k)/(1 + k)^2$ and the dissociation rate constant can be obtained from the slope of the best-fit response.^{112,118-120}

Peak profiling has been used to investigate the dissociation rates of several drugs and small solutes from serum proteins. For example, this method has been used to measure the dissociation rate constants for carbamazepine, imipramine and L-tryptophan with HSA..^{112,118} A typical plot of $(H_R - H_M)$ vs. $(u k)/(1 + k)^2$ that was obtained in this work is provided in Figure 2.7.¹¹⁸ In addition, this method has been used to simultaneously determine the dissociation rate constants of HSA with two chiral metabolites of the drug phenytoin: 5-(3-hydroxyphenyl)-5-phenylhydantoin and 5-(4-hydroxyphenyl)-5-phenylhydantoin.¹²¹ The rate constants for the interactions of β -

Figure 2.7 Peak profiling plots based on Equation 2.19 for describing the dissociation of carbamazepine from immobilized HSA in a high-performance affinity column. Reproduced with permission from Ref. 118.



cyclodextrin with acetaminophen and sertraline have also been measured by this method.¹²²

Peak profiling has similar requirements, advantages and limitations to the plate height method. For instance, peak profiling is again mainly used for systems with relative fast association and dissociation rates and weak-to-moderate strength binding. The dissociation rate constants that have been determined by this method have been in the range of 10^{-1} to 10^1 s^{-1} .^{112,118,121,122} One advantage of peak profiling is it can sometimes be conducted at only a single flow rate, or at higher flow rates than the plate height method. However, a fast sampling rate and stable response is required for work at high flow rates to provide an accurate measure of peak variances and consistent plate height values.¹⁰⁶

Peak fitting methods

Peak fitting has also been used for kinetic analysis in affinity chromatography. This approach differs from those described in the last section in that the amount of applied target can now be sufficiently high to create non-linear elution conditions.¹⁰⁶ Peak fitting can be conducted with either narrow injections of the target (i.e., zonal elution) or continuous application of the target (i.e., frontal analysis).¹⁰⁶ When this method is used with zonal elution, Equation 2.20 can be used to fit the resulting elution profiles.^{123,124}

$$y = \frac{a_0}{a_3} \left[1 - e^{\left(-\frac{a_3}{a_2}\right)} \right] \left[\frac{\sqrt{\frac{a_1}{x}} I_1\left(\frac{2\sqrt{a_1 x}}{a_2}\right) e^{-x\frac{a_1}{a_2}}}{1 - T\left(\frac{a_1 x}{a_2 a_2'}\right) \left[1 - e^{-\frac{a_3}{a_2}} \right]} \right] \quad (2.20)$$

In this equation, y is the intensity of the measured signal at a given point in time in the peak profile, x is the reduced retention time at which y is measured, T is the switching function, and I_1 is a modified Bessel function. The terms a_0 , a_1 , a_2 and a_3 are the best-fit parameters to be obtained by fitting the experimental data to Equation 2.20. These fitted results are then used to estimate the rate constants and equilibrium constant for the interaction between the injected target and immobilized binding agent. For instance, the dissociation rate constant and association equilibrium constant (k_{-1} and K_1) for the system are represented by the terms $1/a_2 t_M$ and a_3/C_0 , respectively, where t_M is the column void time and C_0 is a term related to the concentration of the injected target.^{106,125}

This form of peak fitting has been used to examine the interaction kinetics of the drug verapamil with nicotinic acetylcholine receptor.¹²⁶ Related peak fitting methods have been utilized to estimate the dissociation rate constant for IgG from immobilized protein A in the presence of a pH 3.0 buffer.¹²⁷ A similar approach has been utilized to examine the elution of lysozyme from a Cibacron Blue 3GA column in the presence of buffers that contained various concentrations of sodium chloride.¹²⁸

Peak fitting can also be used with frontal analysis to examine the interaction kinetics between an applied target and an immobilized binding agent. As an example, the apparent association rate constant ($k_{1,app}$) can be measured and used to determine the true association rate constant (k_1) by using Equation 2.21. This equation makes use of the

reaction model in Equation 2.5, with an assumption that dissociation of the target for the binding agent is negligible on the timescale of the experiment.^{106,129}

$$\frac{1}{k_{1,\text{app}}} = \frac{q_x V_M}{F n_{\text{mt}}} + \frac{1}{k_1} \quad (2.21)$$

In this equation, n_{mt} is the global mass transfer coefficient (which is dependent on the packing size and column dimensions), F is the flow rate, V_M is the column void volume, and q_x is the column loading capacity per unit volume of the mobile phase. A plot of $1/k_{1,\text{app}}$ versus q_x that is made according to Equation 2.21 should give a linear relationship with an intercept that is equal to k_1 .¹²⁹ This method makes it possible to correct for the effects of stagnant mobile phase mass transfer on the apparent association rate constant and has been used to estimate the association rate constant of HSA with immobilized anti-HSA antibodies.¹²⁹

Another peak fitting approach that makes use of frontal analysis is based on Equation 2.22.

$$k_{-1} = \frac{2(V_A - V_A^*)}{d\sigma_A^2/dF} \quad (2.22)$$

The terms V_A and V_A^* in this equation are the breakthrough volumes for the retained target and a non-retained solute, respectively, and σ_A^2 is the variance of the breakthrough curve for the target. When using Equation 2.22, a plot of σ_A^2 versus F should give a response that has a slope equal to $(d\sigma_A^2/dF)$.¹⁰⁶ This type of experiment can be conducted at several concentrations of the applied target to provide a series of $(d\sigma_A^2/dF)$ values, which can then be used to find k_{-1} .¹⁰⁶ This method has been used to measure the

dissociation rate constant for *p*-nitrophenyl- α -D-mannopyranoside from immobilized concanavalin A.^{130,131}

One advantage of peak fitting methods is they can be carried out with both zonal elution and frontal analysis under non-linear elution conditions and to study systems with weak-to-moderate binding affinities.¹⁰⁶ The association and dissociation rate constants that have been measured by peak fitting have been in the range of 10^4 to 10^7 $M^{-1}s^{-1}$ and 10^{-1} to 10 s^{-1} , respectively.^{106,116,123,128,131,132} However, it is necessary to test and verify any assumptions that are made in this approach, such as whether mobile phase mass transfer is negligible or needs to be considered when examining the rate of a target's interaction with the immobilized binding agent.^{106,129-131}

Split-peak method

The split-peak method is another technique for carrying out kinetic studies by affinity chromatography.^{7,106} This approach is based on the finite probability that a small fraction of an applied target may elute from the affinity column without interacting with the stationary phase. This effect can be utilized to provide information on the association rate constant k_1 for an injected target with an immobilized binding agent by using an expression such as Equation 2.23.¹³³

$$-\frac{1}{\ln f} = F \left(\frac{1}{k_{m1}V_e} + \frac{1}{k_1 m_L} \right) \quad (2.23)$$

In this equation, f is the non-retained fraction of the target, F is the flow rate, m_L is the moles of immobilized and active binding sites in the column, and V_e is the excluded

volume in the column. The term k_{m1} is the forward mass transfer rate constant for the target as it moves from the flowing mobile phase to the stagnant mobile phase within the support. According to Equation 2.23, a plot of $-1/\ln(f)$ versus F should give a linear relationship when a small amount of target is applied to the column.⁷ If adsorption of the target to the immobilized binding agent is the rate-limiting step in retention, the slope of Equation 2.23 will be $1/(k_1 m_L)$, which can provide the value of the association rate constant k_1 if the value of m_L is also known or obtained through some other means.^{106,133}

The split-peak method was initially used to examine the binding rate of rabbit immunoglobulin G (IgG) to various columns containing immobilized protein A.^{133,134} This method was also used to provide rate information for the optimization of an affinity-based analysis for human IgG in clinical samples,¹³⁵ and to evaluate the association rate constants for IgG on columns containing protein A, protein G, or a mixed-bed of protein A and protein G.¹³⁶ The split-peak method has been modified for use under non-linear elution conditions when the rate-limiting step is the association of a target with the immobilized binding agent. This latter approach has been used to examine the association rates of HSA with immobilized anti-HSA antibodies.¹³⁷⁻¹³⁹ The association rate constants that have been determined by this method have ranged from 10^4 to $10^6 \text{ M}^{-1} \text{ s}^{-1}$.¹³¹⁻¹³⁹

A significant advantage of the split-peak method in kinetic studies is it only requires the measurement of peak areas. This feature makes it easier to perform in comparison with the previous chromatographic methods, in which peak variances or profiles are required.¹⁰⁶ However, the split-peak method can only be used for systems with relatively high affinities and/or slow dissociation rates, which is needed to allow a

good separation to be obtained between the non-retained and retained target fractions.¹⁰⁶ In addition, this technique needs to be carried out under experimental conditions that make it possible to observe the split-peak effect. As shown by Equation 2.23, this effect can be enhanced by increasing the application flow rate for the target or decreasing the size of the column, as well as lowering the amount of active binding agent that is present.¹⁰⁶

Peak decay method

The peak decay method is used to determine the dissociation rate constant for the release of a target from an immobilized binding agent.^{6,7,106} In this technique, the target is first applied to a column that contains the binding agent. One variation of the peak decay method then has a mobile phase applied that contains a high concentration of a competing agent, which will bind to the immobilized agent and prevent the re-association of any target that dissociates from this binding agent.^{6,7} Another variation of this method uses small affinity columns and a large amount of target that is initially applied to the column, which also minimizes the chance that any dissociated target will rebind to the immobilized ligand.^{7,106} In both of these approaches, a high flow rate is usually used during the dissociation step to minimize the effects of stagnant mobile phase mass transfer during dissociation and to prevent the released target from coming into further contact with the immobilized binding agent.¹⁰⁶

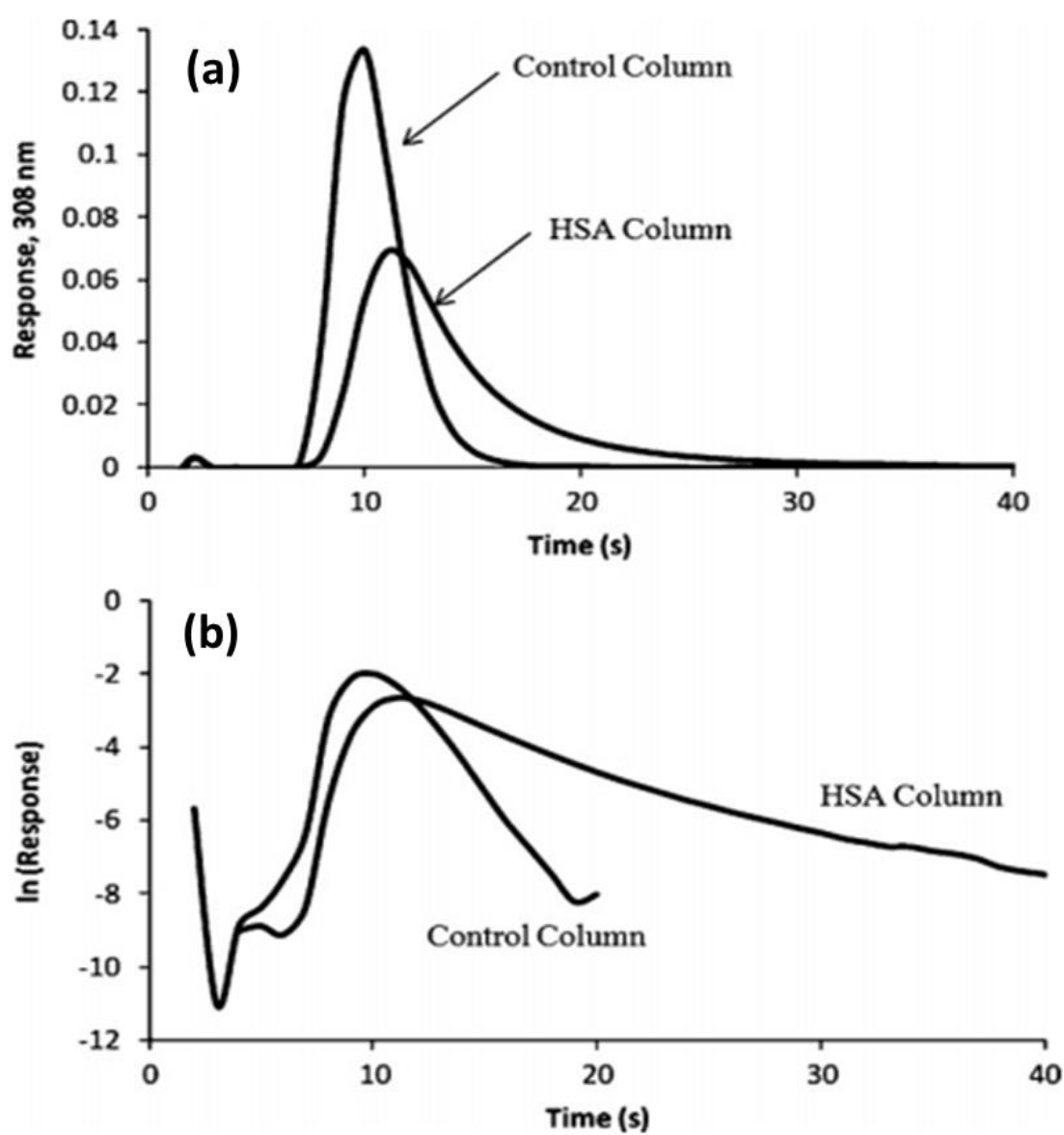
Work under these conditions results in elution of the target from the affinity column in the form of a decay curve. This elution profile can then be converted into a plot of the logarithm of the response versus time, as is described by Equation 2.24.^{7,106}

$$\ln\left(\frac{dm_{\text{Ee}}}{dt}\right) = \ln(m_{\text{Eo}}k_{-1}) - k_{-1}t \quad (2.24)$$

In this equation, m_{Eo} is the initial moles of target that was retained by the immobilized binding agent, m_{Ee} is the moles of target that elutes from the column at time t after the competing agent has been applied or the dissociation step has begun, and k_{-1} is the dissociation rate constant for the target from the immobilized binding agent. Based on Equation 2.24 the slope that is obtained for a plot of the natural logarithm of the response versus time should provide the dissociation rate constant k_{-1} .^{6,140}

The peak decay method was first used to estimate the dissociation rate constant for concanavalin A with the sugar 4-methylumbelliferyl α -D-mannopyranoside by using 4-methylumbelliferyl α -D-galactopyranoside as a competing agent.¹⁴¹ In more recent work, the peak decay method has been adapted to measure the dissociation rate constants of drugs from serum proteins. This is illustrated in Figure 2.8 for racemic warfarin that had been applied to immobilized HSA in a small silica monolith column.¹⁴² Other drugs (e.g., diazepam, imipramine, acetohexamide, tolbutamide, amitriptyline, quinidine, verapamil, amitriptyline, lidocaine, and nortriptyline) and binding agents (e.g., α_1 -acid glycoprotein) have also been studied with this method.^{142,143} The peak decay method has further been employed to study the dissociation rates of various targets from immobilized antibodies during the selection of elution conditions for immunoaffinity chromatography.¹⁴⁴ In addition, this method has been used to characterize the elution

Figure 2.8 Typical results for a peak decay experiment, as obtained from the application of racemic warfarin onto a control monolith column and a monolith column containing immobilized human serum albumin (HSA). The results in (a) give the original elution profiles and the plots in (b) show the natural logarithm of these elution profiles. These results were obtained for a 100 μL injection of 10 μM racemic warfarin. Reproduced with permission from Ref. 143.



kinetics of thyroxine from columns containing anti-thyroxine antibodies or aptamers, and the dissociation of IgG-class antibodies from immobilized protein G.^{145,146}

The peak decay method has been used with application buffers to examine several systems with weak-to-moderate affinities (i.e., $K_1 < 10^6 \text{ M}^{-1}$).¹⁴⁰⁻¹⁴⁴ It has also been used to study the elution conditions needed for systems with stronger binding (e.g., protein G, antibodies and aptamers).^{145,146} The dissociation rate constants that have been measured by the peak decay method range from 10^{-2} to 10^1 s^{-1} .^{6,106,140-146} Data analysis in this method is relatively easy to carry out, because it is based on linear regression of a logarithmic elution profile, and this method is valuable in characterizing elution conditions. However, non-specific interactions of the target within the column must be considered and corrected for by using a control column, especially for targets that may have weak-to-moderate interactions with the immobilized binding agent. This tends to limit the use of this method in these latter cases to the measurement of dissociation rate constants that are less than about $1\text{-}2 \text{ s}^{-1}$.¹⁴⁴ Moreover, the experimental conditions that are required to make dissociation the rate-determining step in elution, and target re-association negligible, may be difficult to obtain for some systems.¹⁴¹⁻¹⁴⁴

Advantages and potential limitations

One general advantage of using affinity chromatography or HPAC to examine the kinetics of a biological interaction is the ability to reuse the same immobilized binding agent for many experiments.⁶⁻¹⁰ This feature helps to improve the reproducibility of the method and lowers the cost per analysis. The variety of approaches that are available for

kinetic measurements in affinity chromatography is another valuable feature of this technique. Altogether, the chromatographic methods that were described in this section have been used to measure association rate constants that have spanned from 10^3 to 10^7 $M^{-1} s^{-1}$ and dissociation rate constants that have ranged from 10^{-2} to $10^1 s^{-1}$. Several of these techniques work well with systems that have relatively weak interactions, a feature which makes these methods complementary to SPR for such work.^{97,106}

Like SPR, these affinity methods are usually “label free” but often use an immobilized binding agent as one of the interacting partners.^{6-10,19} One difference from SPR is that various supports and surfaces can now be used for the immobilizing binding agent since detection is carried out after the target or other sample components have eluted from the column.^{6-10,19} Many detection methods can be used with these affinity columns (e.g., absorbance, fluorescence, or mass spectrometry), which further aids in allowing this group of methods to be used in examining a variety of biological systems.⁶⁻

10

Various immobilization methods are available for coupling binding agents within affinity columns. These methods might again involve the use of amines, thiols, or other groups for the immobilization of proteins or alternative binding agents. It is further possible to use capturing agents such as immobilized streptavidin for biotin-labeled binding agents or protein A for immunoglobulins.^{81,107,111,113,147} The correct selection and validation of the immobilization conditions are needed to provide a binding agent in the affinity column that is a good model for the same binding agent in its native environment. However, as was noted for SPR, there are needs in the methods that can use affinity chromatography to investigate solution-phase reactions.^{7,8,106}

Capillary Electrophoresis

General principles

CE is a second separation technique that has been used to investigate the kinetics of biological interactions. In CE, a narrow-bore capillary is filled with a running buffer or electrolytic solution. A defined volume of sample is then introduced into the capillary, and an electric field is applied across this capillary. The components of the sample are separated based on their differences in migration rates and electrophoretic mobilities. A detector, which is located at the opposite side of the capillary, is used to monitor the migration of these components.¹⁴⁸

When CE is used in kinetic studies, the free forms of P or L in a sample can be separated from their complex PL if there are differences in the electrophoretic mobilities and migration rates of these reactants and product in the capillary. The rate of the interaction for P with L , or for the dissociation of PL , can be determined by monitoring the changes in one or more of these peaks as a function of reaction time.¹⁴⁸⁻¹⁵⁷ Various formats for carrying out such studies are discussed in this section.

Analysis of slow biological reactions

One way CE can be used for kinetic measurements is to study interactions that have long reaction times (e.g., hours) and small dissociation rate constants (i.e., k_{-1} values in the range of 10^{-3} to 10^{-6} s^{-1}).¹⁴⁸⁻¹⁵⁴ To investigate this type of reaction, the target and binding agent can be mixed prior to their injection onto the CE system. Samples of this

reaction mixture are injected at known times. The non-bound and bound target are then separated based on the differences in their electrophoretic mobilities, with the results being used to determine the amount of complex that has formed between the target and binding agent at various reaction times.

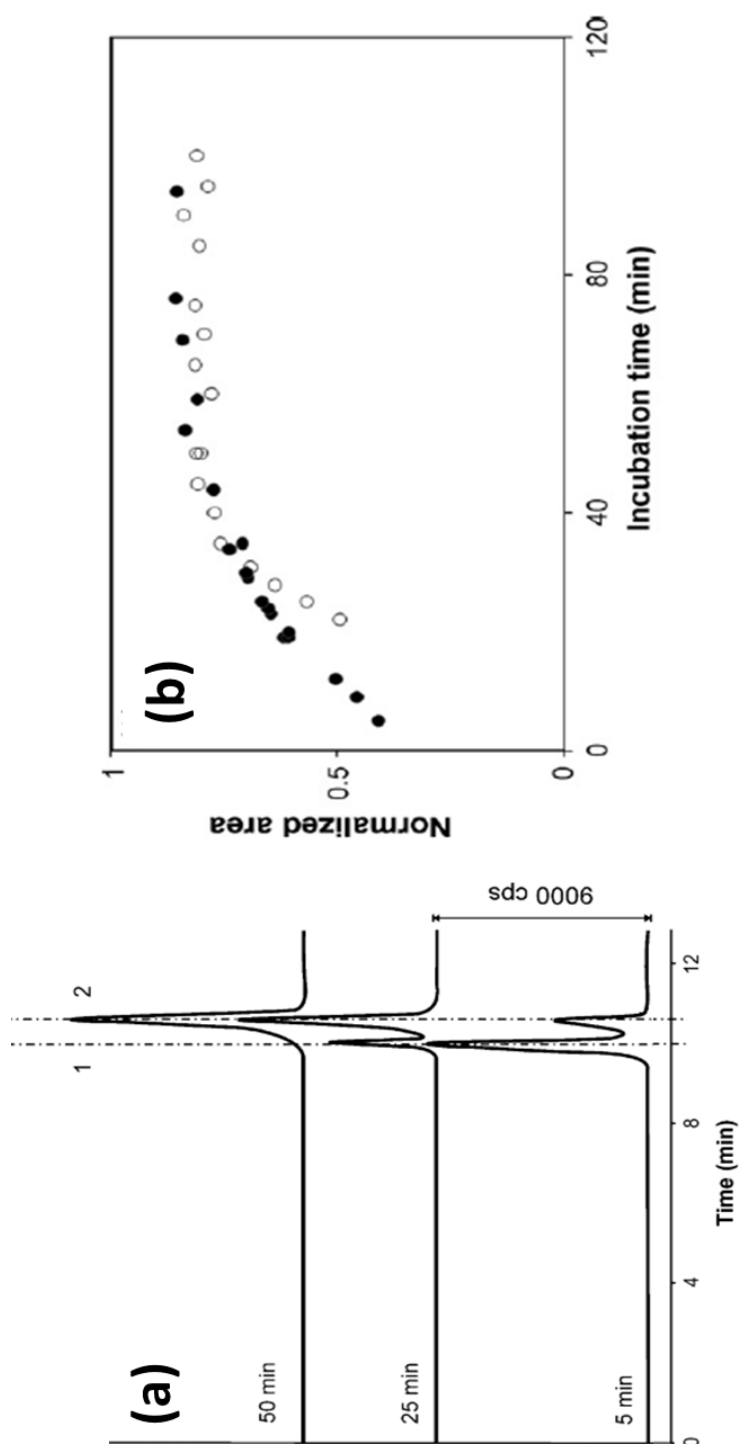
For a reaction that is slow on the timescale of the CE separation and that has slow dissociation, the interaction of target L with binding agent P can be approximately described by the following equation.

$$\ln \frac{[PL]}{[L_{\text{tot}}]} = -k_{\text{obs}}t \quad (2.25)$$

In this equation, $[PL]$ is the measured concentration of the complex at time t , $[L_{\text{tot}}]$ is the total concentration of L , and k_{obs} is the observed rate constant for this interaction.

Figure 2.9 shows an electropherogram that was obtained in this type of experiment. This particular study examined the interaction of a ruthenium(III)-containing drug with HSA and transferrin, with detection being carried out by CE coupled with inductively coupled plasma-mass spectrometry.¹⁴⁹ A similar method has been used to determine rate constants for the interactions of ruthenium(III)-containing drugs with holo-transferrin and for platinum(II)-containing drugs with HSA.^{150,151} Another report examined the reaction of cisplatin with 2'-deoxyguanosine 5'-monophosphate, as based on the use of CE coupled with electrospray ionization mass spectrometry.¹⁵⁵

Figure 2.9 (a) Electropherograms used to study the interaction kinetics of albumin with indazolium *trans*-[tetrachlorobis(1*H*-indazole)ruthenate(III)] (KP1019): peaks, (1) *trans*-[RuCl₄(1*H*-indazole)₂][−], and (2) ruthenium (III)–albumin complex. The plots in (b) show the relative peak areas for the ruthenium (III)-protein complexes as a function of reaction time for experiments conducted with KP1019 and albumin (black circles) or transferrin (open circles). Adapted with permission from Ref. 149.



Kinetic capillary electrophoresis

Kinetic capillary electrophoresis (KCE) is another method that can be used to determine kinetic parameters for biological interactions. This is a type of CE in which the species in the system of interest are interacting during their separation.^{20,156-159} Various types of KCE have been developed to measure kinetic and thermodynamic parameters for biological interactions. These methods include non-equilibrium capillary electrophoresis of equilibrium mixtures (NECEEM), continuous NECEEM (cNECEEM), sweeping capillary electrophoresis (SweepCE), short SweepCE (sSweepCE), short SweepCE of equilibrium mixtures (sSweepCEEM), plug-plug KCE (ppKCE), and equilibrium capillary electrophoresis of equilibrium mixtures (ECEEM).^{20,156-159} A few examples of these methods are shown in Figure 2.10.




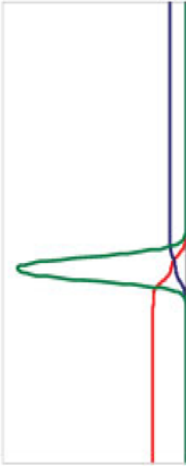

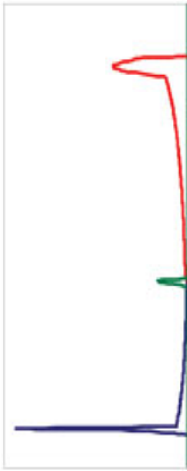
The main model that is used in KCE methods for the measurement of rate constants is the biomolecular reaction between P and L to form PL , as described earlier in Equation 2.5. KCE methods are based on the separation of P , L , and PL according to the differences in their electrophoretic velocities, as represented by v_L , v_P , and v_{PL} , respectively. This separation can be described by the following set of partial differential equations.^{20,156-159}

$$\frac{\partial [L]_{t,x}}{\partial t} + v_L \frac{\partial [L]_{t,x}}{\partial x} = -k_1 [L]_{t,x} [P]_{t,x} + k_{-1} [PL]_{t,x} \quad (2.26)$$

$$\frac{\partial [P]_{t,x}}{\partial t} + v_P \frac{\partial [P]_{t,x}}{\partial x} = -k_1 [L]_{t,x} [P]_{t,x} + k_{-1} [PL]_{t,x} \quad (2.27)$$

$$\frac{\partial [PL]_{t,x}}{\partial t} + v_{PL} \frac{\partial [PL]_{t,x}}{\partial x} = -k_{-1} [PL]_{t,x} + k_1 [L]_{t,x} [P]_{t,x} \quad (2.28)$$

Figure 2.10 Some typical methods used in kinetic capillary electrophoresis, along with their simulated concentration profiles and initial or boundary conditions. The methods that are illustrated here are (a) non-equilibrium capillary electrophoresis of equilibrium mixture (NECEEM), (b) sweeping capillary electrophoresis (SweepCE), and (c) plug-plug KCE (ppKCE). Adapted with permission from Ref. 157.

<p>(a) NECEEM</p>  	<p>Initial Conditions</p> $[P]_{0,x} = [P]\theta_x \theta_{l-x}$ $[L]_{0,x} = [L]\theta_x \theta_{l-x}$ $[PL]_{0,x} = [PL]\theta_x \theta_{l-x}$ $K_1 = [P][L]/[PL]$	<p>Boundary conditions</p> $[P]_{t,0} = 0$ $[L]_{t,0} = 0$ $[PL]_{t,0} = 0$
<p>(b) SweepCE</p>  	<p>Initial Conditions</p> $[P]_{0,x} = [P]$ $[L]_{0,x} = 0$ $[PL]_{0,x} = 0$	<p>Boundary conditions</p> $[P]_{t,0} = [P]$ $[L]_{t,0} = 0$ $[PL]_{t,0} = 0$
<p>(c) ppKCE</p>   <p>Migration time to the detector</p>	<p>Initial Conditions</p> $[P]_{0,x} = [P]\theta_x \theta_{l(p)-x}$ $[L]_{0,x} = [L] \theta_{x-l(l)} \theta_{l(p)+l(l)-x}$ $[PL]_{0,x} = 0$	<p>Boundary conditions</p> $[P]_{t,0} = 0$ $[L]_{t,0} = 0$ $[PL]_{t,0} = 0$

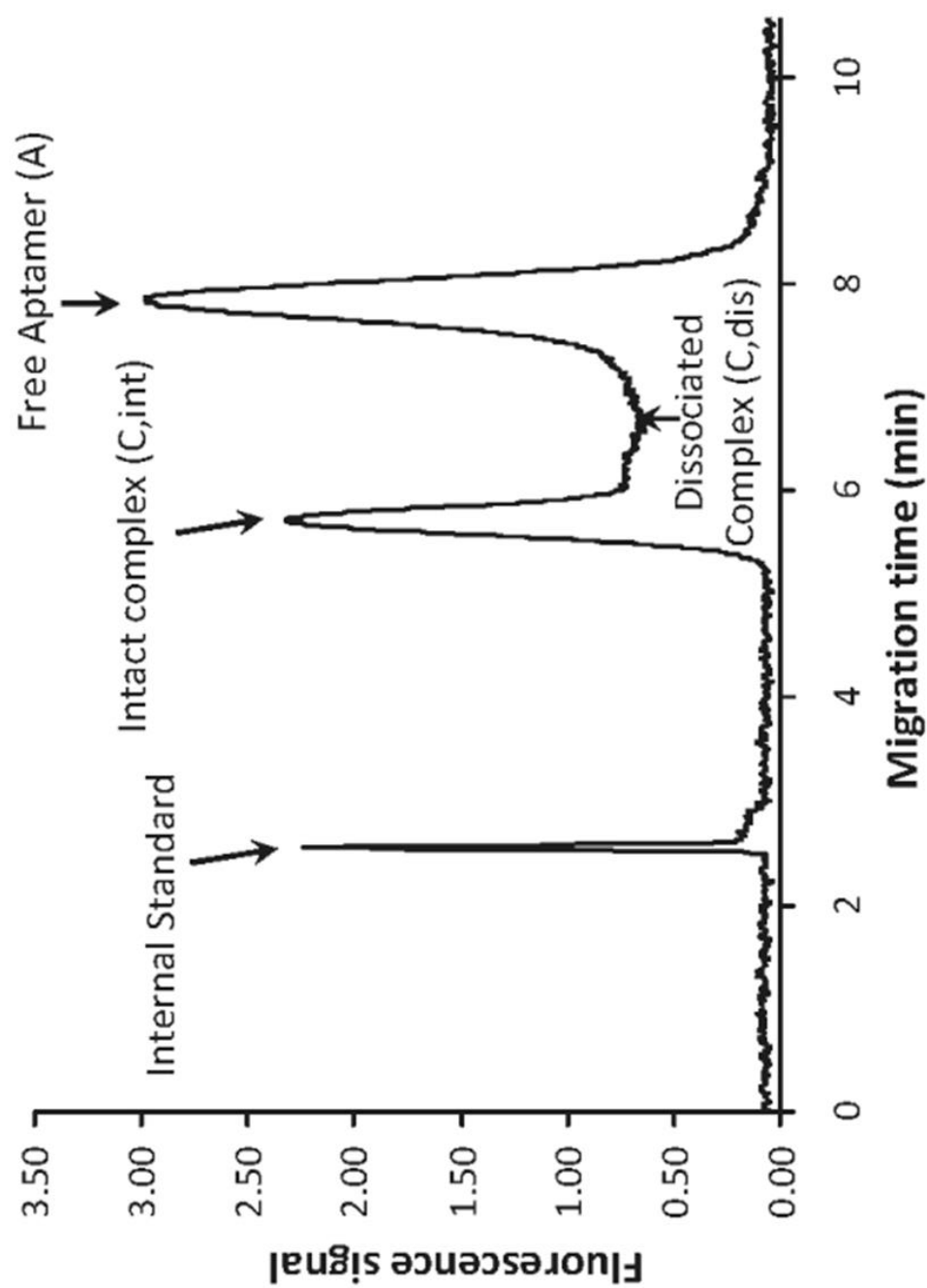
In these equations, $[P]$, $[L]$ and $[PL]$ are the concentrations of P , L and PL at time t (i.e., the time that has elapsed since the beginning of separation), and x is the distance from the injection end of the capillary.

The solution to the expressions in Equations 2.26-2.28 is found by using the initial and boundary conditions for the given separation system. These conditions include the initial distribution of L , P , and PL along the length of the capillary, and the manner in which L , P and PL are injected into and eluted from the capillary. Based on these conditions, the solution to Equations 2.26-2.28 can be determined through numerical or non-numerical methods and by making certain assumptions.^{156,157,160} This solution can then be tested by fitting the experimental data to the predicted electropherograms, and the binding parameters can be determined through non-linear regression.^{156,157,160}

Figure 2.10 includes the initial conditions and boundary conditions for some representative KCE methods.^{20,157} The simulated concentration profiles for these methods are also provided. For example, in NECEEM the capillary is originally filled with only a running buffer. A small sample plug containing a mixture of P and L at equilibrium is injected into this capillary. Separation of the components in this mixture (P , L and PL) occurs as the sample passes through the capillary. However, during this separation the initial equilibrium is disturbed and dissociation occurs for the complex PL , which is reflected in the shape of the resulting electropherogram.

Figure 2.11 shows a typical electropherogram for an NECEEM experiment, as obtained in experiments investigating the interaction of the AlkB protein from *E. coli* with a fluorescent labeled DNA aptamer.¹⁶¹ As the protein-aptamer complex dissociated

Figure 2.11 Electropherogram obtained in studies of the interaction between the AlkB protein and its DNA aptamer by using non-equilibrium capillary electrophoresis of equilibrium mixtures (NECEEM). Adapted with permission from Ref. 161.



during the CE separation, the result was a distribution of the aptamer between the peaks for the complex and free aptamer. The areas of the peaks and overlapping regions in the electrophoreograms, which were related to the concentrations of the reacting components, were measured and used to find the rate constants for this system.¹⁶¹

Examples of applications using other KCE methods can be found in Refs. 20,157-159,162. KCE has been utilized to provide binding strengths and rate constants for several systems, including protein-oligonucleotide, protein-peptide, protein-small molecule, and oligonucleotide-small molecule interactions.^{20,156,157,159,161-168} These methods have been used to measure dissociation rate constants that have ranged from 10^{-4} to 1 s^{-1} ,^{156,157,163,169} and association rate constants that have ranged from 10^1 to $10^7 \text{ M}^{-1} \text{ s}^{-1}$.^{161,162,164,165,166-169}

A multi-method KCE toolbox has also been developed to examine biological interactions. This approach involves proposing a reaction model between L and P , such as the one in Equation 2.5, and then testing this model with several KCE methods. If a significant deviation is seen between the predicted results and the data for one or more methods, the reaction model is modified until a satisfactory fit is obtained by each KCE method. This approach has been used with six KCE methods to study the interactions between single-stranded DNA and ssDNA-binding protein. The results indicated that both specific and non-specific interactions were present in this system.^{20,157}

Advantages and potential limitations

Advantages to using CE for the study of biological interactions are the efficiency, speed and small sample requirements of this method.^{148,151-153} One essential requirement for this approach is that a suitable difference in electrophoretic mobility must be present between the reactants and products of the interaction. The degree of separation of these species and their concentrations must also be sufficient to allow a measurable signal to be obtained that is related to the change in concentration of one or more of these chemicals over time.¹⁷⁰

The CE methods that were discussed in this section have been used to examine a number of systems with a relatively large range of rate constants. For instance, the overall range of dissociation rate constants that have been measured by CE is 10^{-6} to 1 s^{-1} ^{156,157,163,169} and the association rate constants have spanned from 1 to $10^7 \text{ M}^{-1} \text{ s}^{-1}$ ^{161,162,164,165,166-169}

CE allows biological interactions to be studied in solution without the need for immobilization of one of the reagents. It is important to remember, however, that some biomolecules such as proteins can adsorb to bare silica capillaries, as are often used in CE. This may lead to a loss in peak area or create peak tailing. If present, this effect needs to be considered by adding in an additional term into the differential equations in KCE methods. Alternatively, the running buffer's composition or pH can be modified or a coating on the capillary wall can be employed to minimize this adsorption.^{157,171}

Conclusions

This chapter examined various techniques that are used in the study of biological interactions. Traditional or common methods such as stopped-flow analysis and SPR were considered, as well as separation-based measurements based on affinity chromatography or CE. The general principles of these techniques were described, and it was shown how each approach could be utilized to provide information on the rate constants for a biological interaction. Several applications were also provided, and the advantages or potential limitations of each method were discussed.

Most of these methods are used to examine reversible bimolecular interactions or the dissociation of biological complexes. However, some of these approaches are also suitable for examining unimolecular interactions and multistep processes. Some of these techniques (e.g., stopped-flow analysis and CE) are used with solution-phase interactions, while others require an immobilized binding agent (SPR and affinity chromatography). These methods have been used to examine many processes, including the interactions of enzymes with peptides or coenzymes, protein-protein interactions, and the binding of proteins with DNA, RNA or small solutes (e.g., lipids, hormones, drugs, and metal ions). A broad range of rate constants can also be measured by this set of techniques.

The selection of an analytical method for such measurements will depend on the nature of the system being studied, the anticipated rate and complexity of the reaction, and the detectability and concentrations of the reactants or products, among other factors. However, given the set of tools that are already available, it is expected that kinetic measurements of biological systems will continue to grow in their scope and availability.

as work continues in this field. These efforts should make it possible to obtain even more detailed information on the rates and mechanisms of biological interactions, which should be valuable in areas such as pharmaceutical science, clinical chemistry, and biomedical research.

References

1. M.A. Williams, Protein-ligand interactions: fundamentals, in: M.A. Williams, T. Daviter (Eds.), *Protein-Ligand Interactions, Methods and Applications*, Springer, New York, 2013, pp. 3-34.
2. G. Schreiber, G. Haran, H.-X. Zhou, *Chem. Rev.* 109 (2009) 839-860.
3. A. Frostell, L. Vinterback, H. Sjobom, Protein-ligand interactions using SPR systems, in: M.A. Williams, T. Daviter (Eds.), *Protein-Ligand Interactions, Methods and Applications*, Springer, New York, 2013, pp. 139-165.
4. D.G. Myszka, R.L. Rich, *Pharm. Sci. Technol. Today* 3 (2000) 310-317.
5. K. Vuignier, J. Schappler, J. Veuthey, P. Carrupt, S. Martel, *Anal. Bioanal. Chem.* 398 (2010) 53-66.
6. I.M. Chaiken, *Analytical Affinity Chromatography*, CRC Press, Boca Raton, 1987.
7. X. Zheng, Z. Li, S. Beeram, M. Podariu, R. Matsuda, E.L. Pfau Miller, C.J. White II, N. Carter, D.S. Hage, *J. Chromatogr. B* 968 (2014) 49-63.
8. D.S. Hage, Affinity chromatography, in: D. Corradini, E. Katz, R. Eksteen, P. Shoenmakers, N. Miller (Eds.), *Handbook of HPLC*, Marcel Dekker, New York, 1998, pp. 483-498.
9. J.E. Schiel, R. Mallik, S. Soman, K.S. Joseph, D.S. Hage, *J. Sep. Sci.* 29 (2006) 719-737.

10. R. Mallik, D.S. Hage, J. Sep. Sci. 29 (2006) 1686–1704.
11. T.C. Kwong, Clin. Chim. Acta 151 (1985) 193–216.
12. C.K. Svensson, M.N. Woodruff, J.G. Baxter, D. Lalka, Clin. Pharmacokin. 11(1986) 450–469.
13. D.C. Carter, J.X. Ho, Adv. Prot. Chem. 45 (1994) 153–203.
14. J.B. Whitlam, K.F. Brown, J. Pharm. Sci. 70 (1981) 146–150.
15. S. Liu, L. Zhang, X. Zhang, Anal. Sci. 22 (2006) 1515–1518.
16. Y.S.N. Day, D.G. Myszka, J. Pharm. Sci. 92 (2003) 333–343.
17. A. Sulkowska, B. Bojko, J. Rownicka, P. Rezner, W.W. Sulkoński, J. Mol. Struct. 744–747 (2005) 781–787.
18. M.D. Shortridge, K.S. Mercier, D.S. Hage, G.S. Harbison, R. Powers, J. Comb. Chem. 10 (2008) 948–958.
19. D.S. Hage, A. Jackson, M.R. Sobansky, J.E. Schiel, M.J. Yoo, K.S. Joseph, J. Sep. Sci. 32 (2009) 835–853.
20. S.N. Krylov, Electrophoresis 28 (2007) 69–88.
21. S.R. Martin, M.J. Schilstra, Rapid mixing kinetic techniques, in: M.A. Williams, T. Daviter (Eds.), Protein-Ligand Interactions, Methods and Applications, Springer, New York, 2013, pp. 119–138.

22. J.H. Espenson, *Chemical Kinetics and Reaction Mechanisms*, McGraw-Hill, New York, 1981.
23. H.A. Mottola, *Kinetic Aspects of Analytical Chemistry*, Wiley, New York, 1988.
24. A. Gomez-Hens, D. Perez-Bendito, *Anal. Chim. Acta* 242 (1991) 147-177.
25. D. Perez-Bendito, A. Gomez-Hens, M. Silva, *J. Pharm. Biomed. Anal.* 14 (1996) 917-930.
26. H.L. Pardue, *Anal. Chim. Acta*, 216 (1989) 69-107.
27. D. Perez-Bendito, M. Silva, *Kinetic Methods in Analytical Chemistry*, Ellis Horwood, Chichester, 1988.
28. H. Roder, K. Maki, H. Cheng, M.C.R. Shastri, *Methods* 34 (2004) 15-27.
29. J.M. Mason, U.B. Hagemann, K.M. Arndt, *J. Biol. Chem.* 282 (2007) 23015-23024.
30. K.M. Youngman, D.B. Spencer, D.N. Brems, M.R. DeFelippis, *J. Biol. Chem.* 270 (1995) 19816-19822.
31. Z. Wang, W. Watt, N.A. Brooks, M.S. Harris, J. Urban, D. Boatman, M. McMillan, M. Kahn, R.L. Heinrikson, B.C. Finzel, A.J. Wittwer, J. Blinn, S. Kamtekar, A.G. Tomasselli, *Biochim. Biophys. Acta* 1804 (2010) 1817-1831.
32. J.S. Shin, M.H. Yu, *J. Biol. Chem.* 277 (2002) 11629-11635.

33. C.N. Chi, A. Bach, M. Gottschalk, A.S. Kristensen, K. Stromgaard, P. Jemth, J. Biol. Chem. 285 (2010) 28252-28260.
34. E.M. Isin, F.P. Guengerich, J. Biol. Chem. 281 (2006) 9127-9136.
35. A. Adams, J.M. Guss, C.A. Collyer, W.A. Denny, A.S. Prakash, L.P. Wakelin, Mol. Pharmacol. 58 (2000) 649-658.
36. E.M. Isin, F.P. Guengerich, J. Biol. Chem. 282 (2007) 6863-6874.
37. A. Garcon, A. Bermingham, L.Y. Lian, J.P. Derrick, Biochem. J. 380 (2004) 867-873.
38. R.P. Bandwar, S.S. Patel, J. Biol. Chem. 276 (2001) 14075-14082.
39. M. Oertle, C. Richter, K.H. Winterhalter, E.E. Di Iorio, Proc. Natl. Acad. Sci. U.S.A. 82 (1985) 4900-4904.
40. R.D. Gray, J. Biol. Chem. 253 (1978) 4364-4369.
41. O. Corcoran, R.W. Mortensen, S.H. Hansen, J. Troke, J.K. Nicholson, Chem. Res. Toxicol. 14 (2001) 1363-1370.
42. R.W. Mortensen, O. Corcoran, C. Cornett, U.G. Sidelmann, J.C. Lindon, J.K. Nicholson, S.H. Hansen, Drug Metab. Dispos. 29 (2001) 375-380.
43. E. Mahdavian, H.T. Spencer, R.B. Dunlap, Arch. Biochem. Biophys. 368 (1999) 257-264.

44. T. Inobe, M. Arai, M. Nakao, K. Ito, K. Kamagata, T. Makio, Y. Amemiya, H. Kihara, K. Kuwajima, *J. Mol. Biol.* 327 (2003) 183-91.
45. I.G. Gazaryan, B.F. Krasnikov, G.A. Ashby, R.N. Thorneley, B.S. Kristal, A.M. Brown, *J. Biol. Chem.* 277 (2002) 10064-10072.
46. W. Wang, D.K. Smith, K. Moulding, H.M. Chen, *J. Biol. Chem.* 273 (1998) 27438-27448.
47. J.M. Beechem, L. James, L. Brand, *SPIE Proc.* 1204 (1990) 686–698.
48. B.E. Jones, J.M. Beechem, C.R. Matthews, *Biochemistry* 34 (1995) 1867–1877.
49. J. Balbach, V. Forge, N.A.J. van Nuland, S.L. Winder, P.J. Hore, C.M. Dobson, *Nat. Struct. Biol.* 2 (1995) 865–870.
50. C. Frieden, *Biochemistry* 42 (2003) 12439–12446.
51. D.J. Segel, A. Bachmann, J. Hofrichter, K.O. Hodgson, S. Doniach, T. Kiefhaber, *J. Mol. Biol.* 288 (1999) 489–499.
52. T. Terpstra, J. McNally, T.H. Han, N.T. Ha-Duong, J.M. El-Hage-Chahine, F. Bou-Abdallah, *J. Inorg. Biochem.* 136 (2014) 24-32.
53. V. Maes, Y. Engelborghs, J. Hoebeke, Y. Maras, A. Vercruysse, *Mol. Pharmacol.* 21 (1982) 100-107.
54. E.R. Jamieson, S.J. Lippard, *Biochemistry* 39 (2000) 8426-8438.
55. X. Zhao, S. Yu, R.S. Magliozzo, *Biochemistry* 46 (2007) 3161-3170.

56. Y. Feng, N. Xie, M. Jin, M.R. Stahley, J.T. Stivers, Y.G. Zheng, *Biochemistry* 50 (2011) 7033-7044.
57. S. Nijvipakul, D.P. Ballou, P. Chaiyen, *Biochemistry* 49 (2010) 9241-9248.
58. M.A. Moxley, D.F. Becker, *Biochemistry* 51 (2012) 511-520.
59. N. Barbero, L. Napione, S. Visentin, M. Alvaro, A. Veglio, F. Bussolino, G. Viscardi, *Chem. Sci.* 2 (2011) 1804-1809.
60. A.K. Eaton, R.C. Stewart, *Biochemistry* 49 (2010) 5799-5809.
61. B.J. Reeder, D.A. Svistunenko, M.T. Wilson, *Biochem. J.* 434 (2011) 483-492.
62. N. Adamek, M.A. Geeves, *EXS* 105 (2014) 87-104.
63. M. Furch, M.A. Geeves, D.J. Manstein, *Biochemistry* 37(1998) 6317-6326.
64. B. Iorga, N. Adamek, M.A. Geeves, *J. Biol. Chem.* 282 (2007) 3559-3570.
65. M. Bloemink, J. Deacon, S. Langer, C. Vera, A. Combs, L. Leinwand, M.A. Geeves, *J. Biol. Chem.* 289 (2014) 5158-5167.
66. C. Dumortier, M.J. Gorbunoff, J.M. Andreu, Y. Engelborghs, *Biochemistry* 35 (1996) 4387-4395.
67. C. Dumortier, J.L. Potenziano, S. Bane, Y. Engelborghs, *Eur. J. Biochem.* 249 (1997) 265-269.

- 68. M.A. Khan, H. Miyoshi, S. Ray, T. Natsuaki, N. Suehiro, D.J. Goss, J. Biol. Chem, 281 (2007) 28002-28010.
- 69. T. Heidebrecht, A. Fish, E. von Castelmur, K.A. Johnson, G. Zaccai, P. Borst, A. Perrakis, J. Am. Chem. Soc. 134 (2012) 13357-13365.
- 70. D.E. Otzen, K. Blans, H. Wang, G.E. Gilbert, J.T. Rasmussen, Biochim. Biophys. Acta 1818 (2012) 1019-1027.
- 71. D.L. Garland, Biochemistry 17 (1978) 4266-4272.
- 72. L.R. Yarbrough, F.Y. Wu, C.W. Wu, Biochemistry 15 (1976) 2669-2676.
- 73. I.M. Verhamme, P.E. Bock, J. Biol. Chem. 283 (2008) 26137-26147.
- 74. D.J. Scott, A.L. Ferguson, M-T. Gallegos, M. Pitt, M. Buck, J.G. Hoggett, Biochem. J. 352 (2000) 539-547.
- 75. L. Zhao, M.G. Pence, R.L. Eoff, S. Yuan, C.A. Fercu, F.P. Guengerich, FEBS J. 281 (2014) 4394-4410.
- 76. E. Kovacs, J. Toth, B.G. Vertessy, K. Liliom, J. Biol. Chem. 285 (2010) 1799-1808.
- 77. A.M. Wands, N. Wang, J.K. Lum, J. Hsieh, C.A. Fierke, A.K. Mapp, J. Biol. Chem. 286 (2011) 16238-16245.
- 78. Y. Gong, H. Tang, C. Bohne, E. Plettner, Biochemistry 49 (2010) 793-801.
- 79. O. Ecevit, M.A. Khan, D.J. Gross, Biochemistry 49 (2010) 2627-2635.

80. C. Kalidas, *Chemical Kinetic Methods: Principles of Fast Reaction Techniques and Applications*, second ed., New Age International, Delhi, India, 2005.
81. S.D. Long, D.G. Myszka, Affinity-based optical biosensors in: D.S. Hage (Ed.), *Handbook of Affinity Chromatography*, second ed., CRC Press, Boca Raton, FL, 2006, pp. 685–696.
82. J. Homola, S.S. Yee, G. Gauglitz, *Sensors Actuators B: Chem.* 54 (1999) 3-15.
83. H.N. Daghestani, B.W. Day, *Sensors* 10 (2010) 9630-9646.
84. P.A. Van Der Merwe, Surface plasmon resonance, in: S.E. Harding, B.Z. Chowdhry (Eds.), *Protein-Ligand Interactions: Hydrodynamics and Calorimetry*, first ed., Oxford University Press, UK, 2001, pp. 137-170.
85. S.G. Patching, *Biochim. Biophys. Acta.* 1838 (2014) 43-55.
86. P.R. Edwards, C.H. Maule, R.J. Leatherbarrow, D.J. Winzor, *Anal. Biochem.* 263 (1998) 1-12.
87. A.J.T. George, R.R. French, M.J. Glennie, *J. Immunol. Methods* 183 (1995) 51-63.
88. C.T. Campbell, G. Kim, *Biomaterials* 28 (2007) 2380-2392.
89. K.E. Komolov, M. Aguila, D. Toledo, J. Manyosa, P. Garriga, K.W. Koch, *Anal. Bioanal. Chem.* 397 (2010) 2967-2976.

90. C. Bich, M. Scott, A. Panagiotidis, R.J. Wenzel, A. Nazabal, R. Zenobi, *Anal. Biochem.* 375 (2008) 35-45.
91. S. Hearty, P. Leonard, R. O'Kennedy, *Methods Mol. Biol.* 907 (2012) 411-442.
92. H. Zhao, I.I. Gorshkova, G.L. Fu, P. Schuck, *Methods* 59 (2013) 328-335,
93. J. Pollet, F. Delport, K.P. Janssen, K. Jans, G. Maes, H. Pfeiffer, M. Wevers, J. Lammertyn, *Biosens. Bioelectron.* 25 (2009) 864-869.
94. P. Vacha, I. Zuskova, L. Bumba, P. Herman, J. Vecer, V. Obsilova, T. Obsil, *Biophys. Chem.* 184 (2013) 68-78.
95. M.C. Jecklin, S. Schauer, C.E. Dumelin, R. Zenobi, *J. Mol. Recognit.* 22 (2009) 319-329.
96. A. Zhukov, S.P. Andrews, J.C. Errey, N. Robertson, B. Tehan, J.S. Mason, F.H. Marshall, M. Weir, M. Congreve, *J. Med. Chem.* 54 (2011) 4312-4323.
97. G.A. Papalia, S. Leavitt, M.A. Bynum, P.S. Katsamba, R. Wilton, H. Qiu, M. Steukers, S. Wang, L. Bindu, S. Phogat, A.M. Giannetti, T.E. Ryan, V.A. Pudlak, K. Matusiewicz, K.M. Michelson, A. Nowakowski, A. Pham-Baginski, J. Brooks, B.C. Tieman, B.D. Bruce, M. Vaughn, M. Baksh, Y.H. Cho, M.D. Wit, A. Smets, J. Vandersmissen, L. Michiels, D.G. Myszka, *Anal. Biochem.* 359 (2006) 94-105.
98. C. Tassa, M. Liong, S. Hilderbrand, J.E. Sandler, T. Reiner, E.J. Keliher, R. Weissleder, S.Y. Shaw, *Lab. Chip* 12 (2012) 3103-3110.

99. L.S. Jung, K.E. Nelson, C.T. Campbell, P.S. Stayton, S.S. Yee, V. Pérez-Luna, G.P. López, *Sensors Actuators B: Chem.* 54 (1999) 137-144.
100. C. Boozer, G. Kim, S. Cong, H. Guan, T. Londergan, *Curr. Opin. Biotechnol.* 17 (2006) 400-405.
101. R. Karlsson, *J. Mol. Recogn.* 17 (2004) 151-161.
102. C. Jimenez-Castells, S. Defaus, A. Moise, M. Przbylski, D. Andreu, R. Gutierrez-Gallego, *Anal. Chem.* 84 (2012) 6515-6520.
103. T. Natsume, H. Nakayama, O. Jansson, T. Isobe, K. Takio, K. Mikoshiba, *Anal. Chem.* 72 (2000) 4193-4198.
104. C. Hahnefeld, S. Drewianka, F. Herberg, Determination of kinetic data using surface plasmon resonance biosensors, in: J. Decler, U. Reischl (Eds.), *Molecular Diagnosis of Infectious Diseases*, Humana Press, 2004, pp. 299-320.
105. D.J. Winzor, Quantitative affinity chromatography: recent theoretical developments, in: D.S. Hage (Ed.), *Handbook of Affinity Chromatography*, second ed., CRC Press, Boca Raton, FL, 2006, pp. 629-662.
106. J.E. Schiel, D.S. Hage, *J. Sep. Sci.* 32 (2009) 1507-1522.
107. D.S. Hage, P.F. Ruhn, An introduction to affinity chromatography in: D.S. Hage (Ed.), *Handbook of Affinity Chromatography*, second ed., CRC Press, Boca Raton, FL, 2006, pp. 3-13.
108. R.R. Walters, *Anal. Chem.* 57 (1985) 1099A-1114A.

109. P. Cuatrecasas, M. Wilchek, C.B. Anfinsen, Selective enzyme purification by affinity chromatography, *Proc. Natl. Acad. Sci. U.S.A.* 61 (1968) 636–643.
110. J. Turkova, *Affinity Chromatography*, Elsevier, Amsterdam, 1978.
111. D.S. Hage (Ed.), *Handbook of Affinity Chromatography*, second ed., CRC Press, Boca Raton, FL, 2006.
112. J.E. Schiel, C.M. Ohnmacht, D.S. Hage, *Anal. Chem.* 81 (2009) 4320–4333.
113. D.S. Hage, J. Chen, Quantitative affinity chromatography: practical aspects, in: D.S. Hage (Ed.) *Handbook of Affinity Chromatography*, second ed., CRC Press, Boca Raton, FL, 2006, pp. 595–628.
114. B. Loun, D.S. Hage, *Anal. Chem.* 68 (1996) 1218–1225.
115. J. Yang, D.S. Hage, *J. Chromatogr. A* 766 (1997) 15–25.
116. M.J. Yoo, D.S. Hage, *J. Sep. Sci.* 32 (2009) 2776–2785.
117. M.J. Yoo, J.E. Schiel, D.S. Hage, *J. Chromatogr. B* 878 (2010) 1707–1713.
118. Z. Tong, J.E. Schiel, E. Papastavros, C.M. Ohnmacht, Q.R. Smith, D.S. Hage, *J. Chromatogr. A* 1218 (2011) 2065–2071.
119. A.M. Talbert, G.E. Tranter, E. Holmes, P.L. Francis, *Anal. Chem.* 74 (2002) 446–452.
120. I. Fitos, J. Visy, J. Kardos, *Chirality* 14 (2002) 442–448.
121. Z. Tong, D.S. Hage, *J. Chromatogr. A* 1218 (2011) 6892–6897.
122. H. Li, J. Ge, T. Guo, S. Yang, Z. He, P. York, L. Sun, X. Xu, J. Zhang, *J. Chromatogr. A* 1305 (2013) 139–148.
123. J.L. Wade, A.F. Bergold, P.W. Carr, *Anal. Chem.* 59 (1987) 1286–1295.

124. H.C. Thomas, J. Am. Chem. Soc. 66 (1944) 1664-1666.
125. R. Moaddel, I. Wainer, J. Pharm. Biomed. Anal. 43 (2007) 399-406.
126. R. Moaddel, K. Jozwiak, R. Yamaguchi, I.W. Wainer, Anal. Chem. 77 (2005) 5421-5426.
127. W.C. Lee, C.Y. Chuang, J. Chromatogr. A 721 (1996) 31-39.
128. W.C. Lee, C.H. Chen, J. Biochem. Biophys. Methods 49 (2001) 63-82.
129. J. Renard, C. Vidal-Madjor, C. Lapresle, J. Coll. Inter. Sci. 174 (1995) 61-67.
130. P.D. Munro, D.J. Winzor, J.R. Cann, J. Chromatogr. A 659 (1994) 267-273.
131. P.D. Munro, D.J. Winzor, J.R. Cann, J. Chromatogr. 646 (1993) 3-15.
132. S.L. de Lucena, R.G. Carbonell, C.C. Santana, Powder Technol. 101 (1999) 173-177.
133. D.S. Hage, R.R. Walters, H.W. Hethcote, Anal. Chem. 58 (1986) 274-279.
134. D.S. Hage, R.R. Walters, J. Chromatogr. A 436 (1988) 111-135.
135. D.S. Hage, R.R. Walters, J. Chromatogr. 386 (1987) 37-49.
136. J.G. Rollag, D.S. Hage, J. Chromatogr. A 795 (1998) 185-198.
137. J. Renard, C. Vidal-Madjar, B. Seville, C. Labresle, J. Mol. Recognit. 8 (1995) 85-89.
138. J. Renard, C. Vidal-Madjar, J. Chromatogr. A 661 (1994) 35-42.
139. C. Vidal-Madjar, A. Jaulmes, J. Renard, D. Peter, P. Lafaye, Chromatographia 45 (1997) 18-24.
140. J. Chen, J.E. Schiel, D.S. Hage, J. Sep. Sci. 32 (2009) 1632-1641.
141. R.M. Moore, R.R. Walters, J. Chromatogr. 384 (1987) 91-103.
142. M.J. Yoo, D.S. Hage, J. Sep. Sci. 34 (2011) 2255-2263.

143. M.J. Yoo, D.S. Hage, *J. Chromatogr. A* 1218 (2011) 2072-2078.
144. M.A. Nelson, A. Moser, D.S. Hage, *J. Chromatogr. B* 878 (2010) 165-171.
145. E. Pfaunmiller, A.C. Moser, D.S. Hage, *Methods* 56 (2012) 130-135.
146. J.A. Anguizola, Ph.D. Dissertation, University of Nebraska, Lincoln, Nebraska, 2013.
147. H.S. Kim, D.S. Hage, Immobilization methods for affinity chromatography, in: D.S. Hage (Ed.), *Handbook of Affinity Chromatography*, second ed., CRC Press, Boca Raton, FL, 2006, pp. 35-78.
148. A. Bosserhoff, C. Hellerbrand, Capillary electrophoresis, in: G. P. Patrinos, W. Ansorge (Eds.), *Molecular Diagnostics*, Academic Press, Massachusetts, 2005, pp. 67-81.
149. K. Polec-Pawlak, J.K. Abramski, J. Ferenc, L.S. Foteeva, A.R. Timerbaev, B.K. Keppler, M. Jarosz, *J. Chromatogr. A* 1192 (2008) 323-326.
150. S.S. Aleksenko, M. Matczuk, X. Lu, L.S. Foteeva, K. Pawlak, A.R. Timerbaev, M. Jarosz, *Metallomics* 5 (2013) 955-963.
151. A.R. Timerbaev, S.S. Aleksenko, K. Polec-Pawlak, R. Ruzik, O. Semenova, C. G. Hartinger, S. Oszwaldowski, M. Galanski, M. Jarosz, B.K. Keppler, *Electrophoresis* 25 (2004) 1988-1995.
152. S. Iqbal, N. Rahman, J. Iqbal, *Anal. Biochem.* 444 (2014) 16-21.
153. J.R. Petersen, A.A. Mohammad, *Clinical and Forensic Applications of Capillary Electrophoresis*, first ed., Humana: New York, 2001.
154. H. M. Maher, *Biomed. Chromatogr.* 28 (2014) 573-582.

155. G. Grabmann, B. Keppler, C. Hartinger, *Anal. Bioanal. Chem.* 405 (2013) 6417-6424.
156. M. Berezovski, S.N. Krylov, *J. Am. Chem. Soc.* 1247 (2002) 13674-13675.
157. A. Petrov, V. Okhonin, M. Berezovski, S.N. Krylov, *J. Am. Chem. Soc.* 127 (2005) 17104-17110.
158. S.N. Krylov, Kinetic capillary electrophoresis for selection, characterization, and analytical utilization of aptamers, in: M. Mascini (Ed.), *Aptamers in Bioanalysis*, Wiley, New York, 2009, pp. 183-212.
159. S.N. Krylov, *J. Biomol. Screen.* 11 (2006) 115-122.
160. S.M. Krylova, M. Musheev, R. Nutiu, Y. Li, G. Lee, S.N. Krylov, *FEBS Lett.* 579 (2005) 1371-1375.
161. S.M. Krylova, P.M. Dove, M. Kanoatov, S.N. Krylov, *Anal. Chem.* 83 (2011) 7582-7585.
162. V. Okhonin, A.P. Petrov, M. Berezovski, S.N. Krylov, *Anal. Chem.* 78 (2006) 4803-4810.
163. P. Yang, R.J. Whelan, E.E. Jameson, J.H. Kurzer, L.S. Argetsinger, C. Carter-Su, A. Kabir, A. Malik, R.T. Kennedy, *Anal. Chem.* 77 (2005) 2482-2489.
164. J. Bao, S.M. Krylova, O. Reinstein, P.E. Johnson, S.N. Krylov, *Anal. Chem.* 83 (2011) 8387-8390.
165. J. Bao, S.M. Krylova, D.J. Wilson, O. Reinstein, P.E. Johnson, S.N. Krylov, *ChemBioChem.* 12 (2011) 2551-2554.
166. M. Berezovski, A. Drabovich, S.M. Krylova, M. Musheev, V. Okhonin, A. Petrov, S.N. Krylov, *J. Am. Chem. Soc.* 127 (2005) 3165-3171.

- 167. M. Berezovski, S.N. Krylov, *Anal. Chem.* 77 (2005) 1526-1529.
- 168. A.P. Drabovich, M. Berezovski, V. Okhonin, S. N. Krylov, *Anal. Chem.* 78 (2006) 3171-3178.
- 169. V. Okhonin, M. Berezovski, S.N. Krylov, *J. Am. Chem. Soc.* 126 (2004) 7166-7167.
- 170. A.C. Moser, D.S. Hage, *Electrophoresis* 29 (2008) 3279-3295.
- 171. S. de Jong, N. Epelbaum, R. Llyanage, S. N. Krylov, *Electrophoresis* 33 (2012) 2584-2590.

CHAPTER 3

Improvement of Ultrafast Affinity Extraction for Determination of both the Kinetics and Thermodynamics of Drug-Protein Interactions

*Portion of this chapter have previously appeared in X. Zheng, Z. Li, M.I. Podariu, D.S. Hage
“Determination of Rate Constants and Equilibrium Constants for Solution-Phase Drug–Protein
Interactions by Ultrafast Affinity Extraction” Analytical Chemistry 2014, 86, 6454-6460.*

Introduction

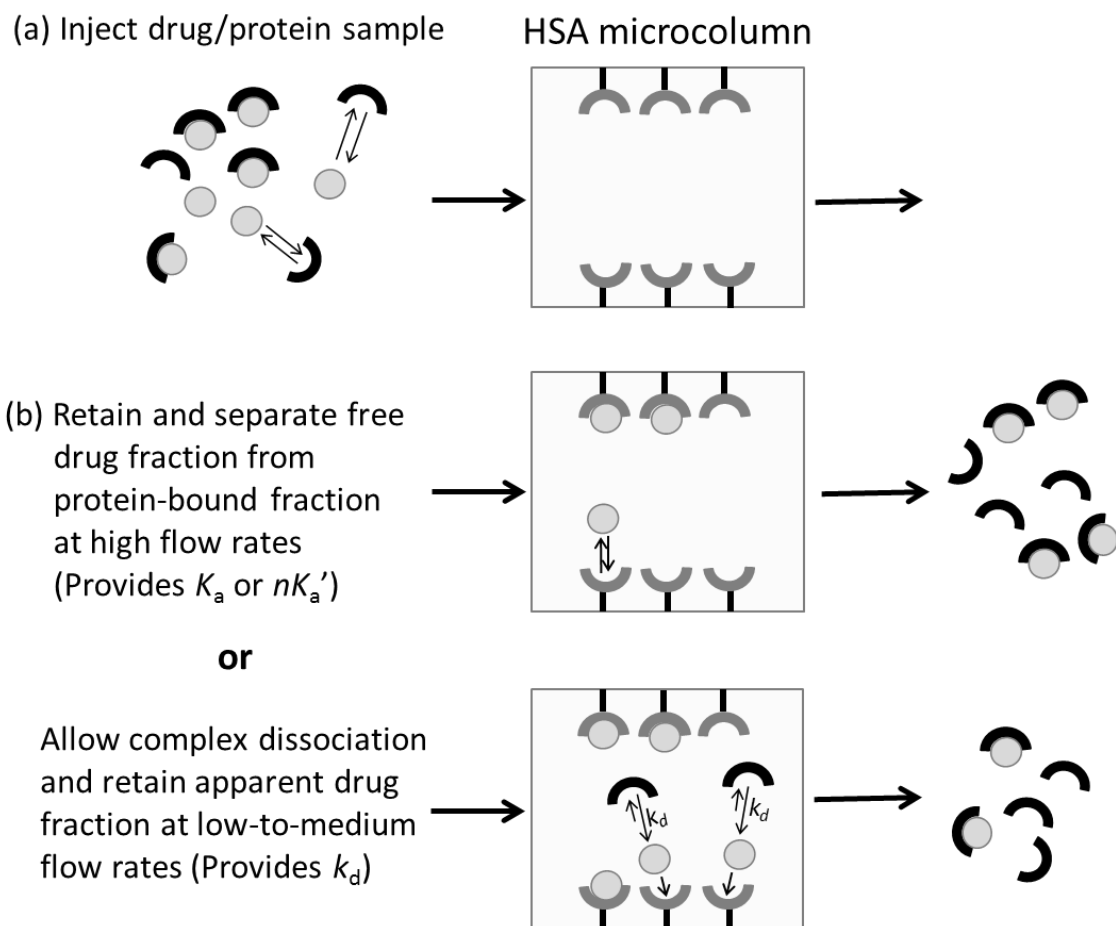
Studies of the interactions between drugs and serum proteins are important in providing information regarding the absorption, distribution, metabolism and excretion (ADME) of pharmaceutical agents within the body.¹ Human serum albumin (HSA) is the most abundant transport protein in blood (concentration, 30-50 g/L) and is of interest in many drug-protein binding studies.² This protein can interact with a large variety of drugs, most of which bind to one or two major sites on HSA: Sudlow sites I and II.³⁻⁸ Examples of drugs and small solutes that can bind to this protein include warfarin, azapropazone, benzodiazepines, indoles (e.g., L-tryptophan), sulfonylureas, and long-chain fatty acids.³⁻⁸

Many techniques have been used to examine the interactions of drugs and solutes with HSA. These techniques have included ultrafiltration, equilibrium dialysis, fluorescence spectroscopy, capillary electrophoresis, UV-Vis spectroscopy, solid-phase microextraction, circular dichroism, surface plasmon resonance, nuclear magnetic resonance spectroscopy, and X-ray crystallography.⁹⁻¹⁵ High-performance affinity

chromatography (HPAC) is another technique that has been used to characterize these interactions via developing methods to measure the equilibrium constants or rate constants for solute-protein interactions.^{1,8,14} These approaches have included zonal elution and frontal analysis for the determination of equilibrium constants; and plate height measurements, peak profiling, or peak decay analysis for kinetic studies.¹⁴⁻¹⁷ One limitation of these past HPAC methods is that they require the use of separate experiments or conditions for determining equilibrium constants and rate constants.^{14,18-23} Also, these methods generally use an immobilized protein or binding agent as one of the components of the interaction that is being examined. This feature means proper validation with model systems and reference methods are ideally required to ensure these HPAC approaches are providing a satisfactory model of how the same protein or binding agent will behave in its soluble or native state.¹⁸⁻²³

An alternative HPAC method based on ultrafast affinity extraction has recently been described for estimating the equilibrium constants of drugs with HSA, or similar biological interactions, in solution.^{14,25,26} As illustrated in Figure 3.1, this method uses an affinity microcolumn that contains an immobilized binding agent, such as an antibody or serum protein, for extraction of the free (or non-protein bound) fraction of a drug or solute in a sample. If the sample residence time in the column is sufficiently small to avoid appreciable release of the drug/solute from proteins in the sample, the amount of extracted drug/solute can then be used to measure the free fraction of this compound or the equilibrium constant for binding by this drug or solute to a soluble protein in the sample.^{25,26} This approach has been shown to give equilibrium constants that are in good agreement with those estimated for solution-phase systems when using ultrafiltration as a

Figure 3.1 General scheme for measuring a free drug fraction by ultrafast affinity extraction. (a) A sample containing a drug/protein mixture is injected onto an affinity microcolumn that contains an immobilized binding agent for the drug, such as HSA. (b) As the sample passes through the microcolumn at a suitably high flow rate, only the free drug fraction will be extracted; this creates a separation of the free and protein-bound forms of the drug in the sample and provides data that can be used to estimate the association equilibrium constant (K_a) or global affinity constant (nK_a') for the interaction. (c) If a slower flow rate is used for sample injection, part of the protein-bound fraction of the drug in the sample may dissociate as it passes through the microcolumn, increasing the apparent free drug fraction; these conditions provide data that can be used to estimate the dissociation rate constant (k_d) for the system. Reproduced with permission from X. Zheng, Z. Li, M.I. Podariu, D.S. Hage, *Anal. Chem.* 86 (2014) 6454-6460.



reference method. In addition, this method requires only microliter-size samples and provides binding data within a few minutes of injection.^{25,26}

In this chapter, a new method based on ultrafast affinity extraction is described in which both the rate constants and equilibrium constants can be quickly determined for a drug-protein interaction in solution. This work will use HSA as a model protein and will examine several drugs that are known to bind to this protein.¹⁸⁻²³ The theory of this approach will be described and various experimental parameters will be considered in the optimization of this technique. This method will then be used to examine the interactions of each tested drug with HSA, and the resulting rate constants and equilibrium constants will be compared with those reported for other techniques. The advantages and requirements of this method will be discussed, as well as the possible extension of this approach to other systems and applications.^{8,27}

Experimental

Materials and reagents

HSA (Cohn fraction V, essentially fatty acid free, $\geq 96\%$ pure), acetohexamide, chlorpromazine, gliclazide, tolbutamide, racemic verapamil, and racemic warfarin were obtained from Sigma (St. Louis, MO, USA). The reagents for the bicinchoninic acid (BCA) protein assay were from Pierce (Rockford, IL, USA). The Nucleosil Si-300 silica (7 μm particle diameter, 300 Å pore size) was purchased from Macherey Nagel (Düren, Germany). All buffers and aqueous solutions were prepared using water from a

Nanopure system (Barnstead, Dubuque, IA, USA) and were passed through Osmonics 0.22 μm nylon filters from Fisher (Pittsburgh, PA, USA)

Apparatus

The columns were packed using a Prep 24 pump from ChromTech (Apple Valley, MN, USA). The chromatographic system consisted of a PU-2080 Plus pump, an AS-2057 autosampler, and a UV-2075 absorbance detector from Jasco (Easton, MD, USA). An Alltech water jacket (Deerfield, IL, USA) and a Fisher Isotemp 3013D circulating water bath were used to maintain a column temperature of $37.0 (\pm 0.1) ^\circ\text{C}$ during all experiments. ChromNAV v1.18.04 software and LCNet from Jasco were used to control the system. Chromatograms were analyzed through the use of PeakFit v4.12 software (Jandel Scientific, San Rafael, CA, USA).

Column preparation

The stationary phase used in these studies consisted of HSA immobilized onto Nucleosil Si-300 silica by the Schiff base method.¹⁸ A control support was prepared in the same manner but with no HSA being added during the immobilization step. The protein content of the final HSA support was determined in triplicate by a BCA assay using HSA as the standard and the control support as the blank, giving a value of $65 (\pm 2)$ mg HSA/g silica or an effective concentration of $\sim 440 \mu\text{M}$ HSA in the affinity microcolumns. The supports were placed into stainless steel columns with an inner

diameter of 2.1 mm and lengths of 1 mm (using a frit-in-column design)²⁸ or 5 to 10 mm (using traditional stainless steel HPLC housings and end fittings). The packing solution was pH 7.4, 0.067 M potassium phosphate buffer and the packing pressure was 3000-4000 psi (20-28 MPa). The columns were stored in pH 7.4, 0.067 M phosphate buffer and at 4 °C when not in use.

Chromatographic studies

The mobile phase used for sample application, elution and sample preparation was pH 7.4, 0.067 M phosphate buffer. All mobile phases were degassed for 30 min prior to use. Each affinity microcolumn was used for approximately 200 sample injections to provide optimum retention and peak resolution; however, these columns were found to be stable for at least 300-400 injections and over six months of use. The free fraction measurements were typically made by injecting 1 μ L samples that contained 10 μ M of the desired drug or a mixture of 10 μ M drug and 20 μ M soluble HSA, although other drug and protein concentrations were also considered. These mixtures were incubated for at least 30 min prior to injection, with both the sample and mobile phase being preheated to 37 °C before passage through the affinity microcolumn.

The dissociation rate constants and equilibrium constants for each drug with soluble HSA were measured by using the general scheme in Figure 3.1. For the direct measurement of equilibrium constants, an injection flow rate was used that was sufficiently high to minimize dissociation of drug-protein complexes in the sample during their passage through the column. By using lower flow rates, and longer residence times

for the sample in the column, the conditions were adjusted so that some of the drug-protein complex could dissociate during passage through the column, thus increasing the apparent free drug fraction and making it possible to determine the dissociation rate constant for the drug with the soluble protein. In both types of studies, the free drug fractions were measured by dividing the drug's baseline-corrected retained peak area by the total peak area for the same drug in the absence of any soluble protein. The baseline of each chromatogram was normalized using the autofit and subtract baseline method of PeakFit 4.12 prior to data analysis. No significant nonspecific binding with the control support was seen for most drugs examined in this study.¹⁸⁻²² Some nonspecific binding was seen for verapamil, as reported previously;²¹ however, this nonspecific binding did not have any notable effect on the free fractions that were measured for this drug with soluble HSA.

Results and Discussion

Optimization of free drug fraction measurements

Several model drugs were examined in this chapter. Warfarin is an anticoagulant known to have single-site binding to HSA at Sudlow site I.^{15,18,29-30} Verapamil is a calcium channel blocking agent and chlorpromazine is an anti-psychotic drug that each have a primary binding site at or near Sudlow site I.^{21,31} Tolbutamide, acetohexamide, and gliclazide are sulfonylurea drugs used to treat type 2 diabetes and have two major binding regions on HSA, which occur at Sudlow sites I and II.^{19-20,22} The association equilibrium constants (K_a , in the case of single-site binding) or global affinity constants (nK_a' , in the case of multi-site binding) for these drugs with HSA at 37 °C and pH 7.4 are

in the general range of 10^4 - 10^6 M⁻¹, as is typical for the binding of many drugs with this protein.^{1,18-24} Dissociation rates from HSA have been examined previously by other methods for four of these drugs (i.e., warfarin, verapamil, acetohexamide and tolbutamide),^{15,17} while the other two drugs (i.e., gliclazide and chlorpromazine) have not been the subject of prior kinetic studies.

In this study, a drug was injected in either the presence or absence of excess soluble HSA onto an HSA microcolumn according to the scheme given in Figure 3.1. As the sample passed through the microcolumn at a moderate-to-high flow rate, the protein-bound fraction of the drug and the excess soluble protein eluted as a non-retained peak, while the free fraction of the drug was extracted, retained and later eluted from the column. Results were obtained within 2-10 min for all of the tested drugs (depending on the column size, degree of retention and the flow rate) and within 2-6 min for drugs with low-to-moderate affinities for HSA.

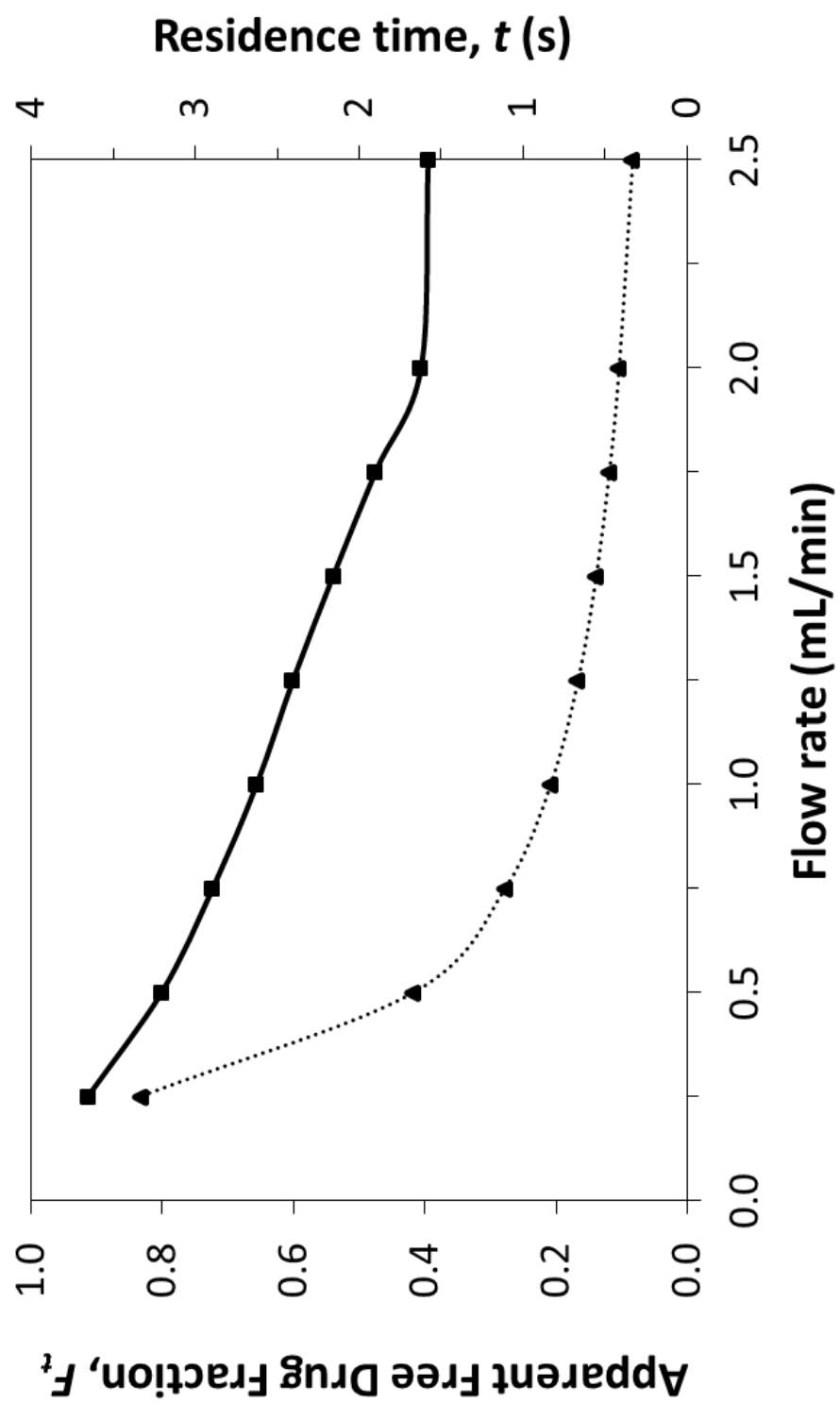
The injected samples that were typically used in this study contained a two-fold mole excess of HSA versus each drug (i.e., 20 μ M HSA and 10 μ M drug). These concentrations avoided the use of an excess of drug vs. protein in the samples and provided free drug fractions that could be readily detected. It has been shown in prior work with ultrafast affinity extraction that therapeutic levels of similar drugs^{26,32,38} and larger concentrations of soluble HSA,²⁶ including physiological levels, could be used in this type of experiment. However, these latter conditions were not required for the purpose of this current study. Samples containing other drug and/or protein concentrations were also examined, with no significant changes being noted in the either

the rate constants or equilibrium constants that were measured under these alternative conditions.

As shown in Figure 3.2, the relative size of the free drug fraction was affected by the flow rate used for sample injection. This effect has been noted for other applications of ultrafast affinity extraction and is due to the change the flow rate created in the time allowed for dissociation of the protein-bound form of the drug as the sample passed through the column.^{25,26,32,38} The extraction efficiency for the drug can also vary with the flow rate for some types of affinity microcolumns, but this parameter was 95% or higher for the HSA microcolumns and experimental conditions used in this study^{25,26} and did not lead to any significant changes in the relative size of the retained peaks as a function of flow rate.

The overall effect of changing the flow rate, and drug-protein dissociation in the sample, is also illustrated in Figure 3.2. At low-to-moderate flow rates (i.e., < 2.0 mL/min, in this example for a tolbutamide/HSA mixture), the apparent free drug fraction increased with a decrease in the flow rate, due to increased dissociation of the drug from soluble HSA as the sample passed through the column. However, the measured free drug fraction approached a constant value when the flow rate reached a certain critical value (e.g., ≥ 2.0 mL/min, or a column residence time of ~ 420 ms or less for the tolbutamide/HSA mixture). This effect was employed by using the latter conditions and high flow rates to estimate the original free drug fraction that was present at equilibrium in the sample and lower flow rates to provide data on the rate of a drug's dissociation from a soluble protein in the sample.

Figure 3.2 Effect of injection flow rate on the column residence time (dashed line) and apparent free drug fractions (solid line) for 1 μ L samples of 10 μ M tolbutamide and 20 μ M soluble HSA injected onto a 5 mm \times 2.1 mm i.d. HSA microcolumn at pH 7.4 and 37 $^{\circ}$ C. Reproduced with permission from X. Zheng, Z. Li, M.I. Podariu, D.S. Hage, *Anal. Chem.* 86 (2014) 6454-6460.



Column size is another factor to consider when performing a free fraction analysis by ultrafast affinity extraction. Like flow rate, this factor will affect the time allowed for drugs to dissociate from proteins during passage of a sample through the column, following the same trend as illustrated in Figure 3.2. In addition, both the column size and flow rate will affect the backpressure of the system (e.g., typical column pressures of 1.9-3.2 MPa for 5-10 mm \times 2.1 mm i.d. columns at 3.5 mL/min). However, the column size will also affect the elution time of the retained free drug fraction and the resolution of this peak from the non-retained peak due to the protein-bound drug and excess protein in the sample.²⁵

It was found that drugs with relatively strong binding to HSA (e.g., warfarin, tolbutamide and acetohexamide; affinities, $\sim 10^5$ - 10^6 M⁻¹)^{18-22,29,30} provided measurable free fractions when using relatively short 5 mm \times 2.1 mm i.d. HSA microcolumns. Such columns not only gave good retention for these drugs, but they made it easy to obtain short column residence times for measurement of the small free drug fractions that could occur in such systems. Most drugs with weaker binding to HSA (e.g., gliclazide and verapamil; affinities, $\sim 10^4$ - 10^5 M⁻¹)^{21,22} were examined by using longer 10 mm \times 2.1 mm HSA microcolumns. These longer microcolumns provided higher drug retention while still providing column residence times sufficient to examine the larger free fractions that were present in such systems. An exception to this trend was chlorpromazine, which had fast dissociation kinetics and moderate binding to HSA.²³ In this specific case, a 1 mm \times 2.1 mm id. HSA microcolumn was used.

Determination of dissociation rate constants

Measurements of the apparent free drug fractions at low-to-moderate flow rates were used in this study to estimate the dissociation rate constant for a drug with a soluble protein in the same sample. This experiment was described by the reactions shown in Equations 3.1 and 3.2, which occurred simultaneously as a mixture of the drug/analyte and soluble protein (as represented by A and P, respectively) was applied to an affinity microcolumn that contained an immobilized binding agent for the drug, P(s).



The reaction in Equation 3.1 describes the binding and equilibrium that has taken place between A and P in the sample prior to entering the column, while Equation 3.2 describes the binding and extraction of the free form of A by the immobilized agent P(s) in the microcolumn. The terms k_a and k_d in Equation 3.1 represent the second-order association rate constant and first-order dissociation rate constant of A with P in solution. The term $k_{a(s)}$ in Equation 3.2 is the second-order association rate constant for A as it interacts with the immobilized binding agent.

The system in Equations 3.1-3.2 was simplified in this study by using a large excess of the immobilized binding agent versus the soluble protein. For instance, the 1-10 mm \times 2.1 mm i.d. microcolumns contained a 76- to 760-fold larger HSA content than a 1 μ L solution of 20 μ M HSA. In addition, each of these columns had at least a 22-fold

larger molar concentration of HSA than was present in even the initial, undiluted samples and mixtures that contained soluble HSA. These conditions meant that P(s) was present in a large excess versus soluble P when using the model described by using Equations 3.1 and 3.2. This also meant that the pseudo-first order rate constant $k_a [P]$ for the binding of A with P was much less than the pseudo-first order rate constant $k_{a(s)} [P(s)]$ for the extraction of A (i.e., assuming k_a and $k_{a(s)}$ had comparable values, as has been noted to be the case for soluble HSA and the type of immobilized HSA used in this study).^{1,29,39}

The result of these experimental conditions is that the extraction of A by the immobilized binding agent was much faster than the association of A with P. This, in turn, made it possible to ignore this latter process and simplify the reaction in Equation 3.1 to that shown in Equation 3.3.



It was then possible with this revised model to obtain the integrated rate expressions given in Equations 3.4 and 3.5

$$\ln \frac{(1-F_0)}{(1-F_t)} = k_d t \quad (3.4)$$

$$\ln \frac{1}{(1-F_t)} = k_d t - \ln(1 - F_0) \quad (3.5)$$

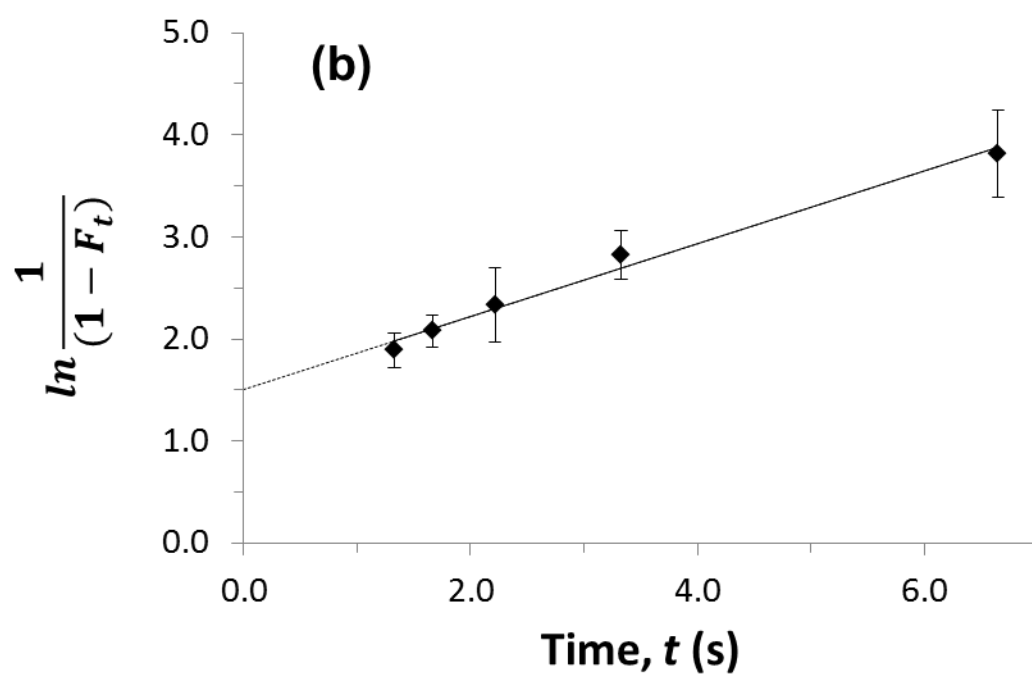
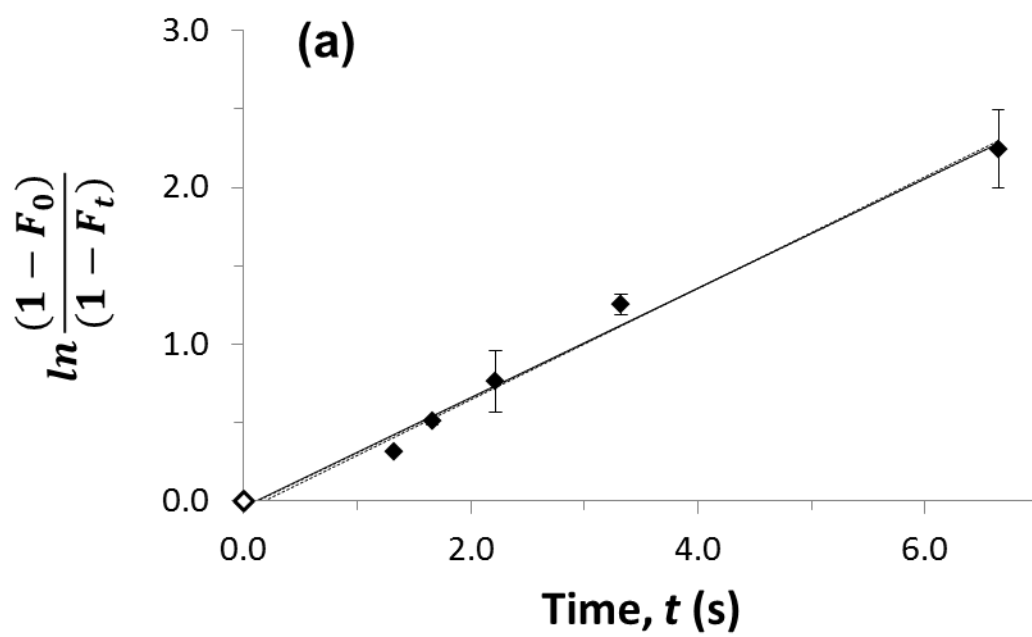
In these equations, F_0 is the original free fraction of A in the sample, and F_t is the apparent free fraction after AP has been allowed to dissociate for time t . The value of t is equal to the column void time and can be calculated by employing the flow rate and the column void volume (e.g., as found by using the known support porosity, packing density,

and column size). Equations 3.4-3.5 indicate that a plot of either $\ln[(1 - F_0)/(1 - F_t)]$ or $\ln[1/(1 - F_t)]$ versus t should provide, under the appropriate experimental conditions, a linear relationship in which the slope is directly related to the dissociation rate constant k_d as A is released from its complex with soluble agent P in the sample.

Some typical plots that were obtained when using Equations 3.4 and 3.5 are provided in Figure 3.3. Both types of plots gave a linear response for all of the tested drugs, with correlation coefficients ranging from 0.988 to 0.998 ($n = 5$ to 8) over dissociation times that allowed measurable changes to be made in the apparent free fractions. The plots that were prepared according Equation 3.4 gave intercepts that were essentially equal to zero, regardless of whether an experimental point at $t = 0$ and $F_t = F_0$ for the original sample was included in the data set. For plots made according to Equation 3.5, a positive non-zero intercept was obtained that was related to the value of F_0 .

The usable time range for these dissociation studies was dependent on the affinity of each drug for soluble HSA (which affected the value of F_0) and the dissociation rate for the soluble drug-protein complex. The lower end of this usable time range occurred when the free fraction grew close to its equilibrium value (i.e., conditions under which little dissociation occurred). These times were as low as 100-277 ms for chlorpromazine or warfarin and as high as 950 ms for verapamil. The ranking of these drugs with respect to this time was correlated with a decreasing order in the overall affinities of the drugs for HSA, with the sole exception of chlorpromazine due to its relatively high dissociation rate. The upper end of the usable time range occurred when the drug had sufficient time to reach essentially complete dissociation. For most of the tested drugs, this upper limit

Figure 3.3 Measurement of the dissociation rate constant for verapamil and soluble HSA at pH 7.4 and 37 °C, as determined by measuring apparent free drug fractions using ultrafast affinity extraction. The samples contained 10 μ M verapamil and 20 μ M soluble HSA. The results were analyzed by using (a) Equation 3.4 or (b) Equation 3.5. The solid line in (a) shows the result that was obtained when a point at the origin was included (\diamond), and the dashed line shows the result obtained when this point was not included; the equations for these two best-fit lines were $y = 0.35 (\pm 0.02) x - 0.04 (\pm 0.06)$ and $y = 0.36 (\pm 0.02) x - 0.06 (\pm 0.09)$, respectively. In (b), the best-fit equation was $y = 0.36 (\pm 0.02) x + 1.51 (\pm 0.09)$. The correlation coefficients for these plots ranged from 0.993 to 0.995 ($n = 5$). The error bars represent a range of ± 1 S.D. and, in some cases, were comparable in size to the data symbols. Reproduced with permission from X. Zheng, Z. Li, M.I. Podariu, D.S. Hage, *Anal. Chem.* 86 (2014) 6454-6460.



occurred over the range of 1.7-6.7 s and, again with the exception of chlorpromazine, followed approximately the same order as seen with the lower time limits for these drugs and the affinities of these drugs for soluble HSA.

Table 3.1 summarizes the k_d values that were obtained in this study. The relative precision of these dissociation rate constants ranged from ± 3 -9%. The measured k_d values differed by only 7-20% from the literature values that have been reported for acetohexamide, tolbutamide and racemic verapamil.^{15,17} In the case of warfarin, the results of this study fell within the overall range of all previously-reported values for racemic warfarin or its enantiomers.^{9,15,40} Although gliclazide and chlorpromazine did not have prior k_d values that have been reported, the dissociation rate constants measured for these drugs did fit within the range that would be expected for drugs with similar affinities to HSA.^{15,17,41,42} The same trends were seen for k_d values that were measured by ultrafast affinity extraction when 1) a point at the intercept, and representing the original sample, was included during analysis of the data by using Equation 3.4; 2) when Equation 3.4 was used with no such point being included in the data set; or 3) when the data were examined by using Equation 3.5.

Measurement of association equilibrium constants

It was also possible by using ultrafast affinity extraction to obtain the association equilibrium constant (K_a), or the global affinity constant (nK_a') in the case of a system with multi-site binding,^{1,24} for each drug with soluble HSA. For instance, Equation 3.6 can be used for this purpose by employing the free drug fraction that is measured for a

Table 3.1 Dissociation rate constants measured for various drugs with soluble HSA by using ultrafast affinity extraction on HSA microcolumns^a

Drug	Dissociation rate constant, k_d (s ⁻¹)		
	Estimate, Equation 3.4 ^b	Estimate, Equation 3.5	Literature [Ref.]
Warfarin	0.80 (\pm 0.05)	0.72 (\pm 0.05)	0.41-2 [9,15,40]
Tolbutamide	0.59 (\pm 0.03)	0.58 (\pm 0.04)	0.49 (\pm 0.15) [15]
Acetohexamide	0.67 (\pm 0.03)	0.63 (\pm 0.03)	0.58 (\pm 0.02) [15]
Verapamil	0.35 (\pm 0.02)	0.36 (\pm 0.02)	0.38 (\pm 0.05) [17]
Gliclazide	0.61 (\pm 0.02)	0.59 (\pm 0.04)	Not reported
Chlorpromazine	3.96 (\pm 0.13)	3.35 (\pm 0.30)	Not reported

^aThe k_d values were measured at pH 7.4 and at 37 °C. Each of the injected samples contained 10 μ M of the drug and 20 μ M HSA. The values in the parentheses represent a range of \pm 1 S.D., as determined from the slopes of the best-fit lines constructed according to Equations 3.4 and 3.5.

^bThese values were found by using Equation 3.4 when a point at the origin was included in the data set.

Reproduced with permission from X. Zheng, Z. Li, M.I. Podariu, D.S. Hage, Anal. Chem. 86 (2014) 6454-6460.

drug/protein mixture at equilibrium (F_0) and under injection conditions that minimize release of the drug from soluble proteins as the sample passes through the column.²⁵

$$K_a = \frac{1-F_0}{F_0([P]_{\text{tot}} - [A]_{\text{tot}} + [A]_{\text{tot}}F_0)} \quad (3.6)$$

In this Equation 3.6, $[A]_{\text{tot}}$ and $[P]_{\text{tot}}$ are the total concentrations of the drug and soluble protein in the original sample, respectively. This equation was derived for a drug and protein interaction that involves 1:1 binding, but the same expression can be used to estimate the global affinity constant for a multi-site drug-protein interaction under a given set of concentration conditions.^{25,32,35,37}

The K_a (or nK_a') values that were obtained by using direct measurements of F_0 are provided in Table 3.2. These values had precisions of ± 7 -36% and differed by less than 7% for the drugs with single reference values obtained under similar temperature conditions. In the case of warfarin, the measured K_a fell within the range of previously-reported values. A second method for estimating K_a was carried out that utilized the value of F_0 that was obtained from the intercept of a plot made according Equation 3.5 during the determination of dissociation rate constants. This second set of values, which are also given in Table 3.2, had precisions of ± 8 -22% and differed from the literature results by less than 23% or, in the case of warfarin, were similar to the range of previously-reported values.

A comparison of these two approaches indicates that there are distinct advantages to each method for measuring the equilibrium constant for a drug-protein interaction. As the data in Table 3.2 suggest, the approach that uses fast flow rates and ultrafast affinity

Table 3.2. Equilibrium constants measured for various drugs with soluble HSA by using ultrafast affinity extraction on HSA microcolumns^a

Association equilibrium constant, K_a, or global affinity constant, nK_a' (M^{-1})			
Drug	Estimate, Equation 3.6	Estimate, Equations 3.5 and 3.6	Literature [Ref.]
Warfarin	$2.4 (\pm 0.4) \times 10^5$	$1.6 (\pm 0.2) \times 10^5$	$2.0\text{-}5.7 \times 10^5$ [18,29,30]
Tolbutamide	$1.1 (\pm 0.4) \times 10^5$	$0.9 (\pm 0.2) \times 10^5$	$1.1 (\pm 0.1) \times 10^5$ [19] ^b
Acetohexamide	$1.8 (\pm 0.5) \times 10^5$	$1.3 (\pm 0.1) \times 10^5$	$1.7 (\pm 0.1) \times 10^5$ [20] ^b
Verapamil	$1.5 (\pm 0.4) \times 10^4$	$1.6 (\pm 0.2) \times 10^4$	$1.4 (\pm 0.1) \times 10^4$ [21] ^c
Gliclazide	$8.0 (\pm 0.6) \times 10^4$	$6.9 (\pm 1.0) \times 10^4$	$7.9 (\pm 0.1) \times 10^4$ [22] ^b
Chlorpromazine	$6.2 (\pm 0.5) \times 10^4$	$4.9 (\pm 0.5) \times 10^4$	6.4×10^4 [23]

^aThese results were measured at pH 7.4 and at 37°C. The values in parentheses represent a range of ± 1 S.D., as determined by error propagation.

^bThe global affinity constants for these drugs were calculated from data in the given references.

^cThis value represents the average association equilibrium constant for *R*- and *S*-verapamil at their high affinity site on HSA.

Reproduced with permission from X. Zheng, Z. Li, M.I. Podariu, D.S. Hage, Anal. Chem. 86 (2014) 6454-6460.

extraction to directly measure F_0 can provide the more precise estimate of K_a or nK_a . However, this method does require obtaining appropriate flow rate conditions for such a measurement and is carried out at separate flow rates from those that would be used to measure a dissociation rate constant. The second approach, in which the value of F_0 is obtained from the intercept of a plot made according to Equation 3.5, provides a slightly less precise estimate of the equilibrium constant but can be carried out with the same experiments and conditions as those used to find k_d . This makes the latter method attractive for the simultaneous and rapid determination of both k_d and K_a . This approach would also be useful for the estimation of equilibrium constants at column pressures or peak resolutions that may prevent the use of sufficiently high flow rates for the direct determination of F_0 and K_a .

Estimation of association rate constants

It was possible from the measured K_a and k_d values to also estimate the second-order association rate constant (k_a) for each drug with soluble HSA, as found by using the relationship $k_a = k_d K_a$. This method provided the actual k_a value for a drug-protein system with 1:1 interactions or the net, apparent value of k_a for a system with multi-site interactions. The average k_a for racemic warfarin that was determined by this approach was $1.7 (\pm 0.3) \times 10^5 \text{ M}^{-1} \text{ s}^{-1}$ at pH 7.4 and 37°C, which gave good agreement with prior values reported for this drug.^{9,15,40,43} The association rate constants for tolbutamide, acetohexamide and racemic verapamil gave k_a values of $6.4 (\pm 2.4) \times 10^4 \text{ M}^{-1} \text{ s}^{-1}$, $1.1 (\pm 0.3) \times 10^5 \text{ M}^{-1} \text{ s}^{-1}$, and $5.4 (\pm 1.5) \times 10^3 \text{ M}^{-1} \text{ s}^{-1}$, respectively, which were comparable to

the results calculated from previously-reported k_d and K_a or nK_a' values for these systems.^{15,17,19-21} Gliclazide and chlorpromazine gave k_a values of $4.7 (\pm 0.5) \times 10^4 \text{ M}^{-1} \text{ s}^{-1}$ and $2.1 (\pm 0.3) \times 10^5 \text{ M}^{-1} \text{ s}^{-1}$, which agreed with the range of values that have been reported for drugs with comparable affinities and dissociation rates for HSA.^{15,17,41,42}

Conclusions

In this chapter, a new method based on ultrafast affinity extraction and affinity microcolumns containing immobilized HSA was developed and used to measure both the rate constants and equilibrium constants for drug-protein interactions involving soluble HSA. The effects of column size and flow rate were considered in these experiments, and several approaches for these measurements were examined and compared. The dissociation rate constants obtained by this approach gave good agreement with previous rate constants that have been reported for the same drugs or for other solutes with comparable affinities for HSA. The equilibrium constants determined by this method also showed good agreement with the literature.

The results indicated that ultrafast affinity extraction can be an effective method for studying both the kinetics and thermodynamics of a drug-protein interaction in solution. An important advantage of this method is it can directly examine both the equilibrium processes and interaction rates that occur between a drug and the soluble form of a protein, thus avoiding any effects immobilization may have on such interactions.¹⁸⁻²³ The moderate-to-high flow rates and small columns used in this method make this technique fast, with analysis times on the order of minutes per sample being

possible.^{25,26} In addition, this approach is not limited to HSA or the drugs examined in this study but could be applied to other systems (e.g., the interactions of drugs or small biomolecules with other soluble proteins or to surface receptors on injected particles). Possible applications for this method include the high-throughput screening of drug candidates and the rapid characterization of solute-protein interactions.^{1,9,14,17,24}

References

1. D. S. Hage, A. Jackson, M. R. Sobansky, J. E. Schiel, M. J. Yoo, K. S. Joseph, J. Sep. Sci. 32 (2009) 835-853.
2. T. Peters, Jr., All About Albumin: Biochemistry, Genetics, and Medical Applications, Academic Press, San Diego, CA, 1996.
3. G. Sudlow, D. J. Birkett, D. N. Wade, Mol. Pharmacol. 12 (1976) 1052-1061.
4. U. Kragh-Hansen, Pharmacol. Rev. 33 (1981) 17-53.
5. U. Kragh-Hansen, V. T. Chuang, M. Otagiri, Biol. Pharm. Bull. 25 (2002) 695-704.
6. D. C. Carter, X. M. He, S. H. Munson, P. D. Twigg, K. M. Gernert, M. B. Broom, T. Y. Miller, Science 244 (1989) 1195-1198.
7. R. Brodersen, J. Biol. Chem. 254 (1979) 2364-2369.
8. D. S. Hage, J. Anguizola, O. Barnaby, A. Jackson, M. J. Yoo, E. Papastavros, E. Pfaunmiller, M. Sobansky, Z. Tong, Curr. Drug. Metab. 12 (2011) 313-328.
9. R. L. Rich, Y. S. Day, T. A. Morton, D. G. Myszk, Anal. Biochem. 296 (2001) 197-207.
10. R. Matsuda, C. Bi, J. Anguizola, M. Sobansky, E. Rodriguez, J. V. Badilla, X. Zheng, B. Hage, D. S. Hage, J. Chromatogr. B 966 (2014) 48-58.
11. F. Ding, G. Zhao, S. Chen, F. Liu, Y. Sun, L. Zhang, J. Mol. Struct. 929 (2009)

159-166.

12. D. Leis, S. Barbosa, D. Attwood, P. Taboada, V. Mosquera, *Langmuir* 18 (2002) 8178-8185.
13. H. Yuan, J. Pawliszyn, *Anal. Chem.* 73 (2001) 4410-4416.
14. J. E. Schiel, D. S. Hage, *J. Sep. Sci.* 32 (2009) 1507-1522.
15. M. J. Yoo, D. S. Hage, *J. Chromatogr. A* 1218 (2011) 2072-2078.
16. Z. Tong, J.E. Schiel, E. Papastavros, C.M. Ohnmacht, Q.R. Smith, D.S. Hage, *J. Chromatogr. A* 1218 (2011) 2065-2071.
17. M.J. Yoo, D.S. Hage, *J. Sep. Sci.* 34 (2011) 2255-2263.
18. J. Chen, D. S. Hage, *Anal. Chem.* 78 (2006) 2672-2683.
19. K. S. Joseph, J. Anguizola, D. S. Hage, *J. Pharm. Biomed. Anal.* 54 (2011) 426-432.
20. K. S. Joseph, J. Anguizola, A. J. Jackson, D. S. Hage, *J. Chromatogr. B* 878 (2010) 2775-2781.
21. R. Mallik, M. J. Yoo, S. Chen, D. S. Hage, *J. Chromatogr. B* 876 (2008) 69-75.
22. R. Matsuda, J. Anguizola, K. S. Joseph, D. S. Hage, *Anal. Bioanal. Chem.* 401 (2011) 2811-2819.
23. H. S. Kim, I. W. Wainer, *J. Chromatogr. B* 870 (2008) 22-26.

24. D. S. Hage, J. A. Anguizola, A. J. Jackson, R. Matsuda, E. Papastavros, E. Pfaunmiller, Z. Tong, J. Vargas-Badilla, M. J. Yoo, X. Zheng, *Anal. Methods* 3 (2011) 1449-1460.
25. R. Mallik, M. J. Yoo, C. J. Briscoe, D. S. Hage, *J. Chromatogr. A* 1217 (2010) 2796-2803.
26. X. Zheng, M. J. Yoo, D. S. Hage, *Analyst* 138 (2013) 6262-6265.
27. M. J. Yoo, D. S. Hage, *J. Sep. Sci.* 32 (2009) 2776-2785.
28. J. E. Schiel, Ph.D. Dissertation, University of Nebraska, Lincoln, Nebraska, 2009.
29. B. Loun, D. S. Hage, *Anal. Chem.* 66 (1994) 3814–3822.
30. M. J. Yoo, J. E. Schiel, D. S. Hage, *J. Chromatogr. B* 878 (2010) 1707-1713.
31. D. Silva, C. M. Cortez, S. R.W. Louro, *Spectrochimica. Acta. Part A* 60 (2004) 1215–1223.
32. C. M. Ohnmacht, J. E. Schiel, D. S. Hage, *Anal. Chem.* 78 (2006) 7547-7556.
33. T. Jiang, R. Mallik, D. S. Hage, *Anal. Chem.* 77 (2005) 2362-2372.
34. W. Clarke, D. S. Hage, *Anal. Chem.* 73 (2001) 1366-1373
35. W. Clarke, J. E. Schiel, A. Moser, D. S. Hage, *Anal. Chem.* 77 (2005) 1859–1866.
36. W. Clarke, A. R. Chowdhuri, D. S. Hage *Anal. Chem.* 73 (2001) 2157–2164.
37. J. E. Schiel, Z. Tong, C. Sakulthaew, D. S. Hage, *Anal. Chem.* 83 (2011) 9384–

9390.

38. C. A. Burtis, E. R. Ashwood, D. E. Bruns (Eds), Tietz Textbook of Clinical Chemistry and Molecular Diagnostics, 4th ed.; Saunders: St. Louis, MO, 2006.
39. J. Yang, D. S. Hage, J. Chromatogr. A 766 (1997) 15-25.
40. J. Chen, J. E. Schiel, D. S. Hage, J. Sep. Sci. 32 (2009) 1632-1641.
41. J. Yang, D. S. Hage, J. Chromatogr. A 725 (1996) 273-285.
42. J. E. Schiel, C. M. Ohnmacht, D. S. Hage, Anal. Chem. 81 (2009) 4320-4333.
43. B. Loun, D. S. Hage, Anal. Chem. 68 (1996) 1218-1225.

CHAPTER 4

Combination of Ultrafast Affinity Extraction and Multi-Dimensional HPAC for the Analysis of Free Fractions for Chiral Drugs

Portion of this chapter have previously appeared in X. Zheng, M.J. Yoo, D.S. Hage "Analysis of Free Fractions for Chiral Drugs Using Ultrafast Extraction and Multi-Dimensional High-Performance Affinity Chromatography" Analyst 2013, 138, 6262-6265.

Introduction

Many drugs and small solutes exist in multiple forms in biological systems. Drugs are often reversibly bound to carrier agents such as serum proteins in the circulatory system, causing these drugs to exist in two forms: a free fraction and bound fraction.¹⁻⁴ Because the free drug fraction is generally thought to be the biologically-active form,^{3,4} there has been ongoing interest in the creation of improved tools for measuring free drug fractions and for studying drug-protein interactions in clinical and pharmaceutical samples.^{1,2,5} The methods of equilibrium dialysis and ultrafiltration are often used for this work but can have long analysis times and large sample requirements (e.g., equilibrium dialysis) or can introduce errors due to nonspecific adsorption to a membrane (e.g., ultrafiltration or equilibrium dialysis).⁶

Chromatographic approaches based on high-performance affinity chromatography (HPAC) and ultrafast affinity extraction have recently been proposed as an alternative means for measuring free drug or free hormone fractions.^{1,2,7-9} In this type of approach,

small columns containing immobilized antibodies^{1,2,7,8} or other binding agents, such as immobilized transport proteins,⁹ are employed to extract the free form of a target drug or solute on a time scale that minimizes release of the target from its protein-bound form in a sample. Potential advantages of this approach include its speed, small sample requirements, good precision and low detection limits, especially when used with detection based on chemiluminescence or near-infrared fluorescence.^{1,7,8} However, previous systems based on this method have been designed to look at only a specific drug or solute (e.g., warfarin, phenytoin and thyroxine)^{1,2,7-9} rather than samples that may contain multiple or related forms of the same target (e.g., a mixture of drug enantiomers).

This chapter will describe the development of a multi-dimensional HPAC system that uses ultrafast affinity extraction and chiral chromatography to simultaneously examine the free forms of drug enantiomers in complex samples (e.g., serum) and to study the binding of such drugs with proteins. *R/S*-Warfarin and its binding protein human serum albumin (HSA) were used as models to develop and evaluate this approach. Warfarin is an anticoagulant often used as a racemic mixture for the treatment of thromboembolic diseases, with the *R*- and *S*-enantiomers having noticeable differences in their pharmacokinetics and protein binding properties.^{3,10,11} HSA (molar mass, 66.5 kDa) is the main binding protein for warfarin and many other drugs in serum and is known to have strong interactions with both *R*- and *S*-warfarin at a region on this protein known as Sudlow site I.^{10,12,13} The data obtained in this study should provide important information on interaction between protein and two drug enantiomers, as well as data that can be used in future work to extend this method to other chiral analytes.

Experimental

Materials and reagents

The HSA (Cohn fraction V, essentially fatty acid free), human serum (from male AB plasma, H4522, lot 039K0728; sterile filtered and tested negative for HIV-1/HIV-2, hepatitis B and hepatitis C), and racemic warfarin (98% pure) were from Sigma (St. Louis, MO, USA). The reagents for the bicinchoninic acid (BCA) protein assay were from Pierce (Rockford, IL, USA). The Nucleosil Si-300 silica (7 μm particle diameter, 300 Å pore size) was purchased from Macherey Nagel (Düren, Germany). All buffers and aqueous solutions were prepared using water from a Nanopure system (Barnstead, Dubuque, IA, USA) and were passed through Osmonics 0.22 μm nylon filters from Fisher (Pittsburgh, PA, USA)

Apparatus

The affinity columns were packed using a Prep 24 preparative pump from ChromTech (Apple Valley, MN, USA). The chromatographic system consisted of a PU-2080 Plus HPLC pump from Jasco (Easton, MD, USA), two six-port Lab Pro valves (Rheodyne, Cotati, CA, USA), and a Shimadzu RF-10AXL fluorescence detector (Kyoto, Japan). An Alltech water jacket (Deerfield, IL, USA) and an Isotemp 3013D circulating water bath from Fisher were used to maintain a temperature of 37.0 (± 0.1) °C for the columns during all experiments described in this chapter. The chromatographic data were collected and processed using in-house programs written in LabView 5.1 (National Instruments, Austin, TX, USA). The ultrafiltration studies were performed using a

5702RH centrifuge from Fisher and tubes containing Ultracel YM-T cellulose membranes (30 kDa cut-off), as obtained from Millipore (Billerica, MA, USA).

Column preparation

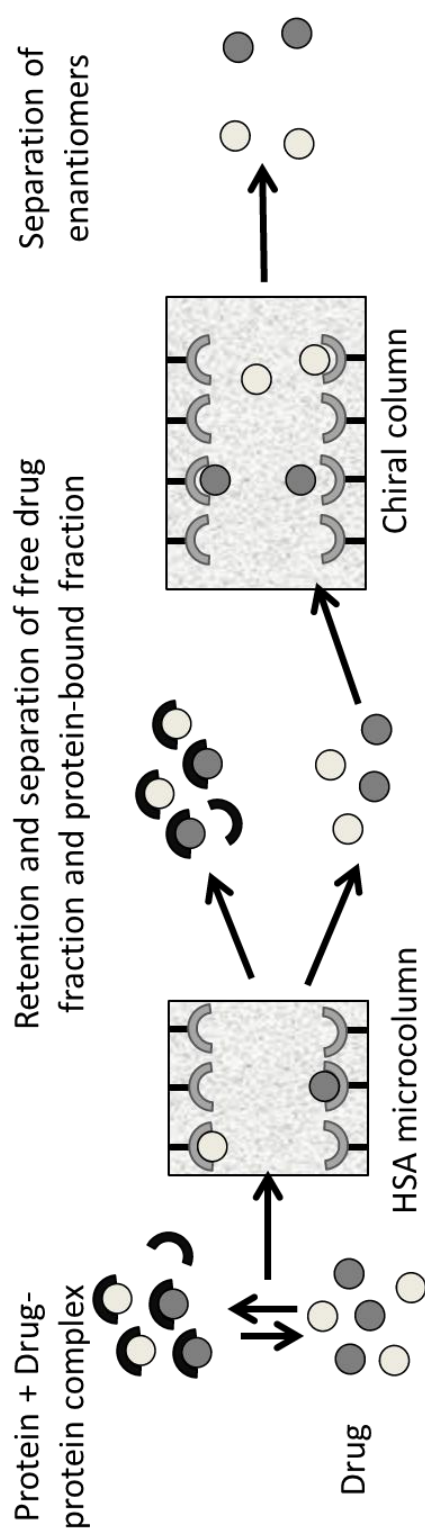
The stationary phase used in these studies consisted of HSA that was immobilized on Nucleosil Si-300 silica by the Schiff base, as performed according to the literature.⁸ Control supports were prepared in the same manner but with no HSA being added during the immobilization step. The protein content of the final HSA support was determined in triplicate by a BCA assay using HSA as the standard and the control support as the blank.

An HPLC column packer was used to place the supports into stainless steel columns with dimensions of 1 cm \times 2.1 mm i.d., or 5 cm \times 2.1 mm i.d. The columns with dimension of 3 mm \times 2.1 mm i.d. used a frit-in-column design, as described in Ref. 14. The longer columns were prepared using traditional stainless steel HPLC housings and end fittings. The packing solution for all of these columns was pH 7.4, 0.067 M potassium phosphate buffer, and the packing pressure was 4000 psi (28 MPa).

Chromatographic studies

Figure 4.1 shows the general separation and analysis strategy that was used in this study to examine the free fractions of *R*- and *S*-warfarin. Ultrafast extraction based on an immobilized HSA microcolumn was first used to separate the free and protein-bound fractions of *R*- and *S*-warfarin in the presence of a sample that contained soluble HSA. In

Figure 4.1 General scheme for separation of the free and protein-bound fractions of a drug and resolution of the enantiomers in free drug fraction through the use of ultrafast extraction and multi-dimensional HPAC. Reproduced with permission from X. Zheng, M.J. Yoo, D.S. Hage, *Analyst* 138 (2013) 6262-6265.



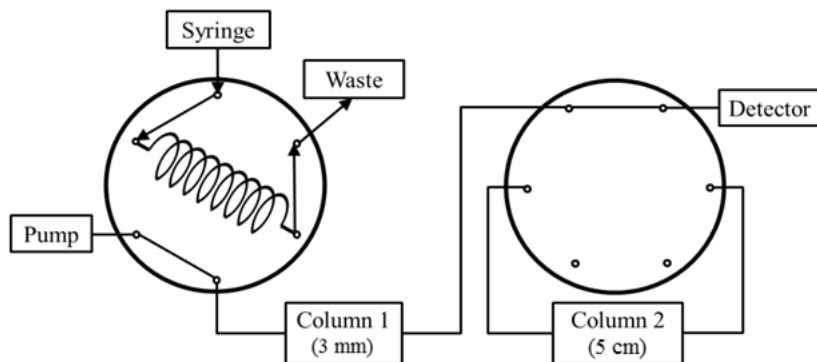
this process, the protein-bound drug and proteins in the sample were eluted in a non-retained peak from the microcolumn, while the free drug fraction in the sample was extracted and retained. This retained free drug fraction was later eluted from the microcolumn under isocratic conditions and delivered to a second, larger HSA column, which was utilized as a chiral stationary phase for the separation and measurement of the captured drug enantiomers.¹⁰

To be specific, this work utilized a multi-dimensional system in which a 3 mm × 2.1 mm i.d. HSA microcolumn was used for the extraction of free drug fractions and a 5 cm × 2.1 mm i.d. HSA column was used for chiral separations of the retained free drug fractions. The sample loading, injection and column switching were controlled by two separate Rheodyne six port valves (Cotati, CA, USA), as shown in Figure 4.2. The mobile phase was pH 7.4, 0.067 M potassium phosphate buffer in the free drug extractions and in the initial chiral separations. All samples containing racemic warfarin and HSA were prepared in this buffer and incubated for at least 1 h before injection to allow equilibrium to be established between the free and protein-bound fractions of the drug in the sample.⁹

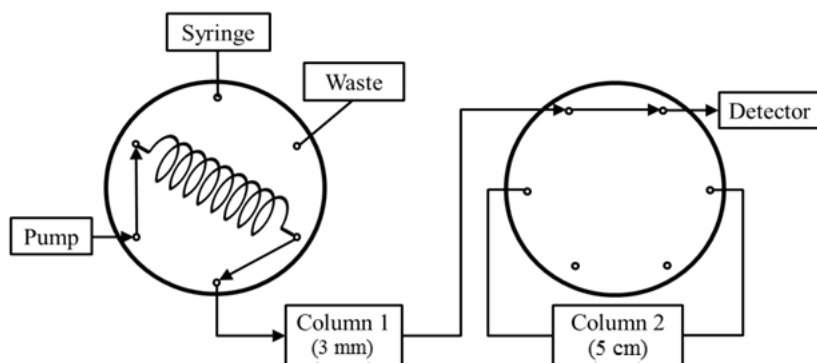
The initial studies examining the free fraction extraction of *R*- and *S*-warfarin used a 1.0 µL sample of 10 µM racemic warfarin or a 10 µM racemic warfarin/20 µM HSA mixture that was injected onto a 3 mm × 2.1 mm i.d. HSA microcolumn at flow rates ranging from 0.5 mL/min to 6.0 mL/min. In the final method that was developed in this study, a 1.0 µL sample injection was made onto the 3 mm × 2.1 mm i.d. HSA microcolumn at a flow rate of 5.0 mL/min for extraction of the free drug fraction. Eighteen seconds later, a switching valve was used to transfer the eluting free drug

Figure 4.2 Valve configurations used in the multi-dimensional HPAC system. The first valve was used for (a) loading and (b) injecting a sample onto an HSA microcolumn for a free fraction separation. (c) The second valve was switched when the protein-bound drug complex and excess protein had been passed through the HSA microcolumn and the free drug fraction had just begun to exit this microcolumn. The free drug fraction, or a representative portion, was then passed on to a second and longer HSA column for a chiral separation. Reproduced with permission from X. Zheng, M.J. Yoo, D.S. Hage, *Analyst* 138 (2013) 6262-6265.

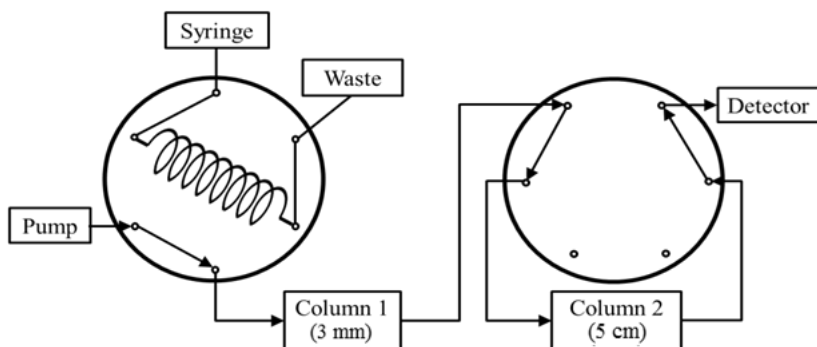
(a) Sample Loading



(b) Sample Injection and Free Drug/Protein-Bound Drug Separation



(c) Column Switching/Chiral Separation of Free Drug Fraction



fraction to a longer 5 cm \times 2.1 mm i.d. HSA column for use in a chiral separation at 0.5 mL/min. The aqueous samples used in these latter studies contained 5 μ M racemic warfarin or a 5 μ M warfarin/10 μ M HSA mixture; 30 μ M racemic warfarin or 30 μ M warfarin/600 μ M HSA, to examine the use of this method at clinically-relevant concentrations; and a mixture of 30 μ M racemic warfarin and human serum (which contained approximately 600 μ M HSA) to study the feasibility of using this system with human serum samples. The warfarin enantiomers were detected by monitoring their fluorescence at an excitation wavelength of 310 nm and an emission wavelength of 390 nm. The concentrations of *R*- and *S*-warfarin in each sample were determined by comparing the resulting peak areas to those obtained for warfarin standards.

Ultrafiltration studies

Before sample introduction, each ultrafiltration device was washed three times with 1 mL water and spun at 1500 \times g for 5 min. The devices were then washed three times in the same manner with 1 mL of pH 7.4, 0.067 M potassium phosphate buffer. Any remaining buffer in the device was removed by spinning the filtration device at 1500 \times g for 15 min. Immediately after these washing and pretreatment steps, a 1 mL sample containing warfarin or warfarin plus HSA, as prepared in pH 7.4, 0.067 M potassium phosphate buffer or human serum, was introduced into three ultrafiltration devices and spun at 1500 \times g and 37°C for 2.5 min or 6.0 min, respectively (Note: different spinning periods were used to make sure that no more than 0.5 mL of the sample passed into the filtrate vial, thus allowing for accurate free drug fraction measurements).¹⁵

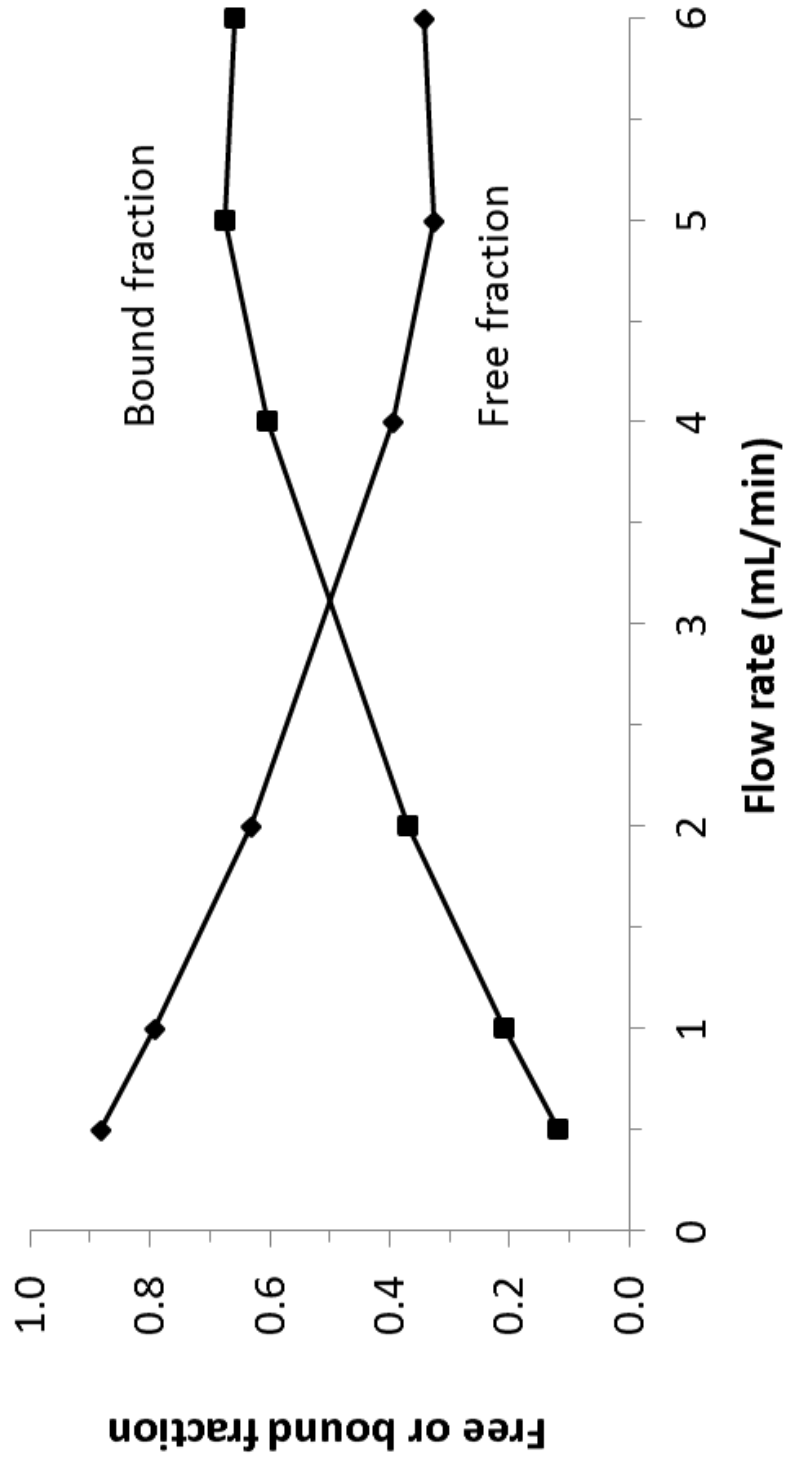
The resulting filtrates were collected for the measurement of their warfarin concentrations by using an HPLC-based chiral separation. This was accomplished by making a 5 μ L injection of each filtrate sample at 1.0 mL/min onto a 1 cm \times 2.1 mm i.d. HSA column. The mobile phase in this case consisted of pH 7.4, 0.067 M potassium phosphate buffer containing 1.5% (v/v) 1-propanol. The elution of warfarin enantiomers from this column was again monitored by using a fluorescence detector, as described in the previous section, and the concentrations of *R*- and *S*-warfarin in each filtrate were determined by comparing the resulting peaks areas to those that were obtained by the same approach when using warfarin standards.

Results and Discussion

Optimization of conditions for multi-dimensional affinity system

Studies were first performed with this system to find the optimum flow rate conditions for extraction of the free fraction of *R/S*-warfarin without creating significant interferences from the portion of the drug that was originally bound to sample proteins but was released as the initial free drug fraction was removed. Figure 4.3 shows the apparent free drug fractions that were obtained for warfarin/HSA mixtures at various flow rates and at 37 °C in pH 7.4, 0.067 M phosphate buffer when using a 3 mm \times 2.1 mm i.d. HSA microcolumn for ultrafast affinity extraction. Based on a measured protein content of 57 (\pm 1) mg HSA/g silica, the microcolumn was determined to contain 4.0 nmol HSA. The amount of warfarin applied per injection in Figure 4.3 was 0.25% of the estimated binding capacity. Experiments with injections of only *R/S*-warfarin indicated

Figure 4.3 Effect of flow rate on the measurement of free fractions in mixtures of racemic warfarin and HSA when using ultrafast affinity extraction. Conditions: 1.0 μL of 10 μM warfarin or 10 μM warfarin/20 μM HSA injected onto a 3 mm \times 2.1 mm i.d. HSA microcolumn. Reproduced with permission from X. Zheng, M.J. Yoo, D.S. Hage, *Analyst* 138 (2013) 6262-6265.

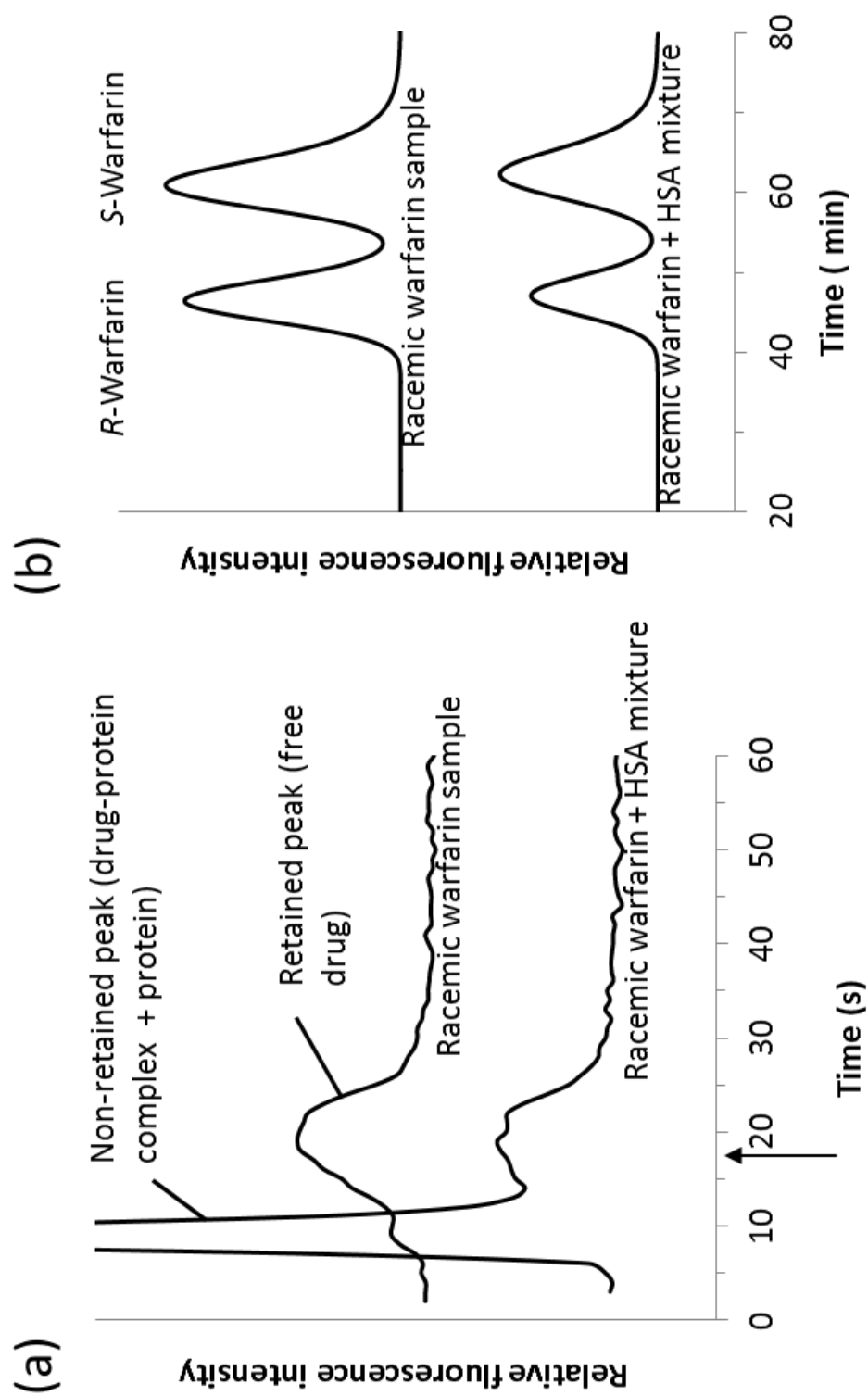


that more than 99% extraction occurred for this drug's enantiomers under these injection conditions and at all of the flow rates tested in this study.

In Figure 4.3, the apparent free drug fractions that were measured for a mixture of warfarin with soluble HSA was elevated at lower flow rates because the longer extraction period provided in the microcolumn under these conditions allowed for some dissociation of this drug from its protein-bound fraction in the sample, as noted previously.^{1,9} This process was decreased at higher flow rates and had no significant effect on the measured free fractions at a flow rate of 5.0 mL/min or higher, which corresponded to a residence time of 100 ms or less for the sample on the HSA microcolumn.

A second set of studies examined the ability of the multi-dimensional HPAC system to separate warfarin enantiomers in the retained free drug fraction (see Figure 4.4). Samples containing 1.0 μ L of 5 μ M warfarin or a 5 μ M warfarin/10 μ M HSA mixture were applied to the multi-dimensional system. The upper peak in Figure 4.4(a) was obtained by injecting only warfarin onto the HSA microcolumn at 5 mL/min. The free fraction of warfarin that was extracted by this microcolumn eluted with a retention time of approximately 17-20 s. This figure also shows a chromatogram that was obtained when the same amount of warfarin and a two-fold mole excess of soluble HSA were injected onto the HSA microcolumn under identical conditions. In this case, a large non-retained peak was now observed at 5-7 s due to the elution of the soluble HSA and protein-bound fraction of warfarin. The second retained peak in this case represented the free fraction of warfarin that was extracted by, and later eluted from, the HSA microcolumn.

Figure 4.4 Chromatograms for 1.0 μL injections of 5 μM racemic warfarin or 5 μM racemic warfarin plus 10 μM HSA on (a) an HSA microcolumn at 5.0 mL/min or (b) a chiral HSA column at 0.5 mL/min after sample passage through the HSA microcolumn. The arrow in (a) shows the time at which a valve was switched to pass the retained components from the HSA microcolumn onto the larger HSA column that was used for the chiral separation. These results were obtained at 37 $^{\circ}\text{C}$ using pH 7.4, 0.067 M phosphate buffer as the mobile phase for both columns. Reproduced with permission from X. Zheng, M.J. Yoo, D.S. Hage, *Analyst* 138 (2013) 6262-6265.



The free warfarin fraction, or a representative portion of this fraction, that was extracted by the HSA microcolumn was then eluted in the presence of the pH 7.4 phosphate buffer onto a 5 cm \times 2.1 mm i.d. HSA column at 0.5 mL/min for a chiral separation. The chromatograms in Figure 4.4(b) show the peaks that were obtained for *R*- and *S*-warfarin in samples that contained only racemic warfarin or racemic warfarin plus soluble HSA. With this combined approach, it was possible to simultaneously study the free fractions for both *R*- and *S*-warfarin in the original sample. Although the chiral separation obtained with the pH 7.4 buffer in Figure 4.4(b) provided baseline resolution for the warfarin enantiomers and was sufficient for these exploratory studies, the speed of this latter step could be reduced to less than 10 min by using a more efficient HSA monolith column and/or by adding an organic modifier to the mobile phase.^{10,16,17}

Measurement of free drug fractions for warfarin enantiomers

The free fraction of *R*- or *S*-warfarin in a mixture of racemic warfarin and soluble HSA was calculated by dividing the concentration of the enantiomer's free fraction, as represented by lower peaks in Figure 4.4(b), by the concentration measured for the enantiomer and at the same total sample concentration but with no soluble protein present, as represented by the upper peaks in Figure 4.4 (b). The concentrations of the *R*- and *S*-warfarin fractions were determined by comparing the sizes of these peaks to those obtained with the same chromatographic system and using warfarin standards. The free fractions for *R*- and *S*-warfarin in various samples were measured by this approach based on multi-dimensional HPAC and by employing a reference method that made use of

ultrafiltration followed by a chiral separation using an HSA column. The results that were obtained by each method are summarized in Table 4.1.

Table 4.1 shows that there was good agreement between the free fractions that were measured in Figure 4.4 by the multi-dimensional HPAC method and by ultrafiltration followed with a chiral separation. For a sample that contained 5 μM racemic warfarin and 10 μM soluble HSA, the absolute difference in these free fractions was 1-6%, with the results showing no significant difference at the 95% confidence level. In addition, these measured free fractions agreed with the range of 33-43% that was predicted for R- and S-warfarin based on the known binding constants of this system.^{9,10}

The multi-dimensional HPAC method was also used to examine other samples. One of these samples contained 30 μM racemic warfarin and 600 μM HSA, representing a clinically- relevant concentration of HSA and a typical therapeutic concentration for warfarin.¹⁸ Good agreement between the multi-dimensional HPAC system and reference method was again obtained, with an absolute difference in the measured free fractions of 0.3-0.5% and no significant differences at the 95% confidence level. In addition, the measured free fractions were consistent with a range of approximately 0.5-2% that was estimated from the reported binding constants for the warfarin-HSA interaction.^{9,10} The free fractions of the warfarin enantiomers were also examined in human serum that was spiked with a therapeutic level of this drug. The results for the multi-dimensional HPAC system and reference method were again comparable, with an absolute difference of 0.2-0.5% and no significant differences being noted at the 95% confidence level.

Table 4.1 Free drug fractions measured for *R*- and *S*-warfarin in samples containing soluble HSA or human serum

Sample & Analyte	Measured free fraction ^a	
	Multi-dimensional HPAC	Ultrafiltration + chiral separation
<i>Racemic warfarin (5 μM) + HSA (10 μM)</i>		
<i>R</i> -Warfarin	42 (\pm 4)%	41 (\pm 4)%
<i>S</i> -Warfarin	38 (\pm 5)%	32 (\pm 3)%
<i>Racemic warfarin (30 μM) + HSA (600 μM)</i>		
<i>R</i> -Warfarin	1.8 (\pm 0.8)%	1.5 (\pm 0.5)%
<i>S</i> -Warfarin	1.3 (\pm 0.2)%	1.8 (\pm 0.2)%
<i>Racemic warfarin (30 μM) + human serum^b</i>		
<i>R</i> -Warfarin	2.7 (\pm 1.7)%	2.5 (\pm 0.2)%
<i>S</i> -Warfarin	1.1 (\pm 0.3)%	1.6 (\pm 0.7)%

^aThese values were obtained at 37 °C in pH 7.4, 0.0067 M potassium phosphate buffer. The numbers in parentheses represent \pm 1 S.D. (n = 3).

^bThe human serum contained approximately 600 μ M HSA.

Reproduced with permission from X. Zheng, M.J. Yoo, D.S. Hage, Analyst 138 (2013) 6262-6265.

Simultaneous estimation of association equilibrium constants for R- and S-warfarin with soluble HSA

The multi-dimensional HPAC system was next used as a screening tool to determine the association equilibrium constants for *R*- and *S*-warfarin with HSA. This was accomplished by using the free fraction data along with a single-site binding model. For a drug and protein interaction that involves 1:1 binding, the relationship between the free fraction (F) and the association equilibrium constant (K_a) for this interaction can be described by using Equations 4.1 and 4.2,

$$F = \frac{C_d - [D-P]}{C_d} \quad (4.1)$$

$$K_a = \frac{[D-P]}{(C_d - [D-P])(C_p - [D-P])} \quad (4.2)$$

in which C_d is the total concentration of drug in the original sample, C_p is the total concentration of protein in the sample, $[D-P]$ is the concentration of the drug-protein complex in the original sample.⁹

In this study, both *R*- and *S*-warfarin were present in a sample containing racemic warfarin and both enantiomers were able to interact with any HSA that was present. Thus, the free fractions for these two enantiomers (F_R and F_S) and their association equilibrium constants ($K_{a,R}$ and $K_{a,S}$) were calculated separately, as described by Equations 4.3-4.6,

$$F_R = \frac{C_R - [R-P]}{C_R} \quad (4.3)$$

$$K_{a,R} = \frac{[R-P]}{(C_R - [R-P])(C_p - [R-P] - [S-P])} \quad (4.4)$$

$$F_S = \frac{C_S - [S-P]}{C_S} \quad (4.5)$$

$$K_{a,S} = \frac{[S-P]}{(C_S - [S-P])(C_p - [R-P] - [S-P])} \quad (4.6)$$

where C_R and C_S represent the concentrations of *R*- and *S*-warfarin in the original sample. According to the information provided by their supplier, the *R*- and *S*-warfarin were present in identical amounts in their original racemic mixture. Under these conditions, the relationship of their concentrations with C_d can be described by Equation 4.7.

$$2 C_R = 2 C_S = C_d \quad (4.7)$$

According to Equations 4.3-4.7 and the data of free drug fractions that were measured in this study, the overall association equilibrium constants for each drug with HSA can thereafter be obtained. For instance, by using Equation 4.3 the concentration of the *R*-warfarin/HSA complex ($[R-P]$) could be calculated from the measured free fraction of *R*-warfarin (F_R). Substituting the value of $[R-P]$ into Equation 4.4 then made it possible to obtain $K_{a,R}$.⁹ The same process was employed for the calculation of $K_{a,S}$ by using Equations 4.5 and 4.6. The results that were obtained by this process are shown in Table 4.2.

Table 4.2 shows the initial results that were obtained for the 5 μ M warfarin/10 μ M HSA mixture. This table also lists previous binding constants that have been reported for *R*- and *S*-warfarin at Sudlow site I of HSA under the same pH and temperature conditions.¹⁰ Under these conditions, the association equilibrium constants that were

Table 4.2 Association equilibrium constants for *R*- and *S*-warfarin with soluble HSA based on a single-site binding model

Sample & Analyte	Association equilibrium constant, K_a (M^{-1}) ^a		
	Multi-dimensional HPAC	Ultrafiltration + chiral separation	Literature value [Ref. 10]
<i>Racemic warfarin (5 μM) + HSA (10 μM)</i>			
<i>R</i> -Warfarin	$2.0 (\pm 0.4) \times 10^5$	$2.1 (\pm 0.4) \times 10^5$	$2.1 (\pm 0.2) \times 10^5$
<i>S</i> -Warfarin	$2.4 (\pm 0.6) \times 10^5$	$3.2 (\pm 0.4) \times 10^5$	$2.6 (\pm 0.4) \times 10^5$
<i>Racemic warfarin (30 μM) + HSA (600 μM)</i>			
<i>R</i> -Warfarin	$1.0 (\pm 0.4) \times 10^5$	$1.2 (\pm 0.4) \times 10^5$	$2.1 (\pm 0.2) \times 10^5$
<i>S</i> -Warfarin	$1.3 (\pm 0.2) \times 10^5$	$0.9 (\pm 0.1) \times 10^5$	$2.6 (\pm 0.4) \times 10^5$
<i>Racemic warfarin (30 μM) + Human serum</i> ^b			
<i>R</i> -Warfarin	$0.6 (\pm 0.4) \times 10^5$	$0.7 (\pm 0.1) \times 10^5$	$2.1 (\pm 0.2) \times 10^5$
<i>S</i> -Warfarin	$1.6 (\pm 0.5) \times 10^5$	$1.1 (\pm 0.5) \times 10^5$	$2.6 (\pm 0.4) \times 10^5$

^aThese values were measured for the given samples at 37 °C in pH 7.4, 0.067 M potassium phosphate buffer. The numbers in parentheses represent a range of ± 1 S.D. ($n=3$) Values from Ref. 10 were measured under the same conditions by using frontal analysis.

^bThe human serum contained approximately 600 μM HSA.

Reproduced with permission from X. Zheng, M.J. Yoo, D.S. Hage, Analyst 138 (2013) 6262-6265.

estimated by multi-dimensional HPAC and the reference methods continued to show good agreement at the 95% confidence level with one another and with the literature values. Similar calculations to those used for 5 μM warfarin/10 μM HSA mixture sample were carried out for the 30 μM warfarin/600 μM HSA mixture and for the spiked serum samples. As shown in Table 4.2, the association equilibrium constants that were obtained by multi-dimensional HPAC and the reference approach were again consistent with each other; however, the estimated binding constants were 38-71% smaller than the literature values. This latter difference is probably due to the greater uncertainty that was present for these samples in the measurement of their relatively small free fractions. It is also possible there were some deviations from a single-site binding model due to greater nonspecific interactions by warfarin with the much larger amounts of HSA, and other proteins in the case of the serum, in this second group of samples.

Conclusions

In summary, it was shown that a multi-dimensional HPAC system that used ultrafast affinity extraction in combination with a chiral separation could be used to simultaneously measure the free fractions of *R*- and *S*-warfarin in serum or drug-protein mixtures. This approach was also used to estimate the binding constants for these enantiomers with HSA. The results of this method gave good agreement with a reference method that was based on ultrafiltration plus a chiral separation. However, the multi-dimensional HPAC method had several potential advantages over ultrafiltration. For instance, this method required only 1 μL of sample per injection and could isolate the free

warfarin fractions within 20-30 s of injection. In comparison, a 1 mL sample was needed for ultrafiltration and 1 h was required for the separation of a free drug fraction by this approach. It was also possible to directly couple the ultrafast extraction with a chiral separation to automate and complete both steps using a single system. This approach is not limited to warfarin or HSA but could easily be extended to other chiral drugs, or drug mixtures, and their binding proteins through the use of similar affinity microcolumns and chiral stationary phases.

References

1. W. Clarke, J. E. Schiel, A. Moser, D. S. Hage, *Anal. Chem.* 77 (2005) 1859-1866.
2. W. Clarke, A. R. Chowdhuri, D. S. Hage, *Anal. Chem.* 73 (2001) 2157-2164.
3. H. Takahashi, T. Kashima, S. Kimura, N. Muramota, H. Nakahata, S. Kubo, Y. Shimoyama, M. Kajiware, H. Echizen, *J. Chromatogr. B* 701 (1997) 71-80.
4. M. Rowland, T. N. Tozer, *Clinical pharmacokinetics, concepts and applications*, Lippincott, Philadelphia, PA, 1995.
5. F. Herve, S. Urien, E. Albengres, J. C. Duche, J. P. Tillement, *Clin. Pharmacokinet.* 26 (1994) 44-58.
6. J. W. Melten, A. J. Wittebrood, J. J. Hubb, G. H. Faber, J. Wemer, D. B. Faber, *J. Pharm. Sci.* 74 (1985) 692-694.
7. J. E. Schiel, Z. Tong, C. Sakulthaew, D. S. Hage, *Anal. Chem.* 83 (2011) 9384-9390.
8. C. M. Ohnmacht, J. E. Schiel, D. S. Hage, *Anal. Chem.* 78 (2006) 7547-7556.
9. R. Mallik, M. J. Yoo, C. J. Briscoe, D. S. Hage, *J. Chromatogr. A* 1217 (2010) 2796-2803.
10. B. Loun, D. S. Hage, *Anal. Chem.* 66 (1994) 3814-3822.
11. W. E. Evans, J. J. Schentag, W. J. Jusko, eds, *Applied pharmacokinetics: principles of therapeutic drug monitoring*, Applied Therapeutics, Inc. Vancouver, WA, 1992.
12. X. M. He, D. C. Carter, *Nature* 358 (1992) 209-215.
13. G. Sudlow, D. J. Birkett, D. N. Wade, *Mol. Pharmacol.* 12 (1976) 1052-1061.
14. J.E. Schiel, Ph.D. Dissertation, University of Nebraska, Lincoln, Nebraska, 2009.

15. J.B. Whitlam, K.F. Brown, J. Pharmaceut. Sci. 70 (1980) 146-150.
16. R. Mallik, D. S. Hage, J. Pharm. Biomed. Anal. 46 (2008) 820-930.
17. E. L. Pfaunmiller, M. Hartmann, C. M. Dupper, S. Soman, D. S. Hage, J. Chromatogr. A 1269 (2012) 198-207.
18. C. A. Burtis, E. R. Ashwood, D. E. Bruns (Eds), Tietz Textbook of Clinical Chemistry and Molecular Diagnostics, 4th ed.; Saunders: St. Louis, MO, 2006.

CHAPTER 5

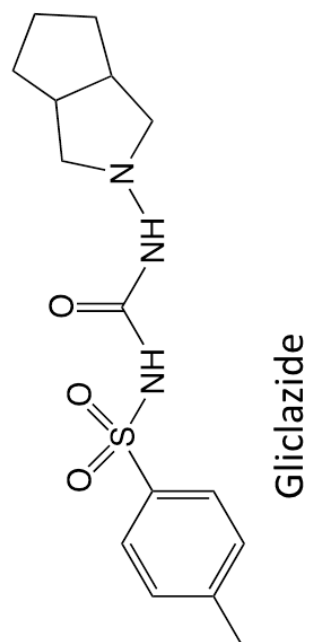
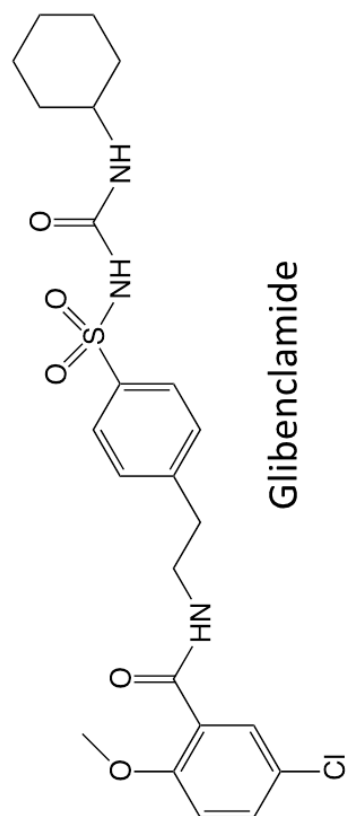
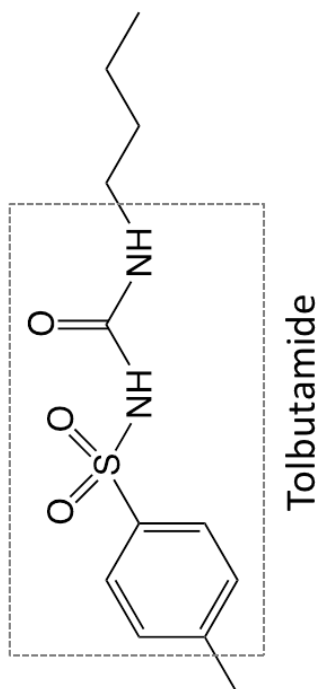
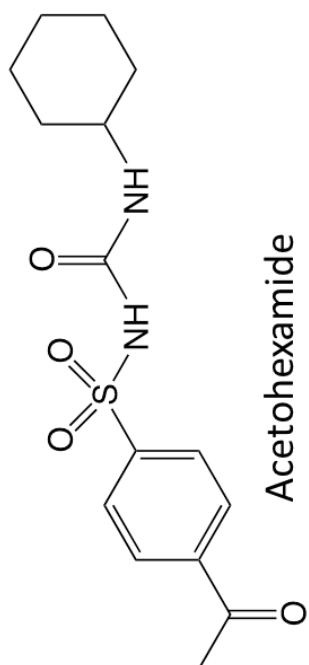
The Use of Ultrafast Affinity Extraction and Multi-Dimensional HPAC to Study the Interactions of Sulfonylurea Drugs with Normal or Glycated Human Serum Albumin

Portion of this chapter have previously appeared in X. Zheng, R. Matsuda, D.S. Hage “Analysis of Free Drug Fractions by Ultrafast Affinity Extraction: Interactions of Sulfonylurea Drugs with Normal or Glycated Human Serum Albumin” Journal of Chromatography A 2014, 1371, 82-89.

Introduction

Diabetes is a disease that is associated with insulin deficiency or glucose intolerance, which can both result in elevated levels of glucose in the bloodstream.¹ Recent reports by the International Diabetes Federation and the American Diabetes Association have indicated that diabetes affects 366 million people in the world and 25.8 million people in the U.S.^{1,2} Type II diabetes accounts for about 90-95% of the confirmed cases of diabetes and results from insulin resistance.^{1,2} Sulfonylurea drugs are commonly used to treat type II diabetes by stimulating the release of insulin, thereby decreasing the level of glucose in blood.³ Figure 5.1 shows the general structure of a sulfonylurea drug.^{4,5} Examples of common first-generation sulfonylurea drugs are acetohexamide and tolbutamide; second-generation drugs include gliclazide and glibenclamide, which tend to be more easily excreted and effective than the first-generation sulfonylurea drugs.⁶

Figure 5.1 Structures of common sulfonylurea drugs. The portion within the dashed box represents the core structure of these drugs. Reproduced with permission from X. Zheng, R. Matsuda, D.S. Hage, J. Chromatogr. A 1371 (2014) 82-89.



Sulfonylurea drugs are highly bound to serum proteins and, in particular, to human serum albumin (HSA).^{7,8} HSA is the most abundant serum protein, accounting for 60% of the total serum protein content and having a normal concentration of 35-50 g/L (526-752 μ M).^{9,10} HSA has a mass of 66.5 kDa and is composed of 585 amino acids. HSA functions as a transport protein for many low mass hormones, fatty acids, and drugs in the bloodstream.⁹ There are two major drug binding sites on HSA, which are often known as Sudlow sites I and II.^{9,11,12}

The elevated levels of glucose in blood during diabetes can result in the non-enzymatic glycation of proteins.¹³⁻¹⁶ Early stage glycation involves the nucleophilic addition of a free amine group on a protein to a reducing sugar (e.g., glucose); advanced glycation products can also form through further reactions.^{7,18-20} It has been found that there can be a 2- to 5-fold increase in the amount of HSA that is glycated in diabetic patients when compared with healthy individuals.^{7,21} Structural investigations of glycated HSA have further found that glycation-related modifications can often occur at or near Sudlow sites I and II.²²⁻²⁵ In addition, glycation has been shown to cause changes in the affinity of various sulfonylurea drugs for HSA.²⁶⁻³⁴ Such changes are of concern because it has been proposed that they may affect the free, or non-protein bound, and active fraction of these drugs in the bloodstream.^{7,26,32,34}

Various methods have been developed in the past to measure free drug fractions.³⁵⁻⁴⁴ Two common methods used for free drug analysis are equilibrium dialysis and ultrafiltration. However, these techniques often require long separation or analysis times (ranging from 15-30 min to hours) and relatively large sample volumes (i.e., typically in the milliliter range). In addition, the non-specific adsorption of drugs to the

membranes or components of these methods can introduce errors in the free fraction measurements.^{35,37-41} Ultrafast affinity extraction is an alternative technique that has been used to measure the free and protein-bound forms of drugs and hormones in clinical and pharmaceutical samples.^{37-40,45-47} In this method, an affinity microcolumn that contains an immobilized binding agent with relatively fast and strong binding for the drug or hormone of interest is used to extract the free form of this analyte on a time scale that minimizes dissociation of the same analyte from its protein-bound form in the sample. The advantages of this approach include its speed, ease of automation, good correlation with reference methods, and need for only a small amount of the analyte and protein.³⁵⁻⁴⁵ This method has been used to measure the free fractions of thyroxine, warfarin and phenytoin in clinical samples.^{38-40,45,46} This technique has also been used to estimate the association equilibrium constants for various drugs with normal HSA.^{37,47} In addition, a multi-dimensional system combining ultrafast affinity extraction with a chiral stationary phase has recently been used to simultaneously measure the free fractions of warfarin enantiomers in complex samples.³⁸

This chapter will examine the development and use of ultrafast affinity extraction in a multi-dimensional system to measure and compare the free fractions of various sulfonylurea drugs in the presence of normal HSA or glycated HSA. The HSA will be glycated *in vitro* at levels similar to those found in patients with prediabetes or diabetes. Various factors, such as column size and flow rate, will be considered in the optimization of this system for determining the free fractions of sulfonylurea drugs. The system will then be used to measure the free fractions and global affinity constants for these drugs with normal HSA or glycated HSA by using samples that have been prepared at typical

therapeutic or physiological concentrations of these drugs and proteins. The results will provide insight concerning how glycation may alter the free fractions of sulfonylurea drugs in the circulatory system. The same results will also provide valuable information as to how ultrafast affinity extraction can be modified and developed for use in the study of drug-protein interactions at clinically-relevant concentrations.

Experimental

Materials and reagents

The HSA (Cohn fraction V, essentially fatty acid free, $\geq 96\%$ pure), tolbutamide, acetohexamide, gliclazide, and glibenclamide were from Sigma (St. Louis, MO, USA). The reagents for the bicinchoninic acid (BCA) protein assay were obtained from Pierce (Rockford, IL, USA). The Nucleosil Si-300 silica (7 μm particle diameter, 300 Å pore size) was from Macherey Nagel (Düren, Germany). All buffers and aqueous solutions were prepared using water from a NANOpure system (Barnstead, Dubuque, IA, USA) and were passed through Osmonics 0.22 μm nylon filters from Fisher Scientific (Pittsburgh, PA, USA).

Apparatus

The microcolumns used in this chapter were packed using a Prep 24 pump from ChromTech (Apple Valley, MN, USA). The HPLC system was comprised of a PU-2080

Plus pump, AS-2057 autosampler, and UV-2075 absorbance detector from Jasco (Easton, MD, USA), plus a six-port Lab Pro valve (Rheodyne, Cotati, CA, USA). An Alltech water jacket (Deerfield, IL, USA) and an Isotemp 3013D circulating water bath from Fisher Scientific were used to maintain a temperature of $37.0 (\pm 0.1) ^\circ\text{C}$ for the columns during all experiments in this chapter. ChromNAV v1.18.04 software and LCNet from Jasco were used to control the system. Chromatograms were analyzed through the use of PeakFit v4.12 software (Jandel Scientific, San Rafael, CA, USA).

Column preparation and protein glycation

Two batches of glycated HSA with different levels of glycation were prepared *in vitro* as described previously.^{29,31} These glycated HSA samples (referred to later in this paper as gHSA1 and gHSA2) were made by incubating normal HSA at $37 ^\circ\text{C}$ and over four weeks with either moderate or high levels of D-glucose (i.e., 5 or 10 mM) in sterile pH 7.4, 0.067 M phosphate buffer. The resulting protein solutions were lyophilized and stored at $-80 ^\circ\text{C}$ until use. The glycation levels of these modified proteins were determined by using a fructosamine assay from Diazyme Laboratories (San Diego, CA, USA), as described in Refs. 29,31. The glycation levels measured for the normal HSA, gHSA1 and gHSA2 samples were $0.24 (\pm 0.15)$, $1.39 (\pm 0.28)$ and $3.20 (\pm 0.13)$ mol hexose/mol HSA, respectively.

Normal HSA was immobilized to Nucleosil Si-300 silica for use as a stationary phase in ultrafast affinity extraction and the multi-dimensional affinity system. This immobilization was carried out by using the Schiff base method, as described in Ref. 48. A control support, in which no HSA was added during the immobilization step, was

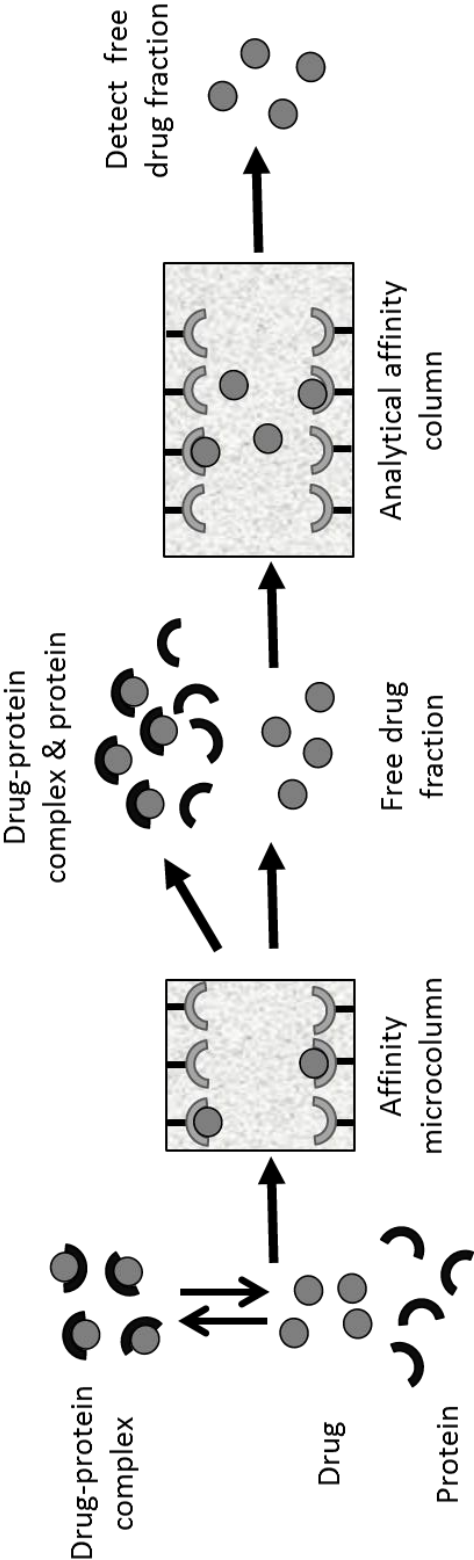
prepared by the same process. A BCA assay was used, according to instructions provided by the manufacturer of this assay, to determine the protein content of the final HSA support by using HSA as the standard and the control support as the blank.²⁹⁻³⁴ This assay gave a protein content of 65 (\pm 2) mg HSA/g silica.

Affinity columns with lengths of 5 to 25 mm and 2.1 mm i.d. were packed into standard stainless steel housings by using pH 7.4, 0.067 M potassium phosphate buffer as the packing solution. The affinity columns with a length of 1 mm and 2.1 mm i.d. were packed in a similar manner but used a frit-in-column design, as described in Ref. 49. The packing pressure was 4000 psi (28 MPa) for the 10 or 25 mm long columns and 3000 psi (20 MPa) for the 1 mm or 5 mm long columns. These columns were stored in pH 7.4, 0.067 M potassium phosphate buffer at 4 °C when not in use.

Chromatographic studies

The multi-dimensional affinity system had two HSA columns that could be connected in series through the use of a six-port valve, as has been shown in Chapter 4.³⁸ In this system, which is illustrated in Figure 5.2, an HSA microcolumn was first used to extract a free drug fraction from a sample. A second HSA column was then placed on-line with the first column to further separate the extracted fraction from other sample components (e.g., drug that had dissociated from proteins in the sample during passage through the first column). The mobile phase for both columns was pH 7.4, 0.067 M potassium phosphate buffer. All samples containing sulfonylurea drugs were dissolved in

Figure 5.2 General scheme for the separation of the free and protein-bound fractions of a drug in a sample and measurement of the free drug fraction through the use of ultrafast affinity extraction and a multi-dimensional affinity system. Reproduced with permission from X. Zheng, R. Matsuda, D.S. Hage, J. Chromatogr. A 1371 (2014) 82-89.



this buffer. The mixtures of the drugs and normal HSA or glycated HSA were prepared by dissolving each protein in the corresponding drug solutions. These drug/protein mixtures were incubated for at least 30 min at 37 °C before injection to allow equilibrium to be established between the free and protein-bound fractions of the drug in the sample.³⁷ Replicate injections ($n = 4$) were made for all samples and standards onto the system. The concentrations of the drugs in the tested samples were representative of the therapeutic ranges for these agents (i.e., 184-370 μM for tolbutamide, 61-216 μM for acetohexamide, 15-31 μM for gliclazide, and 0.08-0.4 μM for glibenclamide).^{50,51} The samples also contained concentrations of normal HSA or glycated HSA that were representative of the physiological levels of this protein (i.e., 526-752 μM).⁵⁰

The column sizes and flow rates that were used for ultrafast affinity extraction were determined as described in next section. The HSA microcolumns that were used for this purpose in the final system had the following dimensions: 5 mm \times 2.1 mm i.d. for tolbutamide and acetohexamide, 10 mm \times 2.1 mm i.d. for gliclazide, and 1 mm \times 2.1 mm i.d. for glibenclamide. A 1.0 μL sample injection was made onto each of these HSA microcolumns at an initial flow rate of 2.25 mL/min for tolbutamide, 2.5 mL/min for acetohexamide, 2.5 mL/min for gliclazide, and 0.35 mL/min for glibenclamide during extraction of the free drug fractions. The valve to which these microcolumns were connected was then placed on-line with the second HSA column at 1.5 min after injection for tolbutamide, 2.2 min for acetohexamide, 0.85 for gliclazide, and 5.0 min for glibenclamide. The flow rate was changed at the same time to 0.50, 0.75, 0.50 or 0.25 mL/min, respectively, for the second portion of the separation. The size of the second HSA column was 10 mm \times 2.1 mm i.d. for tolbutamide and acetohexamide, 25 mm \times 2.1

mm i.d. for gliclazide, and 5 mm \times 2.1 mm i.d. for glibenclamide. The following wavelengths were employed for absorbance detection: 227 nm for tolbutamide, 248 nm for acetohexamide, 226 nm for gliclazide, and 302 nm for glibenclamide. The free drug concentration was determined by comparing the resulting peak area to those obtained for standards containing only the drug. The free fraction was calculated by dividing the free drug concentration by the total concentration of the drug in the sample.^{37,38,47}

Results and Discussion

Optimization of conditions for ultrafast affinity extraction

The residence time for the sample in the extraction column is one factor to consider when using ultrafast affinity extraction to isolate a free drug fraction. One way this factor can be adjusted is by altering the column size that is used for the extraction process.^{37,38,47} A relatively short column will provide a smaller column residence time than a longer column operated at the same flow rate. A shorter column will also have a lower backpressure, allowing work at higher flow rates, while a longer column size should provide higher retention and a better separation of the free drug fraction from other sample components.^{37,47}

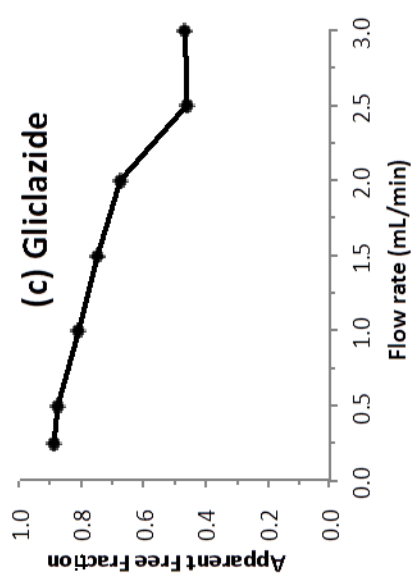
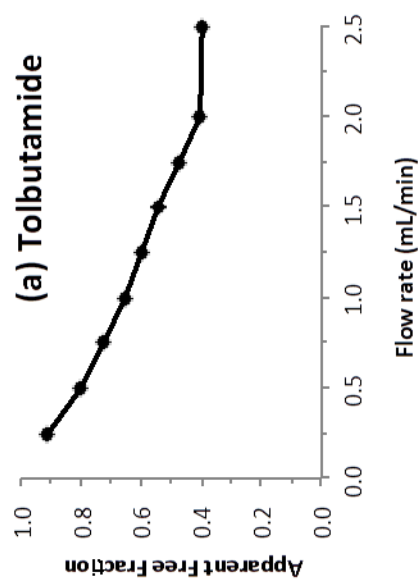
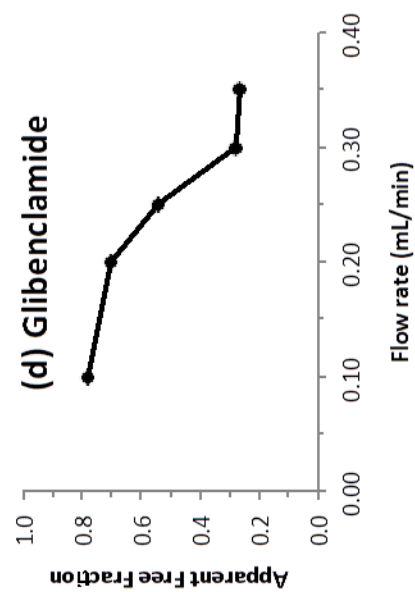
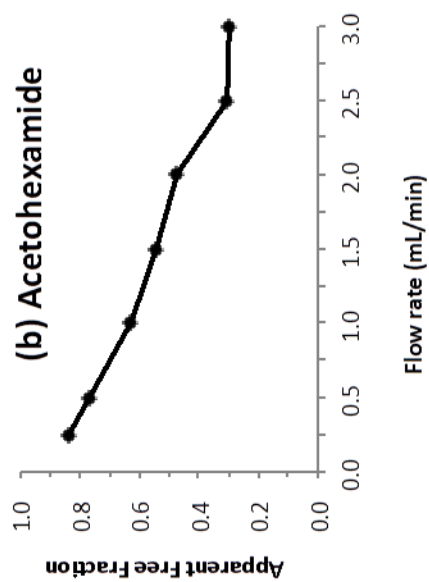
The HSA microcolumns that were used in this chapter for ultrafast affinity extraction had sizes of 1-10 mm \times 2.1 mm i.d. These microcolumns were used at flow rates up to 3.5 mL/min, giving column backpressures of 1.9-3.2 MPa or less under these conditions. The ultrafast affinity extractions that were conducted with gliclazide, which

has relatively weak binding to HSA,^{33,47} used 10 mm × 2.1 mm i.d. microcolumns. The other drugs that were considered, which have stronger binding to HSA,³⁰⁻³⁴ were examined by using 5 mm × 2.1 mm i.d. microcolumns (e.g., for acetohexamide and tolbutamide) or even 1 mm × 2.1 mm i.d. microcolumns (for glibenclamide).

The flow rate that was used for ultrafast affinity extraction was also adjusted to control the sample residence time in the affinity microcolumns (e.g., see Figure 5.3). Low-to-moderate injection flow rates can result in some dissociation of a drug from its complexes with proteins in the sample, giving an apparent free fraction that is higher than what was present in the original sample.^{37-39,46,47} However, this effect can be minimized or made negligible when the flow rate is raised above a certain threshold level, which typically occurs when the sample residence time in the column is on the order of a few hundred milliseconds (ms).^{37-39,47} The size of this effect will vary from one drug to the next, as is shown in Figure 5.3, and depends on such factors as the rate of dissociation of the drug from the soluble proteins and the degree of drug-protein binding that was present in the original sample.⁴⁷

Experiments were conducted early in this work to identify the flow rate conditions that could be used during ultrafast affinity extraction to measure the free fractions of sulfonylurea drugs in the presence of soluble HSA. These initial studies were carried out by injecting 1.0 μL samples that contained 5-10 μM of the desired drug or a mixture containing 5-10 μM of this drug and 5-20 μM of normal HSA. Some typical results are given in Figure 5.3. It was found for tolbutamide that a consistent free drug fraction was obtained when using a minimum flow rate of 2.0 mL/min for sample injections on a 5

Figure 5.3 Effect of injection flow rate on ultrafast affinity extraction of the free fractions for various sulfonylurea drugs. The results were obtained at pH 7.4 and 37 °C for 1.0 μ L injections of (a) 10 μ M tolbutamide in the presence of 20 μ M HSA and injected onto a 5 mm \times 2.1 mm i.d. HSA microcolumn, (b) 10 μ M acetohexamide in the presence of 20 μ M HSA and injected onto a 5 mm \times 2.1 mm i.d. HSA microcolumn, (c) 10 μ M gliclazide in the presence of 20 μ M HSA and injected onto a 10 mm \times 2.1 mm i.d. HSA microcolumn, or (d) 5 μ M glibenclamide in the presence of 5 μ M HSA and injected onto a 1 mm \times 2.1 mm i.d. HSA microcolumn. The values shown for the free fraction on the y-axis have no units, because they represent the ratio of the free drug concentration vs. the total concentration of the same drug in each sample. Reproduced with permission from X. Zheng, R. Matsuda, D.S. Hage, J. Chromatogr. A 1371 (2014) 82-89.



mm \times 2.1 mm i.d. HSA microcolumn (i.e., a column residence time of 415 ms or less). Similar experiments with the other sulfonylurea drugs provided the following conditions for their ultrafast affinity extraction: acetohexamide, 2.5 mL/min or greater when using a 5 mm \times 2.1 mm i.d. HSA microcolumn; gliclazide, 2.5 mL/min or greater when using a 10 mm \times 2.1 mm i.d. HSA microcolumn; and glibenclamide, 0.30 mL/min or greater when using a 1 mm \times 2.1 mm i.d. HSA microcolumn. These conditions for acetohexamide, gliclazide and glibenclamide corresponded to maximum column residence times during the extraction process of 333 ms, 665 ms and 554 ms, respectively. This range of residence times was in good agreement with previous kinetic studies or extraction experiments that have used some of the same analytes or drugs with similar affinities for HSA.^{37-39,47}

Figure 5.4(a) shows some typical chromatograms that were obtained when using a HSA microcolumn for the ultrafast affinity extraction of tolbutamide. These results were generated by using samples containing a therapeutic level of tolbutamide, in the absence or presence of a physiological concentration of HSA, and which were injected onto a 5 mm \times 2.1 mm i.d. HSA microcolumn at 2.25 mL/min. In this example, the non-retained peak for the soluble protein and drug-protein complex appeared within 30-40 sec (s) of injection (Note: injections of only HSA or glycated HSA produced similar non-retained peaks). The peak for the retained, free fraction of tolbutamide had a maximum that appeared at 50-55 s and eluted within 2 min from the HSA microcolumn. Similar chromatograms were generated for gliclazide, acetohexamide, and glibenclamide at therapeutically-relevant concentrations. The non-retained peaks for these other drugs occurred within 0.3-0.6 min (at 2.5 mL/min) or within 3.0 min (at 0.35 mL/min),

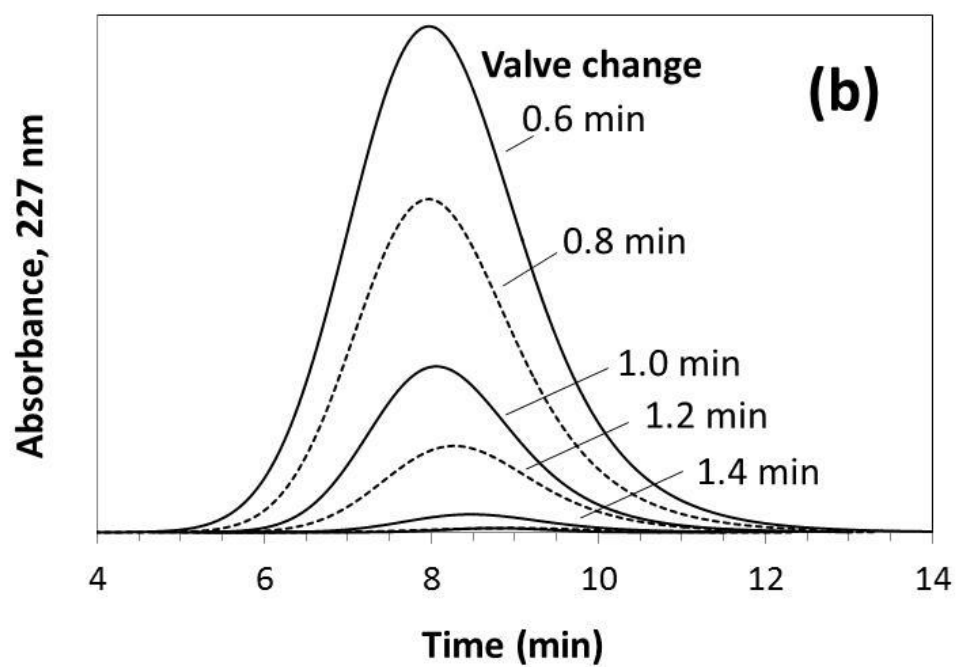
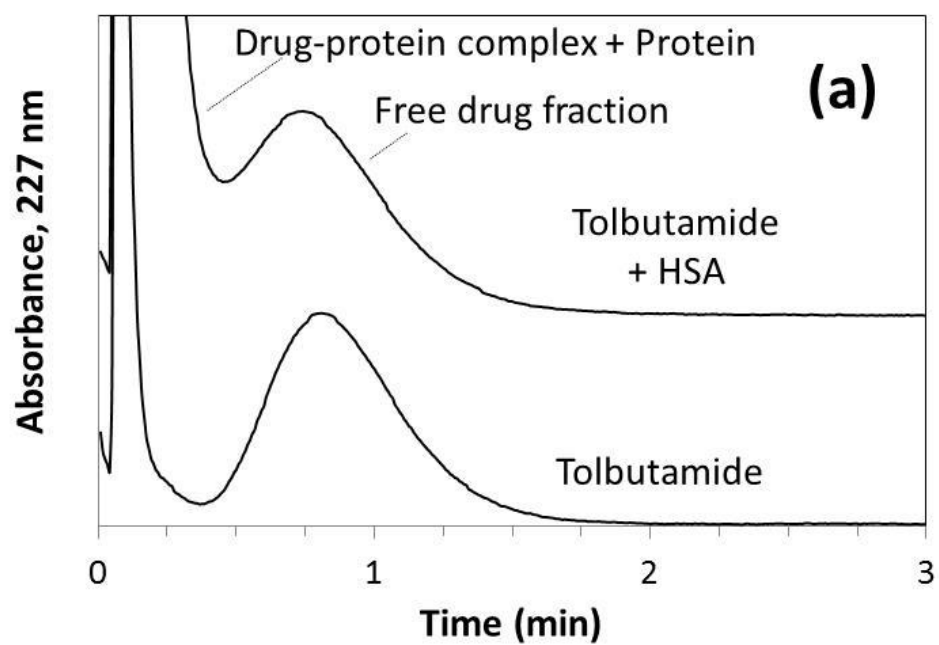
respectively. The retained peaks for these other drugs had maxima occurring at 40-45 s, 65-70 s, or 8.0-8.3 min and eluted within 1.5-2.0 min, 3.5-4.0 min or 13-15 min under the final conditions that were employed for ultrafast affinity extraction.

Optimization of conditions for multi-dimensional affinity system

Baseline resolution was not obtained between the non-retained and retained peaks for most of the sulfonylurea drugs when using only a single HSA microcolumn. This issue was overcome by using a multi-dimensional system with a second HSA column that was placed on-line after the free drug fraction had begun to elute from the first column. Figure 5.4(b) shows some chromatograms that were generated during the second part of this separation. The additional column helped to improve resolution of the retained free drug fraction from other sample components, including any drug that had been released from drug-protein complexes in the sample during passage through the first column.

The results in Figure 5.4(b) were obtained for samples containing 185 μ M tolbutamide/526 μ M HSA and using various times for switching the second column on-line with the first HSA microcolumn. A single retained peak was recovered and observed for tolbutamide on this multi-dimensional affinity system. This peak had a maximum that appeared at 7.8-8.4 min after sample injection, as acquired at a flow rate of 0.50 ml/min when the second HSA column was placed on-line and this column that had a size of 10 mm \times 2.1 mm i.d. Similar chromatograms were observed for acetohexamide, gliclazide and glibenclamide, which gave peaks with maxima at 10.0-10.5 min (final flow rate, 0.75 mL/min; second HSA column size, 10 mm \times 2.1 mm i.d.), 8.4-8.6 min (0.50

Figure 5.4. Typical chromatograms obtained at pH 7.4 and 37 °C on (a) a 5 mm × 2.1 mm i.d. HSA microcolumn at 2.25 mL/min for 1 µL injections of 185 µM tolbutamide in the absence or presence of 526 µM HSA, or (b) the retained peak obtained on a 10 mm × 2.1 mm i.d. HSA column at 0.5 mL/min and that was put in line with the first 5 mm × 2.1 mm i.d. HSA microcolumn after various times following injection of a 1 µL sample 185 µM tolbutamide/526 µM HSA onto the first column at 2.25 mL/min. The change in signal at 5-10 s for the chromatogram in (a) for only tolbutamide was due to a temporary change in pressure that occurred when the sample was injected onto the system. Reproduced with permission from X. Zheng, R. Matsuda, D.S. Hage, *J. Chromatogr. A* 1371 (2014) 82-89.

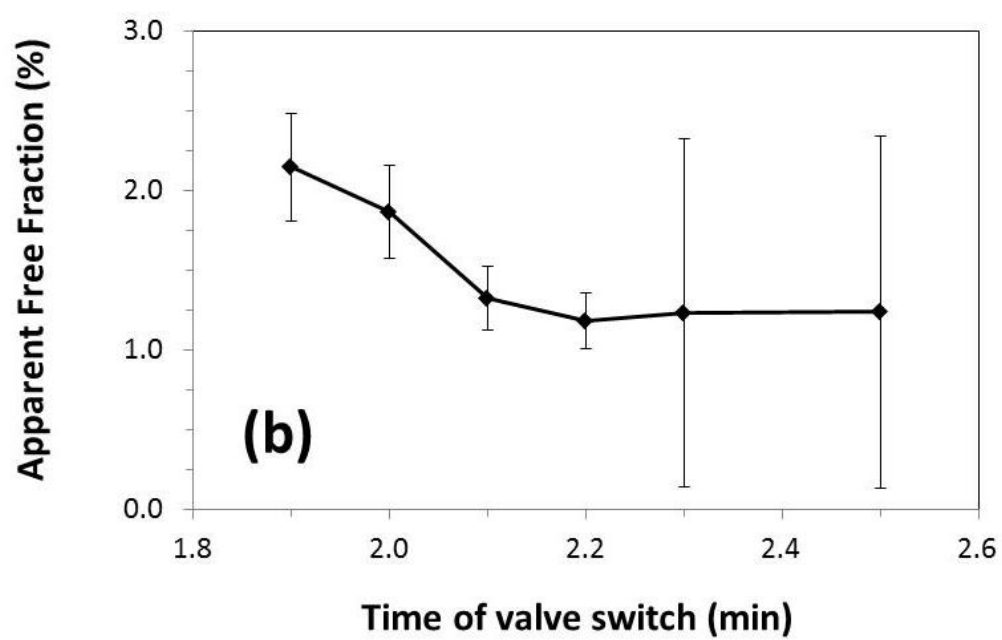
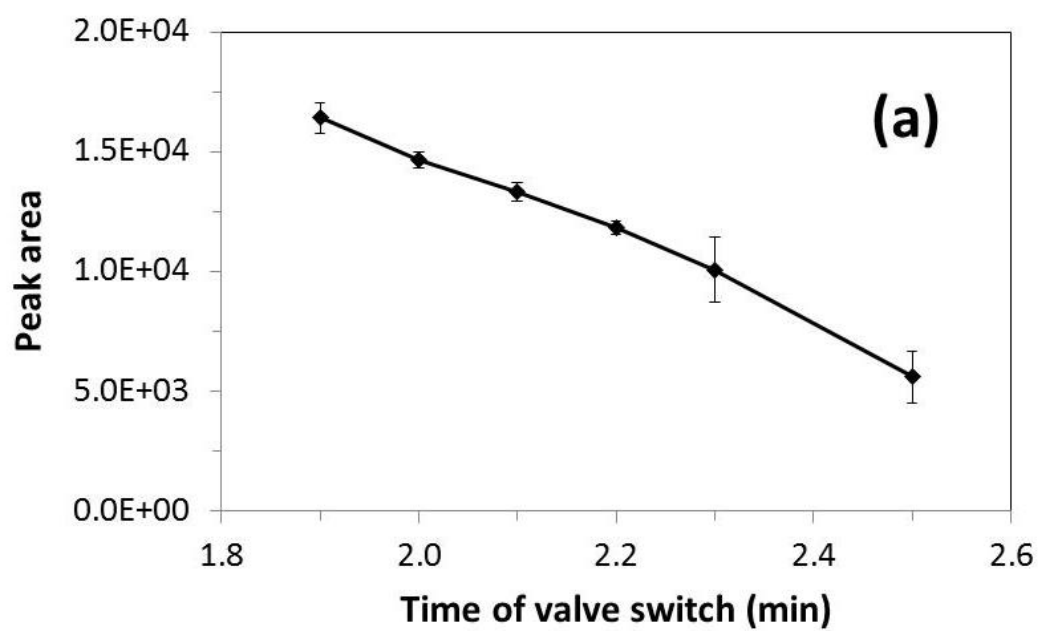


mL/min; 25 mm \times 2.1 mm i.d.), and 27.2-27.7 min (0.25 mL/min; 5 mm \times 2.1 mm i.d.), respectively. The flow rate and column conditions that were utilized for the second part of this multi-dimensional system were again selected based on the retention of each drug on the HSA columns, the backpressures of these columns, and the overall time of analysis.

The time at which the second column was placed on-line with the first column after sample injection was an important factor to consider when measuring small free drug fractions on the multi-dimensional affinity system. Figure 5.5 shows how the peak area and apparent free drug fraction changed for acetohexamide as the time of this switch was varied. Similar trends were noted for the other drugs that were examined in this chapter. The time of this switching event occurred within the time frame that the free drug peak eluted from the first column. As this switching time was increased, the total peak area (i.e., a measure of the recovery) seen for the drug on the second column decreased, as demonstrated in Figure 5.5(a). This effect occurred because less of the retained peak from the first column was passed onto the second column at longer switching times. A correction for this effect was made by comparing the peak areas for the free drugs that were captured from samples to the peak areas that were obtained on the same system for standards with known concentrations of these drugs.

Less contamination due to other sample components, including drugs that had dissociated from proteins in the sample during ultrafast affinity extraction, also occurred as the switching time was increased. This effect resulted in the apparent free fraction dropping and approaching a constant value as the switching time was increased. In Figure 5.5(b), the measured free fraction became a consistent value when a switching

Figure 5.5 Effect of valve switching time on (a) the area of the final peak observed for a 138 μM acetohexamide sample that was applied to the multi-dimensional affinity system, and (b) the apparent free fractions that were measured by this system for a sample that contained 138 μM acetohexamide and 640 μM HSA. These measurements were all made at pH 7.4 and 37 $^{\circ}\text{C}$ using a 5 mm \times 2.1 mm i.d. HSA column operated at 2.5 mL/min, followed by the on-line addition of a 10 mm \times 2.1 mm i.d. HSA column and the use of a flow rate of 0.75 mL/min at the given switching times. The error bars represent a range of ± 1 standard error of the mean ($n = 4$). The times shown for the valve switching event represent the time that has elapsed since sample injection, and were selected to be beyond the elution time for the non-retained sample components leaving the first, affinity microcolumn in this system. Reproduced with permission from X. Zheng, R. Matsuda, D.S. Hage, J. Chromatogr. A 1371 (2014) 82-89.



time of 2.2 min or longer was used for acetohexamide. However, there was also a loss of precision in the measured free fraction if the switching time was too long because only a small amount of the free drug was then being passed onto the second column. This latter effect occurred in Figure 5.5(b) at switching times longer than 2.3 min. The combination of these effects meant that there was a relatively well-defined window of times for the switching event that could be used to provide both reasonable accuracy and precision for free fraction measurements in the multi-dimensional affinity system. Based on these criteria and similar plots to those Figure 5.5(b) for the other drugs that were examined, the switching times that were used in all later parts of this chapter were 2.2 min for acetohexamide, 1.5 min for tolbutamide, 0.85 min for gliclazide, and 5.0 min for glibenclamide.

Measurement of free fractions for sulfonylurea drugs

The next part of this project examined the use of ultrafast affinity extraction and the multi-dimensional system to measure the free fractions of various sulfonylurea drugs in the presence of normal HSA or glycated HSA at typical therapeutic or physiological levels for these agents. Table 5.1 summarizes the results of these measurements. This approach was found to be useful in reliably measuring small free drug fractions (e.g., values as small as 0.09% to 2.58%). This method had a good absolute precision for these values (± 0.02 -0.5%) and a reasonable relative precision (± 3.6 -30%). These free drug fractions also agreed with predicted values based on previously-measured binding constants for the same drugs with similar protein preparations (see Table 5.2).³⁰⁻³⁴ In

Table 5.1 Free drug fractions measured for various sulfonylurea drugs in the presence of normal HSA or glycated HSA (gHSA)

Drug and sample	Measured free fraction ^a		
	Normal HSA	gHSA1	gHSA2
Tolbutamide (275 μ M) + HSA (640 μ M)	2.58 (\pm 0.31)%	2.20 (\pm 0.08)% ^b	1.58 (\pm 0.09)% ^c
Acetohexamide (138 μ M) + HSA (640 μ M)	1.18 (\pm 0.35)%	1.53 (\pm 0.27)%	1.41 (\pm 0.16)%
Gliclazide (23 μ M) + HSA (640 μ M)	2.17 (\pm 0.29)%	2.48 (\pm 0.51)%	1.27 (\pm 0.31)% ^c
Glibenclamide (0.4 μ M) + HSA (526 μ M)	0.09 (\pm 0.02)%	0.11 (\pm 0.03)%	0.14 (\pm 0.02)% ^d

^aThese free drug fraction values were determined at pH 7.4 and 37 °C by using ultrafast affinity extraction and a multi-dimensional affinity system. The values in parentheses represent a range of \pm 1 S.D. ($n = 4$), as determined by error propagation.

^bThis value was significantly different from the result for normal HSA at the 90% confidence level but not the 95% confidence level.

^cThis value was significantly different from the results for normal HSA and gHSA1 at the 95% confidence level.

^dThis value was significantly different from the results for normal HSA at the 95% confidence level and from gHSA1 at the 90% but not the 95% confidence level.

Reproduced with permission from X. Zheng, R. Matsuda, D.S. Hage, J. Chromatogr. A 1371 (2014) 82-89.

addition, these results gave good correlation with free fractions that were determined for some of the same samples when using ultrafiltration as a reference.

The sulfonylurea drugs that were used in this study are known to have strong binding to HSA and to have only small free fractions in serum.^{7,8} The free fractions in Table 5.1 show how this biologically-active fraction can be only a few percent of the total drug content in serum at therapeutic concentrations. These results further show how the size of this fraction can vary with the type of sulfonylurea drug that is being administered. These differences are directly related to the affinities of these drugs for HSA (see Table 5.2) and their total therapeutic concentrations.

The results in Table 5.1 made it further possible to compare the free fractions that were seen for each drug in the presence of normal HSA or HSA with glycation levels similar to those seen in prediabetes (gHSA1) or diabetes (gHSA2). It was found that the level of this glycation and the type of drug that was being examined both affected the change that was noted in the free fraction. For example, going from normal HSA to gHSA1 (which had only a modest level of glycation) produced a possible 0.85- to 1.30-fold change in the free fractions for these sulfonylurea drugs. This level of variation was not significant at the 95% confidence level and was only significant at the 90% confidence level for tolbutamide. However, going from normal HSA to gHSA2 gave changes of 0.59- to 1.56-fold for tolbutamide, glibenclamide, and gliclazide, which were all significant at the 95% confidence level. Acetohexamide was the only exception, which gave only a 1.19-fold change between normal HSA and gHSA2 that was not significant. Similar trends were seen when comparing the free fractions measured in the presence of gHSA1 versus gHSA2.

These variations agree with a previous estimate that HSA glycation may lead to a 0.6- to 1.7-fold change in the free drug fractions for these sulfonylurea drugs (i.e., as based on prior binding studies using both *in vitro* and *in vivo* glycated HSA).^{7,26} Such changes in binding have been attributed to variations in the amount and types of glycation-related modifications that are formed at or near specific regions on HSA (e.g., Sudlow sites I and II) as the overall level of glycation for this protein is increased.²²⁻²⁵ These variations in the free fractions of sulfonylurea drugs are of concern in that they represent a large difference in the actual versus expected dosage of such drugs, with the possible result being either inadequate control of elevated glucose levels (i.e., hyperglycemia) or the production of low glucose levels (hypoglycemia) in patients⁷

Estimation of affinity for sulfonylurea drugs with normal HSA or glycated HSA

The free fraction results that were obtained by ultrafast affinity extraction and the multi-dimensional affinity system were also used to estimate overall affinities of the sulfonylurea drugs with normal HSA or glycated HSA. It is known that these drugs each have at least two major binding regions on HSA,^{7,27,30-34} so in this case the free fractions were used to calculate a global affinity constant (nK_a') for these interactions. These global affinity constants were determined by using Equation 5.1, which can provide either the association equilibrium constant (K_a) for a system with single-site binding or the global affinity constant for a system involving multiple and independent binding regions.^{37,38,47}

$$K_a = \frac{1-F_0}{F_0([P]-[D]+[D]F_0)} \quad (5.1)$$

In this equation, [D] and [P] are the total concentrations of the drug and soluble protein in the original sample, while F_0 is the free fraction measured for the drug in this sample.

Table 5.2 shows the values of nK_a' that were found by using Equation 5.1 and the free fractions from Table 5.1 for the sulfonylurea drugs with normal HSA or glycated HSA. No significant changes in these values were noted when varying the drug or protein concentration within the therapeutic or physiological range of these agents. As an example, the use of samples that contained 185 μM tolbutamide and 526 μM HSA, 185 μM tolbutamide and 752 μM HSA, 370 μM tolbutamide and 526 μM HSA, or 370 μM tolbutamide and 752 μM HSA all gave estimates for nK_a' that were in the range of 0.95- $1.08 \times 10^5 \text{ M}^{-1}$. This indicated there was a negligible effect of sample concentration on the global affinity constants that were estimated through ultrafast affinity extraction. A similar conclusion has been reached in the use of this approach with other drug/protein systems at non-therapeutic concentrations.⁴⁷

The values in Table 5.2 agreed well with global affinity constants that were determined through previous binding data acquired for the same drugs and using comparable preparations of glycated HSA.³⁰⁻³⁴ The values estimated by ultrafast affinity extraction and the multi-dimensional affinity system had a relative precision of ± 6 -29% and differed from these literature results by only 0-22% (average difference, 7%). These global affinity constants also agreed with values that were determined for some of the same samples by using ultrafiltration. For instance, the nK_a' values obtained by ultrafiltration for acetohexamide with the same preparations of HSA and glycated HSA

Table 5.2 Global equilibrium constants estimated for sulfonylurea drugs with normal HSA or glycated HSA (gHSA)^a

Drug & Sample	Global affinity constant, $nK_a (\times 10^5 \text{ M}^{-1})$					
	Normal HSA	Literature value ^b	gHSA1 ^c	Literature value ^b	gHSA2 ^d	Literature value ^b
Tolbutamide (275 μM) + HSA (640 μM)	1.0 (\pm 0.1)	1.1 (\pm 0.1)	1.2 (\pm 0.1)	1.3 (\pm 0.1)	1.7 (\pm 0.1)	1.4 (\pm 0.1)
Acetohexamide (138 μM) + HSA (640 μM)	1.7 (\pm 0.5)	1.7 (\pm 0.1)	1.3 (\pm 0.2)	1.4 (\pm 0.1)	1.4 (\pm 0.1)	1.5 (\pm 0.1)
Gliclazide (23 μM) + HSA (640 μM)	0.73 (\pm 0.10)	0.79 (\pm 0.05)	0.64 (\pm 0.13)	0.64 (\pm 0.05)	1.26 (\pm 0.31)	1.12 (\pm 0.07)
Glibenclamide (0.4 μM) + HSA (526 μM)	21.1 (\pm 4.7)	21.6 (\pm 8.0)	17.3 (\pm 4.7)	18.9 (\pm 8.0)	13.6 (\pm 1.9)	13.7 (\pm 4.0)

^aThe global affinity constants from this study are based on the free drug fractions listed in Table 5.1. All of the values in this table are for drug-protein binding that occurs at pH 7.4 and 37 °C. The values in parentheses represent a range of \pm 1 S.D. ($n = 4$), as determined by error propagation.

^bThe global affinity constants from the literature were calculated by using the association equilibrium constants and binding stoichiometries that had been measured for these drugs at Sudlow sites I and II,³⁰⁻³⁴ as well as at the digitoxin site in the case of glibenclamide.³⁴ A similar range of values has been reported in Ref. 28.

^cThe level of glycation for gHSA1 was similar to that of an *in vitro* glycated HSA sample that was used in the previous binding studies and that contained 1.31 (\pm 0.05) mol hexose/mol HSA).^{29,31-34}

^dThe glycation level for gHSA2 was between the glycation levels for two *in vitro* glycated HSA samples that were used in previous binding studies and that contained 2.34 (\pm 0.13) or 3.34 (\pm 0.14) mol hexose/mol HSA.^{29,31-34}

Reproduced with permission from X. Zheng, R. Matsuda, D.S. Hage, J. Chromatogr. A 1371 (2014) 82-89.

differed by only 0-7.7% (average difference, 4.5%) from the results shown in Table 5.2 based on ultrafast affinity extraction.

Conclusions

This study examined the use and development of ultrafast affinity extraction and a multi-dimensional affinity system for measuring free drug fractions at therapeutic levels. This approach was then used to compare the free fractions and global affinity constants of several sulfonylurea drugs in the presence of normal HSA or glycosylated HSA. Factors that were considered in the optimization of this approach included the column size, flow rate and column residence times that could be used with sulfonylurea drugs during ultrafast affinity extraction with an HSA microcolumn. The flow rate and column size used for the second affinity column in the system were also considered, as well as the time at which this second column was placed on-line with the HSA microcolumn. This system was a general one that could also be adapted for use in coupling an HSA microcolumn with other types of analytical columns, such as those containing reversed-phase, ion-exchange or size-exclusion supports. These latter types of columns will be considered in future work as this approach is further optimized or extended to more complex mixtures of free solutes (e.g., mixtures of drugs or drugs and their metabolites).

This approach holds several advantages. First, the use of affinity microcolumns containing HSA, which has both fast and relatively strong binding to sulfonylurea drugs, made it possible to isolate the free fractions of these drugs under time conditions that minimized dissociation of the protein-bound fractions of the same drugs as the samples

passed through the microcolumns.^{37-40,45-47} Given the relatively fast rate of these dissociation processes, such a separation would be difficult to obtain by using a more conventional reversed-phase or size-exclusion column.^{36,37,40,46,47,52} Another advantage of using an HSA microcolumn for these free drug measurements is that the same immobilized agent, which binds to many pharmaceuticals, could be used for all of the drugs of interest in this study. In addition, the mobile phase for this column was an aqueous buffer with a physiological pH, which should not have significantly affected the drug-protein interactions in the original samples. Finally, the use of these microcolumns for free drug measurements required only 1.0 μL of sample per injection and was able to measure free drug fractions as small as 0.09-2.58% with an absolute precision of ± 0.02 -0.5%.

The free drug fractions and global affinity constants that were determined by this approach showed good agreement with those predicted from previous binding studies or determined through a reference method. This technique was used to examine the possible effects of glycation on the binding of sulfonylurea drugs to HSA. It was found that glycation could affect the free fractions of sulfonylurea drugs at typical therapeutic levels and that the size of this effect varied with the level of HSA glycation. The same multi-dimensional approach could be utilized to examine other drug-protein systems. Possible future applications include the clinical analysis of free drug or hormone levels for disease diagnosis or treatment^{38-40,45,46} and the high-throughput screening of drug-protein interactions.^{36-38,47}

References

1. International Diabetes Federation. IDF Diabetes Atlas; 5th Ed. International Diabetes Federation, Brussels, Belgium, 2011.
2. National Diabetes Fact Sheet: General Information and National Estimates on Diabetes in the United States, 2011, U.S. Centers for Disease Control. U.S. Centers for Disease Control and Prevention, Atlanta, GA, 2011.
3. T.G. Skillman, J.M. Feldman, *Am. J. Med.* 70 (1981) 361-372.
4. R.M. Zavod, J.L. Krystenansky, B.L. Currie, in: W.O. Foye, T.L. Lemke, D.A. Williams (Eds.), *Foye's Principles of Medicinal Chemistry*, Lippincott Williams and Wilkins: Philadelphia, 2008.
5. D.W. Foster, in: K.J. Isselbacher, E. Braunwald, J.D. Wilson, J.B. Martin, A.S. Fauci, D.L. Kasper (Eds.), *Harrison's Principles of Internal Medicine*, McGraw-Hill, New York, 1998, Ch. 29.
6. M.G. Jakoby, D.F. Covey, D.P. Cistola, *Biochemistry* 34 (1995) 8780-8787.
7. J. Anguizola, R. Matsuda, O.S. Barnaby, K.S. Hoy, C. Wa, E. DeBolt, M. Koke, D.S. Hage, *Clin. Chim. Acta* 425 (2013) 64-76.
8. M.J. Crooks, K.F. Brown, *J. Pharm. Pharmacol.* 26 (1974) 304-311.
9. T. Peters, Jr., *All About Albumin: Biochemistry, Genetics, and Medical Applications*, Academic Press, San Diego, CA, 1996.
10. N.W. Tietz (Ed.), *Textbook of Clinical Chemistry*, Saunders, Philadelphia, 1986.
11. M.A. Otagiri, *Drug Metab. Pharmacokinet.* 20 (2005) 309-323.
12. G. Sudlow, D.J. Birkett, D.N. Wade, *Mol. Pharmacol.* 11 (1975) 824-832.

13. D.L. Mendez, R.A. Jensen, L.A. McElroy, J.M. Pena, R.M. Esquerra, Arch. Biochem. Biophys. 444 (2005) 92–99.
14. G. Colmenarejo, Med. Res. Rev. 23 (2003) 275–301.
15. H. Koyama, N. Sugioka, A. Uno, S. Mori, K. Nakajima, Biopharm. Drug. Dispos. 18 (1997) 791–801.
16. N. Iberg, R. Fluckiger, J. Biol. Chem. 261 (1986) 13542–13545.
17. K. Nakajou, H. Watanabe, U. Kragh-Hansen, T. Maruyama, M. Otagiri, Biochim. Biophys. Acta 1623 (2003) 88–97.
18. A. Lapolla, D. Fedele, R. Reitano, L. Bonfante, M. Guizzo, R. Seraglia, M. Tubaro, P. Traldi, J. Mass Spectrom. 40 (2005) 969–972.
19. A. Lapolla, D. Fedele, R. Seraglia, P. Traldi, Mass Spectrom. Rev. 25 (2006) 775–797.
20. Q. Zhang, J.M. Ames, R.D. Smith, J.W. Baynes, T.O. Metz, J. Proteome Res. 8 (2009) 754–769.
21. H.V. Roohk, A.R. Zaidi, J. Diabetes Sci. Technol. 2 (2008) 1114–1121.
22. O.S. Barnaby, C. Wa, R.L. Cerny, W. Clarke, D.S. Hage, Clin. Chim. Acta 411 (2010) 1102–1110.
23. O.S. Barnaby, R.L. Cerny, W. Clarke, D.S. Hage, Clin. Chim. Acta 412 (2011) 277–285.
24. O.S. Barnaby, R.L. Cerny, W. Clarke, D.S. Hage, Clin. Chim. Acta 412 (2011) 1606–1615.
25. C. Wa, R. Cerny, W.A. Clarke, D.S. Hage, Clin. Chim. Acta. 385 (2007) 48–60.

26. J. Anguizola, K.S. Joseph, O.S. Barnaby, R. Matsuda, G. Alvarado, W. Clarke, R.L. Cerny, D.S. Hage, *Anal. Chem.* 85 (2013) 4453-4460.
27. J. Anguizola, S.B.G. Basiaga, D.S. Hage, *Curr. Metabol.* 1 (2013) 239-250.
28. A.J. Jackson, J. Anguizola, E.L. Pfaunmiller, D.S. Hage, *Anal. Bioanal. Chem.* 405 (2013) 5833-5841.
29. K.S. Joseph, D.S. Hage, *J. Pharm. Biomed. Anal.* 53 (2010) 811-818.
30. K.S. Joseph, D.S. Hage, *J. Chromatogr. B* 878 (2010) 1590-1598.
31. K.S. Joseph, J. Anguizola, A.J. Jackson, D.S. Hage, *J. Chromatogr. B* 878 (2010) 2775-2781.
32. K.S. Joseph, J. Anguizola, D.S. Hage, *J. Pharm. Biomed. Anal.* 54 (2011) 426-432.
33. R. Matsuda, J. Anguizola, K.S. Joseph, D.S. Hage, *Anal. Bioanal. Chem.* 401 (2011) 2811-2819.
34. R. Matsuda, J. Anguizola, K.S. Joseph, D.S. Hage, *J. Chromatogr. A* 1265 (2012) 114-122.
35. J.W. Melten, A.J. Wittebrood, J.J. Hubb, G.H. Faber, J. Wemer, D.B. Faber, *J. Pharm. Sci.*, 74 (1985) 692-694.
36. J.E. Schiel, D.S. Hage, *J. Sep. Sci.* 32 (2009) 1507-1522.
37. R. Mallik, M.J. Yoo, C.J. Briscoe, D.S. Hage, *J. Chromatogr. A* 1217 (2010) 2796-2803.
38. X. Zheng, M.J. Yoo, D.S. Hage, *Analyst* 138 (2013) 6262-6265.
39. W. Clarke, J.E. Schiel, A. Moser, D.S. Hage, *Anal. Chem.* 77 (2005) 1859-1866.
40. W. Clarke, A.R. Chowdhuri, D.S. Hage, *Anal. Chem.* 73 (2001) 2157-2164.

41. F.M. Musteata, *Bioanalysis* 3 (2011) 1753-1768.
42. A.B. Ahene, *Bioanalysis* 3 (2011) 1287-1295.
43. S.S. Holm, S.H. Hansen, J. Faber, P. Staun-Olsen, *Clin. Biochem.* 37 (2004) 85-93.
44. O.P. Soldin, S.J. Soldin, *Clin. Biochem.* 44 (2011) 89-94.
45. J.E. Schiel, Z. Tong, C. Sakulthaew, D.S. Hage, *Anal Chem.* 83 (2011) 9384-9390.
46. C.M. Ohnmacht, J.E. Schiel, D.S. Hage, *Anal. Chem.* 78 (2006) 7547-7556.
47. X. Zheng, Z. Li, M.I. Podariu, D.S. Hage, *Anal. Chem.* 86 (2014) 6454-6460.
48. J. Chen, D.S. Hage, *Anal. Chem.* 78 (2006) 2672-2683.
49. J.E. Schiel, Ph.D. Dissertation, University of Nebraska, Lincoln, Nebraska, 2009.
50. C.A. Burtis, E.R. Ashwood, D.E. Bruns (Eds.), *Tietz Textbook of Clinical Chemistry and Molecular Diagnostics*, Saunders, St. Louis, MO, 2006.
51. R. Regenthal, M. Krueger, C. Koeppel, R. Preiss, *J. Clin. Monit.* 15 (1999) 529-544.
52. D.S. Hage, S.A. Tweed, *J. Chromatogr. B* 699 (1997) 499-528.

CHAPTER 6

The Use of Ultrafast Affinity Extraction for Free Fraction Measurements of Various Drugs in Clinical Samples

Portion of this chapter appear in X. Zheng, M. Podariu, D.S. Hage "Analysis of Free Drug Fractions in Human Serum by Ultrafast Affinity Extraction" Analytical and Bioanalytical Chemistry 2015, submitted.

Introduction

Human serum albumin (HSA) is the most abundant transport protein in blood, with a normal concentration of 35-50 g/L (or 526-752 μM).^{1,2} This protein can bind to and transport many drugs through reversible interactions. These interactions, in turn, can affect such processes as drug metabolism, absorption, distribution and excretion.^{3,4} For instance, this binding leads to the creation of both a protein-bound fraction of the drug and a free (or non-bound) fraction. The free fraction for many drugs is generally considered to be the active form because it is this form that can cross cell membranes or bind to receptors.^{2,3,5}

These features make the measurement of free drug fractions and the study of drug-protein interactions in serum of interest when characterizing both existing drugs and new drug candidates.⁵⁻⁸ However, the isolation and measurement of free drug fractions in serum can be difficult due to the many chemicals that are present in such a sample.^{5,9-11} In addition, the free fraction may be only a small part of the total amount of drug that is present. This means it must be possible to measure a relatively small concentration for

this fraction in the presence of a much larger concentration for the corresponding protein and protein-bound fraction.⁵⁻¹¹

Two common methods that are used to measure free drug fractions are ultrafiltration and equilibrium dialysis.^{7,8,12,13} Unfortunately, these methods typically require relatively long separation or analysis times and need moderate-to-large amounts of sample. The adsorption of drugs to the membranes or other system components that are used in these methods also must be considered to avoid introducing errors into the final free fraction values.^{7,8,12,13} Many other analytical methods have also been employed to study drug-protein interactions.¹⁴⁻¹⁶ Examples are surface plasmon resonance, capillary electrophoresis, and nuclear magnetic resonance spectroscopy, as well as equilibrium dialysis and ultrafiltration.^{1,7,8,11-14,17-27} However, many of these techniques employ simple aqueous samples for drug-protein interaction studies and can be difficult to use directly with a complex sample such as serum.^{18-20,24}

Alternative techniques based on ultrafast affinity extraction have recently been developed to measure free drug fractions and to estimate binding parameters for drug-protein interactions in solution.^{3,7,8,10,11,24,28,29} In this approach, the free drug fraction is rapidly extracted from a sample by using a small affinity column that contains a binding agent for the drug of interest. This free fraction is then measured directly as it elutes from the affinity microcolumn^{3,10,24} or indirectly through the use of a method such as an on-line displacement immunoassay.^{7,28,29} Ultrafast affinity extraction has been used in combination with a chiral separation to simultaneously analyze the free fractions for both warfarin enantiomers (i.e., a drug with strong binding to HSA).¹⁰ Affinity microcolumns for ultrafast affinity extraction have also recently been combined with longer affinity

columns to measure the free forms of various drugs in aqueous protein solutions.¹¹ In this latter method, an affinity microcolumn is first used to extract the free drug fraction from a sample, while the second column is used to further separate this free fraction from possible contaminants (e.g., drug that has dissociated from proteins in the sample) prior to measurement of the free fraction.¹¹

In this chapter, ultrafast affinity extraction and a multi-dimensional system will be adapted and used to directly measure the free fractions for various drugs and to study drug-protein interactions in human serum. Several factors will be considered in modifying technique for use with serum. These factors will include the flow rate and column size that are used to isolate the free drug fraction, as well as the conditions that are employed to couple ultrafast affinity extraction with a second affinity column for further separation and measurement of the free fraction.^{3,11} The ability of this method to estimate the overall affinity of drug-protein binding in serum will also be explored. The results should provide important information on the relative advantages or potential limitations of using ultrafast affinity extraction for examining free drug fractions and drug-protein binding directly in biological samples. This information, in turn, should allow the future adaptation of this technique for work with other drugs, proteins or samples of interest in clinical chemistry, pharmaceutical science or biomedical research.

1-6

Experimental

Materials and reagents

The HSA (Cohn fraction V, essentially fatty acid free, $\geq 96\%$ pure), human serum (from male AB plasma, H4522, lot 039K0728; sterile filtered and tested negative for HIV-1/2 and hepatitis B/C), tolbutamide, acetohexamide, gliclazide, diazepam and quinidine were from Sigma Aldrich (St. Louis, MO, USA). The reagents for the bicinchoninic acid (BCA) protein assay were purchased from Pierce (Rockford, IL, USA). The Nucleosil Si-300 silica (300 Å pore size, 7 µm particle diameter) was from Macherey Nagel (Düren, Germany). All buffers and aqueous solutions were prepared using water from a Milli-Q Advantage A 10 system (EDM Millipore Corporation, Billerica, MA, USA) and were passed through Osmonics 0.22 µm nylon filters from Fisher (Pittsburgh, PA, USA).

Apparatus

A Prep 24 pump from ChromTech (Apple Valley, MN, USA) was used to pack the columns that were used in this chapter. The chromatographic system included a PU-2080 Plus pump, an AS-2057 autosampler, and a UV-2075 absorbance detector from Jasco (Easton, MD, USA), plus a six-port LabPro valve from Rheodyne (Cotati, CA, USA). This system was controlled by ChromNAV v1.18.04 software and LCNet from Jasco. A CHM column heater and a TCM column heater controller from Waters (Milford, MA, USA) were used to maintain a temperature of $37.0 (\pm 0.1) ^\circ\text{C}$ for the columns during all experiments. Chromatograms were analyzed by utilizing PeakFit v4.12 software (Jandel Scientific, San Rafael, CA, USA). A temperature-controlled 5702RH centrifuge

from Fisher was used in the ultrafiltration studies, along with Ultracel YM-T cellulose membranes (30 kDa, cut-off) that were purchased from EDM Millipore.

Column preparation

The support and stationary phase used in this chapter consisted of Nucleosil Si-300 silica that had been converted into a diol-bonded form and used to immobilize HSA by the Schiff base method, as described in Ref. 30. A control support, in which no HSA was added during the immobilization step, was prepared by the same process. The protein content of the final HSA support was determined in quadruplicate through a BCA assay by using HSA as the standard and the control support as the blank.³¹⁻³⁵ This assay gave a content of 59 (\pm 1) mg HSA/g silica.

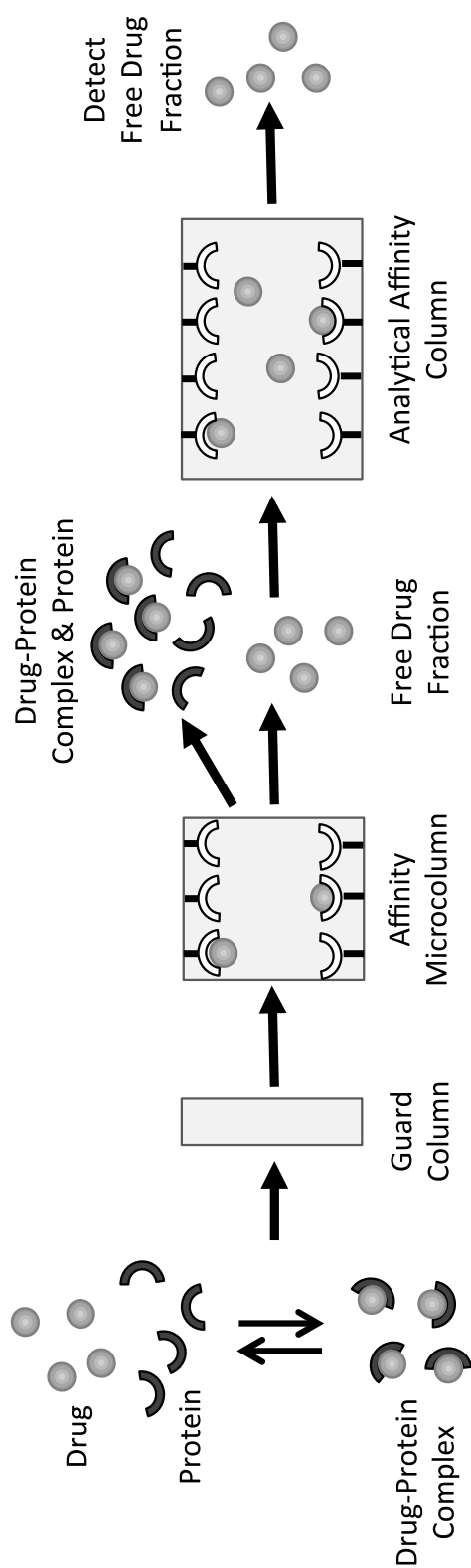
Affinity columns with sizes of 5 \times 2.1 mm i.d., 10 \times 2.1 mm i.d., 20 mm \times 2.1 mm i.d., and 25 mm \times 2.1 mm i.d. were packed into standard stainless steel housings using pH 7.4, 0.067 M potassium phosphate buffer as the packing solution. Guard columns with a size of 1 mm \times 2.1 mm i.d. were packed in a similar manner with the control support but using a frit-in-column design, as described in Ref. 35. The packing pressure was 3000 psi (20 MPa) for the 1 mm and 5 mm long columns and 4000 psi (28 MPa) for the 10 mm, 20 mm and 25 mm long columns. Each of these columns was stored at 4 °C in pH 7.4, 0.067 M phosphate buffer when not in use. The affinity microcolumns that were used for free drug extractions were stable for at least 150 injections. The longer analytical affinity columns could be used for at least 250 injections.

Chromatographic studies

The multi-dimensional affinity system that was used in this study is illustrated in Figure 6.1. A 1 mm \times 2.1 mm i.d. guard column was used to protect the HSA microcolumn from particulate matter in the serum samples. The HSA microcolumn was used to extract the free drug fractions. The second, longer HSA column was later placed on-line with the HSA microcolumn to further separate the extracted free drug fraction from other sample components, such as any drug that had dissociated from proteins in the sample during passage through the HSA microcolumn.¹¹ The following wavelengths were employed for detection: 227 nm, tolbutamide; 248 nm, acetohexamide; 230 nm, diazepam; 226 nm, gliclazide; and 331 nm, quinidine.

The mobile phase used for all of these columns was pH 7.4, 0.067 M phosphate buffer. Most of the drugs were dissolved in this buffer to give working stock solutions which contained approximately 8070 μ M tolbutamide, 730 μ M gliclazide, 123 μ M diazepam or 480 μ M quinidine. These solutions were spiked into a commercial sample of human serum that contained 42 g/L (632 μ M) HSA. These spiked samples were prepared by dissolving approximately 10 μ L of each drug solution into 300 μ L of serum. Samples containing only the drug and no protein were prepared in the same manner but by combining the stock solution of the drug with pH 7.4, 0.067 M phosphate buffer instead of serum. The final samples that were made in this manner contained 275 μ M tolbutamide, 23 μ M gliclazide, 3.5 μ M diazepam or 10 μ M quinidine, which were within the typical therapeutic ranges for these agents (i.e., 184-370 μ M tolbutamide, 15-31 μ M

Figure 6.1 General scheme used for the isolation of a free drug fraction from the drug's protein-bound form and other components in serum through the use of ultrafast affinity extraction and a multi-dimensional HPAC system.



gliclazide, 0.7-7.0 μM diazepam, or 3-15 μM quinidine).^{36,37} The HSA concentration in these drug/serum mixtures was 610-618 μM , which was representative of the normal physiological levels for this protein.³⁶

An alternative approach was used to make the serum samples that contained acetohexamide. In this case, 1 mg of acetohexamide was dissolved directly in 14.28 mL of human serum, with 268 μL of this mixture then being mixed with 150 μL serum. The concentration of acetohexamide in this final spiked serum sample was 138 μM , which was within the normal therapeutic range for this drug (i.e., 61-216 μM).³⁷ The concentration of HSA in the final spiked serum sample was the same as the original content of the serum (i.e., 42 g/L or 632 μM HSA). Samples containing acetohexamide alone were prepared in the same manner but with this drug being dissolved in and diluted with pH 7.4, 0.067 M phosphate buffer instead of serum.

Optimization of the flow rates, column sizes and valve switching times that were used to study the interactions of diazepam or quinidine with HSA will be described in the "Results and Discussion". The HSA microcolumns that were used in the final system to extract the free drug fractions had the following dimensions: 5 mm \times 2.1 mm i.d. for tolbutamide, acetohexamide and diazepam; and 10 mm \times 2.1 mm i.d. for gliclazide and quinidine. The flow rates that were employed to inject samples onto these HSA microcolumns were as follows: 2.25 mL/min, tolbutamide; 2.5 mL/min, acetohexamide or gliclazide; and 3.0 mL/min, diazepam or quinidine. The injection volume was 1 μL for tolbutamide, acetohexamide and gliclazide, and 5 μL for quinidine and diazepam.

The size of the second HSA column in the final system was 10 mm \times 2.1 mm i.d. for tolbutamide, acetohexamide and diazepam, and 25 mm \times 2.1 mm i.d. for gliclazide and quinidine. A six-port valve was used to control the time at which this second column was placed on-line with the first HSA microcolumn. The times for this switching event were 1.2 min after injection for tolbutamide, 1.5 min for acetohexamide, 0.6 min for diazepam, 0.7 min for gliclazide and 0.4 min for quinidine. The flow rate was changed at this same time to 0.50 mL/min for tolbutamide, gliclazide and quinidine, and 0.75 mL/min for acetohexamide and diazepam during the second portion of the separation. The free drug concentration was determined by comparing the resulting peak area to that which was obtained for standards containing only the drug.¹⁰ The free fraction was calculated by dividing the free drug concentration by the total concentration of the drug in the sample.^{3,10,24}

Ultrafiltration studies

Each ultrafiltration tube was washed three times with 1 mL of water, followed by three similar washing steps with pH 7.4, 0.067 M potassium phosphate buffer. The spinning speed and time used in these washing steps were 1500 \times g and 5 min. After the last washing step, the buffer in the tube was decanted. The remaining buffer was removed by spinning the ultrafiltration device at 1500 \times g for 15 min. One mL of a drug or drug/protein sample in pH 7.4, 0.067 M phosphate buffer or in serum, and at the same concentrations as used in the chromatographic studies, was placed into a washed ultrafiltration tube and spun at 1500 \times g and 37 °C. The spinning time for a solution of

the drug alone or a drug in serum was 1.5 min or 10.0 min, respectively, based on data from previous ultrafiltration studies.^{10,11}

The filtrates were injected onto a chromatographic system for measurement of the free drug fraction. The injection volume was 20 μ L for the filtrates containing gliclazide, quinidine or diazepam, and 2 μ L for the filtrates containing tolbutamide or acetohexamide. The columns used in these measurements contained the same immobilized HSA support as used in the affinity microcolumns but had the following dimensions: gliclazide, 10 mm \times 2.1 mm i.d.; quinidine, 20 mm \times 2.1 mm i.d.; and diazepam, tolbutamide or acetohexamide, 5 mm \times 2.1 mm i.d. Standards containing these drugs in pH 7.4, 0.067 M phosphate buffer were injected under the same conditions. The mobile phase was pH 7.4, 0.067 M phosphate buffer, which was applied at flow rates of 0.5 mL/min for gliclazide, quinidine, and tolbutamide; 0.25 mL/min for diazepam; and 0.75 mL/min for acetohexamide. The detection wavelengths and system temperature were the same as described earlier for ultrafast affinity extraction. The concentration of the drug in each filtrate was found by comparing the peak areas obtained for both the filtrate samples and standard solutions. The free drug fraction was calculated in the same manner as described for ultrafast affinity extraction.

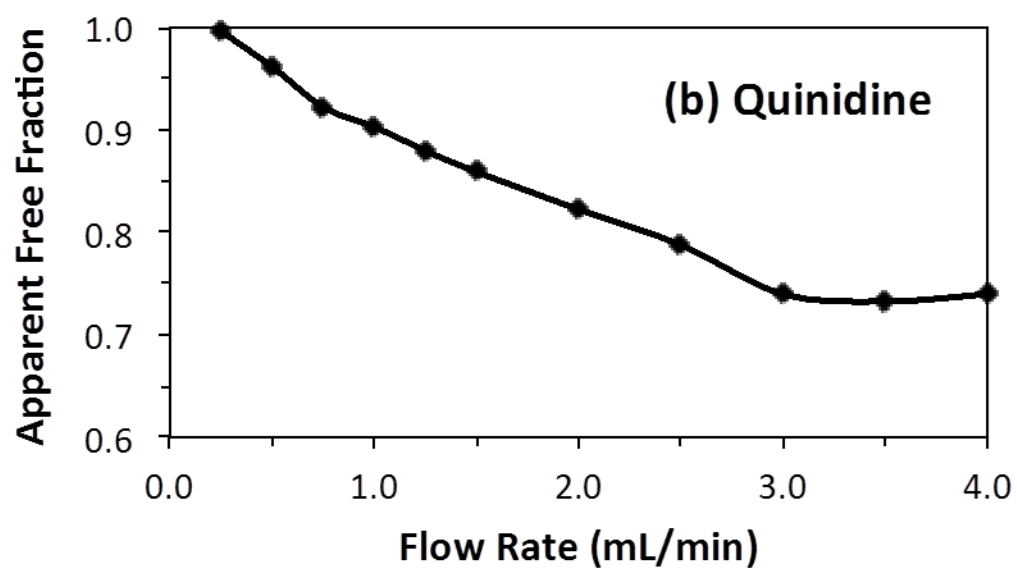
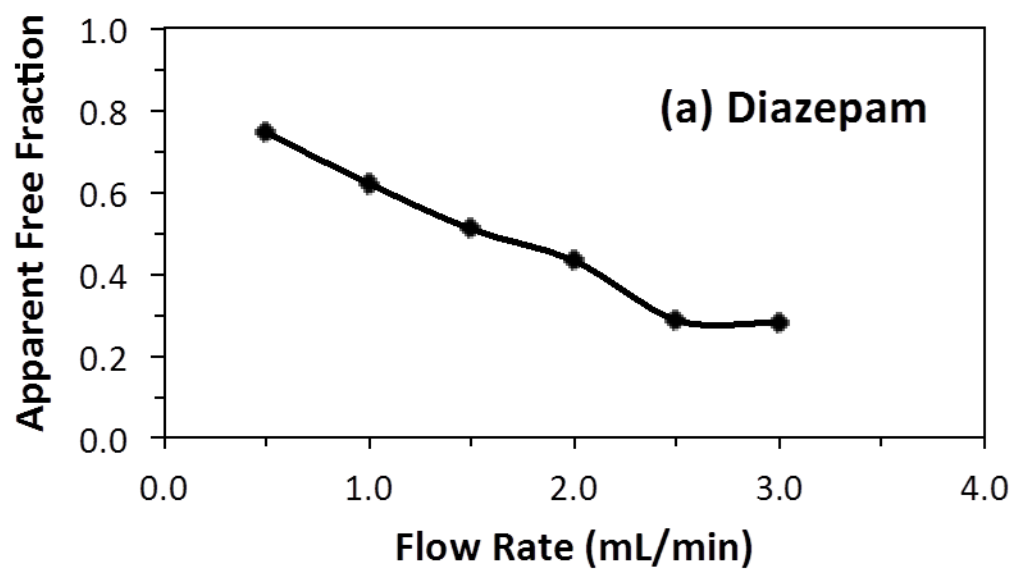
Results and Discussion

Optimization of conditions for ultrafast affinity extraction

The residence time for the sample as it passes through an affinity extraction column is an important factor to consider during the isolation of a free drug fraction from its corresponding drug-protein complex. This time can be adjusted by changing the size of the affinity extraction column or by altering the flow rate.^{3,7,8} For drugs such as tolbutamide and acetohexamide, which have relatively strong binding to serum proteins (i.e., association equilibrium constants or global affinities of $\sim 10^5$ - 10^6 M⁻¹ for soluble HSA), it is known that an HSA microcolumn with a size of 5 mm \times 2.1 mm i.d. can be used to extract and isolate their free fractions in aqueous samples.^{3,11} Diazepam has a similar affinity for soluble HSA, with a binding strength of roughly 2 - 12×10^5 M⁻¹,^{20,38} so the free fraction of this drug was also isolated by using a 5 mm \times 2.1 mm i.d. HSA microcolumn. Glliclazide, which has moderately strong binding to soluble HSA ($\sim 10^4$ - 10^5 M⁻¹), was analyzed by using a longer 10 mm \times 2.1 mm i.d. HSA microcolumn. The same type of longer microcolumn was used with quinidine, which has an affinity for soluble HSA in the range of 0.1 - 5×10^4 M⁻¹.^{1,39}

The effect of the injection flow rate on the measured free drug fractions was also considered. Figure 6.2 illustrates this effect. The data in this figure were obtained for injections of diazepam and quinidine, or mixtures of these drugs with soluble HSA, as made onto 5 mm or 10 mm \times 2.1 mm i.d. HSA microcolumns. It was found that low-to-moderate injection flow rates (i.e., 0.5-2.0 mL/min for diazepam and 0.25-2.50 mL/min for quinidine) resulted in high values for the apparent free drug fractions. However, when the flow rate was raised above 2.5 mL/min for diazepam or 3.0 mL/min for quinidine, a consistent free drug fraction was obtained. The high values seen at low-to-moderate flow rates were caused by dissociation of these drugs from their complexes

Figure 6.2 Measurement of free drug fractions at various injection flow rates. These plots were obtained for 1.0 μL injections of (a) 10 μM diazepam or a 10 μM diazepam/20 μM HSA mixture onto a 5 mm \times 2.1 mm i.d. HSA microcolumn, and (b) 10 μM quinidine or a 10 μM quinidine/20 μM HSA mixture onto a 10 mm \times 2.1 mm i.d. HSA microcolumn. These results were measured at 37 $^{\circ}\text{C}$ in pH 7.4, 0.067 M phosphate buffer.



with soluble HSA while the samples were passing through the affinity extraction microcolumns.^{3,7,10,24,29} However, this dissociation was minimized at higher flow rates as the sample residence time in the column was decreased. This latter situation occurred when the sample residence time was less than 333 millisecond (ms) for diazepam and 554 ms for quinidine. Based on the same type of experiment, the maximum sample residence times that gave similar behavior for the other drugs in this study were 415 ms for tolbutamide, 333 ms for acetohexamide, and 665 ms for gliclazide.¹¹

These flow rate and residence time data were also used to estimate the dissociation rate constant (k_d) for each drug with soluble HSA. This was done by using Equation 6.1 and the apparent free drug fractions that were measured at low-to-moderate flow rates.³

$$\ln \frac{(1-F_0)}{(1-F_t)} = k_d t \quad (6.1)$$

In Equation 6.1, F_0 is the original free fraction of the drug in the sample, as is measured at or above a flow rate that provides minimal dissociation of this drug from soluble proteins in the sample during passage through the affinity extraction column. The term F_t is the apparent free drug fraction that is measured at a given column residence time t . The value of t is also equal to the column void time, which can be calculated by using the flow rate and column void volume.³

As is indicated by Equation 6.1, a drug-protein system that undergoes essentially first-order dissociation as it passes through the affinity extraction column should provide a linear relationship with an intercept of zero when $\ln[(1 - F_0)/(1 - F_t)]$ is plotted against t .

Figure 6.3 shows examples of such linear relationships, as were obtained from the affinity extraction experiments that were conducted with quinidine or diazepam in the presence of soluble HSA. These particular plots gave correlation coefficients of 0.990-0.999 ($n = 5-6$) and intercepts that were equivalent to zero at the 95% confidence level. Similar behavior has been noted for the other drugs that were considered in this study.³ The dissociation rate constants for these systems were then determined from the slopes of the best-fit lines for these plots.

Table 6.1 shows the dissociation rate constants that were estimated by using Equation 6.1 and the ultrafast affinity extraction data. The k_d values for quinidine and diazepam with HSA were $0.58 (\pm 0.02)$ and $0.63 (\pm 0.05) \text{ s}^{-1}$, respectively, which had absolute differences of only $0.05-0.19 \text{ s}^{-1}$ from values in the literature.^{22,40} The relative precisions of these k_d values were ± 3.4 to 7.9% . The same approach, with similar relative precisions and agreement with the literature, has previously provided dissociation rate constant estimates of $0.59 (\pm 0.03) \text{ s}^{-1}$ for tolbutamide, $0.67 (\pm 0.03) \text{ s}^{-1}$ for acetohexamide, and $0.61 (\pm 0.02) \text{ s}^{-1}$ for gliclazide.³

Optimization of conditions for multi-dimensional affinity system

When working with a complex matrix such as serum, the large amount of proteins or other sample components that are present may make it difficult to obtain good resolution between the non-retained and retained peaks on an HSA microcolumn. To avoid this problem, ultrafast affinity extraction was carried out as part of a multi-dimensional affinity system.^{10,11} This was achieved by placing a second and longer HSA

Figure 6.3 Determination of the dissociation rate constants for (a) quinidine and (b) diazepam with soluble HSA by using ultrafast affinity extraction and Equation 6.1. The chromatographic conditions were the same as in Figure 6.2. The equation for the best-fit lines were (a) $y = 0.58 (\pm 0.02) x + 0.01 (\pm 0.03)$ and (b) $y = 0.63 (\pm 0.05) x + 0.02 (\pm 0.05)$. The correlation coefficients for these plots were 0.990 ($n = 5$) and 0.999 ($n = 6$), respectively. The error bars represent a range of ± 1 S.D. ($n = 4$).

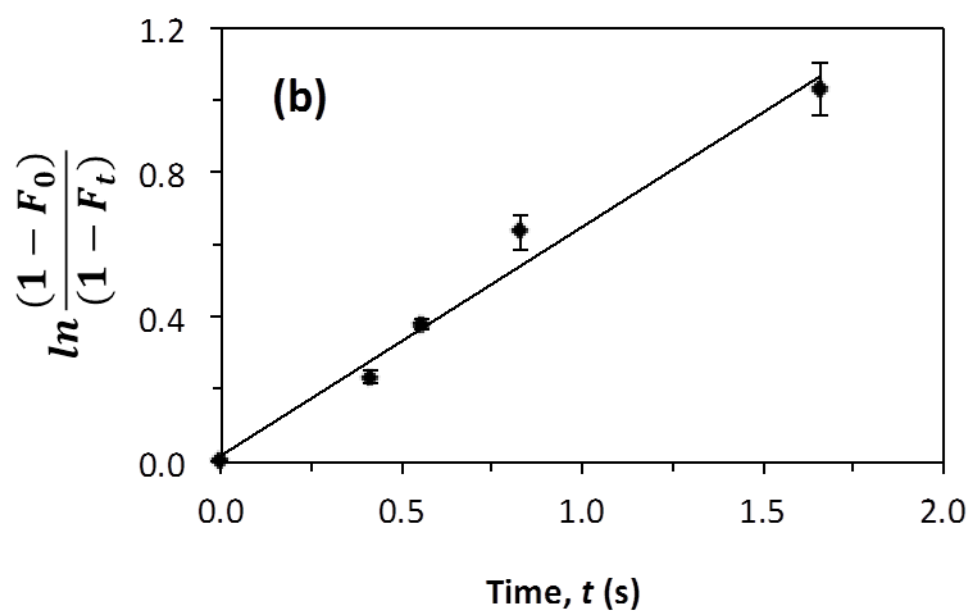
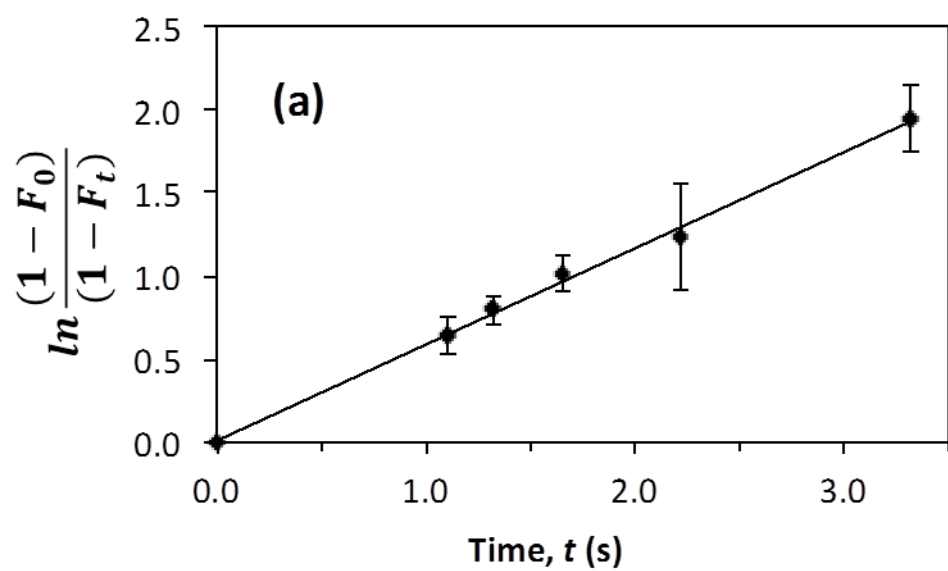


Table 6.1 Dissociation rate constants measured for various drugs with soluble HSA by using ultrafast affinity extraction on HSA microcolumns^a

Drug	Dissociation rate constant, k_d (s ⁻¹)	
	Ultrafast affinity extraction	Literature [Ref.]
Diazepam	0.63 (\pm 0.05)	0.44 [22]
Quinidine	0.58 (\pm 0.02)	0.53 [40]
Tolbutamide ^b	0.59 (\pm 0.03)	0.49 (\pm 0.15) [22]
Acetohexamide ^b	0.67 (\pm 0.03)	0.58 (\pm 0.02) [22]
Gliclazide ^b	0.61 (\pm 0.02)	Not reported

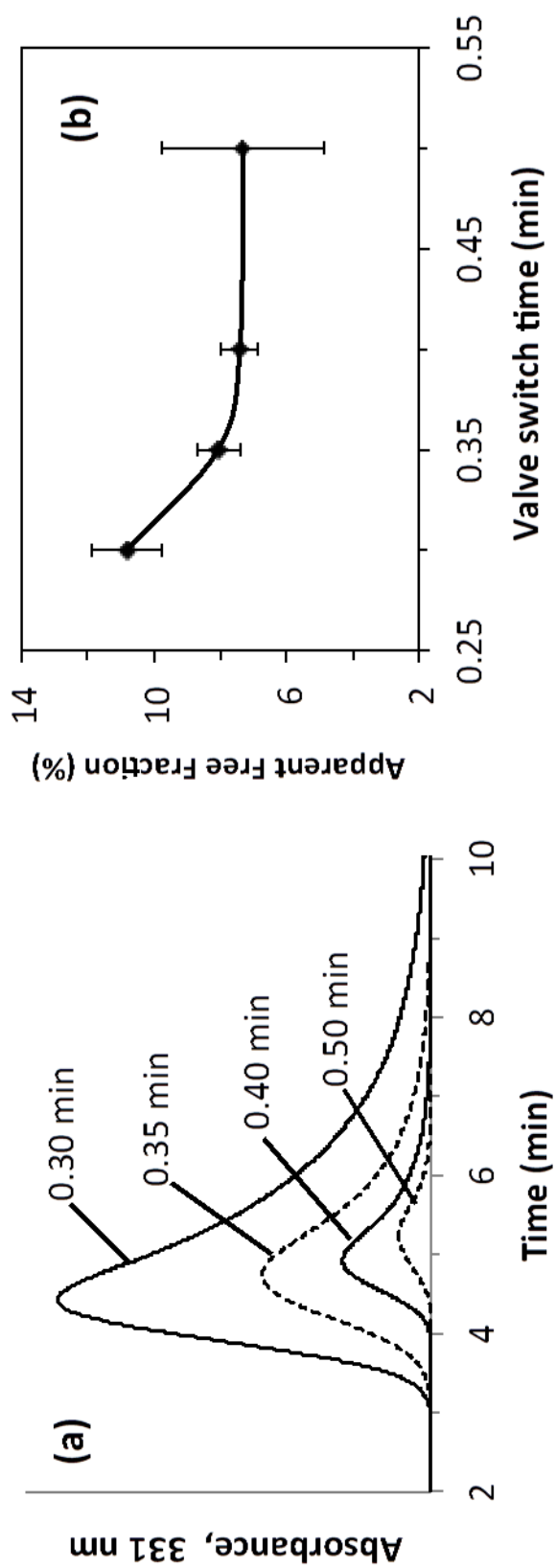
^aThese k_d values were measured at pH 7.4 and at 37 °C. The injected samples contained 10 μ M of a given drug and 20 μ M HSA. The values in the parentheses represent a range of \pm 1 S.D., as determined through error propagation from the slopes of the best-fit lines that were obtained according to Equation 6.1.

^bThese k_d values, as measured by ultrafast affinity extractions were previously reported in Ref. 3.

column on-line after samples had passed through the microcolumn that was used for ultrafast affinity extraction. In this system, part of the free drug fraction that was retained by and later eluted from the affinity microcolumn was delivered to the second column for further separation and analysis. This technique has been shown in prior work to improve the separation of the retained free drug fraction from other sample components, including serum proteins or any protein-bound drug in the sample that had undergone dissociation during its passage through the affinity extraction column.¹⁰

In this multi-dimensional method, the time for switching the valve to place the second column on-line with the first is an important factor to consider, as it determines the amount of a drug and its free drug fraction that are transferred to the second column.^{10,11} This time was optimized by using samples that contained only the drug or a mixture of this drug plus soluble proteins that were each present at typical therapeutic or physiological concentrations. In the case of quinidine, a sample containing 10 μM quinidine in the presence or absence of 600 μM soluble HSA was injected onto a 10 mm \times 2.1 mm i.d. HSA column at an initial flow rate of 3.0 mL/min for ultrafast affinity extraction, as optimized in the previous section. The retained drug was then delivered to a 25 mm \times 2.1 mm i.d. HSA column at various times after sample injection. Figure 6.4(a) provides examples of the retained drug peaks that were transferred to this second column for quinidine when the switching event occurred at 0.30, 0.35, 0.40, or 0.50 min after injection. The flow rate was also decreased to 0.50 mL/min as the second column was placed on-line. It was found in this multi-dimensional system that the retained drug gave a peak maximum that occurred at 4.3-5.2 min after sample injection. Diazepam, tolbutamide, acetohexamide, and gliclazide provided similar chromatograms, in which

Figure 6.4 Effect of valve switching time on (a) the recovery of quinidine at 0.5 mL/min on a 25 mm \times 2.1 mm i.d. HSA column that was put on-line with a 10 mm \times 2.1 mm i.d. HSA microcolumn after various times following the injection of a 5 μ L sample of 10 μ M quinidine onto the first column at 3.0 mL/min, and (b) the apparent free drug fractions that were measured by using the same multi-dimensional system and chromatographic conditions as in (a) with a sample that contained 10 μ M quinidine and 600 μ M HSA. All of the times shown are the elapsed interval after sample injection. The error bars represent a range of ± 1 standard error of the mean ($n = 4$). All of these measurements were made at pH 7.4 and 37 $^{\circ}$ C.



peak maxima were observed at 7.5-7.9 min, 7.6-8.2 min, 9.6-10.0 min, or 7.6-7.8 min, respectively, under the final conditions that are given in the Experimental section.

The timing of the switching event also created some changes in the apparent free drug fractions that were measured. This effect is illustrated in Figure 6.4(b) for injections that were made onto the multi-dimensional system of 10 μM quinidine or a mixture of this drug with 600 μM soluble HSA. It was found that a time for the switching event that was too short caused an overestimation in the free drug fraction, due to contamination of this fraction by dissociation of the original drug-protein complex in the sample. When the time for the switching event was made longer (e.g., at least 0.40 min in Figure 6.4), a consistent value in the measured free fraction was obtained. However, this increase in time also eventually produced a loss in precision for the measured free fraction as the overall area for the transferred drug peak was decreased. These combined effects led to the use of intermediate times for the switching event that provided both good accuracy and reasonable precisions for the measured free fractions. For quinidine, the final switching time that was employed was 0.40 min. The switching times that were optimized and selected for the other drugs were 0.6 min for diazepam, 1.5 min for acetohexamide, 1.2 min for tolbutamide, and 0.7 min for gliclazide.

Measurement of free fractions and binding of drugs to HSA in serum

The use of ultrafast affinity extraction with the multi-dimensional system was next used to measure the free fractions for various drugs that were present at typical therapeutic concentrations in serum. The results are summarized in Table 6.2. These

Table 6.2 Free drug fractions measured for various drugs in human serum^a

Serum content	Ultrafast affinity extraction	Ultrafiltration
Diazepam (3.5 μ M)	0.69 (\pm 0.10)%	Not determined ^b
Quinidine (10 μ M)	7.40 (\pm 0.53)%	7.71 (\pm 0.25)%
Tolbutamide (275 μ M)	2.44 (\pm 0.68)%	2.37 (\pm 0.07)%
Acetohexamide (138 μ M)	1.12 (\pm 0.07)%	1.41 (\pm 0.04)%
Gliclazide (23 μ M)	2.06 (\pm 0.16)%	2.01 (\pm 0.02)%

^aThese values were determined at 37 °C. The values in parentheses were determined by error propagation and represent a range of \pm 1 S.D. (n = 4).

^bThe free fraction of diazepam in this sample was too small to be detected by ultrafiltration but could be detected by ultrafast affinity extraction on the multi-dimensional system.

free fractions were in the general range of 0.7-7.4% for all of the drugs and serum samples that were tested. These results showed good agreement with those that were obtained by ultrafiltration for the same samples, with absolute differences of only 0.05%-0.41%. The results from the multi-dimensional affinity method also gave good absolute precisions for its measured free fractions (± 0.10 -0.68%), as well as reasonable relative precisions (± 6.2 -28%).

The free drug fractions that were measured with the multi-dimensional affinity system were further used to estimate the binding constants for each drug with HSA in the serum samples. These binding constants were calculated by using Equation 6.2, which can be used to provide the association equilibrium constant (K_a) for a system with single-site binding or the global affinity constant (nK'_a) for a system with multiple but independent binding sites.^{3,10,24}

$$K_a \text{ (or } nK'_a) = \frac{1-F_0}{F_0([P]-[D]+[D]F_0)} \quad (6.2)$$

In this equation, F_0 is the free fraction for the drug that is measured in the absence of any appreciable drug-protein dissociation in the sample, while $[D]$ and $[P]$ are the concentrations of the drug and soluble protein in the original sample, respectively. For drugs such as diazepam and quinidine, each having a single major binding site on HSA,^{1,22,41} Equation 6.2 can be used to provide the value of K_a for these interactions. For tolbutamide, acetohexamide and gliclazide, which each have two major binding sites on HSA,³¹⁻³⁴ Equation 6.2 would instead provide an estimate of the global affinity constant for these drug-protein interactions.

Table 6.3 summarizes the values of K_a or nK_a that were determined from the free drug fraction measurements. The relative precisions for these binding constants ranged from ± 6.9 -29%. The values for tolbutamide, acetohexamide, gliclazide and quinidine were all consistent with previous binding constants that have been reported for the same drugs with HSA and at the same temperature and pH.^{1,31-34,39} For instance, the results in Table 6.3 differed from the literature values by only 8.3-15.7% (average difference, 8.9%) or fell within the range of previously-reported values (e.g., in the case of quinidine). The binding constant determined for diazepam with HSA also fell within the range of previous values that have been obtained at the same pH but at room temperature.^{20,38} In addition, all of the binding constants that were measured by ultrafast affinity extraction and the multi-dimensional system agreed with the results that were obtained for the same samples when using ultrafiltration (i.e., K_a or nK_a values that differed by only 2.4-24%).

Conclusions

This study used ultrafast affinity extraction and a multi-dimensional affinity system to measure free drug fractions and to study drug-protein interactions in serum. Several drugs were used to test and illustrate this approach (i.e., quinidine, diazepam, gliclazide, tolbutamide and acetohexamide, with previously-reported affinities for HSA that ranged from 10^3 - 10^6 M^{-1}).^{1,20,31-34,38,39} Various factors were considered when optimizing this system to measure free drug fractions in serum at typical therapeutic concentrations. These factors included the flow rates and column sizes that were used for extraction of the free drug fraction and the times at which the affinity extraction column

Table 6.3 Association equilibrium constants (K_a) or global affinity constants (nK_a') estimated for various drugs with HSA in serum based on free drug fractions

Serum content	Ultrafast affinity extraction	K_a or nK_a' ($\times 10^4 \text{ M}^{-1}$) ^a	
		Ultrafiltration	Literature [Ref.]
Diazepam (3.5 μM)	24 (± 4)	Not determined ^b	22-125 [20,38] ^c
Quinidine (10 μM)	2.0 (± 0.2)	2.0 (± 0.1)	0.16-4.78 [1,39]
Tolbutamide (275 μM)	12 (± 3)	12 (± 1)	10.8 (± 0.3) ^d [31,33]
Acetohexamide (138 μM)	14 (± 1)	11 (± 1)	17.2 (± 1.1) ^d [31,32]
Gliclazide (23 μM)	8.1 (± 0.7)	8.3 (± 0.1)	7.9 (± 0.5) ^d [34]

^aThe ultrafast affinity extraction and ultrafiltration results were measured at 37 °C. The values in parentheses were determined by error propagation and represent a range of ± 1 S.D. ($n = 4$).

^bThe free fraction of diazepam in this sample was too small to be detected by ultrafiltration but could be detected by ultrafast affinity extraction on the multi-dimensional system.

^cThese literature values were determined at pH 7.4 and room temperature.

^dThese literature values were obtained by using the binding stoichiometries and association equilibrium constants that have been estimated at pH 7.4 and 37 °C for the given drugs at Sudlow sites I and II.³¹⁻³⁴ A similar range of values has been reported in Refs. 3 and 11.

was placed on-line with a larger affinity column for use in further isolating and measuring the retained free fraction.

The free drug fractions that were estimated for each drug by this approach were in good agreement with the results that were obtained by ultrafiltration. The binding constants that were estimated from the same data also agreed with those obtained by ultrafiltration and with literature values. However, the approach based on ultrafast affinity extraction had several advantages over traditional methods for free drug measurements and drug-protein binding studies. For instance, ultrafast affinity extraction required much smaller sample volumes per analysis than ultrafiltration (i.e., 1-5 μL versus 1 mL or more).^{3,10,11,24} The ultrafast affinity extraction and multi-dimensional affinity system also provided results within a relatively short period of time (i.e., 5-10 min per sample) and could be used to measure free drug fractions as small as 0.69% in serum with an absolute precision of ± 0.07 -0.68%. The same type of system could be employed in future work to examine alternative drugs and drug-protein interactions in serum. This method should also be adaptable for use in examining the binding of other small solutes (e.g., low mass hormones and fatty acids)^{1,16,21} with serum proteins or other binding agents.

References

1. T. Peters, Jr., All About Albumin: Biochemistry, Genetics, and Medical Applications, Academic Press, San Diego, CA, 1996.
2. N.W. Tietz (Ed.), Textbook of Clinical Chemistry, Saunders, Philadelphia, 1986.
3. X. Zheng, Z. Li, M.I. Podariu, D.S. Hage, Anal. Chem. 86 (2014) 6454-6460.
4. D.S. Hage, A. Jackson, M.R. Sobansky, J.E. Schiel, M.J. Yoo, K.S. Joseph, J. Sep. Sci. 32 (2009) 835-853.
5. T.C. Kwong, Clin. Chim. Acta 151 (1985) 193-216
6. F. Herve, S. Urien, E. Albengres, J. C. Duche and J. P. Tillement, Clin. Pharmacokinet. 26 (1994) 44-58.
7. W. Clarke, J.E. Schiel, A. Moser, D.S. Hage, Anal. Chem. 77 (2005) 1859-1866.
8. W. Clarke, A.R. Chowdhuri, D.S. Hage, Anal. Chem. 73 (2001) 2157-2164.
9. H.A. Krebs, Annu. Rev. Biochem. 19 (1950) 409-430.
10. X. Zheng, M.J. Yoo, D.S. Hage, Analyst 138 (2013) 6262-6265.
11. X. Zheng, R. Matsuda, D.S. Hage, J. Chromatogr. A 1371 (2014) 82-89.
12. J.W. Melten, A.J. Wittebrood, J.J. Hubb, G.H. Faber, J. Wemer, D.B. Faber, J. Pharm. Sci. 74 (1985) 692-694.
13. F.M. Musteata, Bioanalysis 3 (2011) 1753-1768.
14. R. Matsuda, C. Bi, J. Anguizola, M. Sobansky, E. Rodriguez, J.V. Badilla, X. Zheng, B. Hage, D.S. Hage, J. Chromatogr. B 966 (2014) 48-58.
15. K. Vuignier, J. Schappler, J. Veuthey, P. Carrupt, S. Martel, Anal. Bioanal. Chem. 398 (2010) 53-66.

16. X. Zheng, Z. Li, S. Beeram, M. Podariu, R. Matsuda, E.L. Pfaunmiller, C.J. White II, N. Carter, D.S. Hage, *J. Chromatogr. B: Anal. Technol. Biomed. Life Sci.* 968 (2014) 49-63.
17. L.R. Rich, Y.S. Day, T.A. Morton, D.G. Myszka, *Anal. Biochem.* 296 (2001) 197-207.
18. F. Dings, G. Zhao, S. Chen, F. Liu, Y. Sun, L. Zhang, *J. Mol. Struct.* 929 (2009) 159-166.
19. D. Leis, S. Barbosa, D. Attwood, P. Taboada, V. Mosquera, *Langmuir* 18 (2002) 8178-8185.
20. H. Yuan, J. Pawliszyn, *Anal. Chem.* 73 (2001) 4410-4416.
21. J.E. Schiel, D.S. Hage, *J. Sep. Sci.* 32 (2009) 1507-1522.
22. M.J. Yoo, D.S. Hage, *J. Chromatogr. A* 1218 (2011) 2072- 2078.
23. J.E. Schiel, D.S. Hage, *J. Sep. Sci.* 32 (2009) 1507-1522.
24. R. Mallik, M.J. Yoo, C.J. Briscoe, D.S. Hage, *J. Chromatogr. A* 1217 (2010) 2796-2803.
25. A.B. Ahene, *Bioanalysis* 3 (2011) 1287-1295.
26. S.S. Holm, S.H. Hansen, J. Faber, P. Staun-Olsen, *Clin. Biochem.* 37 (2004) 85-93.
27. O.P. Soldin, S.J. Soldin, *Clin. Biochem.* 44 (2011) 89-94.
28. J.E. Schiel, Z. Tong, C. Sakulthaew, D.S. Hage, *Anal. Chem.* 83 (2011) 9384-9390.
29. C.M. Ohnmacht, J.E. Schiel, D.S. Hage, *Anal. Chem.* 78 (2006) 7547-7556.
30. J. Chen, D.S. Hage, *Anal. Chem.* 78 (2006) 2672-2683.

31. K.S. Joseph, D.S. Hage, J. Chromatogr. B 878 (2010) 1590-1598.
32. K.S. Joseph, J. Anguizola, A.J. Jackson, D.S. Hage, J. Chromatogr. B 878 (2010) 2775-2781.
33. K.S. Joseph, J. Anguizola, D.S. Hage, J. Pharm. Biomed. Anal. 54 (2011) 426-432.
34. R. Matsuda, J. Anguizola, K.S. Joseph, D.S. Hage, Anal. Bioanal. Chem. 401 (2011) 2811-2819.
35. J.E. Schiel, Ph.D. Dissertation, University of Nebraska, Lincoln, Nebraska, 2009.
36. C.A. Burtis, E.R. Ashwood, D.E. Bruns (Eds.), Tietz Textbook of Clinical Chemistry and Molecular Diagnostics, Saunders, St. Louis, MO, 2006.
37. R. Regenthal, M. Krueger, C. Koeppel, R. Preiss, J. Clin. Monit. 15 (1999) 529-544.
38. J. Wilting, B.J.T. Hart, J.J. De Gier, Biochim. Biophys. Acta 626 (1980) 291-298.
39. C.T. Ueda, M.C. Makoid, J. Pharm. Sci. 68 (1979) 448-450.
40. M.J. Yoo, D.S. Hage, J. Sep. Sci. 34 (2011) 2255-2263
41. N.A. Kratochwil, W. Huber, F. Muller, M. Kansy, P.R. Gerber, Biochem.Pharmacol. 64 (2002) 1355-1374.

CHAPTER 7

The Use of Ultrafast Affinity Extraction to Study the Interactions of Steroid Hormone with Human Serum Albumin and Sex Hormone Binding Globulin

Portion of this chapter appear in X. Zheng, M. Brooks, D.S. Hage "Analysis of Hormone-Protein Binding in Solution by Ultrafast Affinity Extraction: Interactions of Testosterone with Human Serum Albumin and Sex Hormone Binding Globulin" Analytical Chemistry 2015, submitted.

Introduction

A number of low mass hormones are present in the bloodstream in both a free, or non-bound, form and a protein-bound form.¹⁻³ One example is testosterone, which is a steroid hormone that has a normal plasma concentration of 10-42 nM in adult males.^{1,4} Two important binding proteins for testosterone in blood are human serum albumin (HSA) and sex hormone binding globulin (SHBG).² HSA is the most abundant serum protein, accounting for 60% of the total serum protein content and having a normal concentration of 35-50 g/L (526-752 μ M).^{1,3} Testosterone has been reported to bind to HSA with a low-to-moderate affinity (i.e., $2.0-4.1 \times 10^4 \text{ M}^{-1}$ at 37 °C^{2,5-7}) and at a single site on domain IIA.^{4,8} SHBG is a homodimeric glycoprotein that acts as a transport protein for steroid hormones such as testosterone, dihydrotestosterone and estradiol. The concentration of SHBG in adult males is 10-60 nM.^{1,9} Testosterone has an affinity for SHBG that has been reported to be as high as 10^9 M^{-1} , with binding that occurs at one or two sites per homodimeric unit.^{2,6,10-13} Only about 2% of testosterone is normally present

in its free form in serum, with approximately 53-55% of this hormone being bound to HSA and 43-45% being bound to SHBG.^{2,4}

The free form of testosterone is generally considered to play an important role in the tissue uptake and biological activity of this hormone.^{2,14} However, some studies have shown that the form of testosterone that is bound to HSA in plasma may also be available to tissues.¹⁴ To better understand how each fraction of testosterone affects the biological response of this hormone, it is important to have information regarding the interactions of testosterone with proteins such as HSA or SHBG, and the resulting free fraction of this hormone in blood. The overall binding and rates of these interactions have been of particular interest.¹⁵

Various methods have been used to investigate the interactions between steroid hormones and HSA or SHBG. These methods have included rapid filtration,¹⁵⁻¹⁷ equilibrium dialysis,^{5,17-19} solvent partitioning,^{2,14,20,21} affinity capillary electrophoresis,²² and electron spin resonance spectroscopy.²³ However, some of these methods require relatively large sample volumes or amounts of protein, or may have long analysis times (e.g., equilibrium dialysis, gel filtration and the equilibrium partition method).^{5,7,14,18} In addition, prior binding studies with testosterone in many of these methods have used highly diluted serum or samples that were not prepared at typical physiological concentrations.^{2,15,16} It would be also be desirable in such studies to use a single method that can provide both thermodynamic and kinetic parameters, but previous work examined the interactions between steroid hormones and plasma proteins in separate approaches or experimental conditions to obtain such information.¹⁵⁻²³

Recently, a method based on ultrafast affinity extraction was developed for simultaneously estimating both the equilibrium constants and rate constants for drugs with HSA in solution.²⁴ In this method, an affinity microcolumn that contained an immobilized binding agent with relatively fast and strong binding for the target of interest was used to extract the free form of drugs from their protein-bound form in drug/protein samples. It was found that by varying the flow rate and column size, which altered the time for passage of the sample through the microcolumn, it was possible to obtain information on both the dissociation rate of a drug-protein complex and its binding constant.²⁴⁻²⁶ Advantages noted for this approach have included its ability to be used as a label-free method and to directly examine drug-protein interactions in solution. Other potential advantages are its speed, ease of automation, ability to be used with various HPLC detectors, good correlation with reference methods, and need for only a small amount of the drug and protein.²⁴⁻²⁶ It has further been shown that this method can be modified to measure the free fractions of many drugs at clinically-relevant concentrations.^{25,26}

In this study, ultrafast affinity extraction will be adapted and tested for use in examining the interactions of testosterone with HSA and SHBG in solution. The conditions needed for this type of analysis will be considered to make it allow for both the dissociation rate constants and association equilibrium constants to be obtained for these systems. The results of this study should provide valuable information that can be used to extend ultrafast affinity extraction to the study of other hormone-protein interactions and should provide a more complete picture of these binding processes within the body.

Experimental

Materials and reagents

The HSA (Cohn fraction V, essentially fatty acid free, $\geq 96\%$ pure), testosterone and hexane ($\geq 98.5\%$ pure) were from Sigma (St. Louis, MO, USA). The purified human SHBG was obtained from AbD Serotec ($\geq 90\%$ pure, 1 mg/mL in ammonium bicarbonate; batch number 060613; Raleigh, NC, USA). The reagents for the bicinchoninic acid (BCA) protein assay were obtained from Pierce (Rockford, IL, USA). The Nucleosil Si-300 silica (7 μm particle diameter, 300 Å pore size) was from Macherey Nagel (Düren, Germany). All buffers and aqueous solutions were prepared using water from a NANOpure system (Barnstead, Dubuque, IA, USA) and were passed through Osmonics 0.22 μm nylon filters from Fisher Scientific (Pittsburgh, PA, USA).

Apparatus

The microcolumns used in this study were packed using a Prep 24 pump from ChromTech (Apple Valley, MN, USA). A V-630 UV-Vis spectrophotometer from Jasco (Easton, MD, USA) was used to determine the testosterone concentration during the sample preparation. The HPLC system consisted of a PU-2080 Plus pump, an AS-2057 autosampler, and a UV-2075 absorbance detector from Jasco, plus a six-port Lab Pro valve (Rheodyne, Cotati, CA, USA). A CHM column heater and a TCM column heater controller from Waters (Milford, MA, USA) were used to maintain a temperature of 37.0

(± 0.1) °C for the columns during all experiments in this chapter. ChromNAV v1.8.04 software and LCNet from Jasco were used to control the HPLC system. The chromatograms were analyzed through the use of PeakFit v4.12 software (Jandel Scientific, San Rafael, CA, USA).

Column preparation

HSA immobilized to Nucleosil Si-300 silica was used as the stationary phase for ultrafast affinity extraction and in the multi-dimensional affinity system. This stationary phase was prepared by immobilizing HSA onto aldehyde-activated silica by using the Schiff base method, as described previously.^{27,28} The same material, but with no HSA being added during the immobilization step, was used as a control support. A BCA assay was used to determine the protein content of the final support in triplicate by using HSA as the standard and the control support as the blank.^{27,28} This assay gave a protein content of 66 (± 1) mg HSA/g silica, where the value in parentheses represents a range of ± 1 S.D.

The HSA support and control support were packed into standard stainless steel columns with 2.1 mm i.d. and lengths of 5-25 mm by using pH 7.4, 0.067 M potassium phosphate buffer as the packing solution. The packing pressure was 4000 psi (28 MPa) for 10, 20, or 25 mm long columns and 3000 psi (20 MPa) for the 5 \times 2.1 i.d. mm long columns. These columns were stored in pH 7.4, 0.067 M potassium phosphate buffer at 4 °C when not in use. These affinity microcolumns were each used for up to 40-100 injections, over a period of six months, to provide optimum retention and peak resolution;

however, these types of columns have been previously been found to be stable for at least 300-400 injections.^{24,25}

Preparation of Testosterone Solutions

Due to the low solubility and slow dissolution of testosterone in aqueous solutions, testosterone was dissolved indirectly into pH 7.4, 0.067 M potassium phosphate buffer. This was carried out by first using 2.5 mL hexane to dissolve testosterone at concentrations ranging from 1 to 100 $\mu\text{g/mL}$. A 1.2 mL portion from each of these standard solutions was placed into a series of vials for later use as standard in absorbance measurements. Another 1.2 mL portion of a testosterone/hexane solution was mixed with 3.0 mL of pH 7.4, 0.067 M potassium phosphate buffer. These mixtures were carefully shaken for more than 15 h at room temperature to allow partitioning of the testosterone to occur between the hexane and phosphate buffer.¹⁴ After this mixing step, the hexane and buffer phases were allowed to settle for 30 min to produce two distinct layers. The upper hexane layer and the lower phosphate buffer layer in each vial were then removed and placed into separate vials.

The concentration of testosterone in each hexane solution after the partitioning step was determined by diluting both these solutions and the testosterone/hexane standards ten-fold with pure hexane. The absorbance due to testosterone in each hexane sample or standard was then measured at 231 nm and was used to determine the amount of testosterone that had entered the phosphate buffer layers. The final measured concentrations of testosterone in the pH 7.4 phosphate buffer ranged from 0 to 51.5 μM by this approach. The corresponding solutions of testosterone in pH 7.4, 0.067 M were

then diluted further with the pH 7.4 buffer, as needed, to prepare the working solutions of testosterone for the chromatographic studies.

Chromatographic studies

The mobile phase used for sample preparation and the chromatographic studies was pH 7.4, 0.067 M potassium phosphate buffer. All mobile phases were degassed for 30 min prior to use. The aqueous solutions of testosterone were prepared as described in the previous section. All testosterone/protein mixtures that were used in this work were incubated for at least 30 min at 37 °C prior to injection to allow equilibrium to be established between the free and protein-bound fractions of the hormone in the sample.²⁴⁻
²⁷ Replicate injections ($n = 4$) were made for all samples and standards. Components eluting from the chromatographic system were monitored at 249 nm.

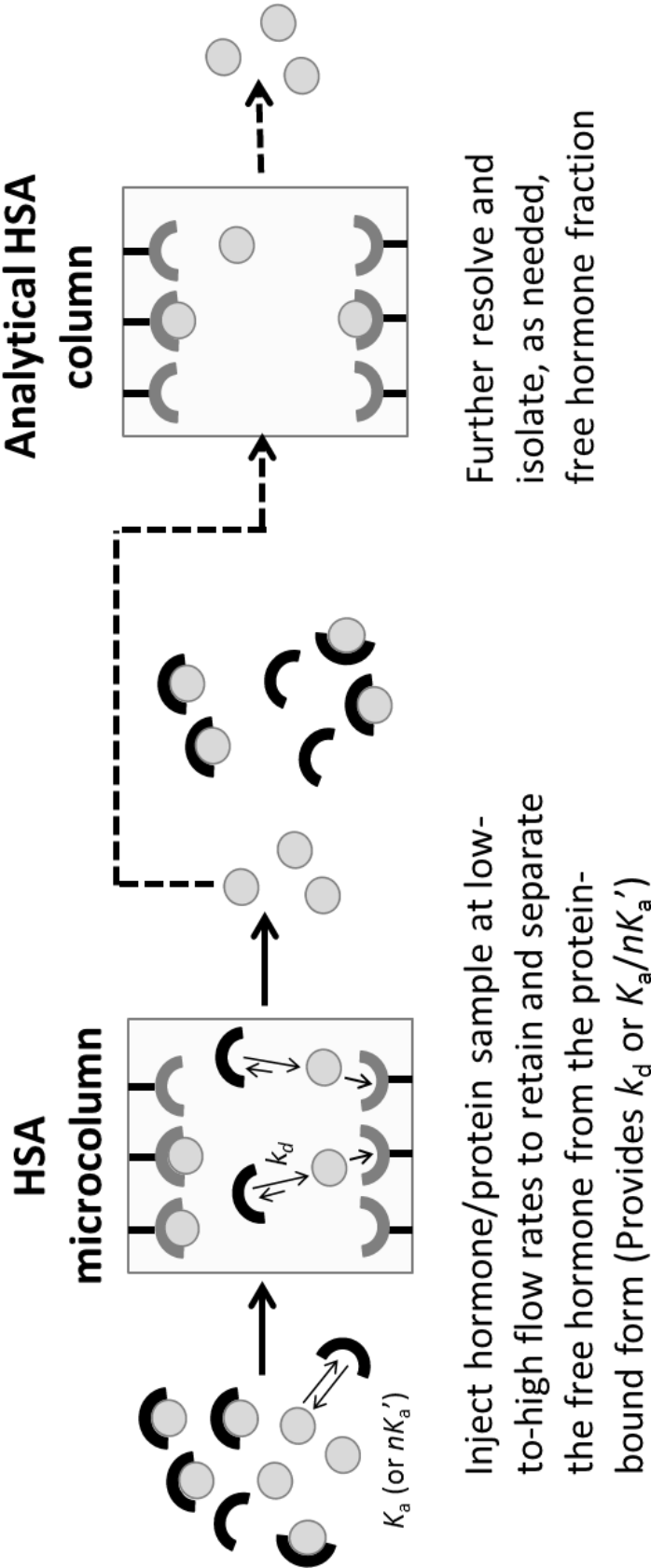
In the measurements of association equilibrium constants and dissociation rate constants for testosterone with HSA, the testosterone samples were prepared by diluting the stock solutions of testosterone, which were prepared as described previously, to a concentration of 20 μ M. The mixtures of testosterone with HSA were prepared by dissolving HSA in the testosterone sample to give a solution containing 20 μ M testosterone and 40 μ M soluble HSA. Samples that contained only testosterone or a mixture of testosterone and HSA were injected onto a 10 mm \times 2.1 mm i.d. HSA microcolumn by using an injection volume of 1 μ L. The flow rate for sample application ranged from 0.1 to 5.0 mL/min. To confirm the results obtained on the 10 mm \times 2.1 mm i.d. HSA microcolumn, a similar experiment was performed by making injections of

samples containing 10 μM testosterone or a mixture of 10 μM testosterone and 20 μM HSA onto a 5 mm \times 2.1 mm i.d. HSA microcolumn. The flow rate for sample application in this case ranged from 0.5 to 2.5 mL/min.

In the measurement of association equilibrium constants or global affinities, a relatively fast flow rate and short column residence time were used for the sample injection, which minimized the time that was allowed for any dissociation of testosterone from its complexes with a protein such as HSA (or SHBG).²⁴ Under these conditions, the measured free fraction should represent the original amount of the free hormone that was present in the sample before its injection, as illustrated in Figure 7.1(a). To determine the dissociation rate constant for testosterone from HSA interaction, low-to-medium flow rates were used to provide longer residence times as the sample passed through the column, as shown in Figure 7.1(a). The apparent free fraction of testosterone in a testosterone/protein mixture that was obtained at a given flow rate was found by dividing the peak area for the free testosterone by the total peak area for the same hormone in a solution that contained the same total amount of testosterone but no soluble protein.

The interactions between testosterone and SHBG were examined in a similar manner. In these experiments, the testosterone/SHBG mixture was prepared by diluting a commercial solution of SHBG (at a concentration of 1 mg/mL in ammonium bicarbonate buffer) with an aqueous solution of testosterone at a concentration of 42.4 nM in pH 7.4, 0.067 M phosphate buffer (i.e., a 0.0018:2 (v/v) mixture). The final mixture contained 42 nM of testosterone and 20 nM of SHBG, which was representative of the physiological concentrations of these agents. Samples containing only testosterone were prepared in

Figure 7.1 General scheme for examining hormone-protein binding by ultrafast affinity extraction. In this approach, a hormone/protein mixture is injected onto an affinity microcolumn that contains an immobilized binding agent for the hormone, such as HSA. A separation of the free and protein-bound forms of the hormone can be obtained on this column and provide apparent free hormone fractions that can be used to estimate the dissociation rate constant for the system (k_d) at low-to-moderate injection flow rates or the association equilibrium constant (K_a) or global affinity (nK_a') for the same system at higher flow rates. If further resolution of the retained free fraction is needed for other sample components, a portion of this fraction can be passed to a second affinity column for further separation prior to the final measurement of the free drug fraction.



the same manner but using pH 7.4, 0.067 M phosphate buffer instead of the SHBG stock solution. The measurements of association equilibrium constants, dissociation rate constant and free fraction were made by injecting 50 μ L samples that contained testosterone or a testosterone/SHBG mixture onto a 20 mm \times 2.1 mm i.d. HSA microcolumn at 0.25-2.0 mL/min.

Measurements of the free fraction and K_a for testosterone with HSA at physiological concentrations were carried out by using ultrafast affinity extraction in a multi-dimensional affinity system (see right portion of Figure 7.7.1). This was needed because of the large excess of HSA that was present versus testosterone (i.e., over a 10^4 -fold mol excess),^{1,3} which made it more difficult to measure the free fraction of testosterone when using only a single column. Work with the multi-dimensional system was carried out using 50 μ L injections of samples that contained 25 nM testosterone or 25 nM testosterone and 600 μ M HSA in pH 7.4, 0.067 M phosphate buffer. A 5 mm \times 2.1 mm i.d. HSA microcolumn was used to extract the free fraction of testosterone at 2.0 mL/min. A second HSA column with a size of 25 mm \times 2.1 mm i.d. was then placed on-line with the first column to further separate the extracted fraction from other sample components (e.g., HSA or testosterone that had dissociated from soluble HSA). This second column was placed on-line with the first column at 0.35-0.40 min after the sample injection, with the flow rate being changed at the same time to 0.50 mL/min. The free testosterone concentration was determined by comparing the peak areas obtained on the second column to those obtained on the same system for testosterone standards.^{25,26} The free fraction was found by dividing the measured free testosterone concentration by the total concentration of the hormone in the sample.

Results and Discussion

Optimization of ultrafast affinity extraction for testosterone-protein binding studies

The flow rate and column size are two important factors to consider in ultrafast affinity extraction, as they determine the time allowed for the dissociation of the protein-bound form of a solute as the sample passes through the column.²⁴⁻²⁸ For instance, a shorter column or a higher flow rate can provide a shorter time for samples to pass through the column, which would help minimize dissociation of the solute from its complex with soluble protein. This effect is illustrated in Figure 7.2 when using various flow rates for the injection of mixtures of testosterone with HSA or SHBG onto 5 mm or 20 mm \times 2.1 mm i.d. HSA microcolumns.

At low-to-medium flow rates, the apparent free fraction for testosterone increased with a decrease in flow rate. This effect occurred up to a flow rate of 2.0 mL/min for the testosterone/HSA data in Figure 7.2 and up to a flow rate of 1.25 mL/min for the testosterone/SHBG samples. This was caused by an increase in dissociation of the hormone from its complex with soluble HSA or SHBG as the samples passed through the affinity extraction column over longer periods of time. In addition, the use of a larger affinity extraction column also provided a higher apparent free testosterone fraction when compared to a smaller column that was used at the same flow rate. This difference was also a result of the longer time that was allowed for solute-protein dissociation as the sample passed through the larger column at the given flow rate.^{24,25}

Figure 7.2 Effect of the injection flow rate on the measurement of the apparent free fraction of testosterone in the presence of soluble HSA or SHBG. These results were acquired at pH 7.4 and 37 °C for 1 μ L injections of 10 μ M testosterone/20 μ M HSA made onto a 5 mm \times 2.1 mm i.d. HSA microcolumn (top), or 50 μ L injections of 42 nM testosterone/20 nM SHBG made onto a 20 mm \times 2.1 mm i.d. HSA microcolumn (bottom). Other conditions are given in the text.

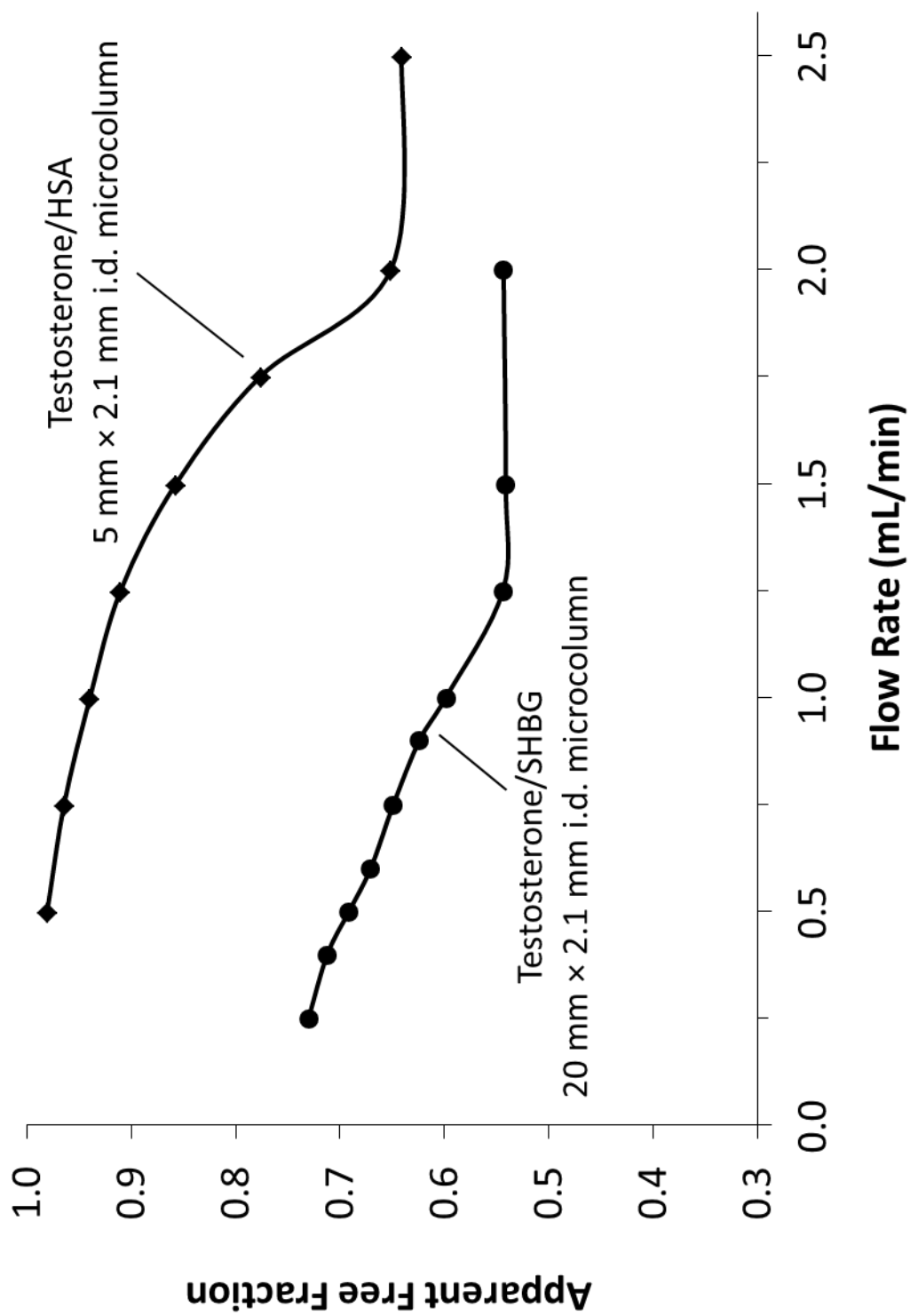


Figure 7.3 shows some typical chromatograms that were obtained from injections of testosterone and HSA onto a 5 mm \times 2.1 mm i.d. HSA microcolumn. The non-retained peak, which was due to HSA and testosterone's complex with the soluble HSA in the sample, eluted in approximately 1 min or less from this column, depending on the application flow rate. The observed elution time for the peak due to the retained free fraction of testosterone occurred at 0.3 min (at 2.5 mL/min) to 1.5 min (at 0.5 mL/min), and showed a separation from the protein-bound fraction of testosterone fraction in the sample. Similar separations were obtained on 10 mm \times 2.1 mm i.d. HSA microcolumns, in which the non-retained peak and retained peak eluted within 8 s to 4 min and 25 s to 10 min, respectively, at flow rates ranging from 0.10 to 5.0 mL/min.

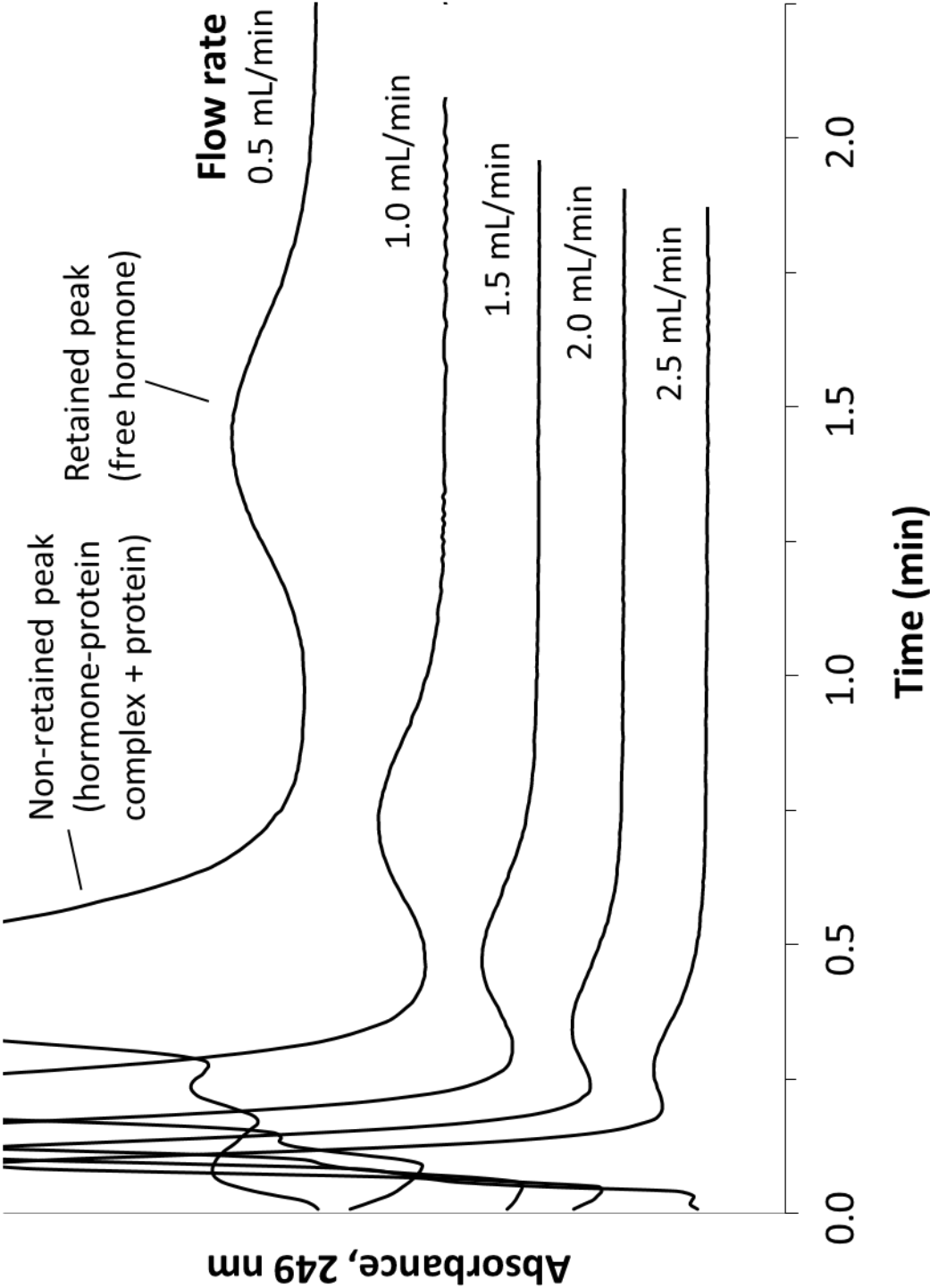
The apparent free hormone fractions that were measured in the low-to-moderate flow rate range were used to estimate the dissociation rate constant for the complex of testosterone with soluble HSA (or later SHBG). This was accomplished by using the apparent free fractions that were measured at each flow, or column residence time, and plotting these results according to a first-order integrated rate expression, such as given by Equation 7.1 or 7.2.²⁴

$$\ln \frac{(1 - F_0)}{(1 - F_t)} = k_d t \quad (7.1)$$

$$\ln \frac{1}{(1 - F_t)} = k_d t - \ln(1 - F_0) \quad (7.2)$$

In these two equivalent equations, F_t is the apparent free fraction that was measured at a given column residence time t , and F_0 is the original free fraction of the same solute in the original sample. The term t is also equal to the column void time and can be

Figure 7.3 Chromatograms obtained at various flow rates for 1 μ L injections of 10 μ M testosterone and 20 μ M HSA onto a 5 mm \times 2.1 mm i.d. HSA microcolumn at pH 7.4 and 37 $^{\circ}$ C.

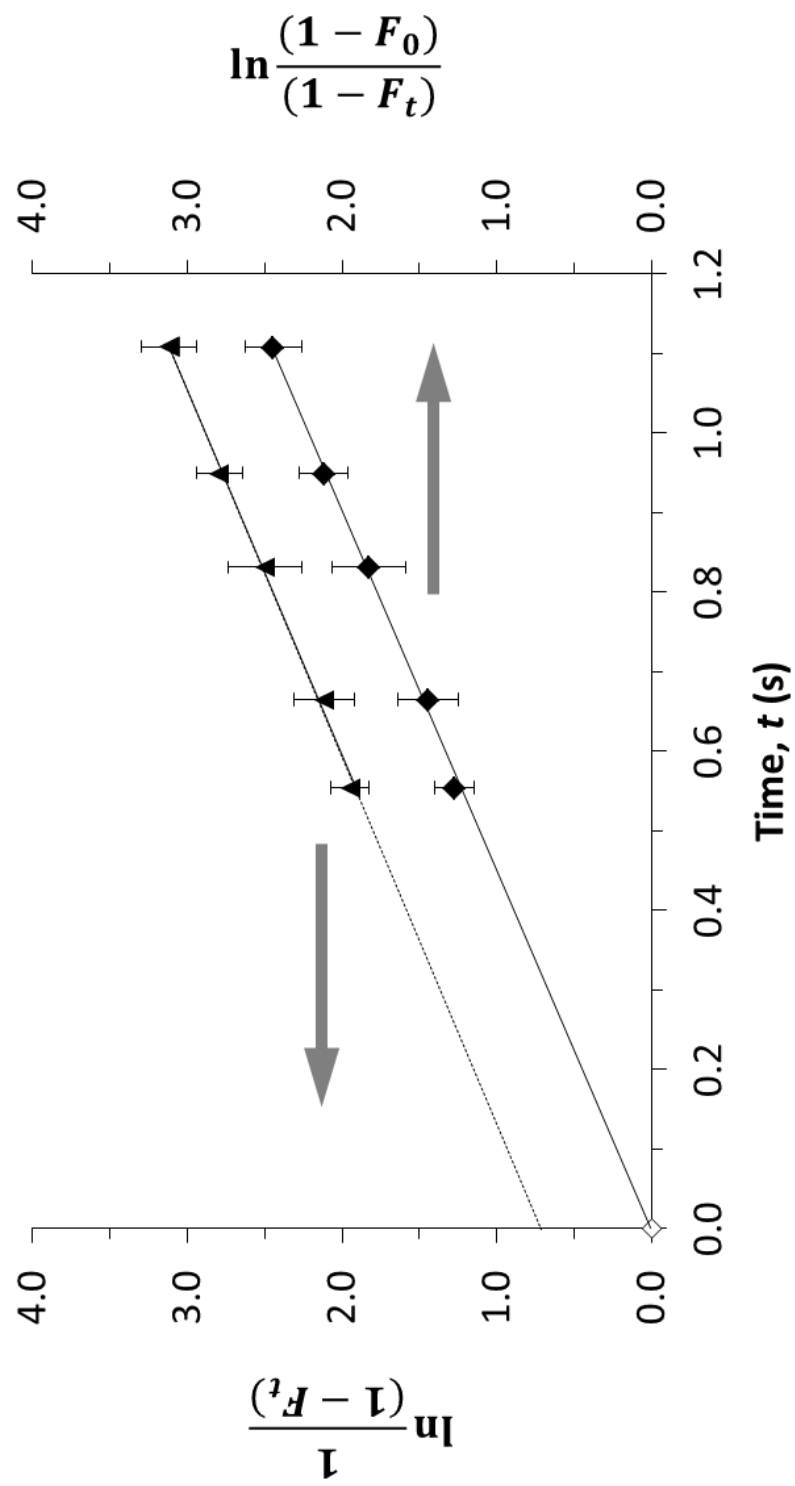


calculated by employing the flow rate and column void volume or by measuring the elution time of a non-retained solute.²⁴

Equations 7.1 and 7.2 predict that a solute-protein system that follows first-order dissociation should provide a plot for either $\ln[(1 - F_0)/(1 - F_t)]$ or $\ln [1/(1 - F_t)]$ against t that gives a linear relationship. Examples of such plots are given in Figure 7.4 for experiments examining the interaction of testosterone with soluble HSA by using a 10 mm \times 2.1 mm i.d. HSA column. In each case, the dissociation rate constant k_d can be determined from the slope of the best-fit line. When using Equation 7.1, a measurement or estimate for F_0 is also required and the intercept of the resulting fit should be essentially equal to zero. A plot constructed according to Equation 7.2 does not require this information and instead gives a positive intercept that can be used to obtain the value of F_0 .

It can be seen in Figure 7.2 that the measured free fraction for testosterone approached a constant value once the column residence time reached a certain minimum value. In the example for the injection of a testosterone/HSA mixture onto a 5 mm \times 2.1 mm i.d. HSA microcolumn, this occurred when the flow rate was greater than or equal to 2.0 mL/min, or a column residence time of around 416 milliseconds (ms) or less. At or above this flow rate, dissociation of testosterone from its protein-bound form was minimal due to the short column residence that was present. The free fraction of testosterone that was measured at or about this optimum flow rate was then employed to determine the free fraction of testosterone in the original sample (F_0). If it was known or assumed that the sample prior to injection was at equilibrium, the association equilibrium

Figure 7.4 Measurement of the dissociation rate constant for testosterone from HSA at pH 7.4 and 37 °C by using ultrafast affinity extraction. The sample contained 20 μM testosterone/40 μM HSA, which was injected onto a 10 mm \times 2.1 mm i.d. HSA microcolumn. These results were analyzed by using Equation 7.2 (top) or Equation 7.1 (bottom), where the latter included a point at the origin. The equations for the best-fit lines were $y = 2.17 (\pm 0.08) x + 0.71 (\pm 0.06)$ and $y = 2.20 (\pm 0.03) x + 0.01 (\pm 0.03)$, respectively. The correlation coefficients for these plots ranged from 0.998 to 0.999 ($n = 5-6$). The error bars represent a range of ± 1 S.D. ($n = 4$).



constant (K_a) for testosterone with the soluble protein could then also be calculated from the value of (F_0) and the known contents of the sample. For a solute and soluble protein with a 1:1 interaction, this can be accomplished by using Equation 7.3,

$$K_a = \frac{1 - F_0}{F_0([P]_0 - [A]_0 + [A]_0 F_0)} \quad (7.3)$$

where $[A]_0$ and $[P]_0$ are the original concentrations of the analyte and soluble protein in the injected sample, respectively.²⁴⁻²⁸ If multiple but independent binding sites are present for the solute with the protein, the value that is obtained by Equation 7.3 is instead the global affinity constant, nK_a' , where n represents the number of sites that are involved in the interaction.²⁴⁻²⁷

Determination of binding strength for testosterone with HSA

The binding parameters for testosterone with HSA were examined by using a 10 mm × 2.1 mm i.d. HSA microcolumn for ultrafast affinity extraction. This type of microcolumn and column size have previously been shown to be useful in this method for studying the interactions of HSA with drugs that have low-to-moderate strength interactions (e.g., affinities in the range of 10^4 - 10^5 M⁻¹), which are comparable to the affinities that have been reported for testosterone with HSA.^{2,5-7,24,25} The experiments with this particular microcolumn were carried out by injecting 1.0 µL samples that contained 20 µM testosterone and 40 µM HSA at flow rates ranging from 0.1 to 5.0 mL/min. A consistent free hormone fraction was obtained when the flow rate was at or

above 4.5 mL/min of this particular column, or when the column residence time for the sample was less than or equal to about 370 ms.

Figure 7.4 shows the results that were obtained when these data were plotted according to Equations 7.1 and 7.2. Linear responses were obtained for both types of plots, with correlation coefficients that ranged from 0.998 to 0.999 ($n = 5-6$). The value of K_a for testosterone with HSA values were determined by either utilizing the extrapolation method based on Equations 7.2 and 7.3 or by only using Equation 7.3 but with a known F_0 value that was measured at the optimum flow rate. As shown in Table 7.1, the value of K_a that was obtained through these methods was $3.2-3.5 \times 10^4 \text{ M}^{-1}$ at pH 7.4 and 37 °C, which gave excellent agreement with values of $2.0-4.1 \times 10^4 \text{ M}^{-1}$ that have been previously determined for the same system by using other methods.^{2,5,7}

To verify these parameters, the ultrafast affinity experiment was repeated by using two-fold lower concentrations of both testosterone and HSA and a shorter HSA microcolumn (i.e., 5 mm \times 2.1 mm i.d.). This shorter column made it possible to still obtain good retention for the free fraction of testosterone but also had half of the column residence time of the 10 mm \times 2.1 mm i.d. column when used at the same flow rate. In this second set of experiments, 1.0 μL samples that contained 10 μM testosterone and 20 μM HSA were applied at 0.5 to 2.5 mL/min. As shown in Figure 7.2, a minimum flow rate of only 2 mL/min was now required to obtain a consistent free hormone fraction on this shorter column but the column residence time obtained at this flow rate (416 ms) was comparable to the maximum allowable residence time that was observed when using the longer 10 mm \times 2.1 mm i.d. HSA microcolumn.

Table 7.1 Equilibrium constants and rate constants for the interactions of testosterone with HSA^a

Samples ^c	Association equilibrium constant, $K_a (\times 10^4 \text{ M}^{-1})$		Dissociation rate constant, $k_d (\text{s}^{-1})$		Association rate constant, $k_a (\times 10^4 \text{ M}^{-1} \text{s}^{-1})^b$
	Equation 7.3	Equations	Equation 7.1	Equation 7.2	Equations 7.2-7.3
	only	7.2-7.3			
10 μM Testosterone/20 μM HSA	3.2 (\pm 0.2)	3.3 (\pm 0.6)	2.07 (\pm 0.03)	2.08 (\pm 0.12)	6.7 (\pm 0.6)
20 μM Testosterone/40 μM HSA	3.5 (\pm 0.3)	3.2 (\pm 0.5)	2.20 (\pm 0.04)	2.17 (\pm 0.08)	7.6 (\pm 0.7)
Literature values [Refs.]	2.02-4.06 [3,5,7]		3.5 (\pm 0.4) [16]		

^aAll of these values were measured at pH 7.4 and 37 °C. The values in parentheses represent a range of \pm 1 S.D. ($n = 4$).

^bThe k_a values were calculated by using the formula $k_a = k_d K_a$, where K_a was determined by using experimentally measured free fraction values and Equation 7.3, and k_d was found by using Equation 7.2.

^cThe samples containing 10 μM testosterone/20 μM HSA were analyzed using a 5 mm \times 2.1 mm i.d. HSA microcolumn, and the samples containing 20 μM testosterone/40 μM HSA were analyzed using a 10 mm \times 2.1 mm i.d. HSA microcolumn.

The data that were obtained when using the 5 mm \times 2.1 mm i.d. HSA microcolumn again gave linear relationships when they were plotted according to either Equations 7.1 or 7.2. The correlation coefficients for these plots ranged from 0.998 to 0.999 ($n = 3-4$). The values of K_a that were determined from this plots were $3.2-3.3 \times 10^4 \text{ M}^{-1}$, as shown in Table 7.1. These values were within 3.1-8.6% of those measured on the 10 mm \times 2.1 mm i.d. column and fell within the range of values that have been reported in the literature.^{2,5,7} The relative precisions of the K_a values that were measured by ultrafast affinity extraction ranged from ± 6.3 to 18.2% when using both sizes of HSA microcolumns and samples that contained 10-20 μM testosterone plus 20-40 μM HSA. Further experiments were carried out using the 5 mm \times 2.1 mm i.d. HSA microcolumn as part of a multi-dimensional affinity system and with samples containing physiological levels of both testosterone and HSA (i.e., 25 nM testosterone and 600 μM HSA). The free fraction of testosterone measured in this condition was 4.94-4.99%, with precisions of $\pm 0.23-1.05\%$. These data gave a value for K_a of $3.2 (\pm 0.1) \times 10^4 \text{ M}^{-1}$, which agreed with these other experimental results and reference values. The consistency of these values also confirmed that the ultrafast extraction results and measured association equilibrium constants for testosterone with HSA were independent of concentration, as would be expected for a system involving one or more saturable sites.

Determination of rate constants for interactions of testosterone with HSA

The dissociation rate constants for testosterone and HSA were estimated by fitting the data in Figure 7.4 (which were obtained on a 10 mm \times 2.1 mm i.d. HSA microcolumn)

directly to Equation 7.2 or to Equation 7.1 with a point included at the origin. Plots gave a value for k_d of 2.17-2.20 s^{-1} at pH 7.4 and 37 °C. This set of values was consistent with a k_d of 3.5 (± 0.4) s^{-1} that has been previously determined by rapid filtration assay at the same temperature and pH using radiolabeled testosterone and a Krebs-tricine buffer.¹⁶

A shorter HSA microcolumn (5 mm \times 2.1 mm i.d.) was also used to measure the dissociation rate constant for testosterone with HSA. The k_d values that were obtained are also given in Table 7.1. These dissociation rate constants differed by only 4.2 to 5.9% from those obtained on the 10 mm \times 2.1 mm i.d. HSA microcolumn. The relative precisions of the k_d values that were determined by using both types of HSA microcolumns were in the range of ± 1.4 to 5.8%.

The K_a and k_d values that were determined in this study were also utilized to calculate the second-order association rate constant (k_a) for testosterone with soluble HSA, based on the relationship $k_a = k_d K_a$. Table 7.1 summarizes the values that were used in these calculations and the estimates of k_a that were obtained. The k_a values of $6.7\text{--}7.6 \times 10^4 \text{ M}^{-1}\text{s}^{-1}$ that were found gave good agreement with the range of association rate constants that have been reported for HSA with other solutes (e.g., gliclazide and chlorpromazine) that have similar association equilibrium constants and/or dissociation rate constants for this protein to those seen here for testosterone.²⁴

Determination of the binding strength for testosterone with SHBG

The binding affinity for testosterone-SHBG interaction followed a similar procedure as for testosterone with HSA. The samples in this case were prepared at therapeutic-relevant concentrations: 42 nM testosterone and 20 nM SHBG. The injection volume also increased to 50 μL for a better detection of testosterone at low concentrations. A single HSA affinity microcolumn that has a size of 20 mm \times 2.1 mm i.d. were used in this study to measure the free fraction of testosterone in the sample containing this hormone and SHBG.

Figure 7.2 shows the apparent free hormone fractions that were measured at flow rates ranging from 0.25 to 2.0 mL/min. The effect of flow rate on hormone-protein dissociation occurred in the column was minimized as the flow rate was raised. A constant free fraction was obtained when the flow rate was above 1.25 mL/min, or when the column residence time was at least 2.66 s. At or above the optimum flow rate, the original free fractions of testosterone that was present at equilibrium in the samples were estimated, giving a value of 54.4 (\pm 1.7)% at 1.25 mL/min, 54.1 (\pm 1.3)% at 1.5 mL/min, and 54.3 (\pm 1.6)% at 2.0 mL/min. This information can be used to determine the global affinity constant for testosterone with SHBG according to Equation 7.3. As summarized in Table 7.2, the estimated value for nK_a' was $1.1 (\pm 0.1) \times 10^9 \text{ M}^{-1}$ at pH 7.4 and 37 $^\circ\text{C}$ when taking an average of the values that were measured at the optimum flow rates (i.e., 1.25, 1.5 and 2 mL/min).

The apparent free fraction values that were measured at various low-to-moderate flow rates were also used to estimate the global association equilibrium constant based on Equations 7.2 and 7.3. As shown in Table 7.2, the value of nK_a' that was obtained was $1.0 (\pm 0.6) \times 10^9 \text{ M}^{-1}$, which differed by only 9.1% from the results determined based on

Table 7.2 Equilibrium constants and rate constants for the interactions of testosterone with SHBG^a

Samples	Global affinity constant, $nK_a' (\times 10^9 \text{ M}^{-1})$		Overall dissociation rate constant, $k_d (\text{s}^{-1})$		Overall association rate constant, $k_a (\times 10^7 \text{ M}^{-1} \text{ s}^{-1})^b$
	Equation 7.3 ^c	Equations	Equation 7.1	Equation 7.2	Equations 7.2-7.3
		7.2-7.3			
42 nM Testosterone/20 nM SHBG	1.1 (± 0.1)	1.0 (± 0.6)	0.058 (± 0.002)	0.057 (± 0.004)	6.3 (± 0.7)
Literature values [Refs.]	0.3-1.9 [3, 5,7,29]		0.032-0.059 [15,30,31] ^d		

^aAll of these values were measured at pH 7.4 and 37 °C, except where otherwise indicated. The values from ultrafast affinity extraction were obtained on a 20 mm \times 2.1 mm i.d. HSA microcolumn. The values in parentheses represent a range of ± 1 S.D. ($n = 4$), except where otherwise indicated.

^bThese k_a values were calculated by using the formula $k_a = k_d (nK_a')$, where nK_a' was determined by using experimentally measured free fraction values and Equation 7.3, and k_d was found by using Equation 7.2.

^cThese nK_a' values were obtained by taking the average of the values that were measured at 1.25, 1.50 and 2.00 mL/min.

^dThe value of k_d was measured at 37 °C and pH 7.4 in Ref. 15, at 37°C and pH 7.2 in Ref. 30 and at 37.5 °C and pH 8 in Ref. 31.

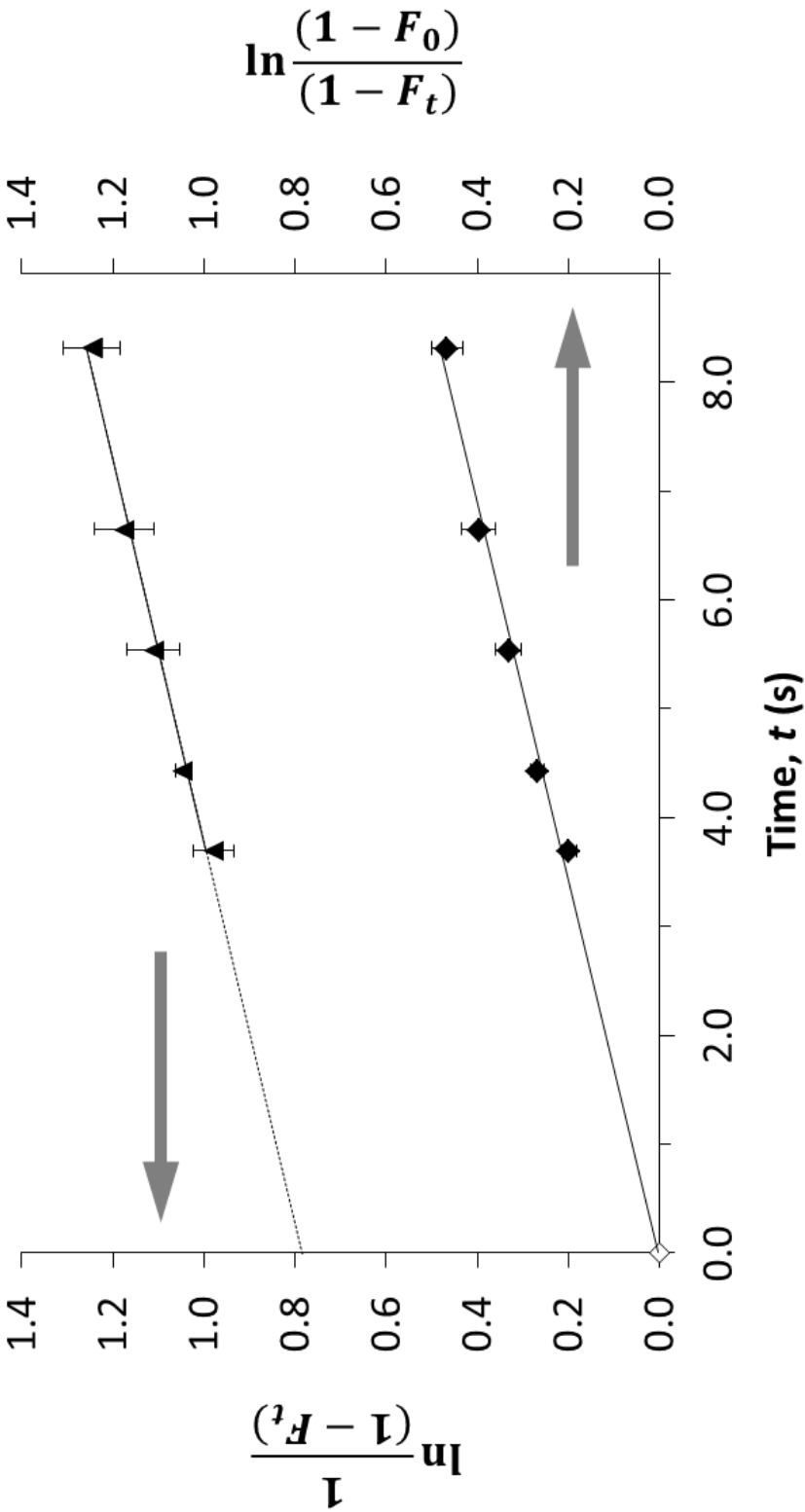
experimentally measured free fraction values and Equation 7.3. Both of these two values fit within the range of the affinity constants that were determined through other methods for the same binding system.^{2,5,7,29}

Determination of rate constants for the interactions of testosterone with SHBG

The rate constants for testosterone with SHBG were determined by using Equations 7.1 and 7.2 and the apparent free fraction values that were measured for this system at various flow rates. Figure 7.5 shows some typical plots that were obtained, which gave linear responses with correlation coefficients that ranged from 0.991 to 0.997 ($n = 5-6$). The overall dissociation rate constants that were determined from these plots were 0.057-0.058 s⁻¹, which agreed well with reference values (see Table 7.2).^{15,30,31} The relative precision for the measured k_d values was $\pm 3.4-7.0\%$.

The overall second-order association rate constant for testosterone with soluble SHBG was calculated from the measured values for k_d and nK_a' shown in Table 7.2. The estimated k_a was $6.3 (\pm 0.7) \times 10^7 \text{ M}^{-1}\text{s}^{-1}$. This value was larger than a value of $1.75 \times 10^6 \text{ M}^{-1}\text{s}^{-1}$ that has been reported for the same binding system at 4 °C,³¹ but was comparable to the result obtained for a system with a similar affinity for the interaction of testosterone with progesterone-binding globulin (guinea pig, 4 °C; nK_a' , $2.4 \times 10^9 \text{ M}^{-1}$; k_d , $9.5 \times 10^{-3} \text{ s}^{-1}$; k_a , $2.2 \times 10^7 \text{ M}^{-1}\text{s}^{-1}$).³²

Figure 7.5 Measurement of the overall dissociation rate constant for testosterone from SHBG at pH 7.4 and 37 °C by using ultrafast affinity extraction. The sample contained 42 nM testosterone/20 nM SHBG, which was injected onto a 20 mm × 2.1 mm i.d. HSA microcolumn. These results were analyzed by using Equation 7.2 (top) or Equation 7.1 (bottom), where the latter included a point at the origin. The equations for the best-fit lines were $y = 0.057 (\pm 0.004) x + 0.785 (\pm 0.027)$ and $y = 0.058 (\pm 0.002) x + 0.002 (\pm 0.012)$, respectively. The correlation coefficients for these plots ranged from 0.991 to 0.997 ($n = 5-6$). The error bars represent a range of ± 1 S.D. ($n = 4$).



Conclusions

This work used ultrafast affinity extraction and a multi-dimensional affinity system to examine the hormone-protein interaction and to measure the free hormone fractions at therapeutic levels. The information obtained included the dissociation rate constants and association equilibrium constants for the testosterone-HSA and testosterone-SHBG interactions. The obtained results gave good agreement with previous values that have been reported for the same binding systems based on other analytical approaches. However, the ultrafast affinity extraction based HPAC method has various advantages. This method is able to provide the both the binding constant and rate constant in a single experiment. This allows the measurements to be accomplished with small consumptions of samples and time. The ultrafast extraction can also be coupled with a multi-dimensional system to estimate the free fraction of hormone in samples prepared at therapeutic and physiological concentrations. In addition, the amount of samples required for each sample injection is very small, which significantly decreases the cost for this method.

The results obtained in this work demonstrates that the ultrafast affinity extraction method can be a general approach that could not only be used on drug-protein binding studies, as has been reported previously,²⁵⁻²⁷ but also be adapted for use with other binding studies such as the interactions between hormone and plasma proteins. Another important finding is that this method can be used to study the analyte-protein interaction with very strong binding (testosterone/SHBG; affinities, $\sim 10^9 \text{ M}^{-1}$) by the use of an affinity column, which has weaker binding to this analyte (testosterone/HSA; affinities, $\sim 10^4 \text{ M}^{-1}$). Therefore, it is possible to extend the ultrafast affinity extraction method to

study broad types of biological interactions with small limitations of the binding strength among the analyte.

References

1. N.W. Tietz (Ed.), Textbook of Clinical Chemistry, Saunders, Philadelphia, 1986.
2. R. Sodergard, T. Backstrom, V. Shanbhag, H. Carstensen, J. Steroid. Biochem. 16 (1982) 801-810.
3. T. Peters, Jr., All About Albumin: Biochemistry, Genetics, and Medical Applications, Academic Press, San Diego, CA, 1996.
4. N.A. Kratochwil, W. Huber, F. Muller, M. Kansy, P.R. Gerber, Biochem. Pharmacol. 64 (2002) 1355-1374.
5. A. Vermeulen, L. Verdonck, Steroids 11 (1968) 609-635.
6. N.A. Mazer, Steroids 74 (2009) 512-519.
7. C.W. Burke, D.C. Andersson, Sex-hormone-binding globulin is an oestrogen amplifier, Nature 240 (1972) 38-40.
8. O.S. Matsushita, Y. Isima, V.T.G. Chuang, H. Watanabe, S. Tanase, T. Maruyama, M. Otagiri, Pharm. Res. 21 (2004) 1924-1932.
9. J.F. Dunn, B.C. Nisula, D. Rodbard, J. Clin. Endocrinol. Metab. 53 (1981) 58-68.
10. P.H. Petra, J. Steroid Biochem. Mol. Biol. 40 (1991) 735-753.
11. G.L. Hammond, F.W. Bocchinfuso, J. Steroid Biochem. Mol. Biol. 53 (1995) 543-552.
12. G.V. Awakumov, I. Grishkovskaya, Y.A. Muller, G.L. Hammond, J. Biol. Chem. 276 (2001) 34453-34457.
13. J. Metzger, A. Schnitzbauer, M. Meyer, M. Soder, C.Y. Cuilleron, H. Hauptmann, Biochemistry 42 (2003) 13735-13745.
14. S. Watanabe, T. Sato, Biochim. Biophys. Acta 1289 (1996) 385-396.

15. C.M. Mendel, J. Steroid Biochem. Mol. Biol. 37 (1990) 251-255.
16. C.M. Mendel, M.B. Miller, P.K. Siiteri, J. T. Murai, J. Steroid Biochem. Mol. Biol. 37 (1990) 245-150.
17. C.C. Pan, C.A. Woolever, B.R. Bhavhani, J. Clin. Endocrinol. Metab. 61 (1985) 499-507.
18. N. Jenkins, K. Fotherby, J. Steroid Biochem. 13 (1980) 521-527.
19. M.J. Iqbal, M. Dalton, R.S. Sawers, Clin. Sci. 64 (1983) 307-314.
20. J.A. Schellman, R. Lumry, L.T. Samuels, J. Am. Chem. Soc. 76 (1954) 2808-2813.
21. E.K. Oyakawa, B.H. Levedahl, Arch. Biochem. Biophys. 74 (1958) 17-23.
22. L.K. Amundsen, H. Siren, Electrophoresis 28 (2007) 3737-3744.
23. M. Basset, G. Defaye, E.M. Chambaz, Biochim. Biophys. Acta 491 (1977) 434-446.
24. X. Zheng, Z. Li, M.I. Podariu, D.S. Hage, Anal. Chem. 86 (2014) 6454-6460.
25. X. Zheng, R. Matsuda, D.S. Hage, J. Chromatogr. A 1371 (2014) 82-89.
26. X. Zheng, M.J. Yoo, D.S. Hage, Analyst 138 (2013) 6262-6265.
27. R. Mallik, M.J. Yoo, C.J. Briscoe, D.S. Hage, J. Chromatogr. A 1217 (2010) 2796-2803.
28. C.M. Ohnmacht, J.E. Schiel, D.S. Hage, Anal. Chem. 78 (2006) 7547-7556.
29. W. Rosner, R.N. Smith, Biochemistry 14 (1975) 4813-4820.
30. W. Heyns, P. De Moor, J. Clin. Endocr. Metab. 32 (1971) 147-154.
31. G.F. Lata, H.K. Hu, G. Bagshaw, R.F. Tucker, Arch. Biochem. Biophys. 199 (1980) 220-227.

32. S.D. Stroupe, U. Westphal, J. Biol. Chem. 250 (1975) 8735-8739.

CHAPTER 8

Development of High Capacity Affinity Microcolumns Based on Hybrid Cross-Linking and Protein Immobilization Methods

Portion of this chapter appear in X. Zheng, M. Podariu, D.S. Hage, "Development of Enhanced Capacity Affinity Microcolumns by using a Hybrid of Protein Cross-linking/Modification and Immobilization" Journal of Chromatography A 2015, submitted.

Introduction

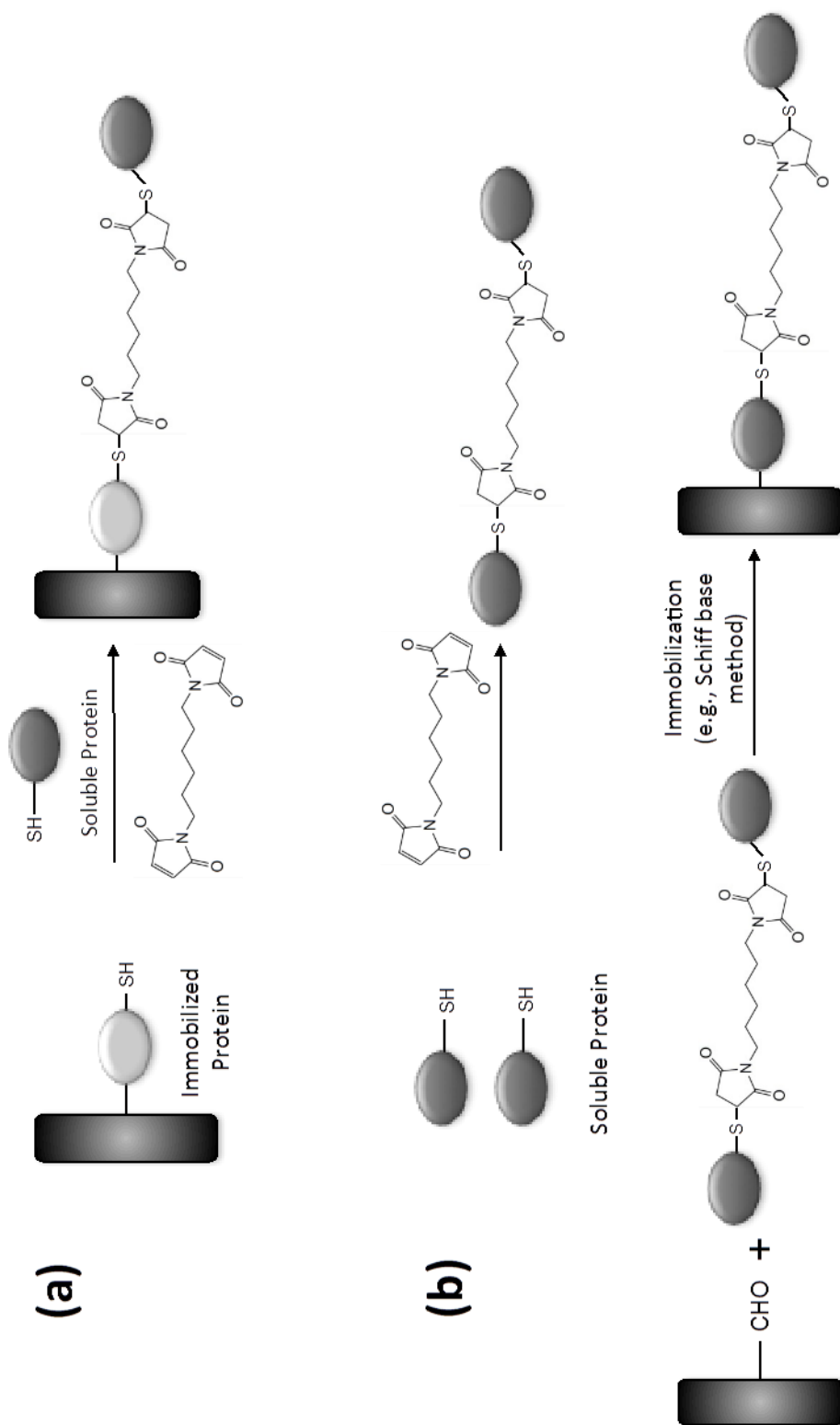
High-performance affinity chromatography (HPAC) is a type of high-performance liquid chromatography that uses biologically-related binding agents such as proteins or antibodies as the stationary phase.¹⁻³ This method has been widely used for chiral separations and the purification or analysis of biological agents, as well as for characterization of the biological interactions.¹⁻⁴ The retention and selectivity of this technique depend on the specific binding of the target analyte to the immobilized binding agent, and the amount of binding sites that are available in the column.⁴ This latter factor is related to, in turn, the total amount of binding agent that is present in the column and its relative activity.^{2,4}

Covalent immobilization is often used in affinity chromatography to couple a binding agent such as protein to a support. For example, this process might involve the use of amine, sulfhydryl, carboxyl, or carbonyl groups on a protein or glycoprotein.^{1,4-9} This general approach can produce affinity columns that have high stabilities and that can

be reused for many sample applications or experiments. However, the amount of protein that can be immobilized is generally limited by the size of protein and the surface area of the support. In addition, effects such as improper orientation of the binding agent or steric hindrance may lead to a decrease in this agent's apparent activity.^{6,9} As a result, it would be useful to have alternative strategies that could avoid such limitations and be used to increase the binding capacity and/or activity of columns that contain proteins as their stationary phases. A specific area in which this is of interest is in work with miniaturized affinity devices and affinity microcolumns, in which an increase in activity helps to provide higher retention and resolution for such devices.¹⁰⁻¹³

This chapter will include the examinations of some possible routes for creating affinity microcolumns with increased binding capacities and activities by using a combination of covalent immobilization and protein cross-linking or modification (see Figure 8.1). Human serum albumin (HSA), which is the most abundant protein in human serum^{2,4,8}, will be used as a model protein and binding agent for these experiments. HSA has been of interest for use in affinity chromatography as a chiral stationary phase⁸ and in studies of the binding by this protein with drugs, long-chain fatty acids, and some hormones.^{8,14-15} This protein is a single chain polypeptide consisting of 585 amino acid residues and has a mass of 66.5 kDa.^{8,14-15} It has two major drug binding sites (i.e., Sudlow sites I and II) but only one free sulfhydryl group (Cys34), which is not located near either of these two sites.^{4,8,14-15} Various methods have previously been developed to immobilize this protein to chromatographic supports, including both amine-based coupling methods^{9,16-21} and the coupling of this protein through Cys34 to maleimide-activated supports.^{5,9} However, these techniques are all inherently limited by the

Figure 8.1 General schemes considered for the preparation of high capacity HSA supports, such as (a) immobilization of HSA followed by modification/cross-linking of the immobilized protein with soluble protein or (b) modifying/cross-linking of soluble HSA, followed by immobilization of the resulting protein products.



available surface area of the support and may be subject to at least some steric hindrance or other immobilization effects.^{6,9}

An alternative approach that will be considered in this chapter is to use the cross-linking or modification of a protein such as HSA, either before or after covalent immobilization, to provide an increase in the amount of active protein that can be placed into small affinity columns. Bismaleimido-hexane (BMH), a homobifunctional cross-linker that reacts specifically with sulfhydryl groups²²⁻²⁷, will be the reagent employed for this approach. The protein content and relative activity of HSA columns that are modified with BMH will be compared to those obtained by using only covalent immobilization. Affinity microcolumns that are made by this hybrid approach will then be examined for use in drug-binding studies and ultrafast affinity extraction, among other applications. The results will be used to determine the advantages or possible limitations of this hybrid modification/immobilization strategy, as well as its potential uses in areas such as high-throughput studies of drug-protein binding, new methods for biointeraction studies, and microscale affinity-based separations.

Experimental

Materials and reagents

The HSA (Cohn fraction V, essentially fatty acid free, $\geq 96\%$ pure), carbamazepine, racemic verapamil, racemic warfarin, dimethyl sulfoxide (DMSO), sodium nitrate, sodium borohydride and sodium cyanoborohydride were obtained from

Sigma (St. Louis, MO, USA). The ethacrynic acid was purchased from Fisher Scientific (Atlanta, GA, USA). The Zeba spin desalting columns (5 mL, 7 kDa cutoff), BMH, and reagents for the bicinchoninic acid (BCA) protein assay were from Thermo Scientific (Rockford, IL, USA). The Nucleosil Si 300 silica (7 μm particle diameter, 300 Å pore size) was purchased from Macherey Nagel (Düren, Germany). All buffers and aqueous solutions were prepared using water from a Milli-Q Advantage A 10 system (EDM Millipore Corporation, Billerica, MA, USA) and were passed through Osmonics 0.22 μm nylon filters from Fisher (Pittsburgh, PA, USA).

Apparatus

The HSA solutions or silica slurries were mixed and allowed to react with added reagents by using a Labquake Shaker from Barnstead Thermolyne (Dubuque, IA, USA). The affinity microcolumns were packed using a Prep 24 pump from ChromTech (Apple Valley, MN, USA). The HPLC system consisted of a PU-2080 Plus pump, an AS-2057 autosampler, and a UV-2075 absorbance detector from Jasco (Easton, MD, USA). An Alltech water jacket (Deerfield, IL, USA) and an Isotemp 3013D circulating water bath from Fisher were used to maintain a temperature of 37.0 (\pm 0.1) °C for the columns during all experiments described in this chapter. ChromNAV v1.18.04 software and LCNet from Jasco were used to control the HPLC system. Chromatograms were analyzed through the use of PeakFit v4.12 software (Jandel Scientific, San Rafael, CA, USA).

Preparation of affinity supports

The reference HSA supports were prepared by immobilizing HSA onto silica that had initially been prepared in a diol-bonded form and then converted into an aldehyde-activated form for use in the Schiff base immobilization method.²⁸ Sodium cyanoborohydride was also placed in the HSA/aldehyde-silica slurry during immobilization to reduce each Schiff base upon its formation, to create a more stable secondary amine linkage. After the Schiff base immobilization reaction had been allowed to occur, the remaining aldehyde groups on the support were reduced by adding sodium borohydride. A control support was prepared in the same manner but with no HSA being added during the immobilization step.²⁸

The BMH-treated HSA silica that was used in the chromatographic studies was prepared according to the strategy shown in Figure 8.1(b). This method involved dissolving 70 mg HSA in 1.0 mL of pH 7.0, 1.5 M potassium phosphate buffer and combining this solution with 30 μ L of 0.072 M BMH in DMSO, giving a mixture with a final concentration of 2 mM BMH and 1 mM HSA (i.e., a 2:1 mol/mol ratio for BMH vs. HSA). This mixture was incubated for 8 h at room temperature, followed by additional mixing for 24 h at 4 °C. A desalting column (5.0 mL volume, 7 kDa cutoff) was used to remove excess reagents from the cross-linked or modified HSA. The pH of this protein solution was slowly adjusted to pH 6.0 by adding a small amount of 50% (v/v) hydrochloric acid, giving a final total volume of approximately 1 mL. This protein solution was then combined with 0.15 g Nucleosil Si-300, which had been already converted into an aldehyde-activated form and washed with pH 6.0, 0.10 M phosphate buffer for use in the Schiff base immobilization method.²⁸ Sodium cyanoborohydride

was also added to this mixture to reduce the Schiff bases upon their formation, and sodium borohydride was again added later to reduce and remove any aldehyde groups that remained after the immobilization process.²⁸ A control support was prepared by the same procedure but with no HSA being placed into the reaction buffer during the cross-linking/modification reaction. All of HSA supports and control supports that are discussed in this chapter were stored in pH 7.4, 0.067 M potassium phosphate buffer and at 4 °C when not in use.

A portion of each HSA support or BMH-treated HSA support was analyzed for its protein content by using a BCA protein assay. This assay was carried out in triplicate using normal HSA as the standard and the control support as the blank. The same assay was also carried out using samples that contained 0.5 μ M soluble BMH or a control support that was prepared from the reference HSA silica after treating this material with a two-fold mol excess BMH, following protein immobilization. The soluble BMH did not have any noticeable effect on the results of the BCA assay, but the BMH-treated HSA control support gave a result that was 37.7% (\pm 2.1%) lower than that obtained for the same support before treatment with BMH. All of the protein assay results reported in this study and that involved BMH-treated HSA have been corrected for this BMH-induced decrease in response, based on the results of these control experiments.

Chromatographic studies

The supports that were used in the chromatographic studies were downward slurry packed into separate 10 mm \times 2.1 mm i.d. microcolumns at 4000 psi (28 MPa) or

into 5 mm \times 2.1 mm i.d. microcolumns at 3000 psi (20 MPa). The packing solution was pH 7.4, 0.067 M potassium phosphate buffer. The microcolumns were stored in the same buffer at 4 °C when not in use. The column-to-column variation in overall support content, as determined by making replicate injections of the tested drugs onto several new columns of the same size and packed with the same HSA support, was \pm 0.4 to 6.8%. The mobile phase used in the chromatographic experiments was pH 7.4, 0.067 M potassium phosphate buffer, except where otherwise indicated. The following wavelengths were employed for absorbance detection: warfarin, 308 nm; verapamil, 229 nm; carbamazepine, 284 nm; ethacrynic acid, 280 nm; and sodium nitrate, 205 nm.

The measurements of retention factors were made by injecting 5 μ L samples that contained 10 μ M of racemic warfarin, racemic verapamil, or carbamazepine dissolved in the mobile phase. All samples were injected in quadruplicate on 5 mm or 10 mm \times 2.1 mm i.d. HSA microcolumns and control columns at 0.1-1.5 mL/min. Sodium nitrate, which has no retention on the HSA reference columns or control columns^{6,29}, was used as a void marker; this compound was injected onto each microcolumn under the same conditions as used for each drug. The extra-column void time was measured by injecting sodium nitrate onto the HPLC system with a zero dead volume connector being used in place of the column.

The retention due to interactions with BMH was measured by injecting each drug in quadruplicate onto a reference 10 mm \times 2.1mm i.d. HSA microcolumn before and after the microcolumn had been treated with BMH. The BMH solution that was used for this treatment contained 1.25 mM of BMH in pH 7.0, 1.5 M potassium phosphate buffer plus 3.5% DMSO. A syringe pump was used to apply this solution to the HSA

microcolumn at 3 $\mu\text{L}/\text{min}$ for 15 h at room temperature. The estimated ratio for BMH versus HSA was 20:1 mol/mol while the BMH solution was passing through the column. This column was then washed with pH 7.4, 0.067 M potassium phosphate buffer for 8 h at 0.25 mL/min and room temperature prior to its used in further retention studies.

The chiral separation of *R/S*-warfarin was obtained by injecting 10 μL of 10 μM racemic warfarin at 1.5 mL/min onto a 10 mm \times 2.1 mm i.d. BMH-treated HSA microcolumn and using a mobile phase that consisted of pH 7.4, 0.067 M potassium phosphate buffer with 1.5% (v/v) 1-propanol. The reversible binding of ethacrynic acid with HSA was examined by injecting 20 μL of 10 μM ethacrynic acid onto 10 mm \times 2.1 mm i.d. BMH-treated HSA or reference HSA microcolumns at 1.5 mL/min.

In the ultrafast affinity extraction experiments, racemic warfarin, racemic verapamil, carbamazepine and HSA were injected onto a 10 mm \times 2.1 mm i.d. BMH-treated HSA microcolumn or reference HSA microcolumn. This was carried out by injecting 1 μL samples that contained 10 μM of each drug or a mixture containing of 10 μM of the drug plus 20 μM soluble HSA. These samples were incubated for at least 30 min prior to injection, with both the sample and mobile phase being preheated to 37 $^{\circ}\text{C}$ before passage through the affinity microcolumn. The flow rates used for ultrafast affinity extraction ranged from 0.25 to 2.5 mL/min for verapamil, 0.25 to 6.0 mL/min for warfarin and 0.05 to 1.0 mL/min for carbamazepine. Each free fraction was calculated by dividing the peak area for the free drug by the peak area for the total drug in the sample.¹⁶⁻¹⁸

Results and Discussion

Optimization of HSA modification

Two possible cross-linking and modification strategies were explored for increasing the HSA content of affinity supports that contain this immobilized protein. This modification and cross-linking could be performed either after protein immobilization, as shown in Figure 8.1(a), or before immobilization, as illustrated in Figure 8.1(b).

In the approach represented by Figure 8.1(a), HSA was first immobilized onto silica, as achieved in this particular study by using the Schiff base method. Soluble HSA and BMH were then incubated with this immobilized HSA silica for cross-linking and modification of the soluble and immobilized forms of this protein. Initial studies of this strategy looked at the amount of soluble HSA that was needed for the cross-linking and modification reaction. A support prepared by using only the Schiff base immobilization method had a protein content of $61.4 (\pm 0.7)$ mg HSA/g silica. A 0.25 mL slurry containing roughly 40 mg of this support (or 2.4 mg immobilized HSA) was incubated with 10 mg/mL of soluble HSA and 0.60 mM BMH in pH 7.0, 0.10 M phosphate buffer that contained 0.15 M NaCl. These conditions gave only a $15.3 (\pm 2.2)\%$ increase in the final protein content of the support. When the concentration of the soluble protein in the slurry was increased to 40 mg/mL, no further increase in the amount of immobilized protein was noted compared to the original protein content of the support. The same amount of soluble HSA and BMH were also added in three portions to the HSA silica in

5 h intervals. This method gave only a small and essentially negligible increase in protein content, or a $3.7 (\pm 2.0)\%$ change, when compared to the original support.

These small or negligible changes in the immobilized protein content when using the strategy in Figure 8.1(a) were probably the result of steric hindrance that prevented the soluble HSA from reaching the immobilized HSA and/or orientation effects that made it difficult for the immobilized and soluble HSA to align properly for cross-linking through their modified or free sulfhydryl groups.⁹ It is also likely that the BMH had cross-linked some of the soluble HSA with other molecules of soluble HSA, which would then not have been available for reacting with the free sulfhydryl groups on the immobilized HSA.

In the second approach, as illustrated in Figure 8.1(b), the HSA was first dissolved in the reaction buffer and then incubated with BMH for cross-linking and modification. After removing the excess BMH, the cross-linked or modified proteins were immobilized by the Schiff base method. This method was performed by dissolving 5 mg or 20 mg of HSA in 1.0 mL of the BMH reaction buffer. This mixture initially contained 0.00, 0.15 mM or 0.75 mM BMH for a 5 mg HSA sample; or 0.00, 0.60 or 3.01 mM BMH for a 20 mg HSA sample, providing a 0:1, 2:1, or 10:1 mol/mol ratio for BMH versus HSA. When the concentration of BMH was 10-fold higher than that of the soluble HSA, the protein content of the final support was increased by $64 (\pm 4)\%$ or $65 (\pm 3)\%$ for the solutions containing 5.0 mg/mL or 20.0 mg/mL of HSA and when compared to an immobilization scheme in which no BMH had been added. When the concentration of BMH was only 2-fold higher than the concentration of soluble HSA, the protein content of the final support increased by $75 (\pm 4)\%$ when using 20.0 mg/mL of soluble HSA.

However, decreasing the BMH content further (e.g., down to a 1:2 mol/mol ratio of BMH versus HSA) did not provide any further increase in the protein content.

The concentration of the reaction buffer that was used in both of the strategies that are shown in Figure 8.1 was also considered. This was done by increasing the concentration of the pH 7.0 potassium phosphate buffer to 1.5 M.^{5,29,30} It has been suggested that increasing the ionic strength of the buffer for this reaction can inhibit charge repulsion of adjacent proteins and increase the rate of nucleophilic addition of a sulfhydryl group to maleimide.³⁰ For the immobilization/modification strategy in Figure 8.1(a), no apparent increase in protein content was found when a higher ionic strength for the buffer was used during the modification reaction. However, an increase as high as 113 (\pm 2)% was observed when this same buffer was used for the modification/immobilization strategy in Figure 8.1(b). This modification/immobilization strategy and set of conditions were later employed in the following sections of this study.

Effects of protein modification on retention

The next set of studies sought to characterize the effects of combining protein modification and immobilization on the retention that was observed for various drugs on HSA columns. One drug that was used in these experiments was warfarin, which is an anticoagulant known to bind to HSA at Sudlow site I.^{19-21,28} Two other drugs that were tested were verapamil, a calcium channel blocking agent that has a primary binding site at Sudlow site I³¹, and carbamazepine, an anticonvulsant that binds to Sudlow site II.³² These drugs represented binding strengths that spanned roughly a 100-fold range in

affinities for HSA, with reported association equilibrium constants (K_a) at 37 °C and pH 7.4 of $2.0\text{--}5.7 \times 10^5 \text{ M}^{-1}$ for racemic warfarin, $1.4 (\pm 0.1) \times 10^4 \text{ M}^{-1}$ for racemic verapamil, and $5.2\text{--}5.5 \times 10^3 \text{ M}^{-1}$ for carbamazepine.^{19-21,28,31-33}

Figure 8.2 shows some typical chromatograms that were obtained for these drugs on BMH-treated HSA microcolumns and reference HSA microcolumns. As is suggested by these results, the BMH-treated HSA columns gave a significant increase in retention for each of the tested drugs. In the case of verapamil, a partial chiral separation with a resolution (R_s) of $0.61 (\pm 0.06)$ could be achieved by the BMH-treated HSA microcolumns in the presence of only pH 7.4 phosphate buffer at some of the flow rates that were used; however, no chiral separation was observed at the same flow rates when using the reference HSA microcolumn, as indicated in Figure 8.2(a). Both types of columns gave at least a partial separation for racemic warfarin in the presence of only pH 7.4, 0.067 M phosphate buffer, with $R_s = 0.59 (\pm 0.02)$ on the reference HSA microcolumn and $0.74 (\pm 0.02)$ on the BMH-treated HSA microcolumn, as shown in Figure 8.2(b). It was possible to increase the extent of the chiral separation for warfarin to nearly baseline resolution ($R_s = 1.32 (\pm 0.05)$) for the BMH-treated HSA microcolumn by including a small amount of 1.5% 1-propanol in the mobile phase, as shown in Figure 8.2(c), while prior work under similar conditions with a reference HSA microcolumn gave a resolution of $1.12 (\pm 0.03)$.¹⁷

Table 8.1 lists the average retention factors that were obtained at 37 °C and pH 7.4 for each drug on 10 mm \times 2.1 mm i.d. microcolumns containing BMH-treated HSA or a reference sample of HSA. For each drug and at each sample flow rate, there was a

Figure 8.2 Chromatograms obtained for the injection of (a) 5 μ L of 10 μ M racemic verapamil onto a 10 mm \times 2.1 mm i.d. BMH-treated HSA microcolumn or a reference HSA microcolumn at 0.25 mL/min and in the presence of pH 7.4, 0.067 M phosphate buffer; (b) 5 μ L of 10 μ M racemic warfarin onto the same columns at 0.5 mL/min and in the presence of pH 7.4, 0.067 M phosphate buffer; or (c) 10 μ L of 10 μ M racemic warfarin onto a 10 mm \times 2.1 mm i.d. BMH-treated HSA microcolumn at 1.5 mL/min and in the presence of pH 7.4, 0.067 M phosphate buffer containing 1.5% (v/v) 1-propanol. All of these separations were carried out at 37 $^{\circ}$ C and using BMH-treated HSA columns that were prepared with the modification/immobilization scheme described in Section of *Optimization of HSA modification*

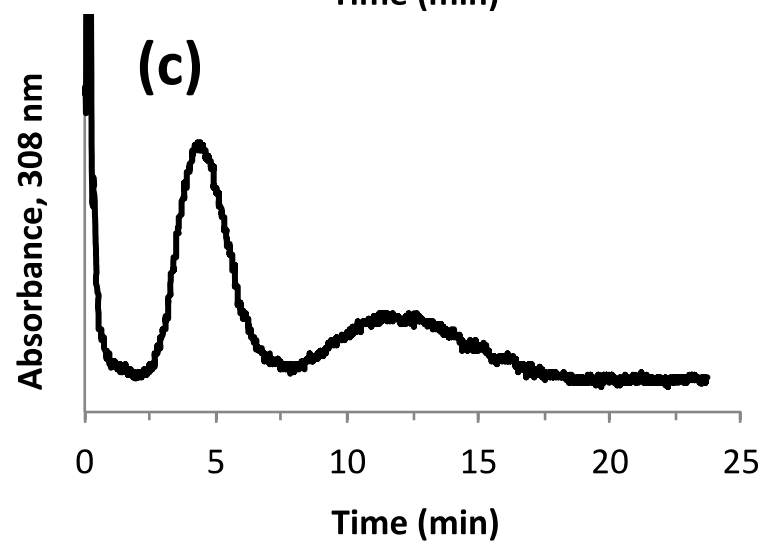
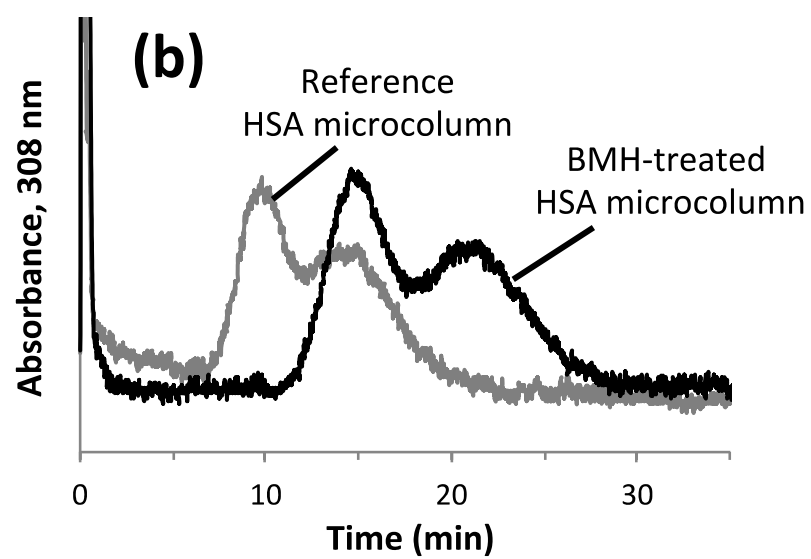
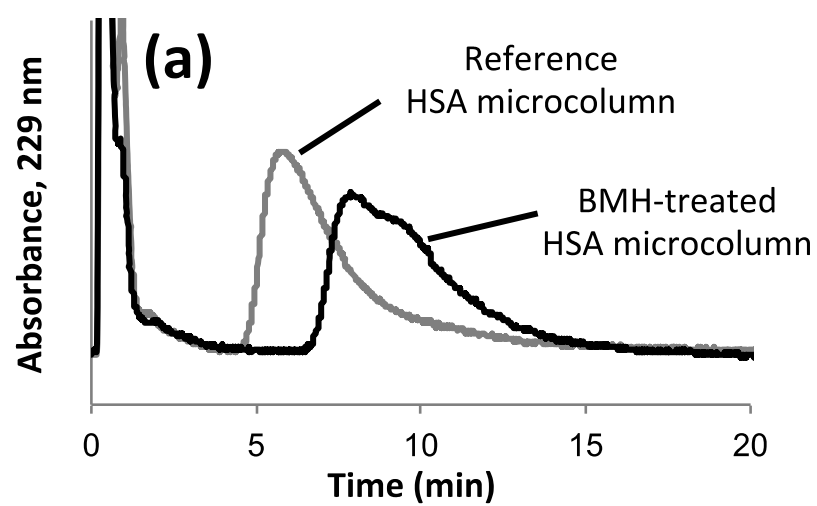


Table 8.1 Retention factors (*k*) measured on BMH-treated HSA supports and standard HSA supports^a

Drug	Flow rate (mL/min)	<i>k</i>, Reference HSA support	<i>k</i>, BMH-treated HSA support	Total change in <i>k</i> (%)	Specific change in <i>k</i> due to HSA (%)
<i>Warfarin</i> ^b	1.50	116 (± 7)	218 (± 3)	88 (± 7)	70 (± 9)
	0.50	124 (± 3)	233 (± 5)	88 (± 5)	70 (± 8)
<i>Verapamil</i> ^b	1.00	13.3 (± 2.2)	35.7 (± 1.5)	168 (± 20)	95 (± 29)
	0.50	14.4 (± 1.2)	37.3 (± 1.5)	159 (± 13)	86 (± 24)
	0.25	13.7 (± 1.6)	35.2 (± 2.2)	157 (± 20)	84 (± 29)
<i>Carbamazepine</i>	0.50	2.3 (± 0.1)	4.6 (± 0.3)	100 (± 14)	96 (± 15)
	0.25	2.1 (± 0.1)	4.2 (± 0.2)	100 (± 11)	96 (± 13)
	0.10	2.1 (± 0.2)	4.3 (± 0.1)	105 (± 11)	100 (± 12)

^aThe retention factors were determined at pH 7.4 and at 37°C for 10 mm × 2.1 mm i.d. columns. The values in parentheses represent a range of ± 1 S.D., as determined by error propagation. The estimated retention due to interactions with BMH were 18.1 (± 6.3)% for warfarin, 73 (± 21)% for verapamil, and 4.3 (± 6.1)% for carbamazepine.

^bThe results provided for warfarin and verapamil were based on the average retention factors for *R*- and *S*-enantiomers.

consistent and significant increase in the total retention factor that was measured on the BMH-treated HSA microcolumns compared to the reference HSA microcolumns. This overall increase ranged from 88% for warfarin to 100-105% for carbamazepine and 157-168% for verapamil. Part of this increase was found to be the result of non-specific interactions by some of the drugs with BHM residues, as determined through control studies that compared retention on a reference HSA column vs. the same column after treatment with BMH, but with no cross-linking to soluble HSA. The increase in retention due to these non-specific interactions was found to be only 4.3 (\pm 6.1)% for carbamazepine and 18.1 (\pm 6.3)% for warfarin; however, this effect lead to 73 (\pm 21)% of the increase in retention that was noted for verapamil. This trend agrees with previous reports in which verapamil has been noted to have much higher non-specific interactions on other types of affinity microcolumns than warfarin, carbamazepine or other drugs.^{18,31}

The retention increase due to the immobilized HSA was determined by correcting the overall change in retention for the increase due to the non-specific interactions with BMH. These corrected values are also included in Table 8.1. The size of this corrected increase in retention was now in the general range of 70-100% for all of the tested drugs, regardless of whether these drugs were known to bind at Sudlow site I (i.e., warfarin and verapamil) or at Sudlow site II (carbamazepine).^{19-21,28,31,32} This increase in protein-based retention was in the same general range as the 75-113% increase in overall protein content that had been noted in the previous section for the BMH-treated HSA supports. The similarity in these values indicates that this increase in retention was directly related to the higher protein content of the BMH-treated HSA supports. This increase was probably also aided by the site-selective nature of the modification process that was used

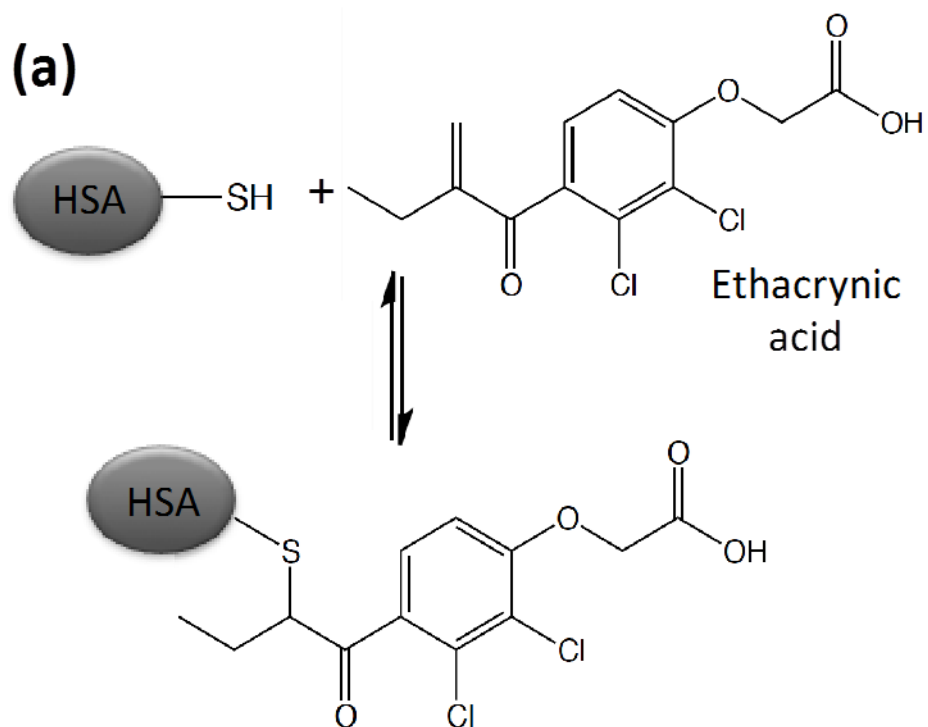
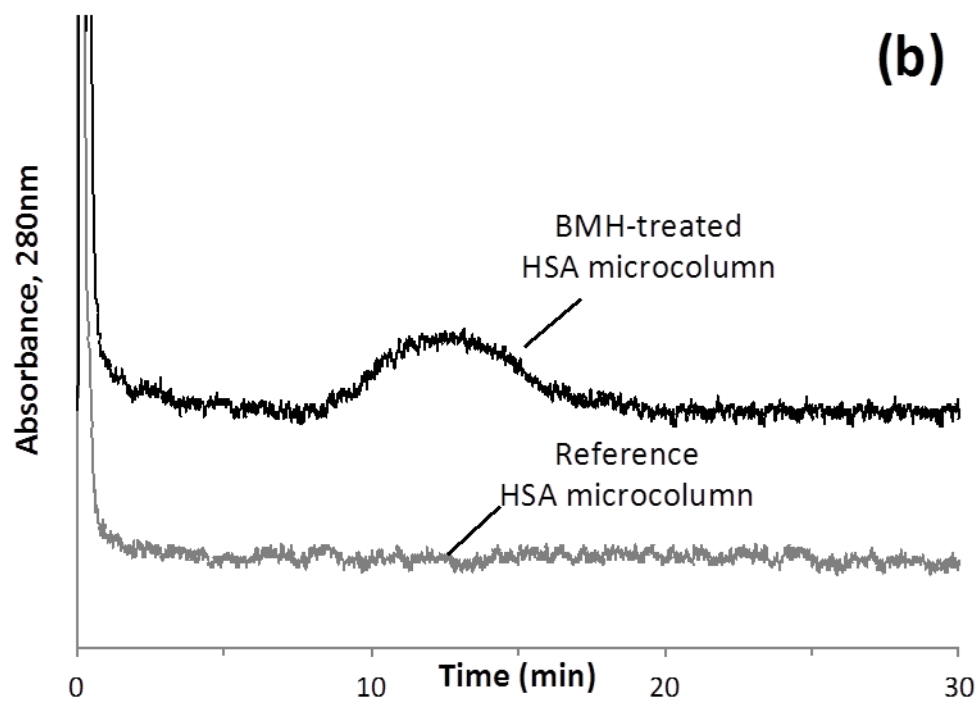
in this study and the fact that Cys34, the modification site, is distant from both Sudlow sites I and II of HSA.^{4,8,14-15}

Use of BMH-treated HSA microcolumns with a sulfhydryl-reactive drug

One unique application that was explored for the BMH-treated HSA microcolumns was their use in studying the reversible binding of a drug that can also undergo a covalent linkage with HSA at Cys34. Ethacrynic acid was used as the model drug for this work. Ethacrynic acid is a diuretic drug that can rapidly form a covalent bond with Cys34 at a neutral pH (see Figure 8.3).³⁴⁻³⁷ In prior work, this drug has been used to modify HSA columns to distinguish between reversible and covalent interactions by other solutes with this protein.³⁵⁻³⁷ However, this drug is also known to be able to reversibly bind at major two sites on HSA (i.e., Sudlow sites I and II).³⁴⁻³⁸ Isothermal titration microcalorimetry and circular dichroism spectroscopy have previously been used to study these latter processes, resulting in estimated binding constants on the order of 10^5 - 10^6 M⁻¹ for these reversible interactions.^{34,36,39,40}

Figure 8.3(b) shows some chromatograms that were obtained when ethacrynic acid was injected at 1.5 mL/min onto a 10 mm × 2.1 mm i.d. reference HSA microcolumn or a BMH-treated HSA microcolumn. On the BMH-treated HSA column, a peak for ethacrynic acid was observed with a retention time of about 12 min. This value corresponded to a retention factor of 502 (± 2) at 37 °C and pH 7.4 and is the type of behavior that would be expected for a strong but reversible drug-protein interaction. However, no peak was seen when the same drug sample was injected onto the reference

Figure 8.3 (a) The reaction between ethacrynic acid and Cys34 on HSA and (b) chromatograms obtained for 20 μL injections of 10 μM ethacrynic acid onto a 10 mm \times 2.1 mm i.d. BMH-treated HSA microcolumn or a reference HSA microcolumn. These results were obtained at 1.5 mL/min and 37 $^{\circ}\text{C}$ using pH 7.4, 0.067 M phosphate buffer as the mobile phase.

(a)**(b)**

HSA microcolumn, as would occur if this drug were quickly and covalently binding to HSA. Injections of ethacrynic acid onto an inert control column with no protein present gave a peak area for ethacrynic acid that differed by only 3.0% from that observed on the BMH-treated HSA microcolumn, indicating that all the injected ethacrynic acid was being eluted and recovered from this microcolumn. Neither the area or position of this peak was affected by including up to 100 μM BMH as a competing agent in the injected sample, confirming that this retention was due to the interaction of ethacrynic acid with HSA rather than with the groups added by BMH to HSA.

The retention factor that was measured for ethacrynic acid on the BMH-treated HSA microcolumn was used to estimate the global affinity constant (nK'_a) for this drug at its reversible binding sites on HSA. This value was determined by using the relationships given in Equations 8.1-8.2.^{4,13,14}

$$k = \frac{(n_1K_{a1} + n_2K_{a2} + \dots + n_nK_{an})m_L}{V_M} \quad (8.1)$$

$$k = \frac{(nK'_a)m_L}{V_M} \quad (8.2)$$

In these equations, the terms K_{a1} through K_{an} represent the association equilibrium constants for the ethacrynic acid at each of its reversible binding sites with HSA, and n_1 through n_n are the mole fractions for each type of site in the column, where nK'_a is the sum of n_1K_{a1} through n_nK_{an} . The term m_L is the total moles of all binding sites for ethacrynic acid in the column, and V_M is the void volume of the column.

The interactions of ethacrynic acid at its two major and reversible binding sites on HSA (i.e., Sudlow sites I and II) are known to have binding constants that are roughly

two orders of magnitude higher than those for any weak binding sites that are present for this drug.^{34,36,38-40} Under these conditions, Equation 8.1 can be simplified to the two-site form given in Equation 8.3,

$$k = \frac{(n_1 K_{a1} + n_2 K_{a2}) m_L}{V_M} = \frac{n K_a' (m_{L1} + m_{L2})}{V_M} \quad (8.3)$$

where n_1 and n_2 are the relative number of sites 1 and 2 (e.g., Sudlow sites I and II) on the binding agent in the column. Equation 8.3 was next combined with the corrected retention factors that had been measured earlier in this chapter on BMH-treated HSA microcolumns for warfarin and carbamazepine (i.e., probes for Sudlow sites I and II) and with the known or measured association equilibrium constants of these drugs with HSA (see next Section). By placing this information and the measured retention factor for ethacrynic acid into Equation 8.3, the global affinity constant for the reversible interactions of ethacrynic acid with HSA was found to be $3.2 (\pm 0.1) \times 10^5 \text{ M}^{-1}$ at 37 °C and pH 7.4. This value was in good agreement with previous literature values of $1.65 \times 10^5 \text{ M}^{-1}$ to $1.2 \times 10^6 \text{ M}^{-1}$ that have been obtained under similar conditions and by using techniques such as circular dichroism or isothermal titration microcalorimetry.^{34,38-40}

Use of BMH-treated HSA microcolumns in ultrafast affinity extraction

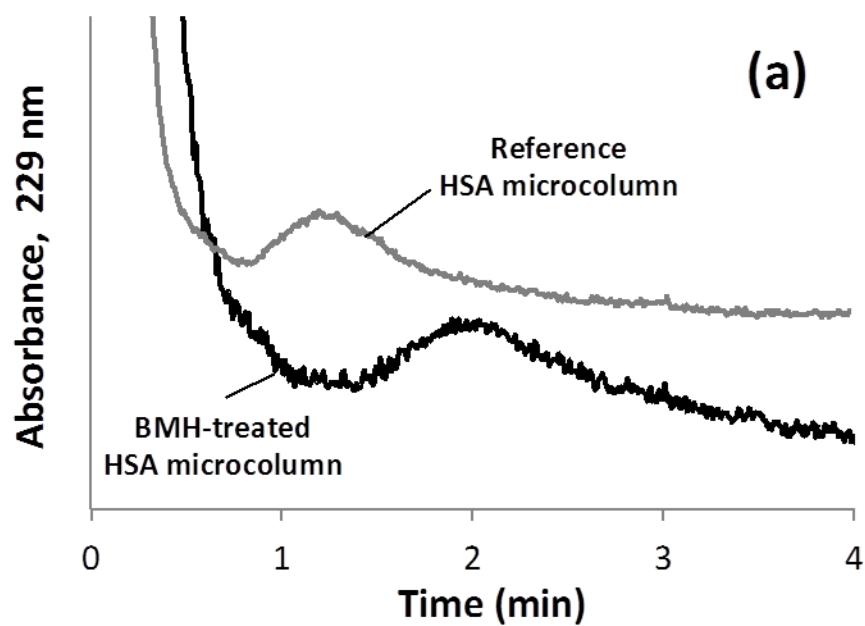
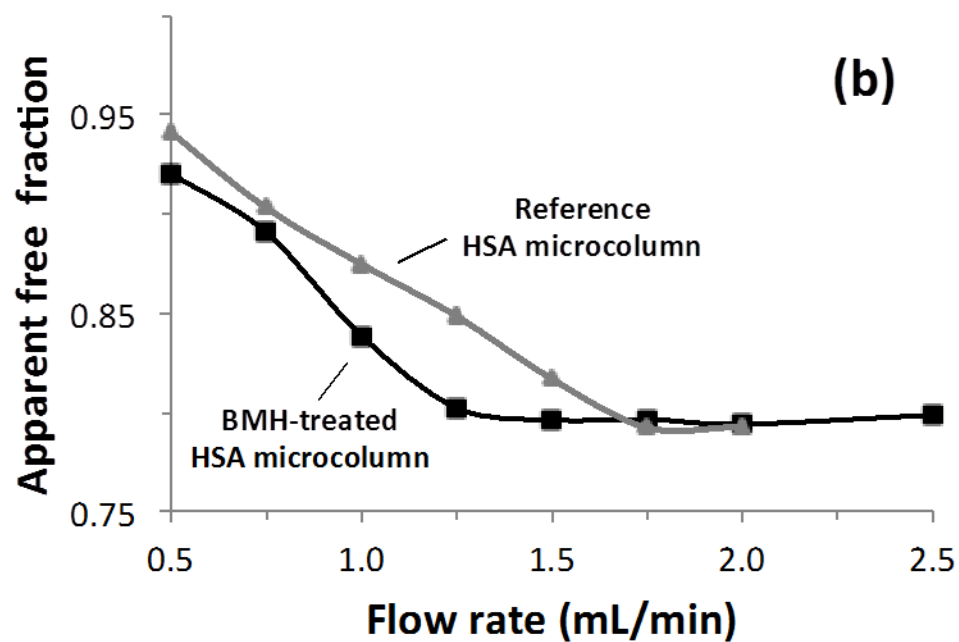
Another application that was considered was the use of the BMH-treated HSA microcolumns in ultrafast affinity extraction and free drug fraction measurements. These experiments were carried out by using samples that contained a drug in the presence or absence of soluble HSA, with small amounts of these samples being injected onto a

BMH-treated HSA microcolumn or a reference HSA microcolumn.¹⁶⁻¹⁸ These injections were made under column size and flow rate conditions that allowed part or all of the non-bound (or free) drug fraction in the sample to be extracted by the immobilized HSA without allowing sufficient time for dissociation of a significant portion of the protein-bound form of the drug in the sample. As shown in Figure 8.4(b), the excess protein and original drug-protein complex eluted as a non-retained peak in this experiment, while the extracted free form of the drug was retained and eluted later from the column. By comparing the retained peak area for the free drug and the total peak area for the same drug in the absence of any soluble HSA, the free drug fraction was then determined for the original sample.¹⁶⁻¹⁸

The residence time of the drug/protein sample in the affinity extraction column is an important factor to consider in this type of free fraction analysis. The use of a relatively long sample residence time may cause dissociation of the protein-bound form of a drug, resulting in a high value for the apparent free fraction. This effect can be minimized by using a short column and/or by increasing the flow rate that is used for sample injection.¹⁶⁻¹⁸ It is also necessary to use a column size and flow rate conditions that allow sufficient resolution to be obtained between the non-retained and retained drug fractions to avoid having high free fraction measurements.¹⁶⁻¹⁸

Figure 8.4(a) shows the results of free fraction measurements for verapamil/HSA mixtures that were injected onto both a BMH-treated HSA microcolumn and a reference HSA microcolumn at various flow rates. The apparent free fraction decreased as the flow rate was increased until a consistent free fraction was obtained when the flow rate was at

Figure 8.4 (a) Effect of flow rate on the apparent free drug fractions measured for 1 μ L samples of 10 μ M verapamil or 10 μ M verapamil plus 20 μ M soluble HSA injected onto a 10 mm \times 2.1 mm i.d. BMH-treated HSA microcolumn (modification/immobilization strategy; black line, ■) or a 10 mm \times 2.1 mm i.d. reference HSA microcolumn (gray, ▲), and (b) chromatograms obtained for 1 μ L injections of 10 μ M racemic verapamil plus 20 μ M HSA onto the same columns at 1.25 mL/min on the BMH-treated HSA microcolumn (black) or at 1.75 mL/min on the reference HSA microcolumn (gray). These results were all acquired at 37 °C and using pH 7.4, 0.067 M phosphate buffer as the mobile phase.



or above 1.25 mL/min on the BMH-treated HSA column. However, the same measurements on the reference HSA microcolumn required a flow rate of at least 1.75 mL/min for consistent free fractions to be obtained (Note: typical chromatograms for verapamil at these flow rates are provided in Figure 8.4(b)). The differences in these flow rate requirements probably reflect the higher retention and better resolution that was between the free and bound drug peaks on the BMH-treated HSA microcolumns, which also helped minimize positive errors in the apparent free drug fraction.^{3,5} The same overall trend, in which lower or equivalent flow rates could be used in the free fraction measurements on the BHM-treated columns, was observed for warfarin and carbamazepine.

The free drug fractions that were measured at or above these optimum flow rates were used to estimate the association equilibrium constants for each drug with soluble HSA. These values were calculated by using Equation 8.4.^{16,17}

$$K_a = \frac{1 - F_0}{F_0([P]_{\text{tot}} - [D]_{\text{tot}} + [D]_{\text{tot}}F_0)} \quad (8.4)$$

In Equation 8.4, F_0 is the free drug fraction that is measured at equilibrium (i.e., at or above a flow rate that minimizes drug-protein dissociation in the sample), while $[D]_{\text{tot}}$ and $[P]_{\text{tot}}$ are the total concentrations of the drug and soluble protein in the original sample. The value of K_a in this equation is the association equilibrium constant for a drug and protein with a single-site interaction, or the global affinity constant for a drug that has multiple but independent binding sites on the protein.^{16,17}

Table 8.2 shows the K_a values that were obtained by using Equation 8.2 and free

Table 8.2 Association equilibrium constants measured for various drugs with soluble HSA by using free fraction analysis on a BMH-treated HSA microcolumn or reference HSA microcolumn^a

Drug	Reference HSA microcolumn	BMH-treated HSA microcolumn	Literature value [Ref.]
Warfarin	$2.5 (\pm 0.2) \times 10^5 \text{ M}^{-1}$	$2.6 (\pm 0.2) \times 10^5 \text{ M}^{-1}$	$2.0\text{-}5.7 \times 10^5 \text{ M}^{-1}$ [19-21,28]
Verapamil	$1.5 (\pm 0.4) \times 10^4 \text{ M}^{-1}$	$1.4 (\pm 0.1) \times 10^4 \text{ M}^{-1}$	$1.4 (\pm 0.1) \times 10^4 \text{ M}^{-1}$ [31]
Carbamazepine	$5.3 (\pm 0.4) \times 10^3 \text{ M}^{-1}$	$5.3 (\pm 0.4) \times 10^3 \text{ M}^{-1}$	$5.2\text{-}5.5 \times 10^3 \text{ M}^{-1}$ [32,33]

^aThese results obtained in this study were measured at pH 7.4 and at 37°C. The values in parentheses represent a range of ± 1 S.D., as determined by error propagation. The results given for warfarin and verapamil are the ranges or average association equilibrium constants for the *R*- and *S*-enantiomers; the value given for verapamil is for the high affinity site of verapamil on HSA.

drug fractions that were measured on the BMH-treated HSA microcolumns or reference HSA microcolumns. The values that were obtained in this chapter had relative precisions in the range of $\pm 7-8\%$ and were based on peak area measurements that could be made within 1 to 6.5 min of sample injection. In each case, there was good agreement between the K_a values that were measured on these columns and with reference values that have been determined under the same pH and temperature conditions. These results confirmed that the BMH-treated HSA microcolumns could be successfully used to quickly estimate K_a values for drug-protein binding based on free drug fraction measurements.

Conclusions

This study developed a new hybrid method to produce enhanced capacity affinity microcolumns containing HSA by combining BMH as a reagent for protein modification or cross-linking with a covalent immobilization method. Various factors were considered in determining the optimum conditions for this method, including the use of BMH modification before or after protein immobilization and the reaction conditions involved in this process. The supports that were obtained in the optimized method had up to a 75-113% increase in protein content when compared to supports that were prepared using only covalent immobilization. These BMH-modified HSA supports also gave a large increase in protein-based retention (i.e., 70-100%) versus a reference support when both types of materials were used in microcolumns to bind various drugs that are known to interact at Sudlow sites I or II of HSA.

The BMH-treated HSA microcolumns were tested for use in estimating free drug fractions and association equilibrium constants for drug-protein interactions. These columns gave results comparable with those determined by reference HSA microcolumns or those reported in literature. In addition, the BMH-treated HSA microcolumns were used to investigate the reversible interactions between HSA and ethacrynic acid, a drug which can also covalently bind to the HSA through its free sulfhydryl group. This type of hybrid modification/immobilization scheme is not limited to HSA but should also be useful in work with other proteins and in the study of alternative drug-protein systems. Possible applications for such columns include the high-throughput analysis of drug-protein binding, protein-based chiral separations, the analysis of free drug fractions in clinical or pharmaceutical samples, and the screening of drug candidates for their protein interactions.¹⁶⁻¹⁸

References

1. R.R. Walters, *Anal. Chem.* 57 (1985) 1099A-1114A.
2. D.S. Hage, *Clin. Chem.* 45 (1999) 593-615.
3. D.S. Hage (Ed.), *Handbook of Affinity Chromatography*, second ed., CRC Press, Boca Raton, FL, 2006.
4. D.S. Hage, *J. Chromatogr. B* 768 (2002) 3-30.
5. R. Mallik, C. Wa, D.S. Hage, *Anal. Chem.* 79 (2007) 1411-1424.
6. A. Jackson, H. Xuan, D.S. Hage, *Anal. Biochem.* 404 (2010) 106-108.
7. M. Wilchek, I. Chaiken, *Methods Mol. Biol.* 147 (2000) 1-6.
8. T. Peters, Jr., *All About Albumin: Biochemistry, Genetics, and Medical Applications*, Academic Press, San Diego, CA, 1996.
9. H.S. Kim, D.S. Hage, Immobilization methods for affinity chromatography, in: D.S. Hage (Ed.), *Handbook of Affinity Chromatography*, second ed., CRC Press, Boca Raton, FL, 2006, pp. 35-78.
10. E. Calleri, G. Fracchiolla, R. Montanari, G. Pochetti, A. Lavecchia, F. Loiodice, A. Laghezza, L. Piemontese, G. Massolini, C. Temporini, *J. Chromatogr. A* 1232(2012) 84-92.
11. X. Mao, Y. Luo, Z. Dai, K. Wang, Y. Du, B. Lin, *Anal. Chem.* 76 (2004) 6941-6947.
12. J. Krenkova, F. Foret, *Electrophoresis* 25 (2004) 3550-3563.
13. X. Zheng, Z. Li, S. Beeram, M. Podariu, R. Matsuda. E.L. Pfau Miller, C.J. White II, N. Carter, D.S. Hage, *J. Chromatogr. B* 968 (2014) 49-63.

14. D.S. Hage, J. Anguizola, O. Barnaby, A. Jackson, M.J. Yoo, E. Papastavros, E. Pfaunmiller, M. Sobansky, Z. Tong, *Curr. Drug Metab.* 12 (2011) 313-328.
15. G. Sudlow, D.J. Birkett, D.N. Wade, *Mol. Pharmacol.* 12 (1976) 1052-1061.
16. R. Mallik, M.J. Yoo, C.J. Briscoe, D.S. Hage, *J. Chromatogr. A* 1217 (2010) 2796-2803.
17. X. Zheng, M.J. Yoo, D.S. Hage, *Analyst* 138 (2013) 6262-6265.
18. X. Zheng, L. Zhao, M.I. Podariu, D.S. Hage, *Anal. Chem.* 86 (2014) 6454-6460.
19. B. Loun, D.S. Hage, *Anal. Chem.* 66 (1994) 3814-3822.
20. M.J. Yoo, D.S. Hage, *J. Chromatogr. A* 1218 (2011) 2072-2078.
21. M.J. Yoo, J.E. Schiel, D.S. Hage, *J. Chromatogr. B* 878 (2010) 1707-1713.
22. G.T. Hermanson, *Bioconjugate Techniques*, second ed., Academic Press, San Diego, CA, 2008.
23. L.L. Chen, J.J. Rosa, S. Turner, R.B. Pepinsky, *J. Biol. Chem.* 266 (1991) 18237-18243.
24. L. Giron-Monzon, L. Manelyte, R. Ahrends, D. Kirsch, B. Spengler, P. Friedhoff, *J. Biol. Chem.* 279 (1991) 49338-49345.
25. N.S. Green, E. Reisler, K.N. Houk, *Protein Sci.* 10 (2001) 1293-1304.
26. F.T. Ishmael, M.A. Trakselis, S.J. Benkovic, *J. Biol. Chem.* 278 (2003) 3145-3152.
27. M.A. Stalteri, S.J. Mather, *Bioconjugate Chem.* 6 (1995) 179-186.
28. J. Chen, D.S. Hage, *Anal. Chem.* 78 (2006) 2672-2683.
29. E.L. Pfaunmiller, M. Hartmann, C.M. Dupper, S. Soman, D.S. Hage, *J. Chromatogr. A* 1269 (2012) 198-207.

30. L. Baugh, T. Weidner, J.E. Baio, P.C.T. Nguyen, L.J. Gamble, P.S. Stayton, D.G. Castner, *Langmuir* 26 (2010) 16434-16441.
31. R. Mallik, M.J. Yoo, S. Chen, D.S. Hage, *J. Chromatogr. B* 876 (2008) 69-75.
32. H.S. Kim, R. Mallik, D.S. Hage, *J. Chromatogr. B* 837 (2006) 138-146.
33. H.S. Kim, D.S. Hage, *J. Chromatogr. B* 816 (2005) 57-66.
34. C. Bertucci, B. Nanni, P. Salvadori, *Chirality* 11 (1999) 33-38.
35. C. Bertucci, B. Nanni, A. Raffaelli, P. Salvadori, *J. Pharm. Biomed. Anal.* 18 (1998) 127-136.
36. G.A. Ascoli, E. Domenici, C. Bertucci, *Chirality* 18 (2006) 667-679.
37. C. Bertucci, I.W. Wainer, *Chirality* 9 (1997) 335-340.
38. K.J. Fehske, W.E. Miller, *Pharmacology* 32 (1986) 208-213.
39. H. Aki, M. Goto, M. Yamamoto, *Thermochim. Acta* 251 (1995) 379-388.
40. H. Aki, M. Goto, M. Kai, M. Yamamoto, *J. Therm. Anal. Cal.* 57 (1999) 361-370.

CHAPTER 9

Summary and Future Work

Summary of Work

The work in this dissertation mainly involved studies of the interactions between drugs or hormones and proteins by using high-performance affinity chromatography (HPAC) and affinity microcolumns. Human serum albumin (HSA) was used as a model protein for binding studies in this work. Chapter 1 introduced the general background for the work that is presented in this dissertation. This chapter included a discussion of the types of microcolumns that can be used for the study of biomolecular interactions, as well as the potential advantages of each type. This chapter also examined how affinity microcolumns have been used to examine biomolecular interactions with HPAC methods such as zonal elution and frontal analysis methods. A specific technique used throughout this dissertation, ultrafast affinity extraction, was also described in this chapter.

Chapter 2 reviewed several analytical methods that have been to study the kinetics of biological interactions. These techniques included common or traditional methods such as stopped-flow analysis and surface plasmon resonance spectroscopy, as well as alternative methods based on affinity chromatography and capillary electrophoresis. This chapter described the general principles and theory behind these approaches, and showed how each technique can be utilized to provide information on the kinetics of biological interactions. Examples of applications, relative advantages or potential limitations were

also given for each method regarding its use in kinetic studies.

Chapter 3 described the development of a method based on ultrafast affinity extraction and HPAC to determine both the dissociation rate constants and equilibrium constants for drug-protein interactions in solution. Several drugs that are known to bind to human serum albumin (HSA) were examined. The dissociation rate constants (k_d) obtained for soluble HSA with each drug gave good agreement with previous rate constants that have been reported for the same drugs or other solutes with comparable affinities for HSA. The association equilibrium constants (K_a) that were determined simultaneously with the k_d values also showed good agreement with the literature.

Chapter 4 described a multi-dimensional system that was based on affinity microcolumns, ultrafast affinity extraction and chiral separations to measure the free fractions of drug enantiomers and to study their binding with serum transport proteins. *R/S*-Warfarin and the HSA were used as models to test this approach. The free fractions of *R*- and *S*-warfarin that were determined by this method gave good agreement with those measured by ultrafiltration. It was also found that this approach could provide a fast estimate of the association equilibrium constants for drug-protein interactions, giving results consistent with the literature and reference methods. This method could also be utilized with clinically-relevant concentrations of warfarin and HSA and could be extended to other chiral drugs and serum proteins or used for the high-throughput screening of drug-protein interactions.

Chapter 5 showed how ultrafast affinity extraction and a multi-dimensional affinity system could be used to investigate the effects of protein modification on drug

binding at therapeutic levels. This approach was used to compare the free fractions and global affinity constants of several sulfonylurea drugs in the presence of normal HSA or glycated forms of this protein, as are produced during diabetes. Various factors were considered in optimizing the multi-dimensional HPAC system, including the flow rates and column sizes that were used to initially extract the free drug fractions and time at which this extracted fraction was passed onto the second column for further separation and analysis. This method was able to measure free drug fractions as small as 0.09-2.58% with an absolute precision of ± 0.02 -0.5%. The results that were obtained indicated that glycation can affect the free fractions of sulfonylurea drugs at typical therapeutic levels and that the size of this effect varies with the level of HSA glycation. Global affinity constants that were estimated from these free drug fractions gave good agreement with those predicted from previous binding studies or that were determined by using a reference method.

Chapter 6 used ultrafast affinity extraction and a multi-dimensional affinity chromatographic system to measure the free fraction of drugs in serum and to examine the interactions of these drugs with HSA. These studies were conducted at typical therapeutic drug concentrations that were spiked into control human serum. The drugs that were examined in this work included quinidine, diazepam, gliclazide, tolbutamide and acetohexamide. The dissociation rate constants for these drugs with HSA were measured during the process of system optimization, giving results in good agreement with previous literature values. With the final multi-dimensional system, free drug fractions in serum were measured with values in the range of 0.69-7.40% and with absolute precisions of ± 0.1 -0.7%. The association equilibrium constants for each drug

with HSA were also estimated from these data and gave values that agreed well with those in the literature under comparable solution conditions.

In Chapter 7, ultrafast affinity extraction was used to study hormone-protein interactions in solution, using the binding of testosterone with the transport proteins human serum albumin and sex hormone binding globulin (SHBG) as models. In this method, an affinity microcolumn containing HSA was used to isolate and measure the free fraction of testosterone in a sample at equilibrium and after allowing various lengths of time for hormone-protein dissociation. The resulting data were used to determine both the association equilibrium constants and dissociation rate constants for testosterone's interactions with soluble HSA and SHBG. The k_d and K_a values that were obtained for testosterone with HSA were 2.07-2.20 s⁻¹ and $3.2\text{-}3.5 \times 10^4$ M⁻¹ at pH 7.4 and 37 °C. The corresponding constants for the interactions of testosterone with SHBG were 0.057-0.058 s⁻¹ and $1.0\text{-}1.1 \times 10^9$ M⁻¹. All of these values gave good agreement with previous literature values. This study indicated that ultrafast affinity extraction could provide information on both the rate constants and binding strengths for hormone-protein interactions in solution and at clinically-relevant concentrations for such agents.

In last chapter, Chapter 8, a hybrid method was developed and examined for increasing the binding capacity and activity of protein-based affinity columns by using a combination of protein cross-linking/modification and covalent immobilization. Various applications of this approach in the study of drug-protein interactions and in use with affinity microcolumns were considered. HSA was utilized as a model protein for this work. Bismaleimido-hexane (BMH, a homobifunctional maleimide) was used to modify and/or cross-link HSA through the single free sulfhydryl group that is present on this

protein. Up to a 75-113% increase in protein content was obtained when comparing affinity supports that were prepared with BMH versus reference supports that were made by using only covalent immobilization. Several drugs that are known to bind HSA (e.g., warfarin, verapamil and carbamazepine) were also found to have a significant increase in retention on HSA microcolumns that were treated with BMH (i.e., a 70-100% increase in protein-based retention). These BMH-treated HSA microcolumns were also used in ultrafast affinity extraction to measure free drug fractions in a drug/protein mixtures, giving association equilibrium constants that had good agreement with literature values. In addition, it was found that the reversible binding of HSA with ethacrynic acid, an agent that can also combine irreversibly with the free sulfhydryl group on this protein, could be examined by using the BMH-treated HSA microcolumns. The same hybrid immobilization method could be extended to other proteins or to alternative applications that may require protein-based affinity columns with enhanced binding capacities and activities.

Future Work

The work presented in this dissertation has shown that ultrafast affinity extraction can be powerful tools for the examination of solute-protein interactions. It was found that this method could allow use of a single experimental system to provide information regarding the free fraction of solutes, their dissociation rate constants for proteins, and the equilibrium constant for the biomolecular reaction. In addition, this method could be used to the study of the samples that are more complex, such as those containing a racemic

mixture of two enantiomers of the solute, human serum or samples that are prepared at clinically-relevant concentrations.

To further improve this method, this system could also be used with other types of analytical columns, such as those containing reversed-phase, ion-exchange or size-exclusion supports. These new combinations could be used to optimize and extend the ultrafast affinity extraction method to systems that have even weaker binding or faster dissociation of the immobilized ligand. This new approach could also be adapted for the study of more complex mixtures of free solutes, such as mixtures of drugs or drugs and their metabolites.

Studies could also be performed to examine the use of ultrafast affinity extraction on alternative types of affinity column to investigate the effects of changing the support or immobilization method on the ability to carry out a free fraction analysis. Examples of supports and immobilization methods that are of interest would include the use of entrapment-based immobilization, the use of covalent immobilization on silica particles versus organic monoliths, or the use of the hybrid immobilization method that was introduced in Chapter 8. This type of study should provide a better understanding of how ultrafast affinity extraction can be used with other types of affinity microcolumns in HPAC method. The optimum chromatographic conditions that are required for each column type could also be examined.

Another application of ultrafast affinity extraction is in the analysis of free drug fractions in sample that contain more than one binding protein. Even though HSA is the most abundant protein in plasma, the target of interest may have much stronger binding

strength to other proteins that are present in serum, but at a much lower concentration. This type of sample will make a consideration regarding the interactions for the target with both types of the binding proteins necessary. The measurement of free target fractions in such a situation will provide more precise information on solute-protein interactions in this type of situation under typical clinical conditions.

Columns that are prepared based on the hybrid immobilization method could be further used to study solutes that have reversible binding plus covalent interactions with free sulfhydryl groups on an immobilized ligand. Other hybrid immobilization strategies can also be explored to improve the capacity and active content of proteins that are immobilized within microcolumns for use in ultrafast affinity extraction or related methods.